THE UNIVERSITY OF CHICAGO

SYNTHESIS AND REACTIVITY OF LOW COORDINATE NICKEL SULFIDE COMPLEXES

A DISSERTATION SUBMITTED TO

THE FACULTY OF THE DIVISION OF THE PHYSICAL SCIENCES

IN CANDIDACY FOR THE DEGREE OF

DOCTOR OF PHILOSOPHY

DEPARTMENT OF CHEMISTRY

BY

FRANK DAVID OLECHNOWICZ

CHICAGO, ILLINOIS

MARCH 2017

TABLE OF CONTENTS

LIST OF TABLES

LIST OF FIGURES

LIST OF SCHEMES

LIST OF CHARTS

ACKNOWLEDGEMENTS

The Ph.D. experience depends on many factors, the most important of which is the research advisor. I am blessed to have two exceptional mentors, Professors Gregory Hillhouse (R.I.P.) and Richard Jordan. Prof. Hillhouse challenged me to be a better chemist through his brand of "tough love", and set an example for how to be both an exceptional chemist and an exceptional person. Prof. Jordan has been incredibly supportive, and it has been a privilege to learn from his example of both scientific rigor and professionalism. I hope all group members, past and present, appreciate his emphasis on effective communication skills, perhaps the most impactful skill I will use for the rest of my career.

I also thank the other members of my committee, Professors Michael Hopkins and John Anderson, for their helpful advice and discussions.

The quality of my Ph.D. experience was greatly enhanced by the member of both the Hillhouse and Jordan groups. Dr. Steve Baldwin was invaluable for his mentorship in synthetic inorganic techniques when I first joined the Hillhouse group. He, together with Junjie Zhai, Chris Hansen, Sarah Del Ciello, Niklas Thompson, and Ryan Witzke, were always willing to talk chemistry as well as life. Likewise, the Jordan group cultivated an upbeat atmosphere, and I wish to thank Becca Black, Tabbetha Bohac, Dr. Nathan Contrella, Dr. Ge Feng, Alison Johnson, Dr. Ka Cheong Lau, Dr. Qian Liu, Erik Reinhart, Joseph Solomon, Shinji Wada, Amanda Waterbury, Dr. Jia Wei, Dr. Ryan Zarkesh, and Dr. Feng Zhai. Additionally, alumni from both groups have provided insight and advice to surviving a Ph.D. and the transition to the next step. Lastly, to Paul Williams and Maxwell Weinberg, who taught me humility, and that what works in theory does not always work in practice.

I am grateful to Mr Rivers, who first set me on the path of Chemistry back in 7th Grade, and to my undergraduate research advisor, Professor Catalina Achim at Carnegie Mellon University, for the opportunity to join the lab as a sophomore and her encouragement in college and beyond.

Much of the work presented in this thesis would not have been possible without the assistance of others. Major thanks are owed to Professor Thomas Cundari, who hosted me at the University of North Texas and gave me an expeditious orientation to Gaussian and GAMESS. Although things didn't work out quite as we had hoped, I am grateful to Dr. John Linehan at Pacific Northwest National Laboratory, for advice and usage of the high pressure PEEK setup. The research described in this thesis has relied on many departmental facilities, and I thank Dr. Antoni Jurkiewicz and Dr. Chang-Jin Qin for their assistance with optical and mass spectroscopies, Zbigniew Gasyna for computational assistance, and Dr. Ian Steel and Dr. Alexander Filatov for their assistance with x-ray crystallography.

I am also grateful to Dr. Vera Dragisich, Laura Luburich, Melinda Moore, Michael Reedy, and Jesse Valle for their assistance with various obligations and responsibilities outside of research, and keeping the department running like a well-oiled machine.

Many good friends within and outside of the Chemistry Department have provided great memories throughout graduate school, and in this regard I am especially grateful to the entire 4^{th} floor of GCIS (who clearly work in an elevated state of mind), and Nick Daly, Cesar Favila, Bart Longacre, Alex Murray, and KC Vavra for helping keep my sanity.

I thank my family and especially my parents, for ineffable support and freedom to pursue my passion wherever it takes me, and for my fiancée Heidi, for her love, support, and patience through the stress and uncertainty of graduate school.

ABSTRACT

This thesis describes the chemistry of Ni complexes supported by an N-Heterocyclic Carbene (NHC) ligand that contain sulfur atoms in different binding modes. The unique steric and electronic properties of NHCs allow for the preparation and interconversion of four different sulfur-based groups. These complexes are markedly different than related complexes in the literature, and can be used as a model to study the H_2 activation step of the hydrodesulfurization process.

Chapter One describes the prevalence of nickel complexes containing bridging thiolate and sulfide groups. These complexes serve key roles in the small molecule activation and electron transport in enzyme active sites, and perform the key activation step of H_2 in the hydrodesulfurization process. Model used to study this activation step exhibit fluxional behavior in solution, which limits the conclusions about the exact mechanistic details. These limitations can be overcome by using an NHC ligand. The core imidazole ring imparts NHC ligands with net electron donor ability that is greater than that of phosphine ligands. Additionally NHC ligands possess lateral steric bulk that can shelter a metal center and support low-coordinate environments.

Chapter Two describes the synthesis and reactivity of the dinuclear bridging disulfide complex $\{(IPr)ClNi\}_2(\mu^2\text{-}\eta^2,\eta^2\text{-}S_2)$ (IPr = 1,3-bis(2,6-diisopropylphenyl)imidazolin-2-ylidene) . This complex can be converted to a mononuclear $(IPr)(AdNC)Ni(\eta^2\text{-}S_2)$ complex with a terminal disulfide, a dinuclear $\{(IPr)Ni(\mu\text{-}S)\}_2$ complex with two bridging sulfides, and a dinuclear $\{(IPr)Ni(\mu\text{-}SH)\}_2$ complex two bridging hydrosulfides. Most interestingly, the bridging sulfide and bridging hydrosulfide complexes are interconverted through reaction with H_2 and H-atom abstractor 2,4,6-^{t}Bu$_3$-phenoxy radical.

In Chapter Three, the hydrogenation of $\{(IPr)Ni(\mu\text{-}S)\}_2$ to $\{(IPr)Ni(\mu\text{-}SH)\}_2$ is probed in depth through a combination of kinetic studies and DFT calculations. These results show that H_2 adds across a Ni-S bond in a heterolytic manner to generate a Ni(H)(μ-S)(μ-SH)Ni

intermediate that rearranges to the product by H atom migration from Ni to the remaining μ-S ligand.

Chapter Four describes the reaction of $\{(IPr)Ni(\mu\text{-}S)\}_2$ with H-BPin to produce $\{(IPr)Ni\}_2(\mu\text{-}SH)(\mu\text{-}SBPin)$. This reaction suggests that heterolytic E-H bond activation by the $Ni_2(\mu\text{-}S)_2$ unit may be a general reaction.

Chapter 1 - Introduction

1.1. Prevalence and Importance of Ni-S Complexes

Nickel complexes bearing sulfur-based ligands, particularly bridging thiolate (μ-SR) and bridging sulfide (μ-S) species, have received much interest because of their important roles in biological and synthetic systems (Figure 1).

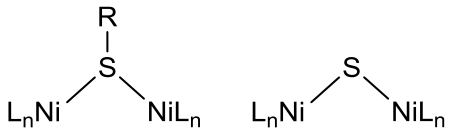

Figure 1. Nickel complexes with bridging thiolate (μ-SR) and bridging sulfide (μ-S) groups.

Nickel plays a prominent role in enzyme active sites, where nickel atoms connected to bridging sulfide and thiolate ligands are vital for small molecule activation and electron transfer reactions (Figure 2).[1] In bacteria and archaea, the [NiFe] Hydrogenase enzyme uses Ni to interconvert H_2 with protons and electrons.[2] In the bacterial enzyme CO Dehydrogenase, a Ni center catalyzes the reversible oxidation of CO to CO_2.[3] In the archaea enzyme Acetyl CoA Synthase, Ni reversibly condenses CO (derived from CO_2) with CoA-SH and a methyl group to generate acetyl-S-CoA.[4]

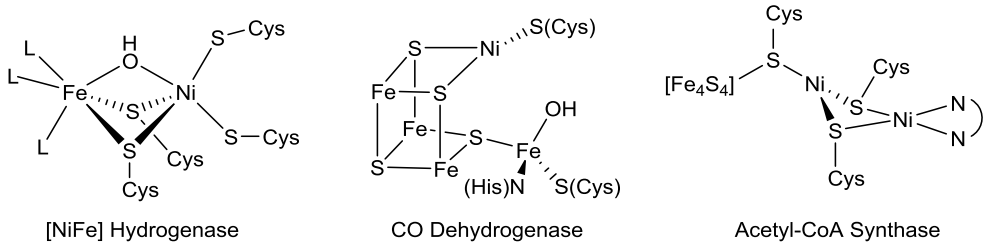

Figure 2. Ni centers supported by bridging thiolate and sulfide ligands in enzyme active sites.

Synthetic Ni catalysts supported by bridging thiolate and sulfide ligands have been developed that perform a wide array of transformations. These species are catalytically active for hydrogenations of C=O and C=C bonds,[5] oxidation of alcohols to aldehydes,[6] Suzuki coupling,[7] alkyne cyclization,[8] thioesterification of CO,[9] copolymerization of CO with ethylene,[10] CO methanation and hydrogenation,[11] decomposition of formic acid,[12] and the electro- and photo-catalytic production of H_2 from water (Figure 3).[13]

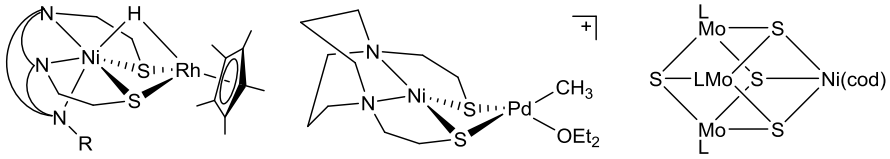

$R_2C=O$ Hydrogenation CO/Ethylene Copolymerization Alkyne Cyclization

Figure 3. Representative nickel catalysts with bridging thiolate and sulfide ligands that perform important chemical reactions.

1.2. Metal Sulfide Catalysts Used In Hydrodesulfurization

Nickel-sulfide catalysts, including heterogeneous catalysts, have been intensively studied for hydrodesulfurization and hydrodenitrogenation reactions.[14] These processes are performed with heterogeneous catalysts on an industrial scale to remove S- and N- containing impurities from petroleum feedstocks to minimize SO_x and NO_x emissions during combustion as fuel (Figure 4). The catalysts employed are typically MoS_2 doped with Ni or Co.[15] Ni is incorporated into the two dimensional lattice in place of Mo, and greatly improves the catalytic activity.

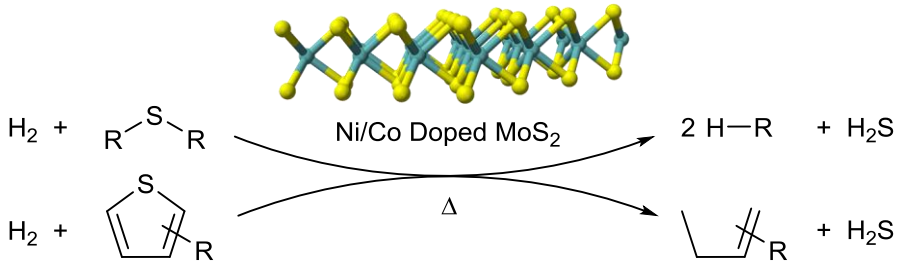

Figure 4. Hydrodesulfurization reactions with the heterogeneous Ni/Co-doped MoS_2 catalyst.

Theoretical investigations of MoS_2 catalysts have predicted that molecular hydrogen is activated heterolytically by the Mo-S-Mo units to form Mo-H and Mo-SH functionalities.[16] These studies implicate Mo-S-Mo units as the active catalyst site and imply that they are essential for the activation of H_2 (Figure 5). Mo-S-Mo sites located at the edges of the 2D lattice, where the unsaturated coordination sphere of the metal can aid in the adsorption and cleavage of H_2, are thought to be more active than those at internal, more coordinatively saturated metal positions within the lattice. Ni has more d electrons than Mo, and is expected to be more stable with a lower coordination number at the edges of the lattice.

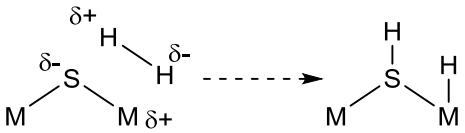

Figure 5. Hypothesized H_2 activation pathway for heterogeneous catalysts.

Heterogeneous catalysts, including MoS_2 and WS_2 systems doped with Ni or Co, have been studied *in situ* and the presence of M-SH groups has been demonstrated by neutron scattering and solid state NMR studies. In contrast, M-H units have only been observed in a RuS_2 system.[17] The heterogeneous nature of these catalysts limits the methods to characterize

H atoms on the surface, and discrete model complexes have been investigated to understand the H_2 coordination and activation.[18]

A desirable model system to investigate the H_2 activation would possess the following properties: 1) multi-nuclear system based on metals used in the hydrodesulfurization process, i.e., Mo, Ni, or Co; 2) homogeneous system that can be easily studied under hydrodesulfurization conditions using spectroscopic techniques; 3) low coordination number, to simulate a metal at the edge of the 2D lattice with open coordination sites.

To date no model systems have exhibited all of these properties simultaneously. Model $Cp_2Mo_2S_4$ systems add H_2 across the S-S bond in a $Cp_2Mo_2(\mu\text{-}S_2)(\mu\text{-}S)_2$ species, to form a $Cp_2Mo_2(\mu\text{-}S)_2(\mu\text{-}SH)_2$ species that reacts further with unsaturated S and N containing substrates (Scheme 1A).[19] However the presence of several product isomers, dynamic reorganization in solution, and multiple side reactions complicated efforts to identify the exact active Mo species in solution.[20] Model systems based on metals not used in hydrodesulfurization have also been studied. The dinuclear dication $[\{L_3Rh(\mu\text{-}S)\}_2]^{2+}$ ($L_3 = CH_3C(CH_2PPh_2)_3$) activates two equiv of H_2 to form $[\{L_3Rh(H)(\mu\text{-}SH)\}_2]^{2+}$ (Scheme 1B).[21] The dinuclear $(Ph_3P)_2Ir(\mu\text{-}S)_2Ir(PPh_3)_2$ complex reacts with two equiv of H_2 to produce $(Ph_3P)_2(H)Ir(\mu\text{-}SH)(\mu\text{-}S)(\mu\text{-}H)Ir(H)(PPh_3)_2$ (Scheme 1C).[22] In both cases, isomerization and dynamic reorganization in solution hindered efforts to draw conclusions about the mechanistic details of the H_2 activation.

Scheme 1. Homogeneous model systems for the H_2 activation step in catalytic hydrodesulfurization.

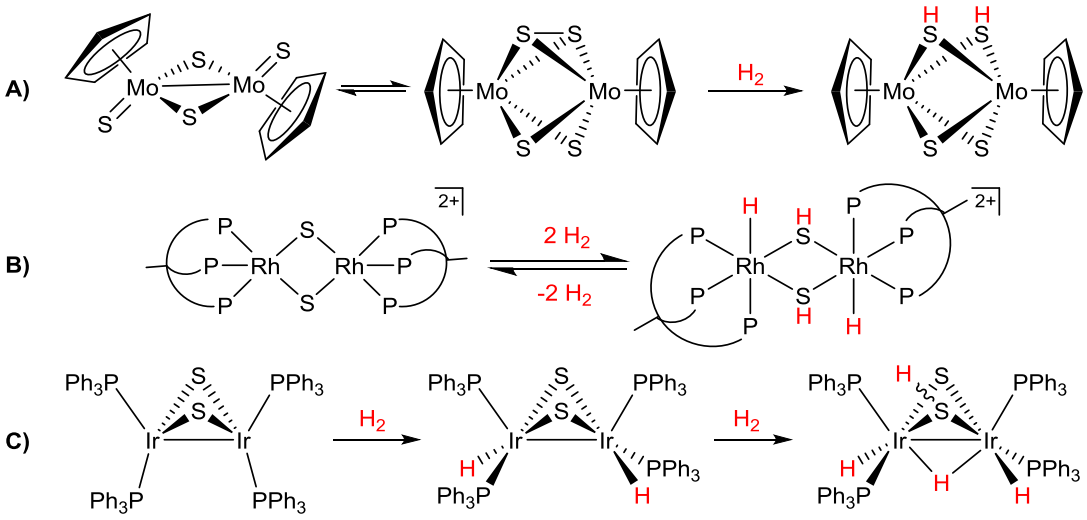

1.3. N-Heterocyclic Carbene Ligands

Chelating phosphines ($R_2P(CH_2)_nPR_2$) and diketiminates (nacnac; $[R^1NCR^2CHCR^2NR^1]^-$) have provided useful scaffolds for isolation of three- and four-coordinate Ni complexes (Figure 6).[23] Typically the P and N atoms are substituted with large groups, which prevent aggregation into multinuclear complexes but also limit access to the inner coordination sphere and thus the potential reactivity. These limitations can be avoided by switching to the N-Heterocyclic Carbene (NHC) ligand class. The unique electronic and steric properties of NHC ligands have enabled significant advances in catalysis and organometallic synthesis.[24]

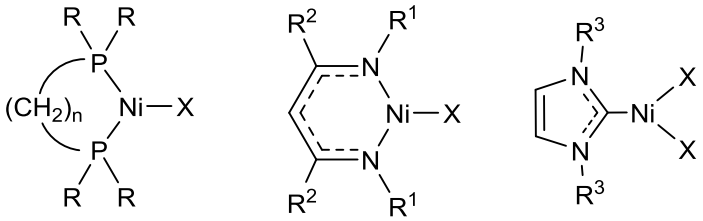

Figure 6. Generic structures of diphosphine, diketiminate, and NHC ligands attached to a 3-coordinate Ni center.

1.3.1. Electronic Properties of NHC Ligands

N-heterocyclic carbenes are charge-neutral, electron-rich, strong σ-donor ligands (Figure 7). NHC ligands bind in a mono-dentate fashion through the central, sp^2-hybridized C atom. The C atom also has an empty p_z orbital, into which the adjacent N atoms can donate their lone pair electrons, resulting in significant negative charge on the carbon and strong σ-donor ability.

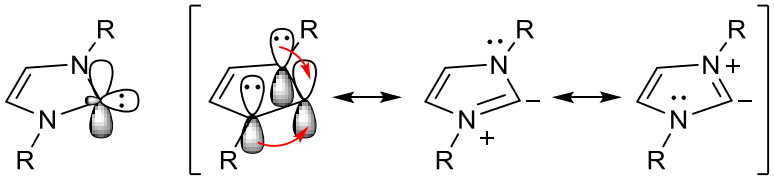

Figure 7. Electronic structure of N-heterocyclic carbene ligands.

The N→C π donation prevents significant π-backbonding from the metal center. DFT calculations predict that π-backbonding contributes <10% of the total Pt-C bond electron density in *cis*-(IPr)-$PtCl_2$(DMSO).[25] Therefore an NHC ligand functions as a strong σ-donor with little π-acceptor character, in contrast to phosphine ligands which are both strong σ-donor and π-acceptor ligands. As a result, the net-donor ability of NHCs is on par with or greater than that of tri-alkyl phosphines, as measured by CO stretching frequencies of metal carbonyl complexes.[26]

NHC-M bonds are typically strong and dissociation of NHC ligands is less common than for phosphine ligands.[27] In the $(CO)_3$Ni-L series, the Ni-L bond dissociation energy of most NHC ligands is >10 kcal/mol greater than that of even P^tBu_3.[28] The donor properties of an NHC ligand can be tuned through modification of the imidazole ring or the N substituents. Common variations include use of a saturated imidazolidine ring, which results in stronger σ-donor ability, and incorporation of amide units into the NHC ring, which strongly decrease the σ-donor ability. Alkyl or aryl groups may be incorporated on the N atoms for more subtle changes in the σ-donor ability (Figure 8).[29]

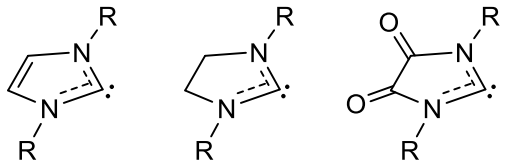

Figure 8. Common ring modifications of N-hetercyclic carbene ligands. R = alkyl or aryl.

1.3.2. Steric Properties of NHC Ligands

In phosphine complexes the substituents on P are two bonds removed from the metal center. The steric profile of a phosphine is well described by the Tolman cone angle, defined as the angle of the cone that circumscribes the phosphine (Figure 9).[30] In an NHC ligand, the substituents are three bonds removed from the metal center, and point toward the metal center, giving rise to an umbrella-like spatial profile. The steric properties of NHC ligands are not well characterized by a cone angle (θ), and are instead best described through the percent buried volume ($\%V_{bur}$), defined as the fraction of volume of a sphere around the metal that is occupied by the ligand.[31] This property allows the large substituents of an NHC to flank the sides of a metal center and has been exploited to isolate three- and even two- coordinate Ni complexes.[32]

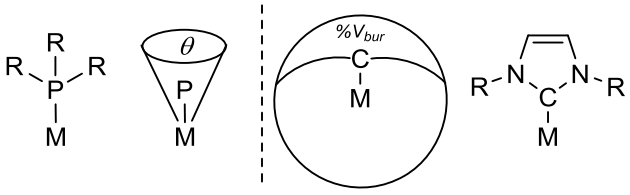

Figure 9. Steric properties of phosphine and NHC ligands.

Like phosphines, NHC ligands can be readily modified to access a wide range of steric properties, which is usually accomplished through tuning of the substituents on the imidazole N atoms (Figure 10).[33] Alkyl substituents ranging from methyl to adamantyl have been reported.

These groups typically have a small steric profile and allow for multiple NHC ligands to coordinate to a single metal center, in some cases up to four at once.[34] Aryl substituents are larger and more variable in size, and typically only one or two N,N-diaryl NHCs are able to coordinate to a metal center. Common aryl substituents include 2,4,6-dimethylphenyl (IMes),[35] di-*iso*propylphenyl (IPr),[36] and 2,6-bis(diphenylmethyl)-4-methylphenyl (IPr*).[37] The M-L bond dissociation energy (BDE) inversely correlates with the buried volume. In the (Cp*)(Cl)Ru(NHC) system, IMes has a BDE 4.5 kcal/mol higher than IPr, for percent buried volumes of 26 and 29% respectively.[38]

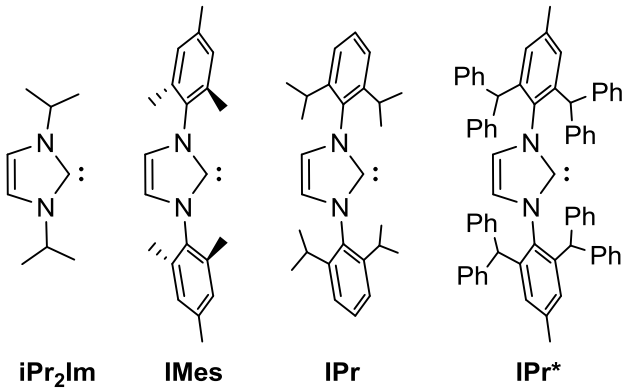

Figure 10. Common NHC ligands with progressively larger steric profiles.

1.3.3. NHC Ligand Synthesis

NHC ligands are easy to synthesize from commercially available building blocks. A typical NHC synthesis is accomplished through three steps (Scheme 2). First, a double condensation reaction with a primary amine and glyoxal produces an α-diimine. Second, a cyclization is accomplished through incorporation of formaldehyde in the presence of a strong acid, to produce an imidazolium salt. Third, the imidazolium salt is deprotonated by a strong base to generate the carbene.[39] In many cases the carbene can be isolated, although it is common to deprotonate *in situ* and immediately metallate with an appropriate metal precursor.

Scheme 2. General Synthesis of N-Heterocyclic Carbene Ligand

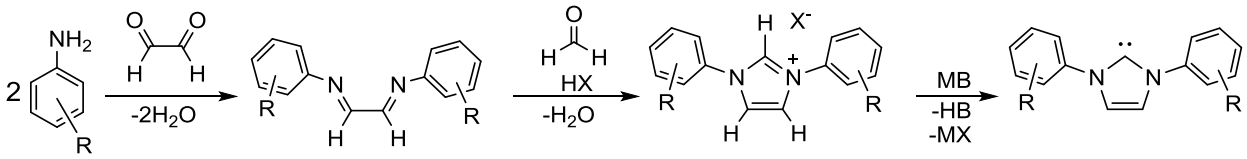

1.4. Thesis Objectives

There are two objectives for this thesis. The first objective is to use an (NHC)Ni scaffold to explore the chemistry of low-coordinate Ni complexes containing sulfur atoms in different binding modes. The second objective is to exploit these results to create a model system that can be used to study the activation of H_2 in the hydrodesulfurization process.

Chapter 2 describes the synthesis and reactivity of the dinuclear bridging disulfide complex $\{(IPr)ClNi\}_2(\mu^2\text{-}\eta^2,\eta^2\text{-}S_2)$. This complex can be converted to a mononuclear $(IPr)(AdNC)Ni(\eta^2\text{-}S_2)$ complex with a terminal disulfide, a dinuclear $\{(IPr)Ni(\mu\text{-}S)\}_2$ complex with two bridging sulfides, and a dinuclear $\{(IPr)Ni(\mu\text{-}SH)\}_2$ complex two bridging hydrosulfides. Most interestingly, the bridging sulfide and bridging hydrosulfide complexes are interconverted through reaction with H_2 and H-atom abstractor 2,4,6-^{t}Bu$_3$-phenoxy radical. In Chapter 3, the hydrogenation of $\{(IPr)Ni(\mu\text{-}S)\}_2$ to $\{(IPr)Ni(\mu\text{-}SH)\}_2$ is probed in depth through a combination of kinetic studies and DFT calculations. These results show that H_2 adds across a Ni-S bond in a heterolytic manner to generate a Ni(H)(μ-S)(μ-SH)Ni intermediate that rearranges to the product by H atom migration from Ni to the remaining μ-S ligand. Chapter 4 describes the reaction of $\{(IPr)Ni(\mu\text{-}S)\}_2$ with H-BPin to produce $\{(IPr)Ni\}_2(\mu\text{-}SH)(\mu\text{-}SBPin)$. This reaction suggests that heterolytic E-H bond activation by the $Ni_2(\mu\text{-}S)_2$ unit may be a general reaction.

1.5. References

(1) (a) Can, M.; Armstrong, F. A.; Ragsdale, S. W. *Chem. Rev.* **2014**, *114*, 4149. (b) Lubitz, W.; Ogata, H.; Rüdiger, O.; Reijerse, E. *Chem. Rev.* **2014**, *114*, 4081. (c) Boer, J. L.; Mulrooney, S. B.; Hausinger, R. P. *Arch. Biochem. Biophys.* **2014**, *544*, 142. (d) Majumdar, A. *Dalton Trans.* **2014**, *43*, 12135. (e) Huynh, M. T.; Schilter, D.; Hammes-Schiffer, S.; Rauchfuss, T. B. *J. Am. Chem. Soc.* **2014**, *136*, 12385. (f) Pinder, T. A.; Montalvo, S. K.; Hsieh, C.-H.; Lunsford, A. M.; Bethel, R. D.; Pierce, B. S.; Darensbourg, M. Y. *Inorg. Chem.* **2014**, *53*, 9095.

(2) (a) Ding, S.; Ghosh, P.; Lunsford, A. M.; Wang, N.; Bhuvanesh, N.; Hall, M. B.; Darensbourg, M. Y. *J. Am. Chem. Soc.* **2016**, *138*, 12920. (b) Schilter, D.; Camara, J. M.; Huynh, M. T.; Hammes-Schiffer, S.; Rauchfuss, T. B. *Chem. Rev.* **2016**, *116*, 8693. (c) Qiu, S.; Azofra, L. M.; MacFarlane, D. R.; Sun, C. *ACS Catal.* **2016**, *6*, 5541. (d) Ulloa, O. A.; Huynh, M. T.; Richers, C. P.; Bertke, J. A.; Nilges, M. J.; Hammes-Schiffer, S.; Rauchfuss, T. B. *J. Am. Chem. Soc.* **2016**, *138*, 9234. (e) Greene, B. L.; Wu, C.-H.; Vansuch, G. E.; Adams, M. W. W.; Dyer, R. B. *Biochemistry* **2016**, *55*, 1813. (f) Chambers, G. M.; Huynh, M. T.; Li, Y.; Hammes-Schiffer, S.; Rauchfuss, T. B.; Reijerse, E.; Lubitz, W. *Inorg. Chem.* **2016**, *55*, 419. (g) Lubitz, W.; Ogata, H.; Rüdiger, O.; Reijerse, E. *Chem. Rev.* **2014**, *114*, 4081.

(3) (a) Manesis, A. C.; Shafaat, H. S. *Inorg. Chem.* **2015**, *54*, 7959. (b) Wang, V. C.-C.; Islam, S. T. A.; Can, M.; Ragsdale, S. W.; Armstrong, F. A. *J. Phys. Chem. B* **2015**, *119*, 13690. (c) Horn, B.; Limberg, C.; Herwig, C.; Braun, B. *Inorg. Chem*. **2014**, *53*, 6867. (d) Oelgeschläger, E.; Rother, M. *Arch. Microbiol.* **2008**, 190, 257.

(4) (a) Bender, G.; Stich, T. A.; Yan, L.; Britt, R. D.; Cramer, S. P.; Ragsdale, S. W. *Biochemistry* **2010**, *49*, 7516. (b) Seravalli, J.; Ragsdale, S. W. *J. Biol. Chem*. **2008**, *283*, 8384. (c) Tan, X.; Martinho, M.; Stubna, A.; Lindahl, P. A.; Munck, E. *J. Am. Chem. Soc.* **2008**, *130*, 6712. (d) Seravalli, J.; Xiao, Y.; Gu, W.; Cramer, S. P.; Antholine, W. E.; Krymov, V.; Gerfen, G. J.; Ragsdale, S. W. *Biochemistry* **2004**, *43*, 3944. (e) Doukov, T. I.; Iverson, T.; Seravalli, J.; Ragsdale, S. W.; Drennan, C. L. *Science* **2002**, *298*, 567. (f) Shin, W.; Anderson, M. E.; Lindahl, P. A. *J. Am. Chem. Soc.* **1993**, *115*, 5522. (g) Shin, W.; Lindahl, P. A. *Biochemistry* **1992**, *31*, 12870. (h) Ragsdale, S. W.; Wood, H. G.; Antholine, W. E. *Proc. Natl. Acad. Sci. U. S. A.* **1985**, *82*, 6811.

(5) (a) Kure, B.; Sano, M.; Nakajima, T.; Tanase, T. *Organometallics* **2014**, *33*, 3950. (b) Kure, B.; Nakajima, T.; Tanase, T. *J. Organomet. Chem.* **2013**, *733*, 28. (c) Kure, B.; Taniguchi, A.; Nakajima, T.; Tanase, T. *Organometallics* **2012**, *31*, 4791. (d) Niu, S.; Zhang, Z.; Xu, J.; Zhang, H.; Xin, Q.; Wei, *Z. Cuihua Xuebao* **1995**, *16*, 464.

(6) Kuiper, J. L.; Shapley, P. A.; Rayner, C. M. *Organometallics* **2004**, *23*, 3814.

(7) Datta, S.; Seth, D. K.; Butcher, R.; Bhattacharya, S. *Inorg. Chim. Acta.* **2011**, *377*, 120.

(8) Takei, I.; Wakebe, Y.; Suzuki, K.; Enta, Y.; Suzuki, T.; Mizobe, Y.; Hidai, M. *Organometallics* **2003**, *22*, 4639.

(9) (a) Beletskaya, I. P.; Ananikov, V. P. *Chem. Rev.* **2011**, *111*, 1596. (b) Ito, M.; Kotera, M.; Matsumoto, T.; Tatsumi, K. *Proc. Natl. Acad. Sci. U.S.A.* **2009**, *106*, 11862.

(10) Rampersad, M. V.; Zuidema, E.; Ernsting, J. M.; van Leeuwen, P. W. N. M.; Darensbourg, M. Y. *Organometallics* **2007**, *26*, 783.

(11) Curtis, M. D.; Schwank, J.; Thompson, L. T.; Williams, P. D. U.S. Patent 4,605,751, Aug 12, **1986**.

(12) Nguyen, N. T.; Mori, Y.; Matsumoto, T.; Yatabe, T.; Kabe, R.; Nakai, H.; Yoonac, K.-S.; Ogo, S. *Chem. Commun.* **2014**, *50*, 13385.

(13) (a) Jiang, J.; Goa, M.; Sheng, W.; Yan, Y. *Angew. Chem. Int. Ed.* **2016**, *55*, 15240. (b) Kong, C.; Min, S.; Lu, G. *ACS Catalysis* **2014**, *4*, 2763.

(14) (a) Gutiérrez, O.; Singh, S.; Schachtl, E.; Kim, J.; Kondratieva, E.; Hein, J.; Lercher, J. A. *ACS Catalysis* **2014**, *4*, 1487. (b) Robbie, A.; Cowley, A. R.; Jones, M. W.; Dilworth, J. R. *Polyhedron* **2011**, *30*, 1849. (c) Torres-Nieto, J.; Brennessel, W. W.; Jones, W. D.; Garcia, J. J. *J. Am. Chem. Soc.* **2009**, *131*, 4120. (d) Vicic, D. A.; Jones, W. D. *J. Am. Chem. Soc.* **1999**, *121*, 4070. (e) Vicic, D. A.; Jones, W. D. *J. Am. Chem. Soc.* **1999**, *121*, 7606.

(15) (a) Kabe, T. *Hydrodesulfurization and Hydrodenitrogenation: Chemistry and Engineering*; Wiley-VCH: New York, **1999**. (b) Topsøe, H.; Clausen, B. S.; Massoth, F. E. Hydrotreating Catalysis, Science and Technology.; Springer-Verlag: Berlin, **1996**.

(16) (a) Wen, X. D.; Zeng, T.; Tend, B. T.; Zhang, F.-Q.; Li, Y. W.; Wang, J.; Jiao, H. *J. Mol. Catal. A: Chem.* **2006**, *249*, 191. (b) Cristol, S.; Paul, J. F.; Payen, E.; Bougeard, D.; Clémendot, S.; Hutschka, F. *J. Phys. Chem. B* **2002**, *106*, 5659. (c) Hwang, D. Y.; Mebel, A. M. *J. Phys. Chem. A* **2002**, 106, 520. (d) Alexiev, V.; Prins, R.; Weber, Th. *Phys. Chem. Chem. Phys.* **2001**, *3*, 5326. (e) Cristol, S.; Paul, J. F.; Payen, E.; Bougeard, D.; Clémendot, S.; Hutschka, F. *J. Phys. Chem. B* **20**, *104*, 11220. (f) Neurock, M.; van Santen, R. A. *J. Am. Chem. Soc.* **1994**, *116*, 4427.

(17) (a) Breysse, M.; Furimsky, E. *Catal. Rev.* **2002**, *44*, 651. (b) Lacroix, M.; Yuan, S.; Breysse, M.; Dorémieux-Morin, C.; Fraissard, J. *J. Catal.* **1992**, *138*, 409.

(18) (a) Diaz de León, J. N. *Applied Catalysis B: Environmental* **2016**, *181*, 524. (b) Rangarajan, S.; Mavrikakis, M. *AIChE Journal* **2015**, *61*, 4036. (c) Sigurdson, S.; Dalai, A. K.; Adjaye, J. *Can. J. Chem. Eng.* **2011**, *89*, 562. (d) Hein, J.; Gutiérrez, O. Y.; Schachtl, E.; Xu, P.; Browning, N. D.; Jentys, A.; Lercher, J. A. *ChemCatChem* **2015**, *7*, 3692.

(19) (a) Lopez, L. L.; Godziela, G.; Rakowski DuBois, M. *Organometallics* **1991**, *10*, 2660. (b) Bernatis, P.; Laurie, J. C. V.; Rakowski DuBois, M. *Organometallics* **1990**, *9*, 1607. (c) Weberg, R. T.; Haltiwanger, R. C.; Laurie, J. C. V.; Rakowski DuBois, M. *J. Am. Chem. Soc*. **1986**, *108*, 6242. (d) Laurie, J. C. V.; Duncan, L.; Haltiwanger, R. C.; Weberg, R. T.; Rakowski DuBois, M. *J. Am. Chem. Soc.* **1986**, *108*, 6234. (e) McKenna, M.; Wright, L. L.; Miller, D. J.; Tanner, L.; Haltiwanger, R. C.; Rakowski DuBois, M. *J. Am. Chem. Soc.* **1983**, *105*, 5329.

(20) (a) Appel, A. M.; Lee, S.-J.; Franz, J. A.; DuBois, D. L.; DuBois, M. R. *J. Am. Chem. Soc.* **2009**, *131*, 5224. (b) Appel, A. M.; Lee, S.-J.; Franz, J. A.; DuBois, D. L.; Rakowski DuBois, M.; Twamley, B. *Organometallics* **2009**, *28*, 749. (c) Appel, A. M.; Lee, S.-J.; Franz, J. A.; DuBois, D. L.; Rakowski DuBois, M.; Birnbaum, J. C.; Twamley, B. *J. Am. Chem. Soc.* **2008**, *130*, 8940. (d) Bursten, B. E.; Cayton, R. H. *Inorg. Chem.* **1989**, *28*, 2846. (e) Casewit, C. J.; Coons, D. E.; Wright, L. L.; Miller, W. K.; Rakowski DuBois, M. *Organometallics* **1986**, *5*, 951.

(21) (a) Ienco, A.; Calhorda, M. J.; Reinhold, J.; Reineri, F.; Bianchini, C.; Peruzzini, M.; Vizza, F.; Mealli, C. *J. Am. Chem. Soc.* **2004**, *126*, 11954. (b) Bianchini, C.; Mealli, C.; Meli, A.; Sabat, M. *Inorg. Chem.* **1986**, *25*, 4617.

(22) (a) Rauchfuss, T. B. *Inorg. Chem*. **2004**, *43*, 14. (b) Linck, R. C.; Pafford, R. J.; Rauchfuss, T. B. *J. Am. Chem. Soc.* **2001**, *123*, 8856. (c) Mueting, A. M.; Boyle, P. D.; Wagner, R.; Pignolet, L. H. *Inorg. Chem.* **1988**, *27*, 271.

(23) (a) Mindiola, D. J.; Waterman, R.; Iluc, V. M.; Cundari, T. R.; Hillhouse, G. L. *Inorg. Chem.* **2014**, *53*, 13227. (b) Iluc, V. M.; Hillhouse, G. L. *J. Am. Chem. Soc.* **2014**, *136*, 6479. (c) Iluc, V. M.; Miller, A. J. M.; Anderson, J. S.; Monreal, M. J.; Mehn, M. P.; Hillhouse, G. L. *J. Am. Chem. Soc.* **2011**, *133*, 13055. (d) Iluc, V. M.; Hillhouse, G. L. *J. Am. Chem. Soc.* **2010**, *132*, 15148. (e) Harrold, N. D.; Waterman, R.; Hillhouse, G. L.; Cundari, T. R. *J. Am. Chem. Soc.* **2009**, *131*, 12872. (f) Waterman, R.; Hillhouse, G. L. *J. Am. Chem. Soc.* **2008**, *130*, 12628. (g) Waterman, R.; Hillhouse, G. L. *J. Am. Chem. Soc.* **2003**, *125*, 13350. (h) Mindiola, D. J.; Hillhouse, G. L. *Chem. Commun.* **2002**, 1840. (i) Mindiola, D. J.; Hillhouse, G. L. *J. Am. Chem. Soc.* **2002**, *124*, 9976. (j) Mindiola, D. J.; Hillhouse, G. L. *J. Am. Chem. Soc*. **2001**, *123*, 4623.

(24) (a) Przyojski, J. A.; Veggeberg, K. P.; Arman, H. D.; Tonzetich, Z. J. *ACS Catal.* **2015**, *5*, 5938. (b) Przyojski, J. A.; Arman, H. D.; Tonzetich, Z. J. *Organometallics* **2013**, *32*, 723. (c) Diez-Gonzalez, S.; Marion, N.; Nolan, S. P. *Chem. Rev.* **2009**, 109, 3612. (d) Hahn, F. E.; Jahnke, M. C. *Angew. Chem. Int. Ed.* **2008**, 47, 3122. (e) Scholl, M.; Ding, S.; Lee, C. W.; Grubbs, R. H. *Org. Lett.* **1999**, *1*, 953.

(25) (a) Fillman, K. L.; Przyojski, J. A.; Al-Afyouni, M. H.; Tonzetich, Z. J.; Neidig, M. L. *Chem. Sci.* **2015**, 6,1178. (b) Fantasia, S.; Peterson, J. L.; Jacobsen, H.; Cavallo, L.; Nolan, S. P. *Organometallics* **2007**, *26*, 5880. (c) Nemcsok, D.; Wichmann, K.; Frenking, G. *Organometallics* **2004**, *23*, 3640. (d) Heinemann, C.; Müller, T.; Apeloig, Y.; Schwarz, H. *J. Am. Chem. Soc.* **1996**, *118*, 2023. (e) Boehme, C.; Frenking, G. *J. Am. Chem. Soc.* **1996**, *118*, 2039.

(26) Kocher, C.; Herrmann, W. A. *J. Organomet. Chem*. **1997**, *532*, 261.

(27) (a) Frémont, P.; Marion, M.; Nolan, S. P. *Coord. Chem. Rev.* **2009**, *253*, 862. (b) Diez-Gonzalez, S.; Nolan, S. P. *Coord. Chem. Rev.* **2007**, *251*, 874.

(28) Glorius, F. *N-Heterocyclic Carbenes in Transition Metal Catalysis (Topics in Organometallic Chemistry)*; Springer: New York, **2007.**

(29) Hopkinson, M. N.; Richter, C.; Schedler, M.; Glorius, F. *Nature*, **2014**, *510*, 485.

(30) (a) Ferguson, G.; Roberts, P. J.; Alyea, E. C.; Khan, M. *Inorg. Chem.* **1978**, *17*, 2965. (b) Tolman, C. A. *Chem. Rev.* **1977**, *77*, 313. (c) Tolman, C. A.; Seidel, W. C.; Gosser, L. W. *J. Am. Chem. Soc.* **1974**, *96*, 523. (d) Tolman, C. A. *J. Am. Chem. Soc.* **1970**, *92*, 2956.

(31) Cavallo, L.; Correa, A.; Costabile, C.; Jacobsen, H. *J. Organomet. Chem.* **2005**, *690*, 5407.

(32) (a) Zhai, J.; Filatov, A. S.; Hillhouse, G. L.; Hopkins, M. D. *Chem. Sci.* **2016**, *7*, 589. (b) Zhai, J.; Hopkins, M. D.; Hillhouse, G. L. *Organometallics* **2015**, *34*, 4637. (c) Hansen, C. B.;

Jordan, R. F.; Hillhouse, G. L. *Inorg. Chem*. **2015**, *54*, 4603. (d) Harrold, N. D.; Hillhouse, G. L. *Chem. Sci*. **2013**, *4*, 4011. (e) Laskowski, C. A.; Miller, A. J. M.; Hillhouse, G. L.; Cundari, T. R. *J. Am. Chem. Soc.* **2011**, *133*, 771. (f) Iluc, V. M.; Laskowski, C. A.; Hillhouse, G. L. *Organometallics* **2009**, *28*, 6135.

(33) (a) Niehues, M.; Kehr, G.; Erker, G.; Wibbeling, B.; Fröhlich, R.; Blacque, O.; Berke, H. *J. Organomet. Chem.* **2002**, *663*, 192. (b) Arduengo, A. J.; Bock, H.; Chen, H.; Denk, M.; Dixon, D. A.; Green, J. C.; Herrmann, W. A.; Jones, N. L.; Wagner, M.; West, R. *J. Am. Chem. Soc.* **1994**, 116, 6641. (c) Berthon-Gelloz, G.; Siegler, M. A.; Spek, A. L.; Tinant, B.; Reek, J. N. H.; Marko, I. E. *Dalton Trans.* **2010**, *39*, 1444. (d) Arduengo, A. J.; Krafczyk, R.; Schmutzler, R. *Tetrahedron* **1999**, *55*, 14523.

(34) Findlay, N. J.; Park, S. R.; Schoenebeck, F.; Cahard, E.; Zhou, S.; Berlouis, L. E. A.; Spicer, M. D.; Tuttle, T.; Murphy, J. A. *J. Am. Chem. Soc.* **2010**, 132, 15462.

(35) Arduengo, A. J.; Dias, H. V. R.; Harlow, R. L.; Kline, M. *J. Am. Chem. Soc.* **1992**, *114*, 5530.

(36) Bohm, V. P. W.; Gstottmayr, C. W. K.; Weskamp, T.; Herrmann, W. A. *Angew. Chem. Int. Ed*. **2001**, *40*, 3387.

(37) Berthon-Gelloz, G.; Siegler, M. A.; Spek, A. L.; Tinant, B.; Reek, J. N. H.; Marko, I. E. *Dalton Trans.* **2010**, *39*, 1444.

(38) Jacobsen, H.; Correa, A.; Poater, A.; Costabile, C.; Cavallo, L. *Coord. Chem. Rev*. **2009**, *253*, 687.

(39) (a) Ref. 37. (b) Arduengo, A. J.; Goerlich, J. R.; Marshall, W. J. *J. Am. Chem. Soc.* **1995**, *117*, 11027. (c) Fehlhammer, W. P.; Bliss, T.; Kernbach, U.; Brüdgam, I. *J. Organomet. Chem.* **1995**, 490, 149.

Chapter 2 - Synthesis and Reactivity of NHC-Supported $Ni_2(\mu^2\text{-}\eta^2,\eta^2\text{-}S_2)$ Bridging Disulfide and $Ni_2(\mu\text{-}S)_2$ Bridging Sulfide Complexes

2.1. Introduction

Nickel complexes bearing sulfur-based ligands, particularly bridging thiolate (μ-SR) and bridging sulfide (μ-S) species, have received much interest because of their important roles in homogenous C-S coupling reactions, hydrodesulfurization processes, and small molecule activation chemistry, and their prevalence in enzyme active sites. Ni compounds supported by bridging thiolate and sulfide ligands are catalytically active for a wide variety of reactions, including hydrogenations of aldehydes, Suzuki coupling, thioesterification, ring cyclization reactions, and copolymerization of CO with ethylene.[40] Heterogeneous Ni-sulfide catalysts for hydrodesulfurization, hydrodenitrogenation, and the photocatalytic production of H_2 from water have also been studied intensively.[41] In the active sites of Nickel CO Dehydrogenase, Hydrogenase, and Acetyl-CoA synthase enzymes, nickel atoms are surrounded by μ-S and μ-SR ligands that are vital for small molecule activation and electron transfer reactions. Model complexes for those active sites have been investigated in depth.[42]

Dinuclear Ni complexes with two bridging thiolate or sulfide ligands, $L_nNi_2(\mu\text{-}SR)_2$ and $L_nNi_2(\mu\text{-}S)_2$ respectively, have been prepared and characterized (Chart 1).[43,44] Bridging sulfide species can be interconverted with bridging disulfide compounds $L_nNi_2(\mu^2\text{-}\eta^2,\eta^2\text{-}S_2)$ by oxidation and reduction.[45] Two additional binding modes have been observed for Ni-disulfide species, the $L_nNi_2(\mu^2\text{-}\kappa^1,\kappa^1\text{-}S_2)$[46] bridging motif and the $L_nNi(\eta^2\text{-}S_2)$ terminal structure.[47] Related $L_nNi(\eta^2$-supersulfido) species are also known.[4845] These three latter motifs exhibit limited thermal stability and little is known about the reactivity of these compounds.

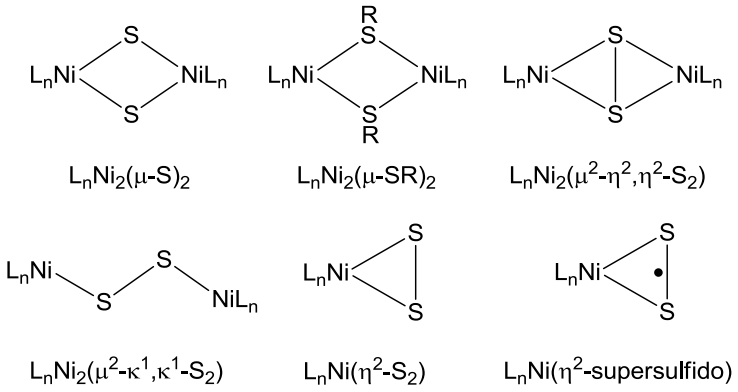

Chart 1. Ni-disulfides and related complexes. $L_nNi_2(\mu\text{-}SR)_2$ complexes may have a Ni-Ni bond.

The $L_nNi_2(\mu^2\text{-}\eta^2,\eta^2\text{-}S_2)$ motif has been observed for a variety of L_n ligand manifolds, including bidentate phosphines and diketiminates, tridentate phosphines and thioethers, and tetradentate aryl and alkyl amines. $L_nNi_2(\mu^2\text{-}\eta^2,\eta^2\text{-}S_2)$ complexes can be synthesized by several pathways, which are shown schematically in Scheme 3, including: (i) salt metathesis of Ni^{II} salts and alkali metal M_2S_2 reagents; (ii) reaction of L_nNi^{I} complexes with S_8; (iii) two-electron oxidation of $L_nNi^{II}(\eta^2\text{-}S_2)$ or $L_nNi_2(\mu\text{-}S)_2$ complexes; (iv) abstraction of S from supersulfido $L_nNi(\eta^2\text{-}S_2)$ complexes by PPh_3, followed by dimerization; (v) reaction of a supersulfido $L_nNi(\eta^2\text{-}S_2)$ complex with an L_nNi^{I} complex; and (vi) thermally driven homolytic cleavage of an $L_nNi^{II}S\text{-}CPh_3$ bond and subsequent dimerization. The only reported reaction of an $L_nNi_2(\mu^2\text{-}\eta^2,\eta^2\text{-}S_2)$ species is the reduction of $[\{(dippnapht)Ni\}_2(\mu^2\text{-}\eta^2,\eta^2\text{-}S_2)]^{2+}$ (**A**, dippnapht = 1,8-bis(diisopropylphosphino)-naphthalene, Chart 2) by KC_8 to generate the bridging sulfide complex $\{(dippnapht)Ni(\mu\text{-}S)\}_2$ (**E**, Chart 2).[44a] This reaction shows that in this case the S_2^{2-} unit rather than the Ni^{2+} centers is the site of reduction.

Scheme 3. Synthesis of $Ni_2(\mu^2\text{-}\eta^2,\eta^2\text{-}S_2)$ Complexes.

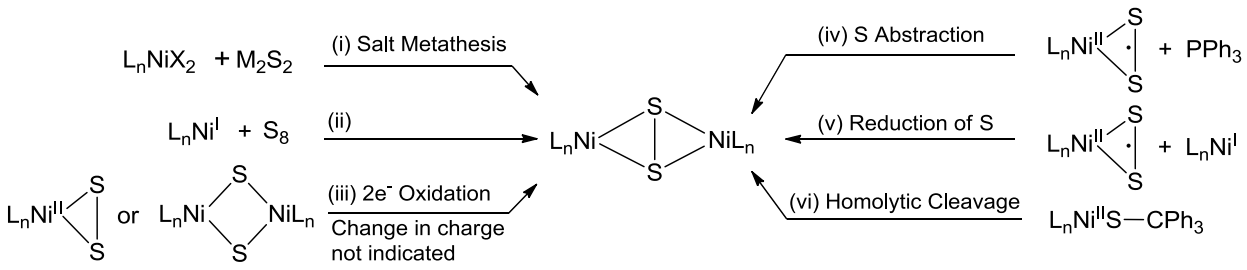

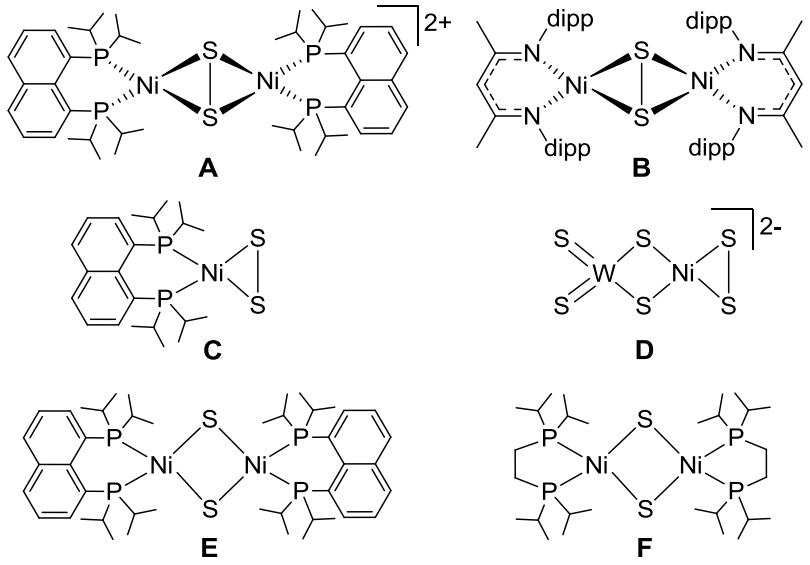

dipp = 2,6-$^{i}Pr_2Ph$

Chart 2. Structural analogues of compounds studied in this chapter.

The objective of this works is to identify an ancillary ligand set that enables synthesis of complexes with a variety of Ni-S binding motifs and studies of their reactivity. We report the synthesis of $\{(IPr)ClNi\}_2(\mu^2\text{-}\eta^2,\eta^2\text{-}S_2)$ (**2**), a bridging disulfide complex supported by a monodentate N-heterocyclic carbene ligand (IPr = 1,3-bis(2,6-diisopropylphenyl)imidazolin-2-ylidene). We also describe the reaction of **2** with isocyanides to produce the terminal disulfide compound $(IPr)(RNC)Ni(\eta^2\text{-}S_2)$ (**3**), and the two-electron reduction of **2** to produce the bridging sulfide species $\{(IPr)Ni(\mu\text{-}S)\}_2$ (**6**). Hydrogenation of $\{(IPr)Ni(\mu\text{-}S)\}_2$ (**6**) yields the bridging

hydrosulfide complex {(IPr)Ni(μ-SH)}$_2$ (**7**), which is converted back to **6** by hydrogen atom abstraction by a phenoxy radical.

2.2. {(IPr)Ni(μ-Cl)}$_2$ as a starting compound

The NHC ligand IPr (1,3-di(2,6-di-*iso*-propylphenyl)imidazolin-2-ylidene) has a percent buried volume of 29%,[49] and this steric profile has been exploited to stabilize 3-coordinate Ni species.[50] The imidazolium chloride salt [IPrH]Cl is commercially available or can be synthesized on >30 gram scale from commercially available di-*iso*-propylaniline.[51]

The free IPr ligand has C_{2V} symmetry, with a C_2 axis that bisects the central imidazole ring through the carbene C. In (PDI)$FeCl_2$ (PDI = 2,6-bis(2,6-di-*iso*-propylphenyl)pyridine), rotation around the N-dipp bond (dipp = 2,6-di-*iso*-propylphenyl) is restricted, with a barrier of 24.0(1) kcal/mol at 298 K.[52] A similar barrier is expected for N-dipp bond rotation in free IPr and in IPr complexes. In free IPr, all four isopropyl groups are equivalent by symmetry on the NMR time scale, and all four methine protons appear as a single resonance in the ^{1}H NMR spectrum (Figure 11). The two methyl groups within a given isopropyl group are inequivalent, and at 298 K two ^{1}H NMR resonances integrating for 12 H each are observed for the methyl groups. These results indicate that the C_{2V} symmetry is maintained in solution. Therefore, the number of methyl and methine resonances observed can be used to identify which symmetry elements are present in IPr complexes.

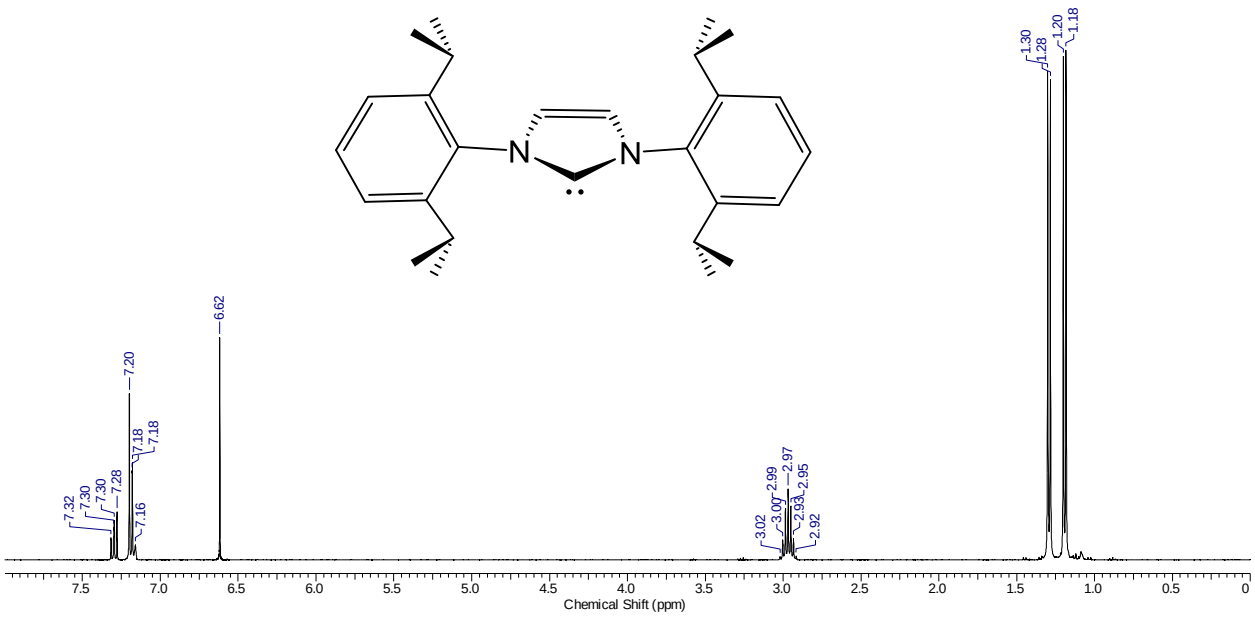

Figure 11. ^{1}H NMR spectrum of free IPr, taken in C_6D_6 at 298 K.

Only a few simple IPr-Ni complexes that could serve as a starting material for the synthesis of low coordinate IPrNi complexes with S-based ligands have been reported. The most versatile is the dinuclear complex {IPrNi(μ-Cl)}$_2$ (**1**),[53] with others including (IPr)Ni(CO)$_n$ (n = 2, 3) and (IPr)Ni(C_3H_7)(Cl).[54] Complex **1** can be synthesized from commercially available Ni(cod)$_2$ and (dme)NiCl$_2$ in a comproportionation reaction (Scheme 4) and isolated in 70% yield in gram scale quantities by recrystallization from the reaction mixture.

Scheme 4. Synthesis of {IPrNi(μ -Cl)}$_2$ (**1**).

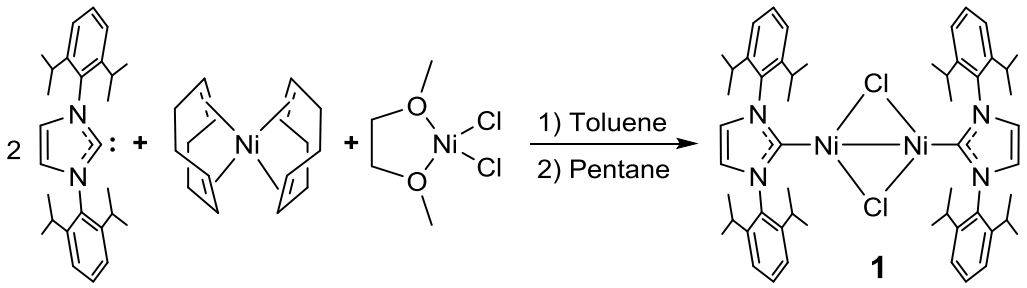

Complex **1** is a d^9-d^9 antiferromagnetically coupled dimer with a diamagnetic ^{1}H NMR spectrum (Figure 12). The central Ni_2Cl_2 core is planar and diamond-shaped, and in the solid state the complex has C_{2V} symmetry. Rotation around the Ni-NHC bond is expected to be fast on the NMR time scale based on VT NMR studies of Pd-NHC complexes. For example, the barrier to rotation around the Pd-NHC bond in (N-butyl, N-(4-methylbenzyl)-NHC*)Pd(Cl)(η^3-allyl) is only 14 kcal/mol.[55] Consistent with this expectation, the ^{1}H NMR spectrum of **1** contains two methyl resonances and one methine resonance, indicative of time-averaged C_{2V} symmetry in solution.

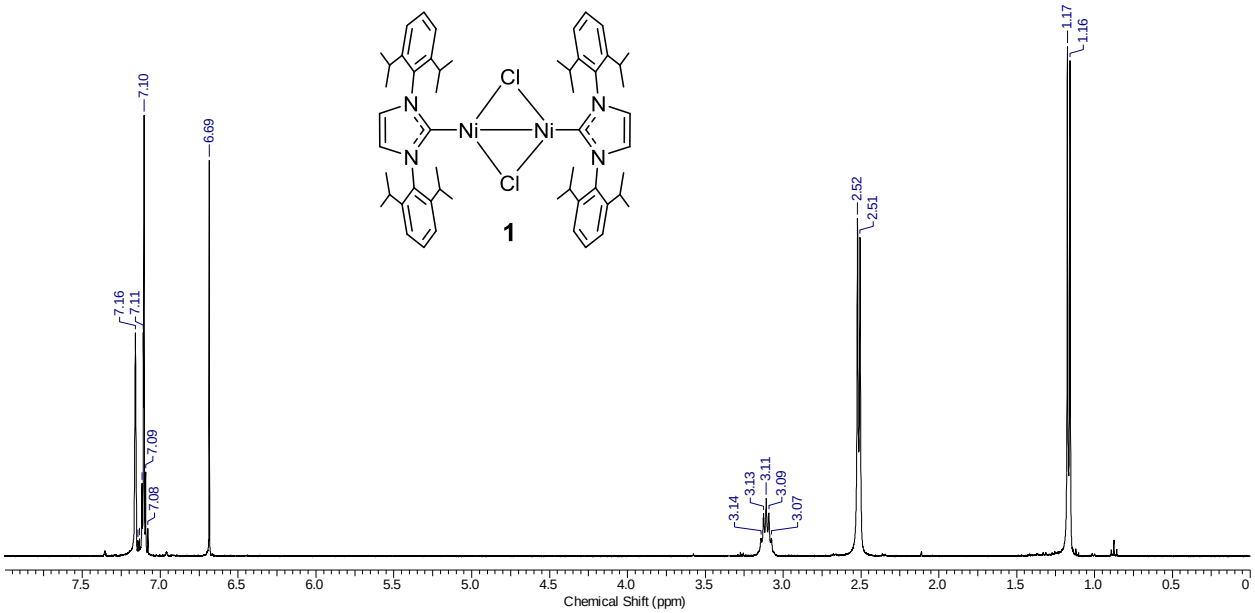

Figure 12. ^{1}H NMR spectrum of {IPrNi(μ-Cl)}$_2$ (**1**), taken in C_6D_6 at 298 K.

2.3. Results and Discussion

2.3.1 Synthesis and structure of {(IPr)ClNi}$_2$(μ^2-η^2,η^2-S_2) (2).

The reaction of {(IPr)Ni(μ-Cl)}$_2$ (**1**) with S_8 in THF affords the bridging disulfide complex {(IPr)ClNi}$_2$(μ^2-η^2,η^2-S_2) (**2**, Scheme 5). Complex **2** was isolated as a dark green powder in 72%

yield by precipitation from the reaction mixture with pentane. No intermediates or other products were observed by ^{1}H NMR. Complex **2** does not react further with S_8 under these conditions. Complex **2** is thermally stable up to 90 °C, at which temperature it decomposes to the known thiourea IPr=S and uncharacterized Ni products.[56]

Scheme 5.

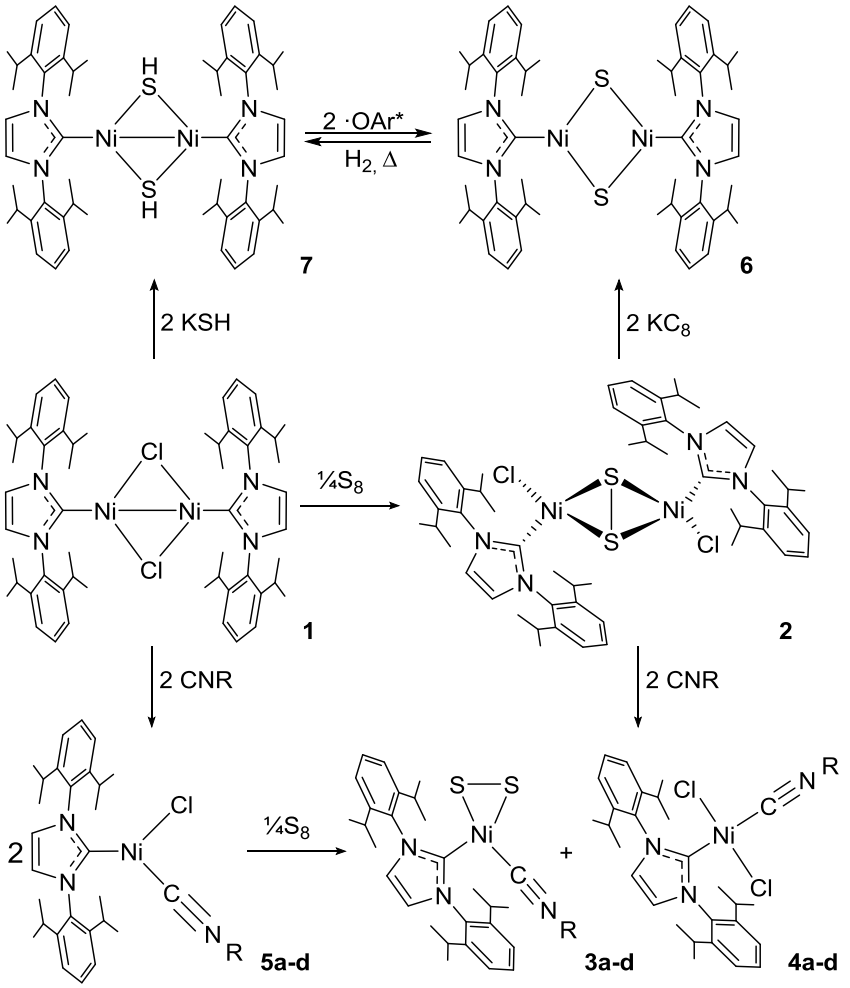

R = Ad (**a**), ^{t}Bu (**b**), *o*-xylyl (**c**), *p*-MeO-Ph (**d**)

Ar* = 2,4,6-^{t}Bu$_3$-Ph

Careful layering of pentane on to a solution of **2** in Et_2O at -35 °C yields X-ray quality crystals. The solid-state structure of **2** is shown in Figure 13. The two Ni centers adopt

distorted square planar geometries, the principal distortion being the acute S-Ni-S angles (S1-Ni1-S2 = 55.15(11)°; S1-Ni2-S2 = 55.63(11)°). The two square planes share an edge that is composed of the S_2^{2-} moiety, forming a butterfly structure which breaks both planes of symmetry from the IPr ligand. Complex **2** has overall approximate C_2 symmetry, where the C_2 axis bisects the S-S bond. The imidazolin-2-ylidene rings are rotated from the corresponding Ni square planes by 51.43(4)° and 52.05(5)°. The dihedral angle between the two Ni square planes is 107.97(11)° and the distance between the two nickel atoms is 3.098(2) Å, beyond the limit of a significant Ni-Ni interaction.[57] The distance between the two sulfur atoms is 2.011(4) Å, consistent with a single bond.[58] The Ni-S distances involving the sulfur atoms that are *trans* to the NHC ligands are ca. 0.06 Å longer than those involving the sulfur atoms that are *trans* to the chloride ligands, consistent with the larger *trans* influence and stronger σ-donor properties of the NHC ligands compared to the Cl^- ligand.[59]

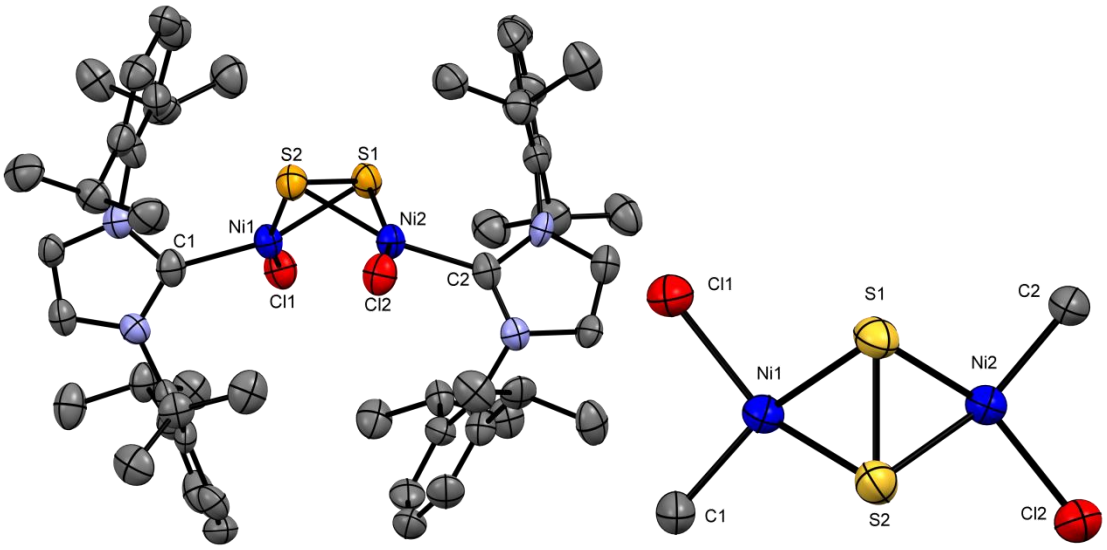

Figure 13. (a) Molecular structure of $\{(IPr)ClNi\}_2(\mu^2\text{-}\eta^2,\eta^2\text{-}S_2)$ (**2**). Hydrogen atoms are omitted. (b) View of core atoms from above, showing pseudo-square planar geometry at each Ni center. Selected bond distances (Å) and angles (°): Ni(1)-Ni(2) = 3.098(2), S(1)-S(2) = 2.011(4), Ni(1)-S(1) = 2.198(3), Ni(1)-S(2) = 2.143(3), Ni(2)-S(1) = 2.123(3), Ni(2)-S(2) = 2.184(3), Ni(1)-C(1) = 1.893(10), Ni(2)-C(2) = 1.891(10), Ni(1)-Cl(1) = 2.156(3), Ni(2)-Cl(2) = 2.143(3); Ni(1)-S(1)-Ni(2) = 91.58(11), Ni(1)-S(2)-Ni(2) = 91.43(12), S(1)-Ni(1)-S(2) = 55.15(11), S(1)-Ni(1)-Cl(1) =

100.73(12), S(2)-Ni(1)-C(1) = 106.1(3), C(1)-Ni(1)-Cl(1) = 96.1(3), S(1)-Ni(2)-S(2) = 55.63(11), S(2)-Ni(2)-Cl(2) = 101.14(12), S(1)-Ni(2)-C(2) = 106.6(3), C(2)-Ni(2)-Cl(2) = 95.5(3).

The ^{1}H NMR spectrum of **2** contains four methyl reosnances and two methine resonances for the isopropyl groups, indicative of C_2 symmetry on the NMR time scale (Figure 14). This result is consistent with the solid state structure and fast Ni-C bond rotation.

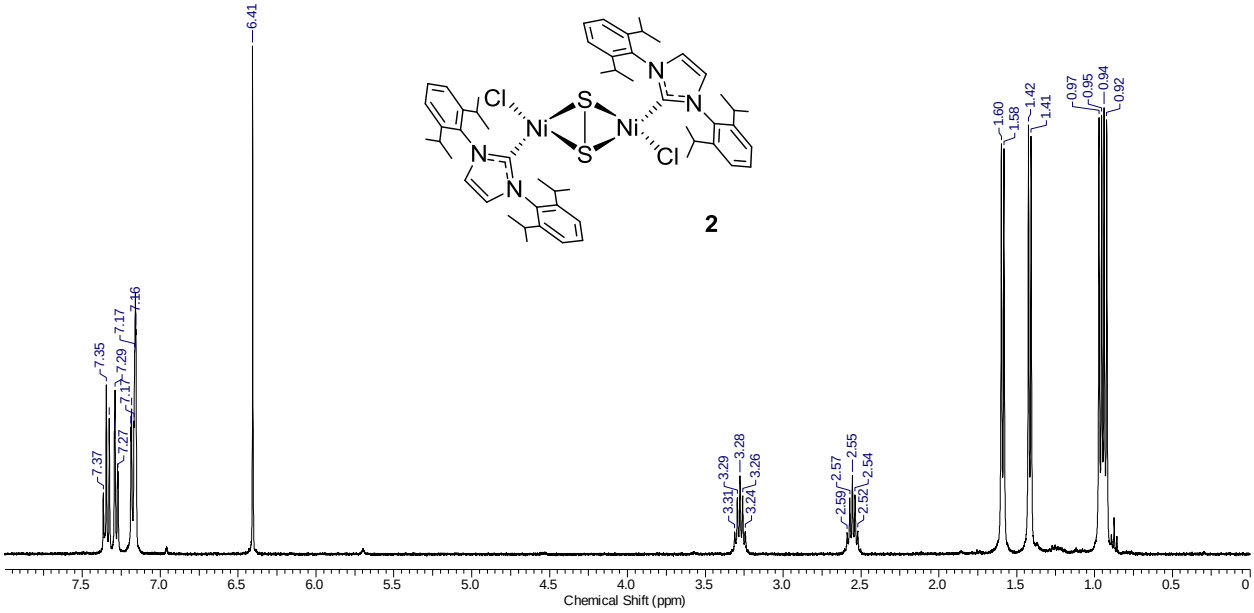

Figure 14. ^{1}H NMR spectrum of {(IPr)ClNi}$_2$(μ^2-η^2,η^2-S_2) (**2**), taken in C_6D_6 at 298 K.

Two close structural analogues of **2**, {(dippnapht)Ni}$_2$(μ^2-η^2,η^2-S_2) (**A**)[44a] and {(dipp-nacnac)Ni}$_2$(μ^2-η^2,η^2-S_2) (**B**, dipp-nacnac = CH{(CMe)(N-2,6-$^{i}Pr_2C_6H_3$)}$_2$),[45c] have been reported (Chart 2). The Ni_2S_2 core of **2** is more contracted than those of **A** or **B**. The S-S distance of **2** is ca. 0.040 Å shorter than those in **A** and **B**, the Ni-S distances *trans* to IPr in **2** fall in between the Ni-S distances in **A** and **B**, and the Ni-S distances *trans* to chloride in **2** are the shortest overall. Additionally, the dihedral angle between the Ni-S-S-Ni planes of **2** is 4.25° and 25.96° smaller, and the Ni-Ni distance in **2** is ca. 0.14 Å and 0.50 Å shorter than the corresponding values for **A**

and **B**. Examination of spacefilling models for **A** and **B** shows that the ^{i}Pr and dipp substituents on the P and N donor atoms on opposite sides of the molecule are in close contact, suggesting that steric repulsion between these groups results in the expansion and flattening of their Ni_2S_2 cores (Figure 15). In contrast, the dipp substitutents in **2** are located on the flanking N atoms rather than the donor C atom. Examination of a spacefilling model for **2** reveals less crowding around the Ni centers and a small gap between the two IPr ligands, indicative of little steric crowding between them. These comparisons suggest that the more compact structure of **2** is electronically preferred.

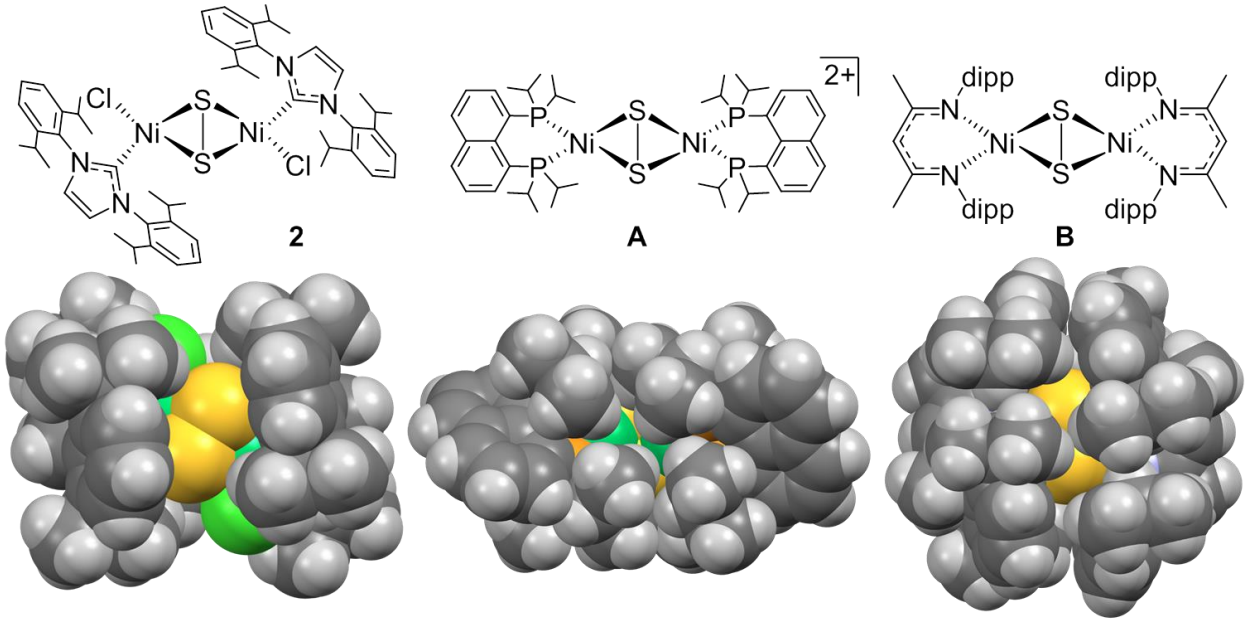

Figure 15. Spacefilling models of $Ni_2(\mu^2\text{-}\eta^2,\eta^2\text{-}S_2)$ disulfide complexes **2**, **A**, and **B**, showing the available volume around each Ni_2S_2 core.

2.3.2 Reaction of {(IPr)ClNi}$_2$(μ^2-η^2,η^2-S_2) (2) with isocyanides.

Complex **2** reacts with 2 equiv of adamantyl isocyanide (AdNC) in Et_2O to afford a 1:1 mixture of (IPr)(AdNC)Ni(η^2-S_2) (**3a**) and *trans*-(IPr)(AdNC)$NiCl_2$ (**4a**, Scheme 5). No intermediates were observed by ^{1}H NMR. **3a** was selectively precipitated from the reaction mixture by addition of pentane and isolated in 88% yield, and **4a** was isolated subsequently

from the filtrate in 76% yield. Close control of stoichiometry is required to obtain clean conversion of **2** to **3a** and **4a** because the product mixture reacts further with AdNC to yield free IPr, $Ni(CNAd)_4$, and other products.

Careful layering of pentane on to a solution of **3a** in Et_2O at -35 °C yields X-ray quality crystals (Figure 16). In the solid state, **3a** adopts an approximate square planar geometry, with the principal distortion being the acute S-Ni-S angle of 58.92(7)°. The imidazolin-2-ylidene ring is rotated from the Ni square plane by 41.9(6)° and the isocyanide is slightly bent away from the IPr ligand with a Ni-C-N angle of 171.3(5)° due to steric interference between these groups. The S-S distance (2.113(2) Å) is 0.1 Å longer than that in **2** but still consistent with a single bond. Two close structural analogues of **3a** exist, one supported by a dippnapht ligand (**C**),[44a] and the other by a chelating tetrathiotungstate ligand (**D**, Chart 2).[47b] The structures of the Ni(η^2-S_2) cores of **3a**, **C**, and **D** are very similar.

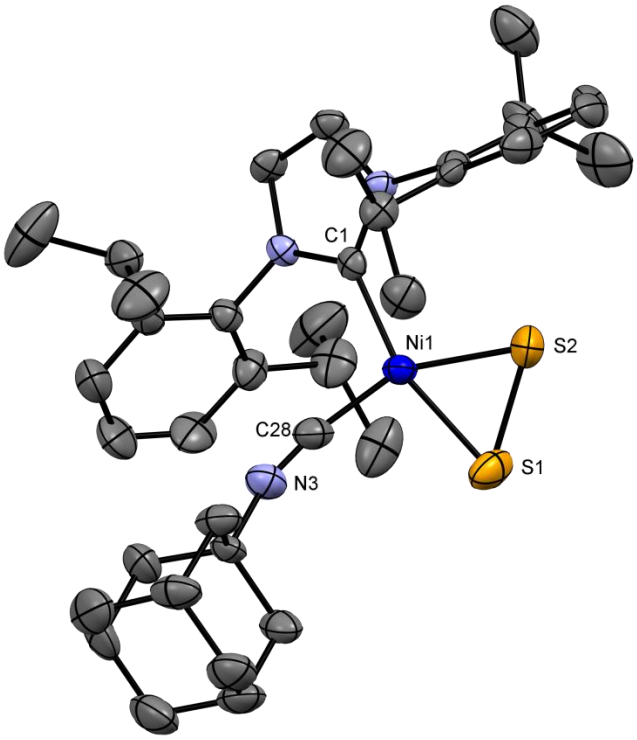

Figure 16. Molecular structure of (IPr)(AdNC)Ni(η^2-S_2) (**3a**). Hydrogen atoms are omitted. Selected bond distances (Å) and angles (°): S(1)-S(2) = 2.113(2), Ni-S(1) = 2.159(2), Ni-S(2) =

2.137(2), Ni-C(1) = 1.904(5), Ni-C(28) = 1.823(6), C(28)-N(3) = 1.152(7); S(1)-Ni-S(2) = 58.92(7), C(1)-Ni-C(28) = 105.0(2), C(1)-Ni-S(2) = 100.60(15), C(28)-Ni-S(1) = 95.7(2), Ni-C(28)-N(3) = 171.3(5).

Crystals of **4a** were grown by layering pentane on to a THF solution of **4a** (Figure 17). In the solid state, **4a** exhibits a square planar geometry and a *trans* arrangement of the AdNC and IPr ligands. The imidazolin-2-ylidene ring is rotated from the Ni square plane by 88.6(6)°. Several other *trans*-(IPr)(L)$NiCl_2$ complexes have been characterized, in which L = IPr,[60] N,N-diisopropyl-imidazolin-2-ylidene,[61] 2,6-lutidine,[62] PPh_3[60] or PMe_3,[63] and all are structurally similar to **4a**.

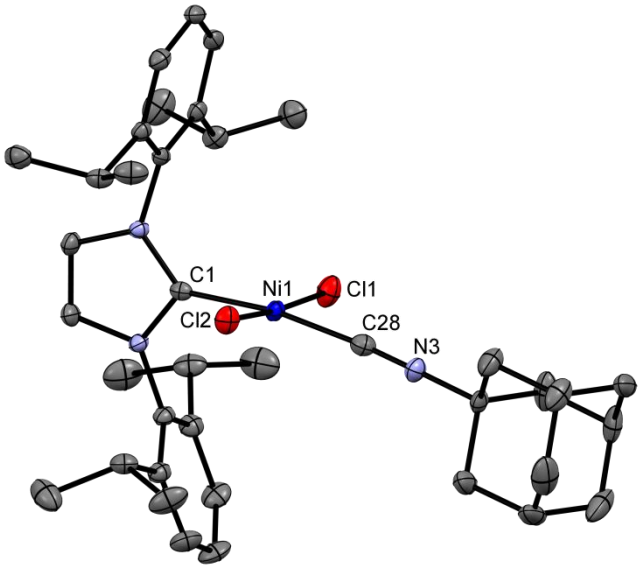

Figure 17. Molecular structure of *trans*-(IPr)(AdNC)$NiCl_2$ (**4a**). Hydrogen atoms are omitted. Selected bond distances (Å) and angles (°): Ni-C(1) = 1.9022(14), Ni-C(28) = 1.871(2), Ni-Cl(1) = 2.1614(4), Ni-Cl(2) = 2.1747(4), C(28)-N(3) = 1.150(2); C(1)-Ni-Cl(1) = 92.02(4), C(1)-Ni-Cl(2) = 90.52(5), Cl(1)-Ni-C(28) = 90.18(5), Cl(2)-Ni-C(28) = 88.12(5), Ni-C(28)-N(3) = 175.97(14).

The ^{1}H NMR spectra of **3a** and **4a** both contain two methyl resonances and one methine resonance (Figure 18), consistent with the solid state structures and fast rotation of Ni-NHC bonds.

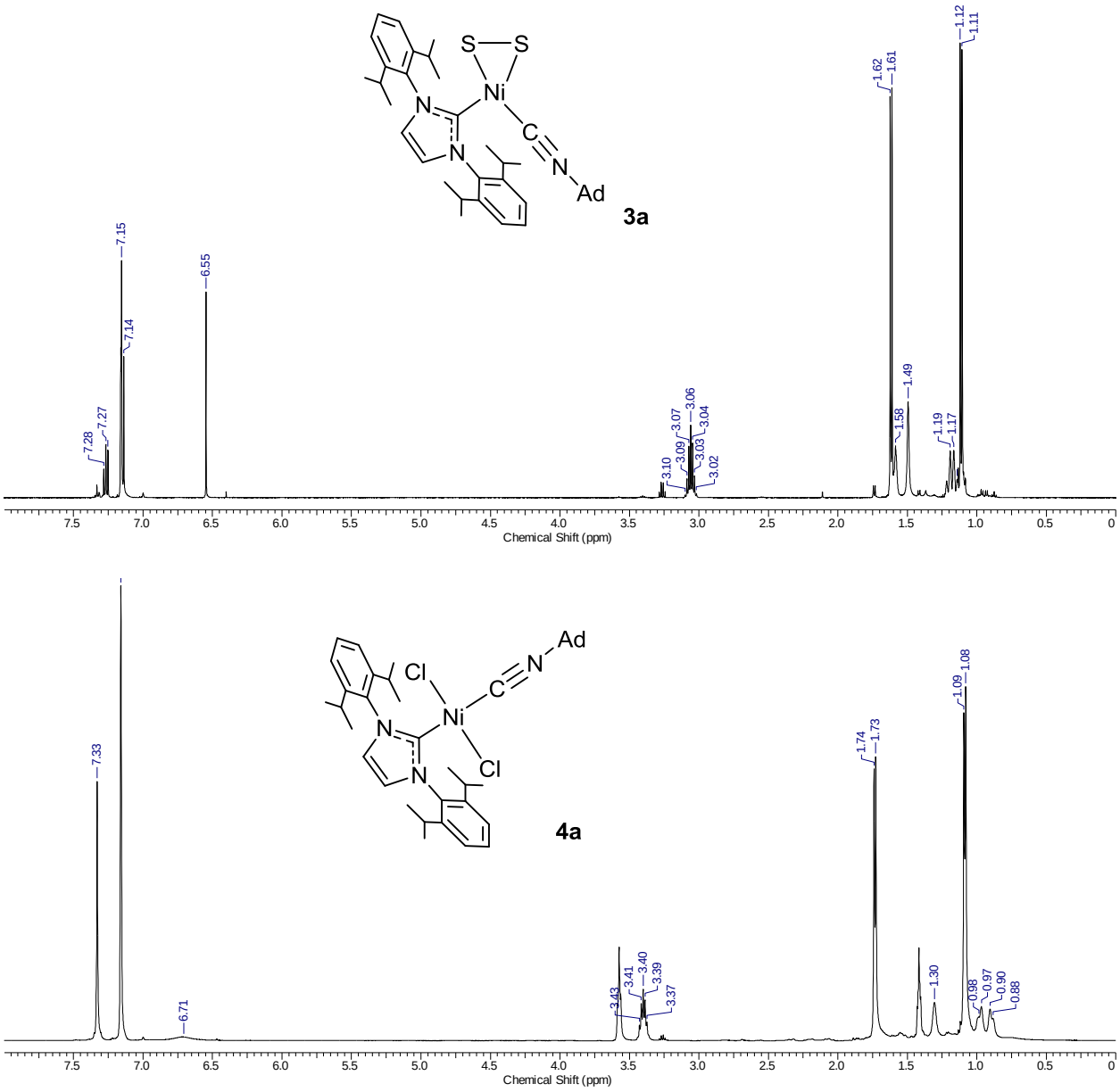

Figure 18. ^{1}H NMR spectra of (IPr)(AdNC)Ni(η^2-S_2) (**3a**) and *trans*-(IPr)(AdNC)$NiCl_2$ (**4a**), taken in C_6D_6 at 298 K.

2.3.3 Alternate synthesis of (IPr)(AdNC)Ni(η^2-S_2) (3a) and *trans*-(IPr)(AdNC)$NiCl_2$ (4a).

Complexes **3a** and **4a** can be prepared by an alternate route involving sequential reaction of **1** with AdNC and S_8 (Scheme 5). The reaction of **1** with 2 equiv of AdNC in Et_2O yields the 3-coordinate Y-shaped complex (IPr)(AdNC)NiCl (**5a**), which precipitates from the

reaction mixture as a white powder in 94% yield. The analogous *tert*-butyl and benzyl isocyanide complexes were previously prepared by this route and characterized crystallographically.[63] The reaction of **5a** with S_8 in THF produces a 1:1 mixture of **3a** and **4a** quantitatively (by NMR), and **3a** and **4a** are isolated in yields comparable to those from the reaction of **2** with AdNC. **5a** reacts with excess AdNC to yield $\{(IPr)NiCl_2\}_2$, free IPr, and $Ni(CNAd)_4$,[63] and therefore close control of stoichiometry is important for clean conversion of **1** to **5a**. However, neither **3a** nor **4a** react further with S_8.

^{1}H NMR studies show that **1** and **2** react with *tert*-butyl (**b**), *ortho*-xylyl (**c**) and *para*-methoxyphenyl (**d**) isocyanides in the same manner as with AdNC, as shown in Scheme 5. The AdNC complexes exhibited the most favorable solubility properties, and therefore lent themselves to the highest isolated yields and full characterization. While the mechanistic details of the conversion of **2** to **3a-d** and **4a-d** are unknown, these reactions show that the disulfide unit is quite robust.

2.3.4 IR spectra of isocyanide complexes.

The isocyanide ν_{CN} bands for **3a** and **4a** (2136 and 2210 cm^{-1} respectively) appear at higher frequencies than the value for free AdNC (2123 cm^{-1}). Therefore, **3a** and **4a** are examples of non-classical isocyanide complexes in which the isocyanide acts as a σ-donor but π-backbonding is minimal.[64] This binding mode is consistent with the poor backbonding properties of d^8 Ni^{II} centers. **4a** exhibits a larger coordination shift in ν_{CN} (87 cm^{-1}) than **3a** (13 cm^{-1}), due to the stronger electron withdrawing effect of the two Cl ligands in **4a** versus the (η^2-S_2) ligand in **3a**. In contrast, the ν_{CN} value for **5a** (2108 cm^{-1}) is 15 cm^{-1} lower than free AdNC value, due to π-backbonding from the d^9 Ni^{I} center.

2.3.5 Reduction of $\{(IPr)ClNi\}_2(\mu^2$-η^2,η^2-$S_2)$ (2) by KC_8.

As noted above, the two-electron reduction of disulfide complex **A** (Chart 2) with KC_8 yields the bridging sulfide complex **E**. DFT analysis of **2** indicates that the LUMO has significant S-S σ* character, which suggests that two-electron reduction should induce a similar S-S bond cleavage reaction. A CV of **2** (THF, $[NBu_4][PF_6]$ as supporting electrolyte) shows an irreversible reduction at E_p = -1.92 V and a quasi-reversible 2-electron reduction at -2.31 V versus the $Cp_2Fe/[Cp_2Fe]^+$ couple, see Experimental Section. Indeed, the reaction of **2** with 2 equiv of KC_8 in THF affords $\{(IPr)Ni(\mu\text{-}S)\}_2$ (**6**), which was isolated as X-ray quality crystals in 90% yield by recrystallization from Et_2O and pentane (Scheme 5).

In the solid state, **6** adopts a bimetallic structure with nearly planar nickel centers (sum of angles: Ni1 = 356.42(6)°, Ni2 = 352.65(6)°, Figure 19). The two imidazolin-2-ylidene rings are perpendicular to each other; one is coplanar with the planar, diamond-shaped Ni_2S_2 core and the other is perpendicular to it. The structure has approximate C_{2v} symmetry with the mirror planes lying along the Ni-Ni vector. The S-S distance is 3.4186(8) Å, indicating that the S-S bond in **2** has been completely cleaved,[57,58] while the Ni-Ni distance is very short (2.3666(5) Å), indicative of a significant Ni-Ni bonding interaction.[65] These pronounced structural changes result in Ni-S-Ni angles (68.81(2)°, 68.89(2)°) that are significantly more acute than those in **2** (~91.5°). The average Ni-S distance in **6** is ca. 0.07 Å shorter than that in **2**, consistent with the higher formal charge of the sulfur in **6** (two S^{2-} ligands) versus **2** (one S_2^{2-} ligand).

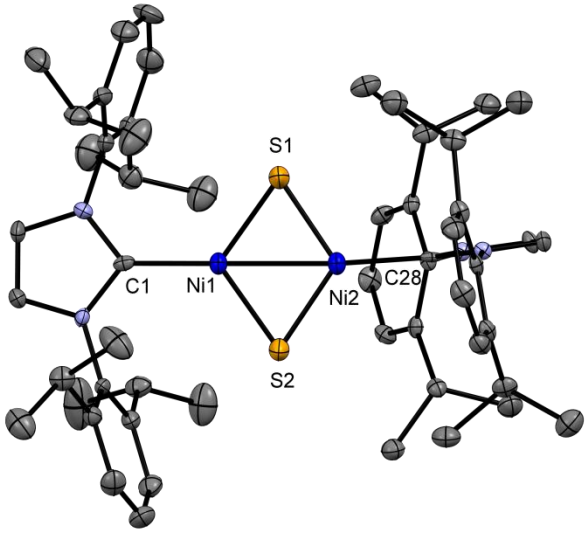

Figure 19. Molecular structure of {(IPr)Ni(μ-S)}$_2$ (**6**). Hydrogen atoms are omitted. Selected bond distances (Å) and angles (°): Ni(1)-Ni(2) = 2.3666(5), S(1)-S(2) = 3.4186(8), Ni(1)-S(1) = 2.0972(6), Ni(1)-S(2) = 2.0950(6), Ni(2)-S(1) = 2.0911(6), Ni(2)-S(2) = 2.0890(6), Ni(1)-C(1) = 1.923(2), Ni(2)-C(28) = 1.899(2); Ni(1)-S(1)-Ni(2) = 68.81(2), Ni(1)-S(2)-Ni(2) = 68.89(2), S(1)-Ni(1)-S(2) = 109.26(2), S(1)-Ni(2)-S(2) = 109.73(2), C(1)-Ni(1)-S(1) = 123.55(6), C(1)-Ni(1)-S(2) = 123.27(6), C(28)-Ni(2)-S(1) = 125.04(6), C(28)-Ni(2)-S(2) = 117.88(6).

In solution the ^{1}H NMR spectrum of **6** contains two methyl resonances and one methine resonance, all three of which are broad (Figure 20). Therefore the C_{2V} symmetry of the solid state structure is maintained in solution. VT NMR across the range 180 to 298 K in either Toluene-d8 or THF-d8 do not show any difference in number or shape of the methyl and methine resonances. This will be addressed in Chapter 3.

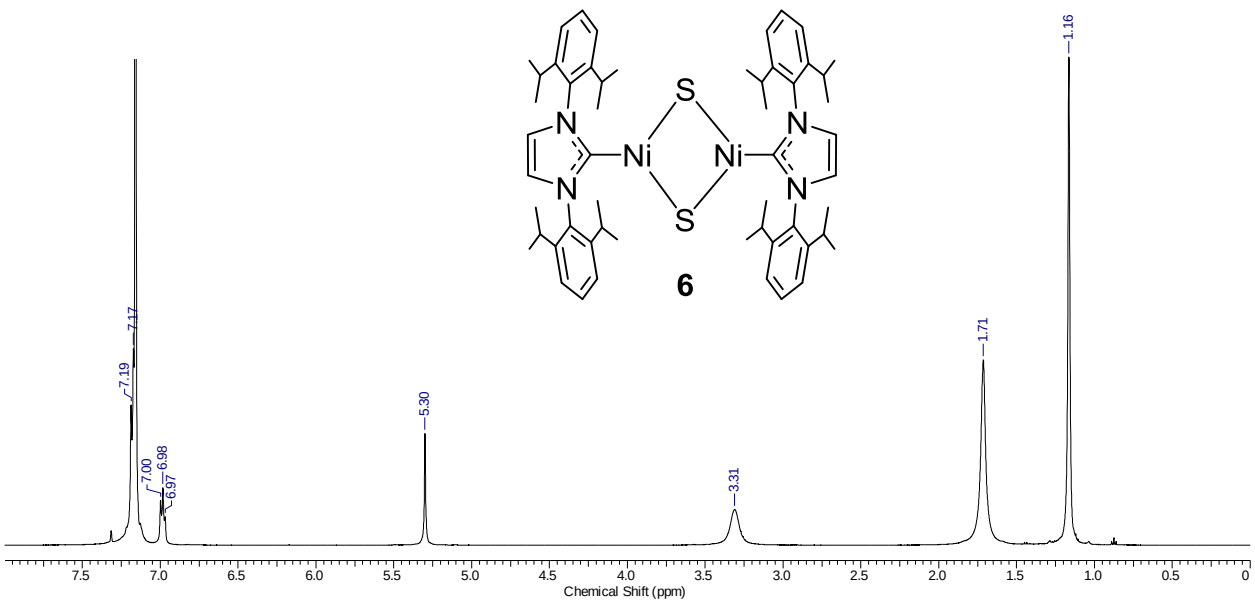

Figure 20. ^{1}H NMR spectrum of {(IPr)Ni(μ-S)}$_2$ (**6**), taken in C_6D_6 at 298 K.

Two analogues of **6** that contain chelating diphosphine ligands in place of IPr have been reported, compounds **E** and **F (**Chart 2). [44b] The Ni_2S_2 core of **6** is more contracted than those in **E** and **F** (Figure 21). Complex **6** exhibits a significantly shorter Ni-Ni distance, by 0.9174 and 0.5744 Å respectively, and shorter Ni-S bonds, on average by ca. 0.08 and 0.10 Å, respectively. The diamond core of **6** is flatter and features a much longer S-S distance (by 0.580 and 0.342 Å respectively) and more acute Ni-S-Ni angles (by 29.44° and 15.16° respectively) compared to those in **E** and **F**. Similar to complexes **A** and **B**, **E** and **F** have bulky ^{i}Pr groups on the P donor atoms, and spacefilling models show that the ^{i}Pr groups on opposite sides of the molecule are in close contact. This observation suggests that steric repulsion between these groups results in the expansion of the Ni_2S_2 core. In contrast, there is less crowding around the Ni centers and a small gap between the two IPr ligands in **6**. This difference suggests that the Ni-Ni bonded structure of **6** is electronically preferred but is precluded by steric crowding in **E** and **F**.[66]

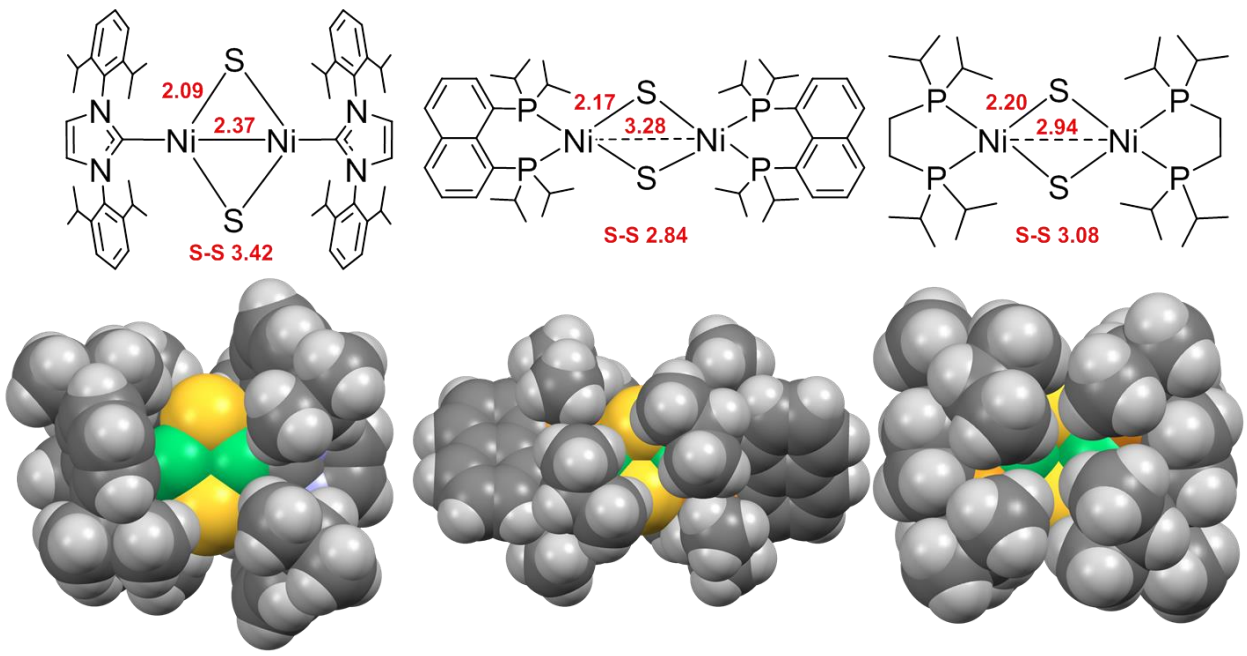

Figure 21. Spacefilling models of $Ni_2(\mu\text{-}S)_2$ bis-sulfide complexes, showing the available volume around each Ni_2S_2 core.

2.3.6 Reaction of {(IPr)Ni(μ-S)}$_2$ (6) with H_2.

Bridging sulfide and hydrosulfide species, $\{L_nM\}_2(\mu\text{-}S)_2$ and $\{L_nM\}_2(\mu\text{-}SH)_2$, are closely related and can be interconverted through acid/base reactions, with a concomitant change in the overall charge.[67] Interestingly, **6** and its neutral hydrosulfide analogue {(IPr)Ni(μ-SH)}$_2$ (**7**) are interconverted through hydrogenation and H atom abstraction reactions (Scheme 5). Complex **6** reacts with 1 atm of H_2 over 24 h at 70 °C in benzene to produce {(IPr)Ni(μ-SH)}$_2$ (**7**) in 85% yield. This reaction is accompanied by a color change from turquoise to yellow and the growth of a ^{1}H NMR resonance at δ = -4.81 (s, 2H), corresponding to the μ-S*H* units in **7**. No intermediates in the conversion of **6** to **7** were observed by ^{1}H NMR. Complex **7** can also be prepared by the salt metathesis reaction of **1** with 2 equiv KSH in a MeOH and THF mixture, followed by a recrystallization from Et_2O and pentane to produce X-ray quality crystals in 92% yield (Scheme 5). However, **6** does not react with common H atom donor sources such as Bu_3SnH, dihydroanthracene, or terpinenes.

In the solid state, **7** assumes a bimetallic structure with planar Ni centers (sum of angles: 359.64(4)°, Figure 22). The SH hydrogens were located and their positions refined isotropically. The $Ni_2(SH)_2$ core forms a diamond with H atoms disordered over both sides of the Ni_2S_2 plane in equal occupancy. The imidazolin-2-ylidene rings are rotated from the Ni plane by 59.4° in opposite directions. This conformation positions the diisopropylphenyl rings directly above the μ-SH groups and the resulting anisotropic shielding explains the high field shift of the μ-SH ^{1}H NMR resonance. The Ni-Ni distance is 2.3601(7) Å, which is typical for Ni(I)-Ni(I) species that exhibit diamagnetic ground states and Ni-Ni sigma bonds (2.314(1) - 2.3910(8) Å),[68] and is essentially unchanged from that in **6**. The Ni_2S_2 core structure of **7** is very similar to that of **6**, the major difference being that the Ni-S distances are ca. 0.1 Å longer, which results in a more acute Ni-S-Ni angle.

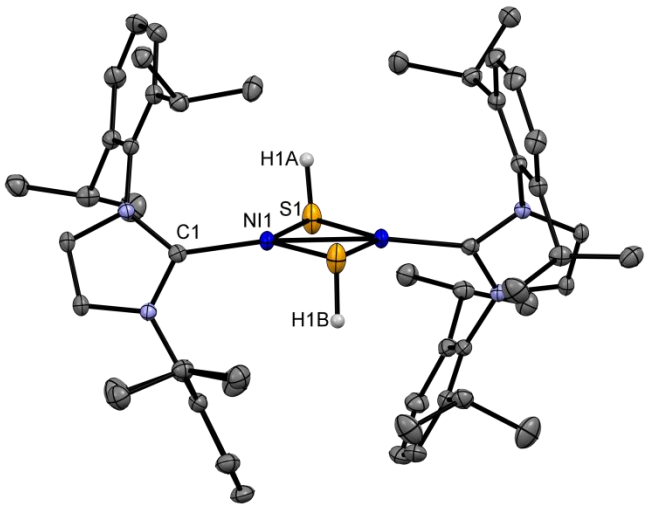

Figure 22. Molecular structure of $\{(IPr)Ni(\mu\text{-}SH)\}_2$ (**7**). Hydrogen atoms except those on S are omitted. H1 is disordered over two sites (A, B; above and below the Ni_2S_2 plane). Selected bond distances (Å) and angles (°): Ni-Ni´ = 2.3601(7), Ni-S = 2.1945(4), Ni-S´ = 2.2042(4), Ni-C(1) = 1.8677(12), S-S´ = 3.7119(6); Ni-S-Ni´ = 64.891(12), S-Ni-S´ = 115.096(12), C(1)-Ni-S = 123.82(4), C(1)-Ni-S´ = 120.72(4).

The ^{1}H NMR spectrum of **7** in solution contains two methyl resonances and one methine resonance, indicating that all four isopropyl groups are equivalent on the NMR time scale. The

two SH protons can be positioned on the same or opposite sides of the Ni_2S_2 diamond, giving rise to syn- and anti- isomers respectively. The syn-isomer has C_{2V} symmetry with all four isopropyl groups equivalent, while the anti-isomer has D_{2h} symmetry with two inequivalent sets of isopropyl groups. The N-dipp bond rotation is assumed to be slow. The observed equivalence of all four isopropyl groups suggests that **7** adopts the syn configuration in solution or that inversion of the S centers is fast on the NMR time scale.

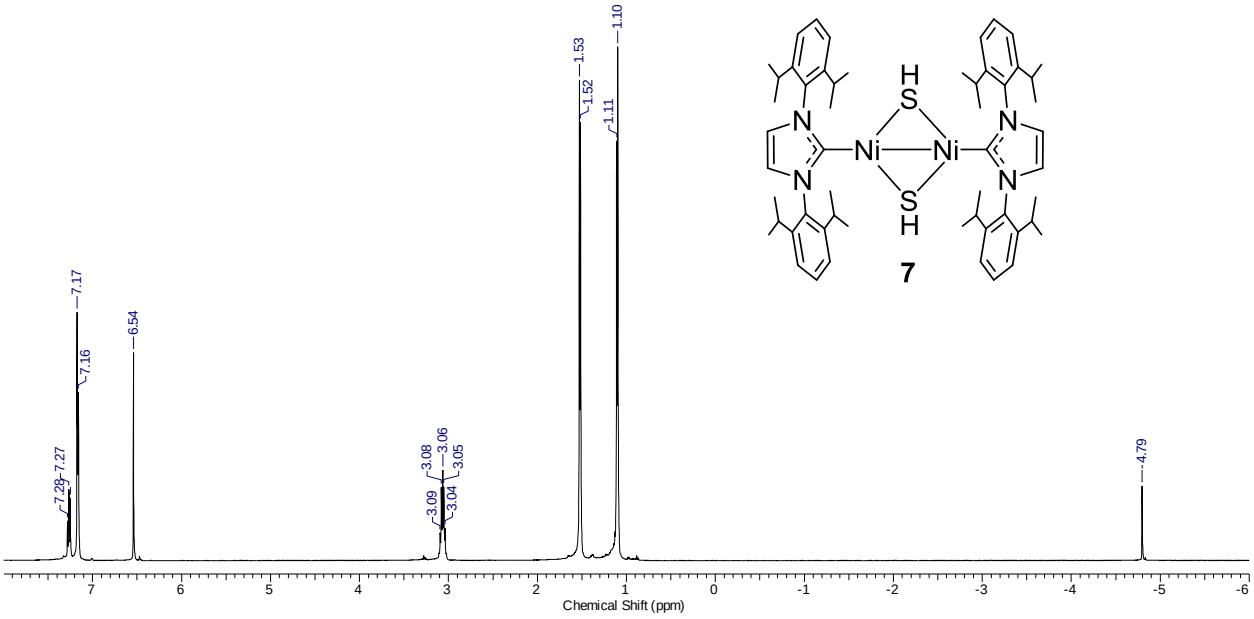

Figure 23. ^{1}H NMR spectrum of {(IPr)Ni(μ-SH)}$_2$ (**7**), taken in C_6D_6 at 298 K.

Few hydrogenations of sulfide ligands have been reported. A terminal titanium sulfido species, Cp^*_2(py)Ti=S, is hydrogenated to produce the terminal thiol-hydride complex Cp^*_2TiH(SH).[69] The Rh(I) [70] and Ir(I) [71] bridging sulfide complexes, [{MeC(CH_2PPh_2)$_3$Rh}$_2$(μ-S)$_2$]$^{2+}$ and [Cp_2Mo(μ-S)$_2$Ir(PPh_3)$_2$]$^+$, produce M(H)(μ-SH)$_2$M(H) species upon double hydrogenation. Ni alkyl and aryl thiolate complexes are known to react with H_2 to produce thiols, which is an important step in the hydrodesulfurization processes.[72]

2.3.7 Hydrogen atom abstraction from {(IPr)Ni(μ-SH)}$_2$ (7).

Compound **7** reacts with 2,4,6-^{t}Bu$_3$-phenoxy radical [73] to produce **6** and the parent phenol in quantitative yield on the NMR scale (Scheme 5). This reaction proceeds with similar high yields on the preparatory scale. Compound **6** does not react further with excess phenoxy radical. Similar H atom transfer and abstraction reactivity was reported recently for the bridging diselenide complex [(Me$_4$[12]aneN$_4$)$_2$Ni$_2$(μ^2-η^2,η^2-Se$_2$)]$^{2+}$.[74] This species reacts with 9,10-dihydroanthracene to produce the monomeric selenol [(Me$_4$[12]aneN$_4$)NiSeH]$^+$, which reacts with 2,4,6-^{t}Bu$_3$-phenoxy radical to regenerate the bridging diselenide.

2.4. Conclusions

The (IPr)Ni scaffold stabilizes low coordinate, mononuclear and dinuclear complexes with a diverse range of sulfur ligands, including μ^2-η^2,η^2-S$_2$, η^2-S$_2$, μ-S, and μ-SH. The 2,6-diisopropylphenyl groups of the IPr ligand provide lateral steric protection of the (IPr)Ni unit, but also allow for the formation of Ni-Ni bonded dinuclear species and electronically preferred, rather than sterically preferred structures. This contrasts with the dominant influence of steric effects on the structures of analogous compounds containing diphosphine ligands. The reaction of {(IPr)Ni(μ-Cl)}$_2$ (**1**) with S$_8$ yields the bridging disulfide species {(IPr)ClNi}$_2$(μ^2-η^2,η^2-S$_2$) (**2**), which exhibits a compact butterfly core structure. Complex **2** reacts with two equiv of AdNC to produce the terminal disulfide complex (IPr)(AdNC)Ni(η^2-S$_2$) (**3a**) and *trans*-(IPr)(AdNC)NiCl$_2$ (**4a**). AdNC breaks up the dimer into two mononuclear species, but the S-S bond is maintained. In contrast, two-electron reduction of **2** with KC$_8$ yields the bridging sulfide complex {(IPr)Ni(μ-S)}$_2$ (**6**). The added electrons cleave the S-S bond, and the unusual sterics of IPr allow the two Ni centers to come into close proximity and form a Ni-Ni bond. The reaction of **6** with H$_2$ yields the bridging hydrosulfide compound {(IPr)Ni(μ-SH)}$_2$ (**7**), which retains a Ni-Ni bond. Complex **7** is converted back to **6** through hydrogen atom abstraction by a phenoxy radical. This work

raises interesting questions related to the bonding of these nickel species and the mechanism of their reactions, and future studies are needed to elucidate these matters.

2.5. Experimental Section

General Procedures. Unless stated otherwise, all operations were performed in an MBraun Lab Master dry box under an atmosphere of purified nitrogen.[75] Anhydrous Et_2O and THF were purchased from Fisher, stirred over sodium metal, and filtered through activated alumina.[76] Anhydrous benzene was purchased from Sigma Aldrich, stirred over sodium metal, and filtered through activated alumina. Pentane and toluene were purchased from Sigma Aldrich and dried by passage through activated alumina and Q-5 columns. C_6D_6 was purchased from Cambridge Isotope Laboratories, degassed by freeze-pump-thaw cycles, and dried over CaH_2 or activated 4 Å molecular sieves. Celite and 4 Å molecular sieves were activated by evacuation overnight at 180 ºC. $\{(IPr)Ni(\mu\text{-}Cl)\}_2$[53b], KC_8[77] , and 2,4,6-^{t}Bu$_3$-phenoxy radical[73] were prepared according to literature preparations. All other chemicals were used as received. Elemental analyses were performed by Midwest Microlab (Indianapolis, IN) or Robertson Microlit (Ledgewood, NJ). NMR spectra were recorded on a Bruker 400 or 500 MHz NMR spectrometer. Chemical shifts were determined by reference to the solvent resonance (^{1}H: residual C_6D_5H in C_6D_6 δ 7.16; ^{13}C: C_6D_6 δ 128.1) and coupling constants are reported in hertz. Infrared spectra were measured as Fluorolube-S20 mulls between CaF_2 plates using a Thermo NEXUS 670 Near-, Far-, and Mid-FTIR with ATR Accessory.

X-ray Data Collection and Structure Refinement. X-ray diffraction data for **2** was collected on a Bruker SMART APEX system with a Charged Coupled Device (CCD) detector and a Mo-target X-ray tube (λ = 0.71073 Å). X-ray diffraction data **3a**, **4a**, **6** and **7** were collected on a Bruker D8 VENTURE with PHOTON 100 CMOS detector system equipped with a microfocus

Mo-target X-ray tube (λ = 0.71073 Å). All data were collected at 100 K using a routine of ϕ and ω scans to survey an entire sphere of reciprocal space and were indexed using the SMART or APEX2 program suits. Data were corrected for absorption effects using the empirical methods as implemented in SADABS. Space groups were determined based on systematic absences and intensity statistics. The structures were solved and refined by full-matrix least-squares procedures using the Bruker SHELXTL (version 6.14) software package (XL refinement program version 2014/7).[78] All non-hydrogen atoms were refined anisotropically. Compound **3a** exhibited disorder in the Ad group, which was modeled by parts and using restraints on one part. Compound **3a** also crystallized with two molecules of THF in the unit cell, one of which was modeled by parts and the second was removed by the Squeeze command. Compound **4a** crystallized with half a molecule of pentane in the unit cell, which could not be modeled and was removed by the Squeeze command. All hydrogen atoms were refined isotropically and fixed at calculated positions except for the H on S1 in **7**, which was located in the difference map, disordered over two positions, and refined isotropically. All structures are drawn with thermal ellipsoids at 50% probability.

Table 1. Crystal Data and Refinement Details

	2	3a·2THF	4a·Et_2O	6	7
Identification Code	FDO01	FDO02	FDO03	FDO04	FDO05
Empirical Formula	$C_{54}H_{72}Cl_2N_4Ni_2S_2$	$C_{38}H_{51}N_3NiS_2$	$C_{38}H_{51}Cl_2N_3Ni$	$C_{54}H_{72}N_4Ni_2S_2$	$C_{54}H_{74}N_4Ni_2S_2$
Formula Weight	1029.6	744.75	679.42	958.69	960.7
Temperature	100(2)	100(2)	100(2)	100(2)	100(2)
Wavelength	0.71073 Å	0.71073 Å	0.71073 Å	0.71073 Å	0.71073 Å
Crystal System	Monoclinic	Orthorhombic	Monoclinic	Monoclinic	Monoclinic
Space Group	P2(1)/c	P2(1)2(1)2(1)	P2(1)/c	P2(1)/n	C 2/c
Unit Cell Dimensions	*a* = 22.365(8) Å	*a* = 14.9869(6) Å	*a* = 12.4795(5) Å	*a* = 18.0741(10) Å	*a* = 23.8714(9) Å
	b = 16.166(6) Å	*b* = 15.7096(7) Å	*b* = 18.3976(7) Å	*b* = 15.2541(9) Å	*b* = 12.3451(5) Å
	c = 15.755(6) Å	*c* = 18.9277(8) Å	*c* = 16.8933(6) Å	*c* = 18.7632(12) Å	*c* = 19.5255(13) Å
	β = 110.240(7)°		β = 93.9125(12)°	β = 94.017(2) °	β = 118.0870(10) °
Volume	5344(3)	4456.3(3)	3869.5(3)	5160.4(5)	5076.4(4)
Z	4	4	4	4	4
Density (calculated)	1.280 Mg/m^3	1.110 Mg/m^3	1.166 Mg/m^3	1.234 Mg/m^3	1.257 Mg/m^3
Absorption Coefficient	0.921	0.561	0.667	0.849	0.863
F(000)	2184	1600	1448	2048	2056
Crystal Size	0.4 x 0.3 x 0.2 mm^3	0.2 x 0.2 x 0.1 mm^3	0.3 x 0.3 x 0.1 mm^3	0.2 x 0.1 x 0.1 mm^3	0.3 x 0.3 x 0.3 mm^3
Theta ranges for data collection	1.59 to 25.22°	1.88 to 27.22°	2.21 to 27.99°	2.02 to 25.79°	2.24 to 27.56°
Index Ranges	-26≤h≤26	-19≤h≤17	-16≤h≤13	-22≤h≤22	-31≤h≤30
	-19≤k≤19	-20≤k≤20	-24≤k≤24	-18≤k≤18	-16≤k≤15
	-18≤l≤18	-24≤l≤24	-22≤l≤22	-22≤l≤22	-25≤l≤25
Reflections collected	50879	100626	93090	111750	54989
Completeness to θ = 25°	99.2%	99.5%	99.9%	99.7%	99.8%
Absorption Correction	multi-scan	multi-scan	multi-scan	multi-scan	multi-scan
Max. and min. transmission	0.8372 and 0.7096	0.927 and 0.894	0.7456 and 0.6913	0.26312 and 0.15614	0.81989 and 0.77226
Refinement Method	Full-matrix least-squares on F^2	Full-matrix least-squares on F^2	Full-matrix least-squares on F^2	Full-matrix least-squares on F^2	Full-matrix least-squares on F^2
Data / restraints / parameter	9562 / 0 / 593	9877 / 298 / 541	9153 / 0 / 405	9881 / 0 / 575	5859 / 0 / 296
Goodness-of-fit on F^2	1.042	1.052	1.03	1.03	1.08
Final R indices [I>2sigma(I)]	R1 = 0.1087, wR2 = 0.2264	R1 = 0.0610, wR2 = 0.1308	R1 = 0.0326, wR2 = 0.0764	R1 = 0.0311, wR2 = 0.0691	R1 = 0.0273, wR2 = 0.0715
R indices (all data)	R1 = 0.1866, wR2 = 0.2601	R1 = 0.0829, wR2 = 0.1402	R1 = 0.0510, wR2 = 0.0828	R1 = 0.0456, wR2 = 0.0749	R1 = 0.0297, wR2 = 0.0736

Synthesis of {(IPr)ClNi}$_2$(μ^2-η^2,η^2-S_2) (2). A suspension of S_8 (0.0283 g, 0.883 mmol) in THF (3 mL) was added dropwise at room temperature over 10 s to a stirred, pale green solution of {(IPr)Ni(μ-Cl)}$_2$ (**1**, 0.313 g, 0.324 mmol) in THF (8 mL). The color of the mixture changed to a dark forest green over the course of 5 s. The mixture was stirred for 45 min and filtered through Celite. The filtrate was concentrated to 4 mL under reduced pressure, chilled to -35 °C, layered with pentane (13 mL), and chilled to -35 °C overnight to induce precipitation. A dark green powder was collected by filtration. This process was repeated to give several crops of product. Yield: 0.225 g (72 %). X-ray quality crystals of **2** were grown by slow diffusion of pentane into an Et_2O solution of **2**. ^{1}H NMR (22 °C, 400 MHz C_6D_6): δ 7.35 (t, J = 8.0, 4H, *p*-$C_6{}^{i}Pr_2H_3$), 7.28 (dd, J = 8.0 and 1.6, 8H, *m*-$C_6{}^{i}Pr_2H_3$), 6.41 (s, 4H, $C_3N_2H_2$), 3.28 (sept, J = 6.4, 4H, PhC*H*Me$_2$), 2.55 (sept, J = 6.8, 4H, PhC*H*Me$_2$), 1.59 (d, J = 7.2, 12H, PhCH(CH_3)$_2$), 1.42 (d, J = 6.6, 12H, PhCH(CH_3)$_2$), 0.96 (d, J = 6.8, 12H, PhCH(CH_3)$_2$), 0.93 (d, J = 7.2, 12H, PhCH(CH_3)$_2$). ^{13}C{^{1}H} NMR (22 °C, 500 MHz, C_6D_6): δ 171.8 (Ni-*C*N$_2$), 146.9 (*o*-$C_6{}^{i}Pr_2H_3$), 146.5 (*o*-$C_6{}^{i}Pr_2H_3$), 136.6 (*i*-$C_6{}^{i}Pr_2H_3$), 130.3 (*p*-$C_6{}^{i}Pr_2H_3$), 125.4 (Ni-CN$_2$*C*$_2$H$_2$), 125.0 (*m*-$C_6{}^{i}Pr_2H_3$), 124.5 (*m*-$C_6{}^{i}Pr_2H_3$), 29.1 (PhCH(CH$_3$)$_2$), 28.9 (PhCH(CH$_3$)$_2$), 26.3 (PhCH(CH$_3$)$_2$), 25.8 (PhCH(CH$_3$)$_2$), 24.3 (PhCH(CH$_3$)$_2$), 23.7 (PhCH(CH$_3$)$_2$). IR (CaF_2, fluorolube): ν (cm^{-1}) 3163, 3123, 3087, 2962, 2927, 2867, 1592, 1558, 1467, 1456, 1402, 1384, 1361, 1331, 1276, 1198, 1149, 1125, 1041, 967. Elemental Analysis Calculated. $Ni_2Cl_2S_2N_4C_{54}H_{72}$: C 62.98; H 7.06; N 5.04. Found: C 62.43; H 6.90; N 5.15.

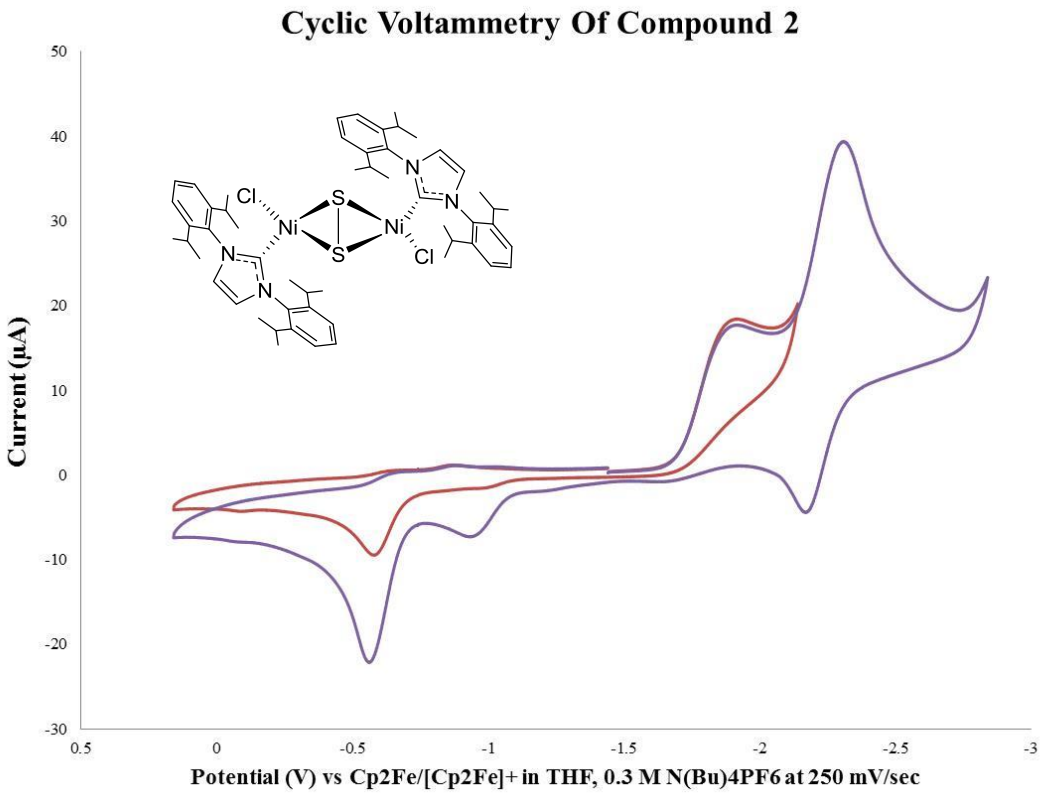

Figure 24. Cyclic Voltammogram of **2** (Potential (V) vs $Cp_2Fe/[Cp_2Fe]^+$ in THF, 0.3 M $N(Bu)_4PF_6$ at 250 mV/sec)

Synthesis of (IPr)(AdNC)Ni(η^2-S_2) (3a). A solution of AdNC (0.0343 g, 0.213 mmol) in Et_2O (2 mL) was chilled to -35 °C and then added dropwise to a chilled, stirred solution of **2** (0.108 g, 0.105 mmol) in Et_2O (8 mL). There was an immediate color change to orange. The solution was stirred for 30 min and filtered through Celite. The volatiles were removed by vacuum and the resulting solid was redissolved in Et_2O (7 mL). The filtrate was chilled to -35 °C and a fluffy yellow solid precipitated, which was collected by filtration. This process was repeated to give several crops of product. Yield: 0.0620 g (88 %). X-ray quality crystals of **3a**·2(THF) were grown by liquid diffusion of pentane into a THF solution of **3a**. ^{1}H NMR (22 °C, 500 MHz C_6D_6): δ 7.27 (t, J = 7.5, 2H, *p*-$C_6{}^{i}Pr_2H_3$), 7.15 (d, J = 7.5, 4H, *m*-$C_6{}^{i}Pr_2H_3$), 6.55 (s, 2H, $C_3N_2H_2$), 3.06 (sept, J = 6.5, 4H, PhC*H*Me_2), 1.61 (d, J = 7, 12H, PhCH(CH_3)$_2$), 1.59 (br, 3H,

$NC(CH_2)_3(CH)_3(CH_2)_3$), 1.49 (br, 6H, $NC(CH_2)_3(CH)_3(CH_2)_3$), 1.18 (dd, J = 13.5 and 12, 6H, $NC(CH_2)_3(CH)_3(CH_2)_3$), 1.11 (d, J = 7, 12H, $PhCH(CH_3)_2$). $^{13}C\{^1H\}$ NMR (22 °C, 500 MHz, C_6D_6): δ 185.8 (Ni-CN_2), 146.2 (*o*-$C_6{}^iPr_2H_3$), 137.3 (*i*-$C_6{}^iPr_2H_3$), 130.2 (*p*-$C_6{}^iPr_2H_3$), 124.3 (Ni-$CN_2C_2H_2$), 124.1 (*m*-$C_6{}^iPr_2H_3$), 43.2 ($NC(CH_2)_3(CH)_3(CH_2)_3$), 35.4 ($NC(CH_2)_3(CH)_3(CH_2)_3$), 29.1 ($PhCHMe_2$), 29.0 ($NC(CH_2)_3(CH)_3(CH_2)_3$), 25.4 ($PhCH(CH_3)_2$), 24.0 ($PhCH(CH_3)_2$). IR (CaF_2, fluorolube): ν (cm^{-1}) 2960, 2930, 2865, 2329, 2136 (ν_{CN}, AdNC), 1456, 1398, 1126, 1041. Anal. Calcd. for $Ni_1S_2N_3C_{32}H_{51}$: C 67.85; H 7.64; N 6.25. Found: C 67.65; H 7.36; N 5.92.

Generation of (IPr)(^{t}BuNC)Ni(η^2-S_2) (3b), (IPr)(*o*-xylylNC)Ni(η^2-S_2) (3c), and (IPr)(*p*-MeO-PhNC)Ni(η^2-S_2) (3d). **3b**, **3c**, and **3d** were generated *in situ* in a manner analogous to **3a**, using ^{t}BuNC, *o*-xylylNC, and *p*-MeO-PhNC in lieu of AdNC. **3b** ^{1}H NMR (22° C, 500 MHz C_6D_6): δ 7.24 (t, J = 7.5, 2H), 7.12 (d, J = 8, 4H), 6.53 (s, 2H), 3.03 (sept, J = 7, 4H), 1.57 (d, J = 7, 12H), 1.09 (d, J = 7, 12H), 0.74 (s, 9H, $C(CH_3)_3$). $^{13}C\{^1H\}$ NMR (22° C, 400 MHz, C_6D_6): δ 185.6, 146.1, 137.3, 130.1, 124.3, 124.1, 30.9 ($C(CH_3)_3$), 30.2 ($C(CH_3)_3$), 29.1, 25.3, 23.9. **3c** ^{1}H NMR (22° C, 500 MHz C_6D_6): δ 7.20 (t, J = 8, 2H), 7.18 (d, J = 8, 2H, *m*-$C_6Me_2H_3$), 7.10 (d, J = 8, 4H), 6.69 (t, J = 7.5, 1H, *p*-$C_6Me_2H_3$), 6.58 (s, 2H), 3.10 (sept, J = 7, 4H), 1.93 (s, 6H), 1.55 (d, J = 7, 12H), 1.07 (d, J = 7, 12H). **3d** ^{1}H NMR (22° C, 500 MHz C_6D_6): δ 7.32 (d, J = 7.5, 2H, *o*-C_6H_4OMe), 7.28 (d, J = 7, 2H, *m*-C_6H_4OMe), 7.22 (t, J = 10, 2H), 7.14 (d, J = 7.5, 4H), 6.58 (s, 2H), 3.07 (sept, J = 6.5, 4H), 3.06 (s, 3H), 1.60 (d, J = 6.5z, 12H), 1.10 (d, J = 7, 12H).

Synthesis of *trans*-(IPr)(AdNC)$NiCl_2$ (4a). **4a** was produced by three independent methods. (1) **4a** was isolated from **3a** by selective precipitation from the reaction mixture of **2** with AdNC. After **3a** was precipitated, the filtrate was concentrated in THF (2 mL), chilled to -35 °C, layered with pentane (4 mL), and chilled to -35 °C overnight. Red crystals were collected by filtration. Yield: 0.0543 g (76 %) (2) A solution of AdNC (0.0474 g, 0.29 mmol) in THF (2 mL) was added dropwise to a stirring solution of trans-$(IPr)_2NiCl_2$ (0.2667 g, 0.29 mmol) in THF (5 mL). There was an immediate color change from blue to red-orange. The solution was stirred for 30 min

and chilled to -35° C, causing precipitation of a beige solid (free IPr). The suspension was filtered in a frit over Celite to remove the IPr byproduct. The filtrate was concentrated by vacuum to 2 mL, layered with pentane (7 mL), and chilled to -35° C overnight to induce precipitation. Red-maroon crystals were collected by filtration. Yield: 0.1498 g (76%). (3) A solution of AdNC (0.0231 g, 0.14 mmol) in THF (2 mL) was added dropwise to a stirring solution of $\{IPrNiCl(\mu\text{-}Cl)\}_2$ (0.1412 g, 0.14 mmol) in THF (4 mL). There was an immediate color change from purple to red-orange. The solution was stirred for 30 min, concentrated by vacuum to 1 mL, layered with pentane (4 mL), and chilled -35° C overnight to induce precipitation. Red-maroon crystals were collected on a frit. Yield: 0.1380 g (84%).

X-ray quality crystals of **4a**·Et_2O were grown by liquid diffusion of pentane into an Et_2O solution of **4a**. ^{1}H NMR (22 °C, 500 MHz C_6D_6): δ 7.33 (s, 6H, m/*p*-$C_6{}^{i}Pr_2H_3$), 6.71 (br, 2H, $C_3N_2H_2$), 3.40 (sept, J = 6.5, 4H, PhC*H*Me_2), 1.73 (d, J = 6.5, 12H, PhCH(CH_3)$_2$), 1.30 (br, 3H, NC$(CH_2)_3$(C*H*)$_3$$(CH_2)_3$), 1.09 (d, J = 6.5, 12H, PhCH(CH_3)$_2$, and br, 6H, NC(CH_2)$_3$$(CH)_3$$(CH_2)_3$), 0.94 (dd, J = 31 and 10.5, 6H, NC$(CH_2)_3$$(CH)_3$(C$H_2$)$_3$). ^{13}C{^{1}H} NMR (22 °C, 500 MHz, C_6D_6): δ 147.4 (*o*-$C_6{}^{i}Pr_2H_3$), 130.7 (*p*-$C_6{}^{i}Pr_2H_3$), 124.4 (*m*-$C_6{}^{i}Pr_2H_3$), 41.3 (NC$(CH_2)_3$(*C*H)$_3$$(CH_2)_3$), 35.0 (NC(*C*$H_2$)$_3$(C*H*)$_3$$(CH_2)_3$), 29.2 (Ph*C*H$Me_2$), 28.6 (NC$(CH_2)_3$$(CH)_3$(*C*$H_2$)$_3$), 26.6 (PhCH(*C*$H_3$)$_2$), 23.6 (PhCH(*C*$H_3$)$_2$). IR ($CaF_2$, fluorolube): ν (cm^{-1}) 3180, 3070, 2966, 2912, 2865, 2210 (ν_{CN}, AdNC), 1965, 1592, 1467, 1405, 1383, 1360, 1345, 1333, 1307, 1199. Anal. Calcd. for $Ni_1Cl_2N_3C_{38}H_{51}$: C 67.17; H 7.57; N 6.18. Found: C 67.43; H 7.82; N 5.94.

Generation of *trans*-(IPr)(^{t}BuNC)$NiCl_2$ (4b), *trans*-(IPr)(*o*-xylylNC)$NiCl_2$ (4c), and *trans*-(IPr)(*p*-MeO-PhCN)$NiCl_2$ (4d). **4b**, **4c**, and **4d** were generated in situ in a manner analogous to **4a**, using ^{t}BuNC, *o*-xylylNC, and *p*-MeO-PhCN in lieu of AdNC. **4b** ^{1}H NMR (22° C, 500 MHz C_6D_6): δ 7.31 (s, 6H), 6.69 (br, 2H), 3.38 (sept, J = 6.5, 4H), 1.71 (d, J = 6.5, 12H), 1.07 (d, J = 7, 12H), 0.38 (s, 9H, C(CH_3)$_3$). ^{13}C{^{1}H} NMR (22° C, 500 MHz, C_6D_6): δ 147.4, 130.7, 124.4, 29.1, 28.5, 26.6, 23.5. IR (CaF_2, fluorolube): ν (cm^{-1}) 2966, 2866, 2361, 2338, 2206, 1465,

1404, 1383, 1341, 1196, 1125. **4c** ^{1}H NMR (22° C, 500 MHz C_6D_6): δ 7.35 (s, 6H), 6.62 (br, 2H), 6.48 (t, J = 7.5, 1H, *p*-$C_6Me_2H_3$), 6.26 (d, J = 7.5, 2H, *m*-$C_6Me_2H_3$), 3.39 (sept, J = 6.5, 4H), 1.78 (s, 6H, *o*-$C_6(CH_3)_2H_3$), 1.74 (d, J = 7, 12H), 1.09 (d, J = 6.5, 12H). **4d** ^{1}H NMR (22° C, 500 MHz C_6D_6): δ 7.36 (s, 6H), 6.71 (br, 2H), 6.14 (d, J = 7, 2H, *o*-C_6H_4OMe), 5.95 (d, J = 9, 2H, *m*-C_6H_4OMe), 3.43 (sept, J = 6.5, 4H), 2.84 (s, 3H, *p*-$C_6H_4OCH_3$), 1.75 (d, J = 6.5, 12H), 1.10 (d, J = 7, 12H).

Synthesis of (IPr)(AdNC)NiCl (5a). A solution of AdNC (0.0268g, 0.166 mmol) in Et_2O (1 mL) was chilled to -35 °C and added dropwise to a chilled, stirred solution of **1** (0.0778 g, 0.0805 mmol) in Et_2O (4 mL). The color of the solution changed to red and after 1 h a beige solid precipitated. The solution was chilled to -35 °C and the beige solid was collected by filtration. Yield: 0.0976 g (94 %). ^{1}H NMR (22 °C, 500 MHz C_6D_6): δ 7.29 (br, 3H, $NC(CH_2)_3(CH)_3(CH_2)_3$), 6.91 (br, 4H, $C_3N_2H_2$), 5.97 (br, 12H, $PhCH(CH_3)_2$), 2.86 (br, 6H, $NC(CH_2)_3(CH)_3(CH_2)_3$), 1.55 (br, 4H, *m*-$C_6{}^iPr_2H_3$), 1.33 (br, 12H + 2H, $PhCH(CH_3)_2$ and *m*-$C_6{}^iPr_2H_3$), 0.99 (br, 6H, $NC(CH_2)_3(CH)_3(CH_2)_3$), 0.25 (br, 4H, $PhCH(CH_3)_2$). IR (CaF_2, fluorolube): ν (cm^{-1}) 2910, 2858, 2108 (ν_{CN}, AdNC), 1457, 1396, 1200. Anal. Calcd. for $Ni_1Cl_1N_3C_{38}H_{51}$: C 70.87; H 7.98; N 6.53. Found: C 70.66; H 8.19; N 6.31.

Synthesis of (IPr)(^{t}BuNC)NiCl (5b), (IPr)(*o*-xylylNC)NiCl (5c), and (IPr)(*p*-MeO-PhNC)NiCl (5d). 5b, **5c**, and **5d** were made in analogous fashion using ^{t}BuNC, *o*-xylylNC, and *p*-MeO-PhNC in lieu of CNAd. **5b** was previously reported.[50d] **5a-d** all have poor solubility in C_6D_6. **5b** ^{1}H NMR (22° C, 400 MHz C_6D_6): δ 10.10 (br, 2 H), 7.43 (br, 6 H), 7.04 (br, 2 H), 5.61 (br, 12 H), 4.36 (br, 4 H), 1.29 (br, 12 H), -0.76 (br, 6 H). **5c** ^{1}H NMR (22° C, 500 MHz C_6D_6): δ 10.10 (br, 1H, *p*-$C_6Me_2H_3$), 7.43 (br, 2H, *m*-$C_6Me_2H_3$), 7.04 (br, 2H), 5.61 (br, 6H + 4H *o*-$C_6(CH_3)_2H_3$), 4.36 (br, 2H), 1.29 (br, 24H), -0.76 (br, 4H). **5d** ^{1}H NMR (22° C, 500 MHz C_6D_6): δ 13.16 (br, 2H, *o*-C_6H_4OMe), 7.27 (br, 4H + 2H, *m*-C_6H_4OMe), 7.00 (br, 2H), 5.71 (br, 12H), 4.06 (br, 3H, *p*-$C_6H_4OCH_3$), 2.57 (br, 4H + 2H), 1.28 (br, 12H).

Synthesis of {(IPr)Ni(μ-S)}$_2$ (6). A suspension of KC_8 (0.0546 g, 0.404 mmol) in THF (3 mL) was chilled to -35 °C, and added dropwise to a chilled, stirred solution of **2** (0.193 g, 0.187 mmol) in THF (4 mL). The mixture was stirred for 3 h, warmed to room temperature, and filtered through Celite, resulting in a blue-black solution. The volatiles were removed by vacuum, and the resulting solid was extracted with pentane (4x 10 mL), providing a turquoise solution. The volatiles were removed by vacuum, and the resulting turquoise solid was dissolved in Et_2O (3 mL), chilled to -35 °C, layered with pentane (7 mL), and chilled to -35 °C overnight. Dark blue crystals were collected by filtration. This process was repeated to give several crops of product. Yield: 0.162 g (90 %). **6** can also be synthesized by alternative reductants including NaHg amalgam and Na naphthalenide, which following analogous purifications provide product in 43% and 48% yields respectively. Complex **6** decomposes over the course of hours in CH_2Cl_2 at room temperature. X-ray quality crystals of **6** were grown by liquid diffusion of pentane into an Et_2O solution of **6**. ^{1}H NMR (22 °C, 500 MHz C_6D_6): δ 7.18 (d, J = 7.5, 8H, *m*-$C_6{}^{i}Pr_2H_3$), 6.99 (t, J = 7.5, 6H, *p*-$C_6{}^{i}Pr_2H_3$), 5.30 (s, 4H, $C_3N_2H_2$), 3.31 (br, 8H, PhC*H*Me$_2$), 1.71 (br, 24H, PhCH(CH_3)$_2$), 1.17 (br, 24H, PhCH(CH_3)$_2$). ^{13}C{^{1}H} NMR (22 °C, 500 MHz, C_6D_6): δ 153.0 (*o*-$C_6{}^{i}Pr_2H_3$), 130.8 (*p*-$C_6{}^{i}Pr_2H_3$), 127.1 (*i*-$C_6{}^{i}Pr_2H_3$), 125.4 (*m*-$C_6{}^{i}Pr_2H_3$), 115.5 (Ni-$CN_2C_2H_2$), 41.1 (Ph*C*HMe$_2$), 26.5 (PhCH(*C*H$_3$)$_2$), 26.2 (PhCH(*C*H$_3$)$_2$). Multiple chemical analyses of spectroscopically pure, crystalline samples of **6** gave poor results (see SI).

Synthesis of {(IPr)Ni(μ-S)}$_2$ (7). A solution of KSH (0.0256 g, 0.355 mmol) in THF (1 mL) and methanol (6 mL) was chilled to -35 °C, and added dropwise to a chilled, stirred solution of **1** (0.168 g, 0.174 mmol) in THF (2 mL) and Et_2O (5 mL). The color of the solution turned to orange, then red, and finally to a murky yellow-green. The solution was stirred for 1 h and warmed up to room temperature. The volatiles were removed by vacuum, producing a yellow-green film, which was extracted with pentane (20 mL) and filtered through Celite. The filtrate was dried by vacuum and the residue was dissolved in Et_2O (3 mL), chilled to -35 °C, layered

with pentane (7 mL), and chilled to -35 °C overnight to produce yellow-green crystals that were collected by filtration. Yield: 0.528 g (92 %). X-ray crystals were grown by liquid diffusion of pentane into an Et_2O solution of **7**. ^{1}H NMR (22 °C, 500 MHz C_6D_6): δ 7.25 (t, J = 7.5, 4H, *p*-$C_6{}^{i}Pr_2H_3$), 7.15 (d, J = 8, 8H, *m*-$C_6{}^{i}Pr_2H_3$), 6.53 (s, 4H, $C_3N_2H_2$), 3.05 (sept, J = 7, 8H, PhC*H*Me_2), 1.50 (d, J = 6.5, 24H, PhCH(CH_3)$_2$), 1.09 (d, J = 6.5, 24H, PhCH(CH_3)$_2$), -4.81 (s, 2H, S*H*). ^{13}C{^{1}H} NMR (22 °C, 500 MHz, C_6D_6): δ 189.5 (Ni-*C*N_2), 146.8 (*o*-$C_6{}^{i}Pr_2H_3$), 137.8 (*i*-$C_6{}^{i}Pr_2H_3$), 129.2 (*p*-$C_6{}^{i}Pr_2H_3$), 123.8 (*m*-$C_6{}^{i}Pr_2H_3$), 123.3 (Ni-$CN_2C_2H_2$), 28.9 (Ph*C*HMe_2), 25.1 (PhCH(*C*H_3)$_2$), 24.2 (PhCH(*C*H_3)$_2$). IR (CaF_2, fluorolube): ν (cm^{-1}) 3125, 3069, 2965, 2868, 2474 (ν_{CN}, SH), 1592, 1538, 1467, 1388, 1362, 1327, 1301, 1198, 1125. Anal. Calcd. for $Ni_2S_2N_4C_{54}H_{74}$: C 67.51; H 7.76; N 5.83. Found: C 67.48; H 7.70; N 5.87.

DFT Calculations. Gaussian 03 (revision E.01) was used for all calculations.[79] The B3LYP functional was used to carry out the geometry optimizations on the model compounds specified in text using the LANL2DZ core potential for Ni and 6-31+g basis set for all other atoms. The validity of the true minima was checked by the absence of negative frequencies in the energy Hessian. For the optimization of {(IPr)ClNi}$_2$(μ^2-η^2,η^2-S_2), the initial structure used was derived from the crystal structure of **2**.

Table 2. Comparison of calculated and experimental metrical parameters for **2**.

Metric	Ni(1)-Ni(2)	S(1)-S(2)	Ni-S (avg)	Ni-Cl (avg)	Ni(1)-S(1)-Ni(2)	Ni-S-S-Ni
DFT (Å)	3.329	2.081	2.274	2.218	94.1	110.77
Structure (Å)	3.096(2)	2.011(4)	2.162(3)	2.152(3)	91.5(1)	107.97(11)

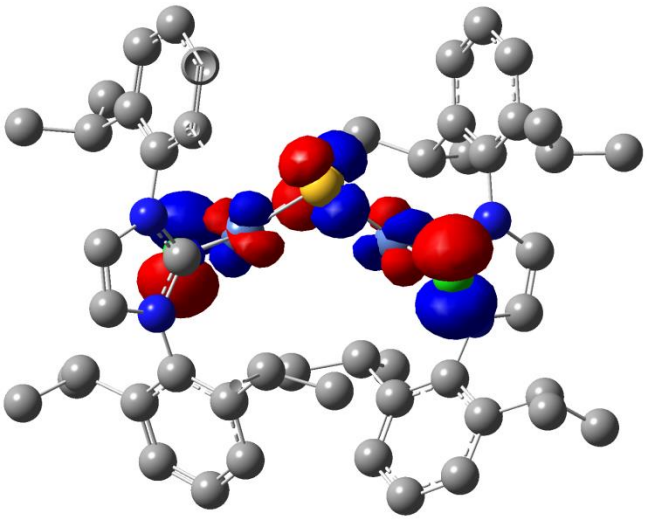

Figure 25. HOMO from structural optimization of **2**, showing a Ni-S π* interaction.

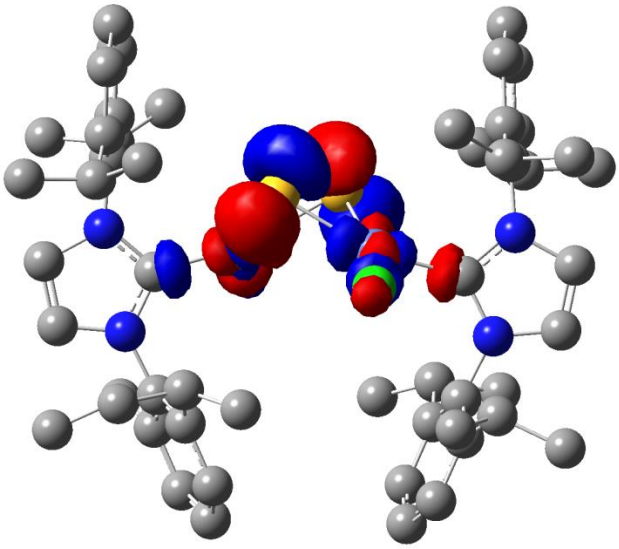

Figure 26. LUMO from structural optimization of **2**, showing a S-S σ* interaction.

2.6. References

(40) (a) Kure, B.; Taniguchi, A.; Nakajima, T.; Tanase, T. *Organometallics* **2012**, *31*, 4791. (b) Beletskaya, I. P.; Ananikov, V. P. *Chem. Rev.* **2011**, *111*, 1596. (c) Datta, S.; Seth, D. K.; Butcher, R.; Bhattacharya, S. *Inorg. Chim. Acta.* **2011**, *377*, 120. (d) Torres-Nieto, J.; Brennessel, W. W.; Jones, W. D.; Garcia, J. J. *J. Am. Chem. Soc.* **2009**, *131*, 4120. (e) Ito, M.; Kotera, M.; Matsumoto, T.; Tatsumi, K. *Proc. Natl. Acad. Sci. U.S.A.* **2009**, *106*, 11862. (f) Rampersad, M. V.; Zuidema, E.; Ernsting, J. M.; van Leeuwen, P. W. N. M.; Darensbourg, M. Y.

Organometallics **2007**, *26*, 783. (g) Takei, I.; Wakebe, Y.; Suzuki, K.; Enta, Y.; Suzuki, T.; Mizobe, Y.; Hidai, M. *Organometallics* **2003**, *22*, 4639.

(41) (a) Kong, C.; Min, S.; Lu, G. *ACS Catalysis* **2014**, *4*, 2763. (b) Gutiérrez, O.; Singh, S.; Schachtl, E.; Kim, J.; Kondratieva, E.; Hein, J.; Lercher, J. A. *ACS Catalysis* **2014**, *4*, 1487.

(42) (a) Can, M.; Armstrong, F. A.; Ragsdale, S. W. *Chem. Rev.* **2014**, *114*, 4149. (b) Lubitz, W.; Ogata, H.; Rüdiger, O.; Reijerse, E. *Chem. Rev.* **2014**, *114*, 4081. (c) Boer, J. L.; Mulrooney, S. B.; Hausinger, R. P. *Arch. Biochem. Biophys.* **2014**, *544*, 142. (d) Majumdar, A. *Dalton Trans.* **2014**, *43*, 12135. (e) Huynh, M. T.; Schilter, D.; Hammes-Schiffer, S.; Rauchfuss, T. B. *J. Am. Chem. Soc.* **2014**, *136*, 12385. (f) Pinder, T. A.; Montalvo, S. K.; Hsieh, C.-H.; Lunsford, A. M.; Bethel, R. D.; Pierce, B. S.; Darensbourg, M. Y. *Inorg. Chem.* **2014**, *53*, 9095.

(43) (a) Beck, R.; Shoshani, M.; Krasinkiewicz, J.; Hatnean, J. A.; Johnson, S. A. *Dalton Trans*. **2013**, *42*, 1461. (b) Robbie, A.; Cowley, A. R.; Jones, M. W.; Dilworth, J. R. *Polyhedron*, **2011**, *30*, 1849. (c) Ito, M.; Matsumoto, T.; Tatsumi, K. *Inorg. Chem.* **2009**, *48*, 2215. (d) Tennyson, A. G.; Dhar, S.; Lippard, S. J. *J. Am. Chem. Soc*. **2008**, *130*, 15087. (e) Melzer, M. M.; Jarchow-Choy, S.; Kogut, E.; Warren, T. H. *Inorg. Chem*. **2008**, *47*, 10187. (f) Redin, K.; Wilson, A. D.; Newell, R.; DuBois, M. R.; DuBois, D. L. *Inorg. Chem.* **2007**, *46*, 1268. (g) Zhu, W.; Marr, A. C.; Wang, Q.; Neese, F.; Spencer, D. J. E.; Blake, A. J.; Cooke, P. A.; Wilson, C.; Schröder, M. *Proc. Natl. Acad. Sci. U. S. A*. **2005**, *102*, 18280. (h) Schneider, J. J.; Spickermann, D.; Blaser, D.; Boese, R.; Rademacher, P.; Labahn, T.; Magull, J.; Janiak, C.; Seidel, N.; Jacob, K. *Eur. J. Inorg. Chem.* **2001**, *5*, 1371.

(44) (a) Iluc, V. M.; Laskowski, C. A.; Brozek, C. K.; Harrold, N. D.; Hillhouse, G. L. *Inorg. Chem.* **2010**, *49,* 6817. (b) Vicic, D. A.; Jones, W. D. *J. Am. Chem. Soc.* **1999**, *121*, 4070.

(45) (a) Mealli, C.; Midollini, S. *Inorg. Chem.* **1983**, *22*, 2785. (b) Pleus, R. J.; Waden, H.; Saak, W.; Haase, D.; Pohl, S. *J. Chem. Soc., Dalton. Trans.* **1999**, 2601. (c) Yao, S.; Milsmann, C.; Eckard, B.; Wieghardt, K.; Driess, M. *J. Am. Chem. Soc.* **2008**, *130*, 13536. (d) Cho, J.; Heuvelen, K. M. V.; Yap, G. P. A.; Brunold, T. C.; Riordan, C. G. *Inorg. Chem.* **2008**, *47*, 3931. (e) Inosako, A.; Kunishita, A.; Kubo, M.; Ogura, T.; Sugimoto, H.; Itoh, S. *Dalton Trans.* **2009**, 9410.

(46) (a) Kieber-Emmons, M. T.; Van Heuvelen, K. M.; Brunold, T. C.; Riordan, C. G. *J. Am. Chem. Soc.* **2009**, *131*, 440. (b) Pelties, S.; Herrmann, D.; de Bruin, B.; Hartl, F.; Wolf, R. *Chem. Commun.* **2014**, *50*, 7014.

(47) (a) Ref. 44a. (b) Xin, Q. X.; Wang, B. Y.; Jin, G. X. *Z. Naturforsch. B* **1996**, *51b*, 1197.

(48) (a) Ref. 45c. (b) Yao, S.; Hrobárik, P.; Meier, F.; Rudolph, R.; Bill, E.; Irran, E.; Kaupp, M.; Driess, M. *Chem. Eur. J.* **2013**, *19*, 1246.

(49) Cavallo, L.; Correa, A.; Costabile, C.; Jacobsen, H. *J. Organomet. Chem.* **2005**, *690*, 5407.

(50) (a) Harrold, N. D.; Corcos, A. R.; Hillhouse, G. L. *J. Organomet. Chem.* **2016**, *813*, 46. (b) Laskowski, C. A.; Bungum, D. J.; Baldwin, S. M.; Ciello, S. A. D.; Iluc, V. M.; Hillhouse, G. L. *J. Am. Chem. Soc.* **2013**, *135*, 18272. (c) Laskowski, C. A.; Morello, G. R.; Saouma, C. T.;

Cundari, T. R.; Hillhouse, G. L. *Chem. Sci*. **2013**, *4*, 170. (d) Laskowski, C. A.; Hillhouse, G. L. *Organometallics* **2009**, *28*, 6114.

(51) Bohm, V. P. W.; Gstottmayr, C. W. K.; Weskamp, T.; Herrmann, W. A. *Angew. Chem. Int. Ed*. **2001**, *40*, 3387.

(52) (a) Rodríguez-Delgado, A.; Cámpora, J.; Naz, A. M.; Palma, P.; Reyes, M. L. *Chem. Commun*. **2008**, 5230. (b) Cámpora, J.; Cartes, M. Á.; Rodríguez-Delgado, A.; Naz, A. M.; Palma, P.; Pérez, C. M. *Inorg. Chem.* **2009**, *48*, 3679.

(53) (a) Jafarpour, L.; Stevens, E. D.; Nolan, S. P. *J. Organomet. Chem.* **20**, *606*, 49. (b) Dible, B. R.; Sigman, M. S.; Arif, A. M. *Inorg. Chem.* **2005**, *44*, 3774.

(54) (a) Dible, B. R.; Sigman, M. S. *J. Am. Chem. Soc.* **2003**, *125*, 872. (b) Dorta, R.; Stevens, E. D.; Hoff, C. D.; Nolan, S. P. *J. Am. Chem. Soc.* **2003**, *125*, 10490.

(55) Dangaloc, M.; Petrov, P.; Vassilav, N. G. *J Organomet. Chem.* **2016**, *824*, 104.

(56) Wei, S.; Wei, X.-G.; Su, X.; You, J.; Ren, Y. *Chem. Eur. J.* **2011**, *17*, 5965.

(57) Bondi, A. *J. Phys. Chem.* **1964**, *68*, 441.

(58) Müller, A.; Jaegermann, W.; Enemark, J. H. *Coord. Chem. Rev.* **1982**, *46*, 245.

(59) Appleton, T. G.; Clark, H. C.; Manzer, L. E. *Coord. Chem. Rev.* **1973**, *10*, 335.

(60) Matsubara, K.; Ueno, K.; Shibata, Y. *Organometallics* **2006**, *25*, 3422.

(61) Liu, Z.-H.; Xu, Y.-C.; Xie, L.-Z.; Sun, H.-M.; Shen, Q.; Zhang, Y. *Dalton Trans.* **2011**, *40*, 4697.

(62) Lee, C. H.; Lutterman, D. A.; Nocera, D. G. *Dalton Trans.* **2013**, *42*, 2355.

(63) Laskowski, C. A.; Hillhouse, G. L. *Organometallics* **2009**, *28*, 6114.

(64) (a) Ito, Y.; Saegusa, T.; Tomita, S. *J. Am. Chem. Soc.* **1971**, *93*, 5656. (b) Cotton, F. A.; Zingales, F. *J. Am. Chem. Soc.* **1961**, *83*, 351. (c) Celik, M. A.; Dash, C.; Adiraju, V. A. K.; Das, A.; Yousufuddin, M.; Frenking, G.; Rasika Dias, H. V. *Inorg. Chem.* **2013**, *52*, 729. (d) La Pierre, H. S.; Arnold, J.; Bergman, R. G.; Toste, F. D. *Inorg. Chem.* **2012**, *51*, 13334. For a discussion of non-classical M-CO complexes see: (e) Lupinetti, A. J.; Strauss, S. H.; Frenking, G. *Progress in Inorganic Chemistry*; Karlin, K. D., Ed.; Wiley: New York, **2001**; Vol. 49, p 1.

(65) Ni(II)-Ni(II) complexes with bridging ligands that exhibit short Ni-Ni distances include: (a) $\{ClNi(\mu\text{-}C(TMS)PMe_3)\}_2$, 2.281(1) Å, König, H.; Menu, M. J.; Dartiguenave, M.; Dartiguenave, Y.; Klein, H. F. *J. Am. Chem. Soc*. **1990**, 112, 5351. (b) $[\{(IPr)Ni\}_2(\mu\text{-}Cl)(\mu\text{-}NMes)][B(Ar^F)_4]$, 2.2911(8) Å, Ref 63. (c) $\{Ni(NPh_2)_2\}_2$, 2.327(2) Å, Hope, H.; Olmstead, M. M.; Murray, B. D.; Power, P. P. *J. Am. Chem. Soc.* **1985**, *107*, 712. (d) $\{Ni(P^tBu_2)_2\}_2$, 2.417(3) Å, Kundu, S.; Brennessel, W. W.; Jones, W. D. *Inorg. Chem.* **2011**, *50*, 9443. (e) $[\{(IPr)Ni\}_2(\mu\text{-}Cl)(\mu\text{-}$

CHSiMe$_3$)][B(Ar^F)$_4$], 2.4312(10) Å, Laskowski, C. A.; Hillhouse, G. L. *Chem. Sci.* **2011**, *2*, 321. (f) [{(IPr)Ni}$_2$(μ-Cl)(μ-CPh$_2$)][B(Ar^F)$_4$], 2.4389(9) Å, Ref 65e.

(66) The change in coordination number between compounds **E** and **F** and compound **6** might also contribute to the change in the structure of the Ni_2S_2 core.

(67) (a) Seyferth, D.; Henderson, R. S.; Song, L.-C. *J. Organomet. Chem.* **1980**, *192*, C1. (b) Kubiak, C. P.; Eisenberg, R. *Inorg. Chem.* **1980**, *19*, 2726. (c) Ruffing, C. J.; Rauchfuss, T. B. *Organometallics* **1985**, *4*, 524. (d) Werner, H.; Luxenburger, G.; Hofmann, W. X.; Nadvornik, M. *J. Organomet. Chem.* **1987,** *323*, 161. (e) Birnbaum, J.; Godziela, G.; Maciejewski, M.; Tonker, T. L.; Haltiwanger, R. C.; Rakowski DuBois, M. *Organometallics* **1990**, *9*, 394. (f) Wang, L. S.; McDonald, R.; Cowie, M. *Inorg. Chem.* **1994**, *33*, 3735. (g) Tang, Z.; Nomura, Y.; Ishii, Y.; Mizobe, Y.; Hidai, M. *Inorg. Chim. Acta* **1998**, *267*, 73. (h) Kuwata, S.; Hidai, M. *Coord. Chem. Rev.* **2001**, *213*, 211. (i) Oster, S. S.; Lachicotte, R. J.; Jones, W. D. *Inorg. Chim. Acta* **2002**, *330*, 118.

(68) Ni(I)-Ni(I) complexes with bridging ligands exhibit short Ni-Ni distances in the range 2.314(1) - 2.3910(8) Å, see: (a) Ref. 43c, (b) Kriley, C. E.; Woolley, C. J.; Krepps, M. K.; Popa, E. M.; Fanwick, P. E.; Rothwell, I. P. *Inorg. Chim. Acta* **20**, *300*, 200. (c) Varonka, M. S.; Warren, T. H. *Organometallics* **2010***, 29*, 717.

(69) Sweeney, Z. K.; Polse, J. L.; Bergman, R. G.; Andersen, R. A. *Organometallics* **1999**, *18*, 5502.

(70) (a) Bianchini, C.; Mealli, C.; Meli, A.; Sabat, M. *Inorg. Chem.* **1986**, *25*, 4617. (b) Ienco, A.; Calhorda, M. J.; Reinhold, J.; Reineri, F.; Bianchini, C.; Peruzzini, M.; Vizza, F.; Mealli, C. *J. Am. Chem. Soc.* **2004**, *126*, 11954.

(71) Kato, H.; Seino, H.; Mizobe, Y.; Hidai, M. *J. Chem. Soc., Dalton Trans.* **2002**, 1494.

(72) (a) Ref. 44b. (b) Vicic, D. A.; Jones, W. D. *J. Am. Chem. Soc.* **1999**, *121*, 7606. (c) Kabe, T. *Hydrodesulfurization and Hydrodenitrogenation: Chemistry and Engineering*; Wiley-VCH: New York, **1999**.

(73) (a) Altwicker, E. R. *Chem. Rev.* **1967**, *67*, 475. (b) Hicks, R. G. *Org. Biomol. Chem*. **2007**, *5*, 1321. (c) Manner, V. W.; Markle, T. F.; Freudenthal, J.; Roth, J. P.; Mayer, J. M. *Chem. Commun.* **2008**, 256.

(74) Wallick, J.; Yap, G. P. A.; Riordan, C. G. *J. Am. Chem Soc.* **2013**, *135*, 14972.

(75) For a general description of air-sensitive techniques and equipment, see: Burger, B. J.; Bercaw, J. E. in *Experimental Organometallic Chemistry*; Wayda, A. L.; Darensbourg, M. Y. Eds.; ACS Symposium Series 357, American Chemical Society; Washington, DC. 1987; pp 79-89.

(76) Pangborn, A. B.; Giardello, M. A.; Grubbs, R. H.; Rosen, R. K.; Trimmers, F. *J. Organometallics* **1996**, *15*, 1518.

(77) Fredenhagen, K.; Cadenbach, G. *Z. Anorg. Allg. Chem*. **1926**, *158*, 249.

(78) Sheldrick, G. M. *Acta Cryst.* **2008** *A64*, 112.

(79) M. J. Frisch, G. W. Trucks, H. B. Schlegel, G. E. Scuseria, M. A. Robb, J. R. Cheeseman, J. A. Montgomery, Jr., T. Vreven, K. N. Kudin, J. C. Burant, J. M. Millam, S. S. Iyengar, J. Tomasi, V. Barone, B. Mennucci, M. Cossi, G. Scalmani, N. Rega, G. A. Petersson, H. Nakatsuji, M. Hada, M. Ehara, K. Toyota, R. Fukuda, J. Hasegawa, M. Ishida, T. Nakajima, Y. Honda, O. Kitao, H. Nakai, M. Klene, X. Li, J. E. Knox, H. P. Hratchian, J. B. Cross, V. Bakken, C. Adamo, J. Jaramillo, R. Gomperts, R. E. Stratmann, O. Yazyev, A. J. Austin, R. Cammi, C. Pomelli, J. W. Ochterski, P. Y. Ayala, K. Morokuma, G. A. Voth, P. Salvador, J. J. Dannenberg, V. G. Zakrzewski, S. Dapprich, A. D. Daniels, M. C. Strain, O. Farkas, D. K. Malick, A. D. Rabuck, K. Raghavachari, J. B. Foresman, J. V. Ortiz, Q. Cui, A. G. Baboul, S. Clifford, J. Cioslowski, B. B. Stefanov, G. Liu, A. Liashenko, P. Piskorz, I. Komaromi, R. L. Martin, D. J. Fox, T. Keith, M. A. Al-Laham, C. Y. Peng, A. Nanayakkara, M. Challacombe, P. M. W. Gill, B. Johnson, W. Chen, M. W. Wong, C. Gonzalez, and J. A. Pople, Gaussian, Inc., Wallingford CT, 2004.

Chapter 3 - Reaction of {(IPr)Ni(μ-S)}$_2$ with Molecular Hydrogen

3.1. Hydrogenation of M-S-M Complexes

Metal-sulfide catalysts, particularly heterogeneous catalysts, have been intensively studied for hydrodesulfurization and hydrodenitrogenation reactions.[80] These processes are performed with heterogeneous catalysts on an industrial scale to remove S- and N- containing impurities from petroleum feedstocks to minimize SO_x and NO_x emissions during combustion as fuel (Figure 27). The catalysts employed are typically MoS_2 doped with Ni or Co.[81] Ni is believed to improve the catalytic activity in two ways. First, Ni can share electrons with Mo centers to promote activity at Mo.[82] Second, Ni can be incorporated at the edges of the two dimensional lattice as square pyramidal sites, which have a 5 kcal/mol lower activation barrier than Mo sites for thiophene hydrogenolysis.[83]

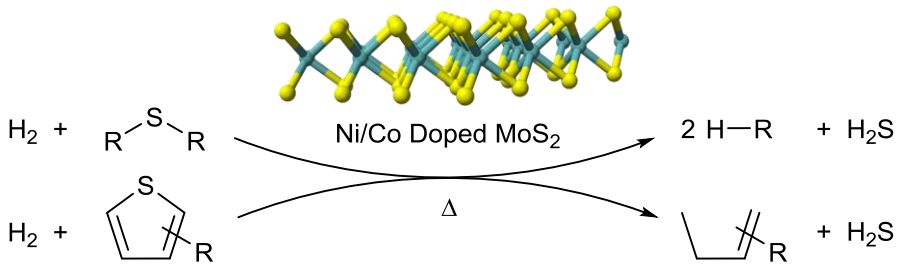

Figure 27. Hydrodesulfurization reactions with the heterogeneous Ni/Co-doped MoS_2 catalyst.

A key step in hydrodesulfurization is the activation of hydrogen. Theoretical investigations of MoS_2 catalysts have predicted that molecular hydrogen is activated heterolytically by the Mo-S-Mo units to form Mo-H and Mo-SH functionalities.[84] These studies implicate Mo-S-Mo units as the active sites and imply that they are essential for the activation of H_2 (Figure 28). Mo-S-Mo sites located at the edges of the 2D lattice, where the unsaturated coordination sphere of the metal can aid in the adsorption and cleavage of H_2, are thought to be

more active than those at internal, more coordinatively saturated metal positions within the lattice. Ni has more d electrons than Mo, and is expected to be more stable in the low-coordination-number sites at the edges of the lattice.

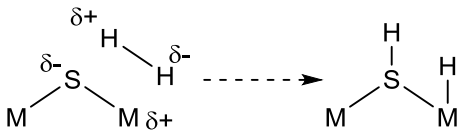

Figure 28. Hypothesized H_2 activation pathway for heterogenous catalysts.

Heterogeneous catalysts, including MoS_2 and WS_2 systems doped with Ni or Co, have been studied *in situ* and the presence of M-SH groups has been demonstrated by neutron scattering and solid state NMR studies. However, M-H units were not detected. An M-H group has only been observed in a RuS_2 catalyst system.[85] The heterogeneous nature of these catalysts limits the methods to characterize H atoms on the surface, and discrete model complexes have been investigated to understand the H_2 coordination and activation.[86]

3.2. Dinuclear Model Systems To Study H_2 Activation

Dinuclear Ni complexes supported by chelating phosphine ligands have been studied for the sulfur-containing heterocycle activation step of hydrodesulfurization (Scheme 6).[87] The Ni_2S_2 and Ni_2S complexes produced are byproducts of disproportionation or aggregation reactions, rather than intermediates in a catalytic cycle. None of those species are reported to react with H_2, although they can be interconverted to hydrosulfide complexes through acid/base reactions, with a concomitant change in the overall charge.[88]

Scheme 6. Dinuclear Ni complexes studied for hydrodesulfurization reactions.

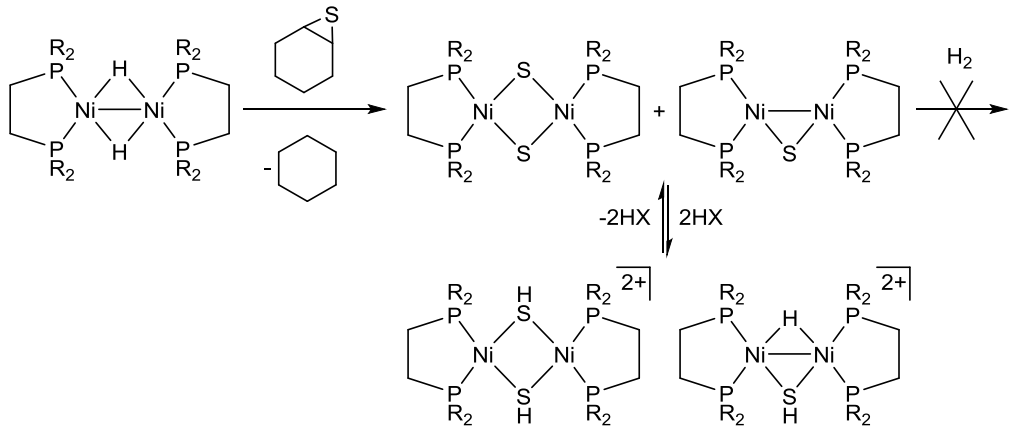

Model $Cp_2Mo_2S_4$ complexes react with H_2 to form Mo(μ-SH)Mo species, which in turn react with unsaturated S- and N- containing substrates to yield Mo(μ-SR)Mo and Mo(μ-SC=NR)Mo species (Scheme 7).[89] The H_2 activation step involves addition of H_2 across the S-S bond (i.e., S-S bond reduction) to form two SH ligands. Multiple isomers are possible in $Mo(S)_2(SH)_2Mo$ systems.[90] The presence of several product isomers, dynamic reorganization in solution, and multiple side reactions complicate efforts to identify the exact active Mo species in solution.[91]

Scheme 7. Model dinuclear Mo complexes studied for hydrodesulfurization reactions.

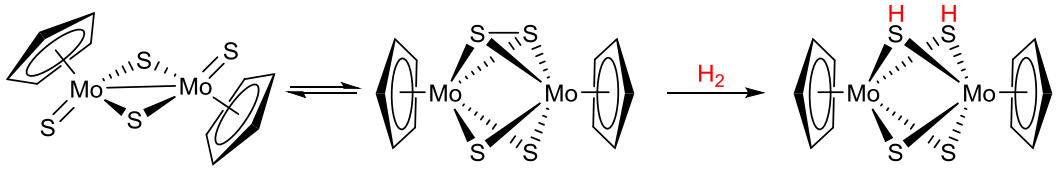

The dinuclear $\{MeC(CH_2PPh_2)_3Rh(\mu\text{-}S)\}_2^{2+}$ system reacts reversibly with H_2 at room temperature (Scheme 8).[92] DFT calculations predict barriers of 7.2 and 8.0 kcal/mol for the two sequential heterolytic H_2 additions across the Rh-S bonds.[92a] VT-NMR reveals the formation of a

mixed hydride μ-hydrosulfide intermediate after the first H_2 activation, in which all P atoms are equivalent on the NMR time scale at -80 °C. DFT calculations predict the existence of this intermediate along with two other local minima, a bis-μ-hydrosulfide complex and a mixed μ-hydride/μ-hydrosulfide/μ-sulfide complex. These species are higher in energy than the hydride-hydrosulfide by 12.3 and 11.6 kcal/mol respectively, but are still energetically accessible. Kinetic observations support the existence of the bis-hydrosulfide, the formation of which would require less reorganization of the core Rh_2S_2 atoms compared to the μ-H/μ-SH/μ-S species. Interconversion of these species requires that the H atom is able to migrate with low energy barriers.

Scheme 8. Hydrogenation of dinuclear Rh(μ-S) species.

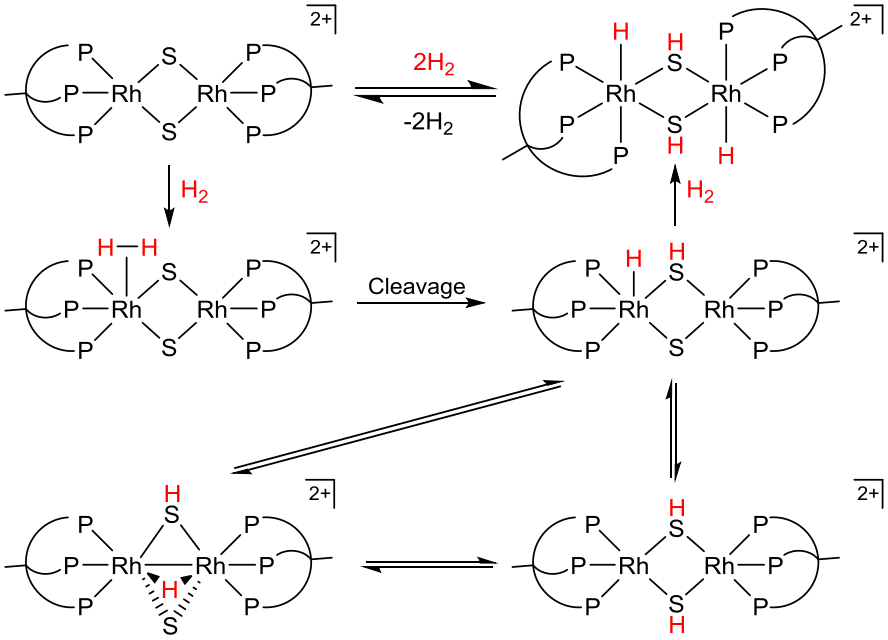

The dinuclear complex $\{(Ph_3P)_2Ir(\mu\text{-}S)\}_2$ reacts with two equiv of H_2 (Scheme 9).[93] This process believed to proceed by oxidative addition at one Ir center followed my H migration to the second Ir center, which produces two hydride ligands and oxidizes the Ir centers from the formally 2+ to the 3+ oxidation states. Computations indicate the second step can occur via two

pathways with similar barriers, 16.5 and 21.0 kcal/mol. The lower energy pathway is the addition of H_2 across the S-S vector to form a bis-hydrosulfide, followed by H migration to produce the hydride and hydrosulfide units. The higher energy pathway is coordination of H_2, followed by heterolytic H-H bond activation to produce a bridging hydride and hydrosulfide ligands. This cleavage is postulated to happen across the Ir-S bond to form a transient terminal hydride, which reorganizes to the bridging hydride species. Addition of D_2 to a $\{(Ph_3P)_2(H)Ir(\mu\text{-}S)\}_2$ or H_2 to the corresponding deutero-complex results in isotopic scrambling at -20 °C, preventing a KIE from being determined.

Scheme 9. Dinuclear Ir complex activates H_2 in both homolytic and heterolytic manners.

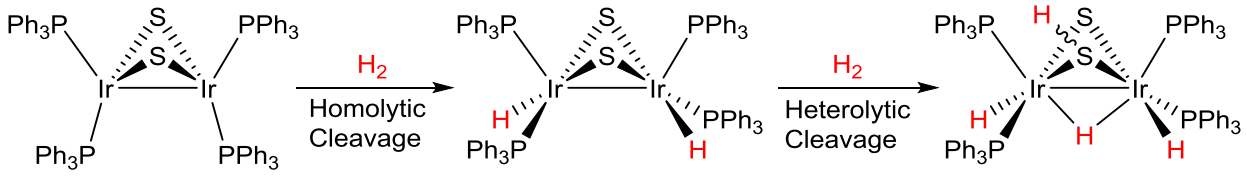

In each of these models, isomerization and dynamic reorganization complicate investigation of the mechanistic details of the H_2 activation. Chapter 2 discussed the hydrogenation reaction of $\{(IPr)Ni(\mu\text{-}S)\}_2$ (**6**) to produce $\{(IPr)Ni(\mu\text{-}SH)\}_2$ (**7**, Scheme 10).[94] This system provides a simple and well-behaved reaction to study the activation of H_2 and develop an improved understanding of how M_2S_2 type complexes react with this substrate.

Scheme 10. Hydrogenation of {(IPr)Ni(μ-S)}$_2$ (**6**) to {(IPr)Ni(μ-SH)}$_2$ (**7**).

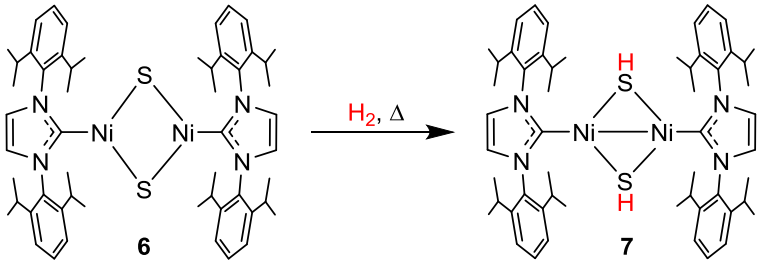

In order to gain a fundamental understanding of this system, a two-pronged approach was utilized. The reaction kinetics were first investigated to establish the rate law, and this information then informed a subsequent computational study. The results show that the rate limiting step is the activation of H_2 by the intact dimeric **6**, which occurs in a heterolytic manner across the Ni-S bond and is followed by a hydrogen migration to form the bis-hydrosulfide product.

3.3. Kinetic Investigation

The goal of the kinetic study was to determine the rate law, to establish if the intact dimer reacts directly with H_2 or must first dissociate into monomeric fragments, and if the H_2 activation is the rate determining step. The reaction of **6** with H_2 to produce **7** was studied by ^{1}H NMR by monitoring the imidazole resonances of the NHC of starting material **6** and the product **7**, with C_6Me_6 as an internal standard. ^{1}H NMR was selected as the preferred method to assay because the imidazole resonances of the starting material and product are sharp and well separated from other resonances.

The reaction order in **6** was determined by examining its consumption during the reaction, and fitting the kinetic data to various rate laws. To determine the order in H_2, runs at multiple pressures were performed. Reactions at 1 atm of H_2 (or D_2) were carried out in a J

Young NMR tube, and reactions at 3 and 6 atm were carried out in a Fischer Porter bottle. Details are provided in the Experimental Section.[95]

The consumption of {(IPr)Ni(μ-S)}$_2$ **6** and the production of {(IPr)Ni(μ-SH)}$_2$ **7** were monitored over the course of the reaction. The only observed species were **6**, **7**, and thermal decomposition products from **7**. At no point were any intermediate species observed. **7** was independently verified to slowly decompose at 80 °C with a first order rate constant of ca. 10^{-6} s^{-1}, to produce IPr=S and an uncharacterized paramagnetic product. This decomposition precluded kinetic analysis by observation of the growth of **7**. **6** is stable at 80 °C, but will decompose slowly at 90 °C. A sample reaction trace for the reaction of **6** with H_2 to produce **7** is shown in Figure 29.

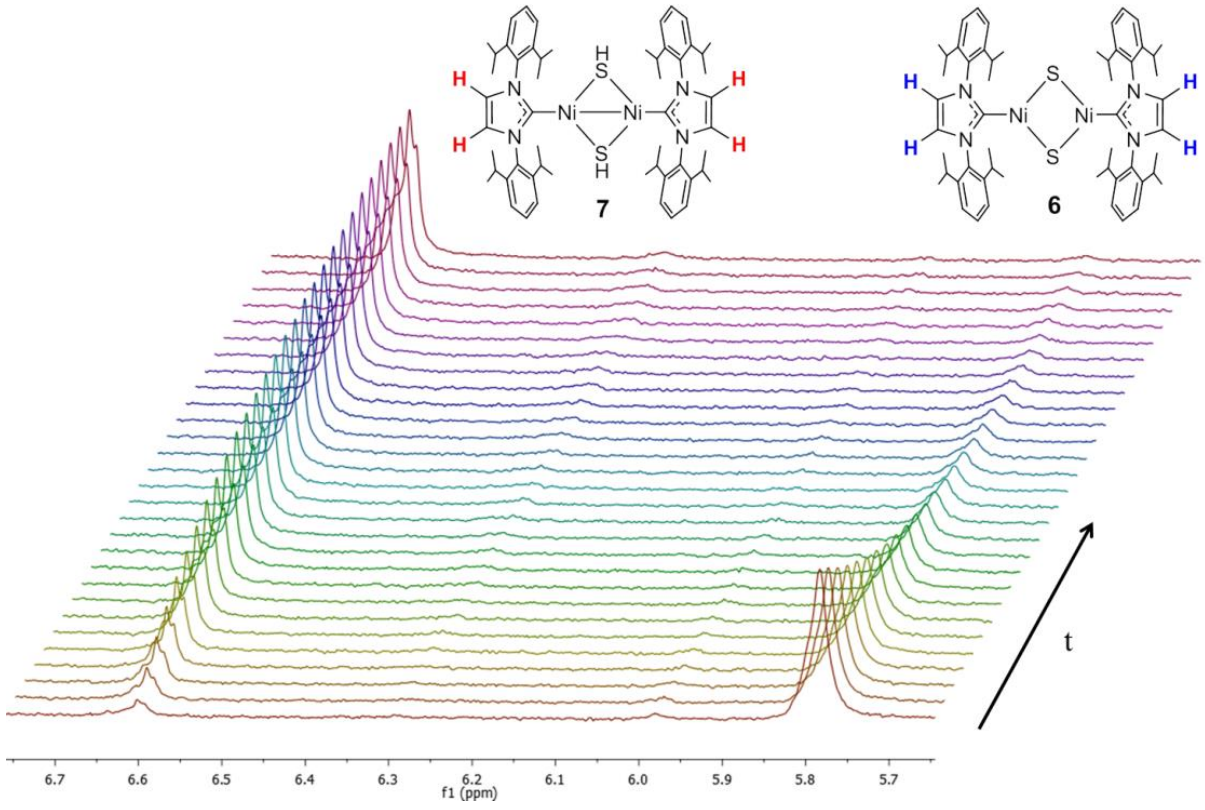

Figure 29. ^{1}H NMR monitoring of the reaction of **6** with H_2 to produce **7**. The imidazole region of the spectrum is shown. Concentration vs time data corresponding to these spectra are given in Figure 30. Conditions were 80 °C, 6 atm H_2, $[\mathbf{6}]_0$ = 0.0037 M.

3.3.1. Determination of Rate Law

The reaction order in **6** was determined by attempting to fit the data to different rate laws, including: 1) a 1st order rate law, which would be expected for direct reaction of the dinuclear {(IPr)Ni(μ-S)}$_2$ structure with H_2; 2) a ½ order rate law, which would be operative if there is dissociation of **6** into a mono-nuclear IPrNi=S species prior to the rate determining step; and 3) a 2nd order rate law, representing the cooperative intermolecular activation of H_2 by two molecules of **6**. These rate laws and their linear forms are shown in Table 3, and fits of the experimental data to 1st, ½, and 2nd order rate laws are shown in Figure 30.

Table 3. Rate laws and their linear forms for the consumption of {(IPr)Ni(μ-S)}$_2$ (**6**).

	Rate Law	Linear Form
1st Order	$\frac{-\mathrm{d}[\mathbf{6}]}{\mathrm{dt}} = \mathrm{k}_{obs}[\mathbf{6}]^1$	$\ln[\mathbf{6}]_t = \ln[\mathbf{6}]_0 - \mathrm{k}_{obs} \cdot t$
½ Order	$\frac{-\mathrm{d}[\mathbf{6}]}{\mathrm{dt}} = \mathrm{k}_{obs}\sqrt{[\mathbf{6}]}$	$\sqrt{[\mathbf{6}]_t} = \sqrt{[\mathbf{6}]_0} - \frac{1}{2}\mathrm{k}_{obs} \cdot t$
2nd Order	$-\frac{1}{2}\frac{\mathrm{d}[\mathbf{6}]}{\mathrm{dt}} = \mathrm{k}_{obs}[\mathbf{6}]^2$	$\frac{1}{\sqrt{[\mathbf{6}]_t}} = \frac{1}{\sqrt{[\mathbf{6}]_0}} + 2k_{obs} \cdot t$

The kinetic data are best fit by the first order rate law, rate = k_{obs}[**6**], as assessed by the R^2 values (Figure 29). This first order dependence indicates that the dinuclear species **6** remains intact in the rate limiting step.

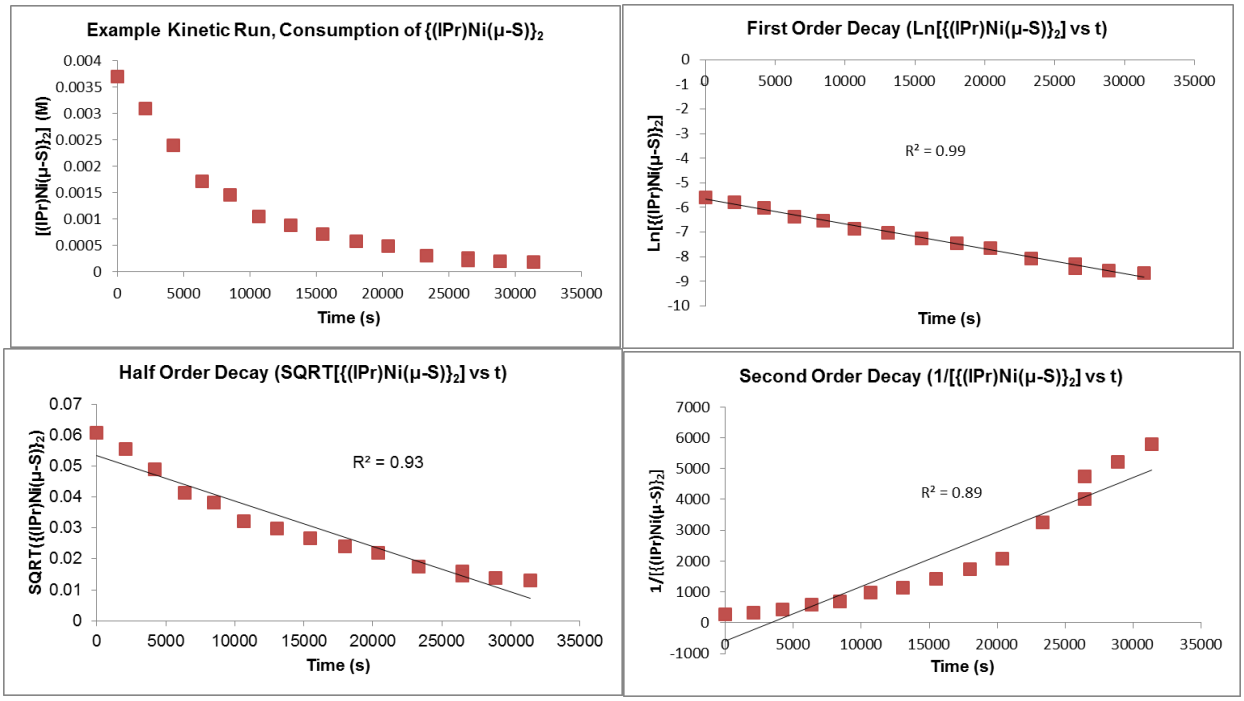

Figure 30. Analysis of the kinetic data for the reaction of **6** with H_2 to form **7** from Figure 29. These data are from the experiment shown in Figure 29. (a) Plot of observed concentration of [**6**] versus time. This data set was fit by rate laws that are (b) 1st order, (c) ½ order, or (d) 2nd order in [**6**], with 1st order demonstrating the closest fit by R^2 value. Conditions were 80 °C, 6 atm H_2, $[Ni_2S_2]_0$ = 0.0037 M.

Kinetic runs at different H_2 pressures were performed in order to determine the order of H_2 in the reaction (Figure 31). The kinetic data show a linear correlation of the reaction rate and increasing H_2 pressure, indicative that the reaction is first order in H_2.[96] Therefore the full rate law is:

$$\text{Rate} = k[Ni_2S_2]P_{H2}$$

$$k = 7.4 \times 10^{-6}\ s^{-1}atm^{-1} \text{ at } 80\ °C$$

This rate law implies that H_2 addition occurs during or before the rate limiting step. These two options can be distinguished through the kinetic isotope effect (KIE).

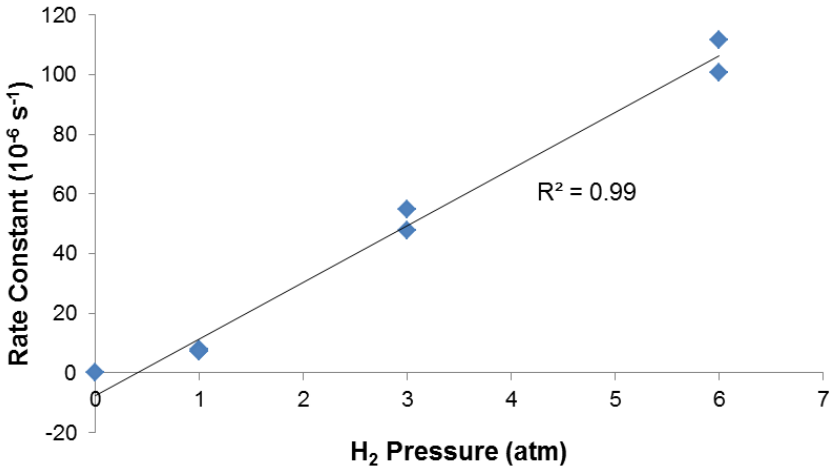

Figure 31. Plot of observed rate constant versus H_2 pressure for the reaction of **6** with H_2. Conditions were 80 °C and $[\mathbf{6}]_0 \approx 0.0037$ M.

3.3.2. Determination of Kinetic Isotope Effect

The potential reaction of **7** with D_2 was investigated by ^{1}H NMR to determine if isotope scrambling occurs on the time scale of the hydrogenation reaction. There is no change in the integration of the μ-SH resonance of **7** relative to the other integral values after 10 hours at 80 °C, typical conditions for the hydrogenation of **6**. This result shows that there is no formation of $\{(IPr)Ni(\mu\text{-}SD)\}_2$ and therefore no isotope scrambling in the system under those conditions.

The rate of the reaction of **6** with D_2 was determined by ^{1}H NMR. In these experiments the (μ-SH) resonance was not observed, confirming the incorporation of D_2 at this site. Duplicate runs at 1 atm D_2 yielded a k value of 4.2 (1) x 10^{-6} $s^{-1}atm^{-1}$, corresponding to a KIE of 1.8 (1). This KIE value is characteristic of a primary isotope effect, and provides evidence that H-H bond cleavage occurs during the rate limiting step of this reaction.

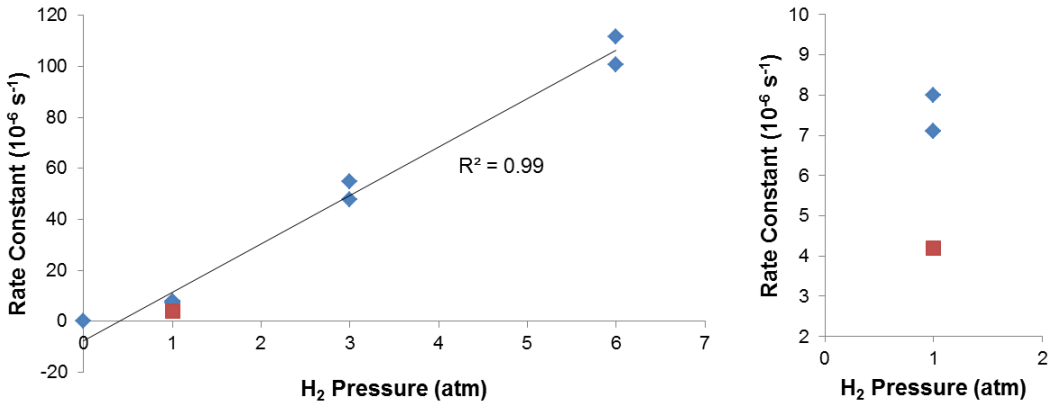

Figure 32. (a) Plot of observed rate constant versus H_2 (blue) and D_2 (red) pressure for the reaction of **6** with H_2. (b) Expansion of the 1 atm data from (a). Conditions were 80 °C and $[\mathbf{6}]_0 \approx$ 0.0037 M.

The 1st order dependence of the reaction rate on **6** indicates that the intact dimer is the active species in the reaction. The primary KIE and 1st order dependence of the reaction rate on H_2 pressure indicate that there is H-H bond cleavage in the rate determining step. However, the kinetic results do not provide detailed information about the transition state or how the H-H bond is cleaved, and therefore a computational study was performed to address these issues.

3.4. Computational Investigation

DFT calculations was undertaken to elucidate the electronic structures of **7**, **6**, and the reaction pathway of the hydrogenation.

3.4.1. Electronic Structure of {(IPr)Ni(μ-SH)}$_2$ (7)

The electronic structure of **7** is straightforward. The complex contains two formally 3-coordinate Y-shaped Ni(I) d^9 centers. Each Ni(I) should be paramagnetic, based on the presence of one unpaired electron in the expected orbital diagram (Figure 33).

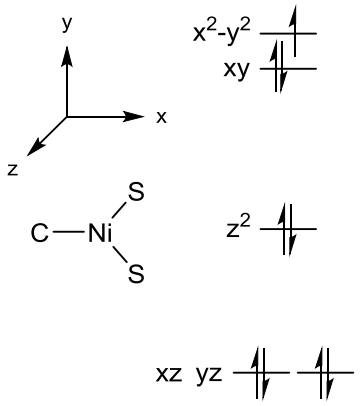

Figure 33. Predicted Orbital Diagram for Mononuclear 3-Coordinate Y-Shaped Ni(I) d^9 center.[97]

Complex **7** exhibits sharp, well resolved ^{1}H and ^{13}C NMR spectra, and the chemical shift values are consistent with an overall diamagnetic structure. Each Ni(I) center has a single unpaired electron, and these pair up to produce a Ni-Ni bond and overall singlet state (Figure 34). The Ni-Ni distance in the solid state falls within the range observed for other σ-bonded Ni(I)-Ni(I) complexes.[98] DFT ONIOM calculations show that the HOMO is a Ni-Ni σ bond for both the α and β spins, and the LUMO is a σ* orbital, corroborating the presence of a σ bond. The S atoms are each connected to two Ni atoms and one H atom, and can be described as covalently bonded to one Ni while acting as a Lewis base to the other Ni center.

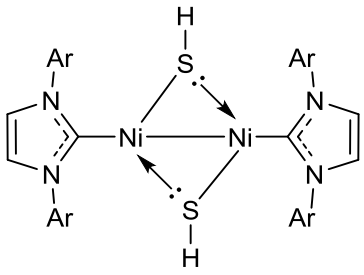

Figure 34. Electronic Structure of dinuclear Ni(I) complex $\{(IPr)Ni(\mu\text{-}SH)\}_2$ (**7**).

3.4.2. Electronic Structure of $\{(IPr)Ni(\mu\text{-}S)\}_2$ (6)

The electronic structure of **6** is more complex. The geometry of the Ni centers is essentially unchanged from **7**. The bridging sulfide ligands are formally 2^- ligands and the Ni centers are formally Ni(II), d^8 centers. Several mononuclear 3-coordinate Y-shaped Ni(II) d^8 complexes are known, and these species are high spin (Figure 35).[99] The crystal-field splitting parameter is small, and less energy is required to populate the d_{x2-y2} than to pair in the d_{xy} orbital, which results in a high-spin triplet ground state.

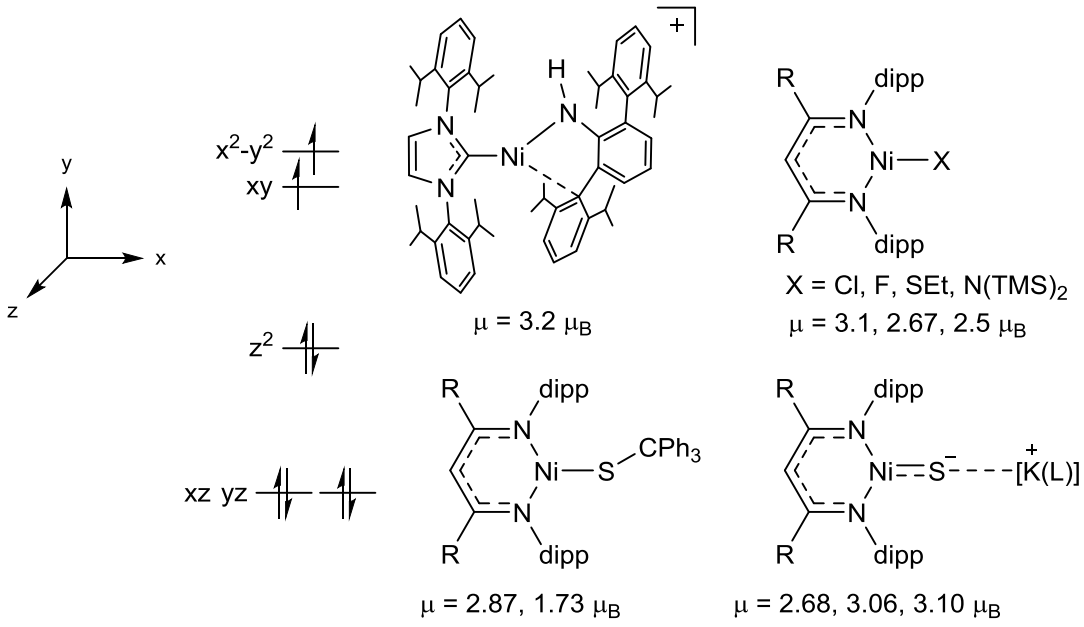

Figure 35. Orbital diagram for and selected examples of mononuclear 3-coordinate Y-shaped high-spin Ni(II) d^8 complexes.

Complex **6** appears to be diamagnetic. The ^{1}H NMR resonances for **6** appear in the normal range (δ 10-0), although the isopropyl resonances are broad and the ^{1}H NMR spectrum is unchanged over the temperature range of 210 to 353 K. The ^{13}C NMR spectrum contains chemical shifts in the normal range (δ 200-0), consistent with a diamagnetic complex, although the carbene carbon resonance was not located. SQUID analysis of **6** was performed on crystalline material and no bulk paramagnetism was observed down to 10 K. EPR analysis of **6**

was performed at 77 K, and no paramagnetic species were observed. Collectively these results imply that neither the ground state, nor a low-lying excited state, have a paramagnetic electronic structure.

Assuming each Ni center has the orbital splitting shown in Figure 35, the 4 electrons could be paired in two possible ways. First, the Ni centers could couple 4 electrons between them, to produce a singlet spin state and a Ni=Ni double bond. However the Ni-Ni distance of 2.3666(5) Å in **6** is in the same range as those in **7** and other antiferromagnetically coupled Ni(I)-Ni(I) complexes,[98] while a much shorter distance would be expected for a Ni(II)=Ni(II) compound. The average Co=Co double bond length is 2.31 Å in dinuclear doubly-bonded Co complexes, which is 6% shorter than the typical Co-Co single bond lengths (2.46 Å).[100] Furthermore, the Ni-S-Ni angle of 68.8° should promote anti-ferromagnetic coupling due to the acuteness of the angle, as has been calculated for bridging alkoxide complexes.[101] To date, neither a Ni=Ni double bond[102] nor coupling of triplet Ni centers in a dinuclear species have been reported.[103] Alternatively, the single electrons in the d_{xy} and d_{x2-y2} orbitals are paired in the d_{xy} orbital, resulting in two diamagnetic Ni centers. However since the Ni geometry of **6** is essentially unchanged from **7**, the orbital order and energy differences would be expected to be very similar.

3.4.3. Choice of Functional Method

A panel of density functionals was tested to determine which would be most suitable for analysis of the electronic structure of **6** (Table 4). A truncated model complex $\{(L)Ni(\mu\text{-}S)\}_2$ (L = 1,3-dimethyl-imidazolin-2-ylidene) was used for faster test calculations (Chart 3). Replacement of the N-Ar groups of **6** with Me groups should not significantly alter the electronic structure of the Ni_2S_2 core. Different types of functionals were screened, including: 1) Hartree-Fock (HF) method; 2) M06 and M06-2X;[104] 3) B97D and B97D3;[105] 4) BHandHLYP;[106] 5) BP86;[107] 6) BLYP;[108] 7) B3LYP;[109] 8) and B3PW91.[110]

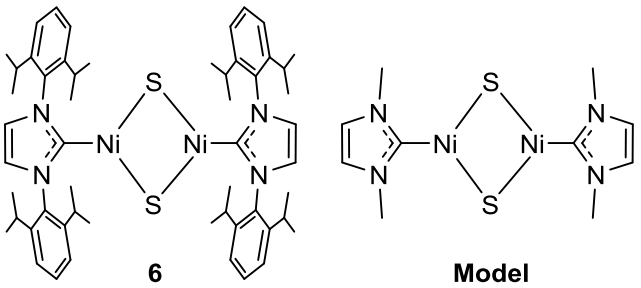

Chart 3. Full and truncated model complexes used for DFT calculations.

Of those functionals surveyed, BP86 was the most accurate in reproducing the crystal structure geometry, predicting Ni-Ni, Ni-S, and Ni-C bond distances for the model compound that are within 0.01 Å of the experimental distances for **6**, consistent with literature reports that this functional is quite accurate in geometry optimization (Table 4).[111] BLYP, B97D(3), and B3PW91 were also accurate to within 1% for all metrical parameters, which is within the expected errors of the calculation. Among the BP86, BLYP, B97D, B97D3, and B3PW91 functionals, B3PW91 contains the electron exchange component that is closest to an exact solution to the wavefunction.[110] B3LYP is the most frequently used functional, and for most cases it calculates results quickly and reasonably accurately. However, B3LYP does not reproduce the geometry of **6** as well as other functionals examined, within 2% for all metrical parameters, perhaps because the parameterization of the functional was based on corrections optimized for small molecules.[112] B3PW91 has been shown to give better results for larger molecules and metal-containing systems,[113] and since it gave good geometric results it was chosen for further study of **6**.

Table 4. Comparison of experimental and DFT-calculated distances for different functionals. Experimental distances are from the solid state structure of **6**, while DFT optimizations were performed on the truncated model complex.

	Exp	BP86	BLYP	B97D	B97D3	B3PW91	B3LYP	M06	BHandHLYP	HF	M06-2X
Ni-Ni	2.37	2.36	2.39	2.35	2.37	2.39	2.43	2.42	2.31	2.27	2.61
Ni-S	2.09	2.11	2.13	2.11	2.12	2.11	2.12	2.11	2.07	2.08	2.19
Ni-C	1.91	1.89	1.91	1.88	1.87	1.88	1.89	1.87	1.94	2.03	1.95

DFT calculations with B3PW91 and 6-31+G(d) as functional and basis set respectively predicted that several spin states separated by small energy differences are accessible for **6** (Figure 36). The predicted energetic order of spin states is Trip (0) < OSS (3.13) < CSS (5.69), where Trip = Triplet, OSS = Open Shell Singlet, and CSS = Closed Shell Singlet and the free energies are given in kcal/mol. A quintet spin state was also investigated, however, the optimized structure was very poor (Ni-Ni distance 2.50 Å). For an ONIOM calculation with the full IPr ligand, the energy gap values were comparable to the truncated ligand model: Trip (0) < OSS (1.82) < CSS (5.00) in kcal/mol. This spin state order is maintained across all functionals examined, with slight differences in relative energy spacing.

All three spin states have three filled d-orbitals on each Ni center. In addition, the triplet state has a Ni-Ni sigma bond and one unpaired electron on each Ni with the same spin; the open shell singlet has a Ni-Ni sigma bond and one unpaired electron on each Ni with opposite spins; and the closed shell singlet has no Ni-Ni bond and a paired set of electrons localized on each Ni.

However, as noted above, NMR, EPR, and SQUID data clearly establish that **6** has a diamagnetic ground state. In the Ni_2S_2 core of **6**, the atoms have close contacts with high orbital overlap, giving rise to the potential for a highly coupled system. As all of the DFT functionals surveyed produced the same spin state order, it is likely that the inability to predict the correct ground state reflects the limitations of the DFT method in dealing with such highly

correlated systems. Therefore, a more advanced multi-configurational SCF method is required to obtain a more accurate description of the electronic structure of **6.**

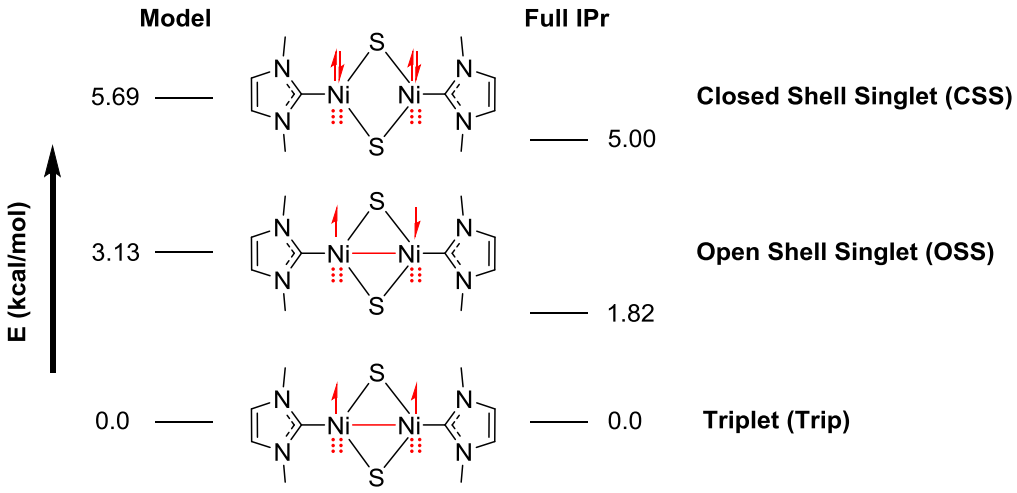

Figure 36. Spin states and energy levels for B3PW91/6-31+G(d)-optimized complexes with truncated model and full IPr ligands.

3.4.4. Multi-Configurational Electronic Structure Calculations

Complete Active Space Self Consistent Field (CASSCF)[114] is a method that can handle highly correlated systems, especially open-shell systems and ground states that are quasi-degenerate. These calculations require an input of a specified number of orbitals and electrons, the "Active Space." A DFT method is first used to calculate preliminary HF orbitals of a complex, and those orbitals with appropriate metal and ligand-based character are then selected as inputs for a CASSCF calculation. From these inputs a linear combination of configuration determinants is used to approximate the exact wavefunction. In CASSCF, coefficients of both the determinants and the basis functions in the molecular orbitals are varied, while in DFT only a single determinant is used and the molecular orbitals are varied. For CASSCF, all possible permutations of the electrons in the active space orbitals are calculated, with each permutation weighted and combined to yield the overall electronic structure. This is

similar to the aromatic π-system of benzene, which is made from the combination of p_π orbitals on C atoms, and could be represented by resonance structures with alternating single and double bonds.

CASSCF analysis was performed on the CSS, OSS, and Trip states for the truncated model system. The coordinates from B3PW91 geometry optimizations were used as the input coordinates. A general HF wavefunction description of each spin state was first calculated. Orbitals close to the HOMO/LUMO gap were comprised primarily of Ni and S orbitals (no NHC-based orbitals). Eight orbitals and eight electrons were selected as the active space to provide good coverage of these Ni and S based orbitals, while also being not inordinately computationally demanding (Figure 37).

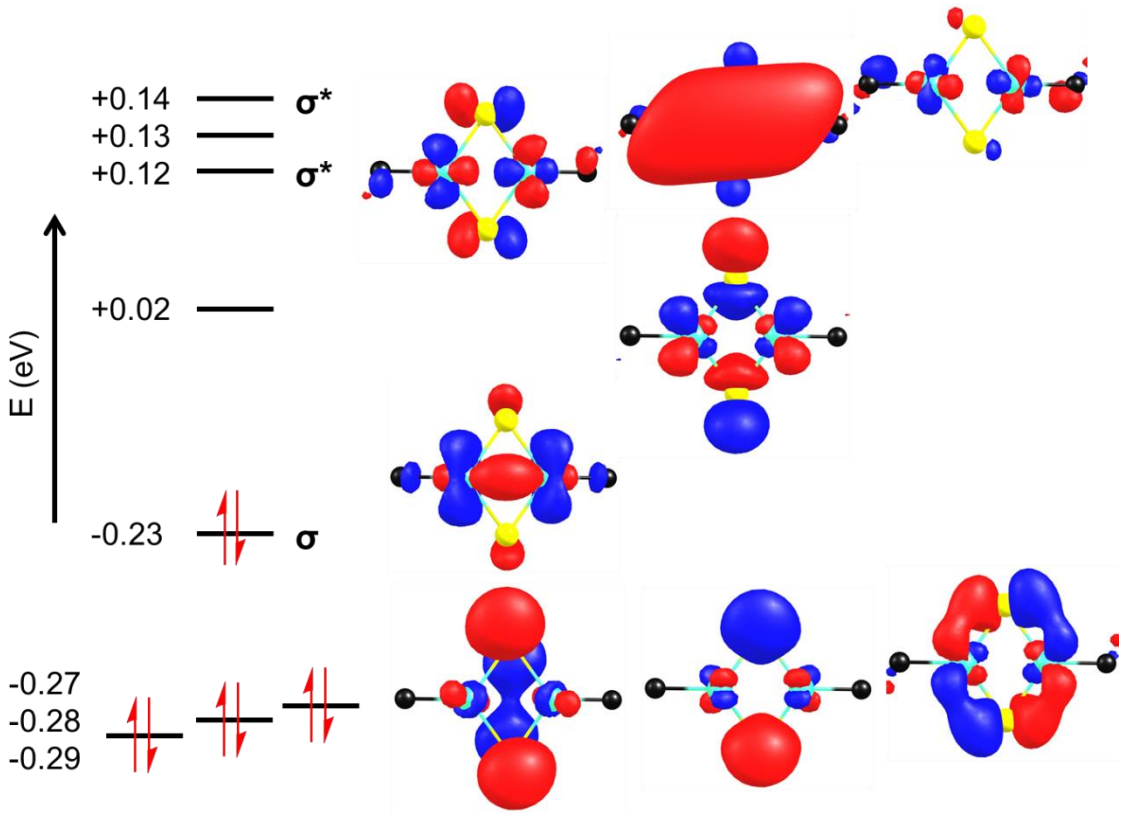

Figure 37. Active space orbitals used for closed shell singlet CASSCF calculation. Orbitals were determined in GAMESS by the HF method, using the truncated $\{(L)Ni(\mu\text{-}S)\}_2$ (L = 1,3-dimethyl-imidazolin-2-ylidene) complex.

CASSCF analysis of the CSS and OSS spin states produced an electronic structure that has two filled orbitals, four singly occupied molecular orbitals, and two empty orbitals (Figure 38). The four SOMOs have Ni-Ni σ, δ*, δ, and σ* character respectively. The two unpaired electrons on each Ni center antiferromagnetically couple across the Ni-Ni vector to produce an overall singlet spin state. Despite this antiferromagnetic coupling of triplet centers, the formal bond order is 0, since there are equal numbers of bonding and antibonding electrons. This is a rare example of antiferromagnetic coupling in two triplet Ni centers. The presence of two unpaired electrons on each Ni center in **6** may explain the temperature-independent broadness of the isopropyl ^{1}H NMR resonances and the inability to locate the carbene C ^{13}C NMR resonance noted above.[115]

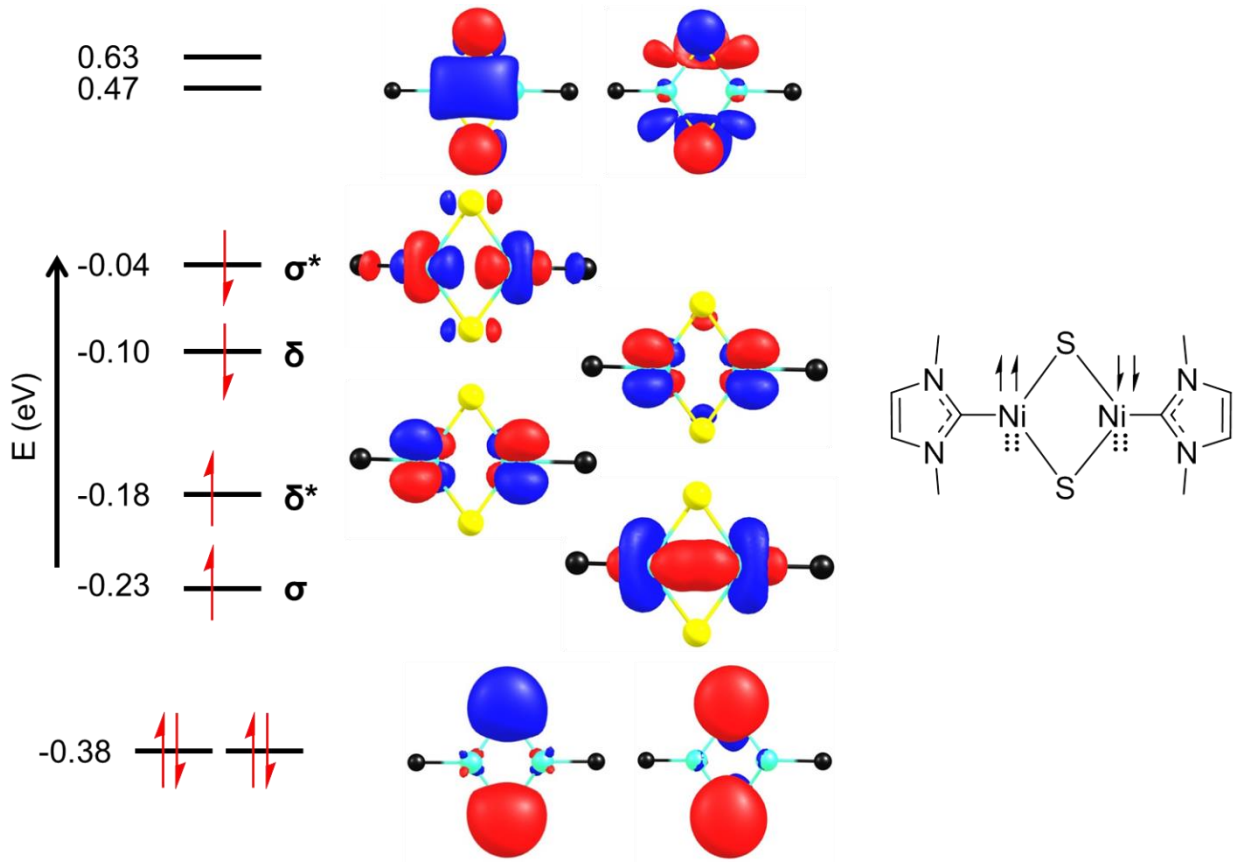

Figure 38. Ground state electronic structure of **6** determined by CASSCF analysis of the CSS and OSS spin states.

The orbital diagram produced from the CASSCF analysis is similar to that derived from the Angular Overlap Model (Figure 39).[116] The AOM molecular orbitals are produced by the union of two monomeric high-spin Ni(II) fragments, each with two unpaired electrons in the d_{xy} and d_{x2-y2} orbitals, which are significantly above the d_{xz}, d_{yz}, and d_{z2} orbitals. The bonding and antibonding combinations of d_{xy} and d_{x2-y2}, which exhibit σ- and π-symmetries, are very close in energy and are all singly occupied. The primary discrepancy between the CASSCF and AOM diagrams is that CASSCF has δ and δ* orbitals based on $d_{yz,}$ while AOM has π and π* orbitals based on d_{xy}. This discrepancy could arise from the HF-calculated orbitals selected for the active space, which exhibit d_{yz} contribution in the LUMO and HOMO-2 orbitals, while those with d_{xy} contribution, HOMO-8 and HOMO-11, were not included.

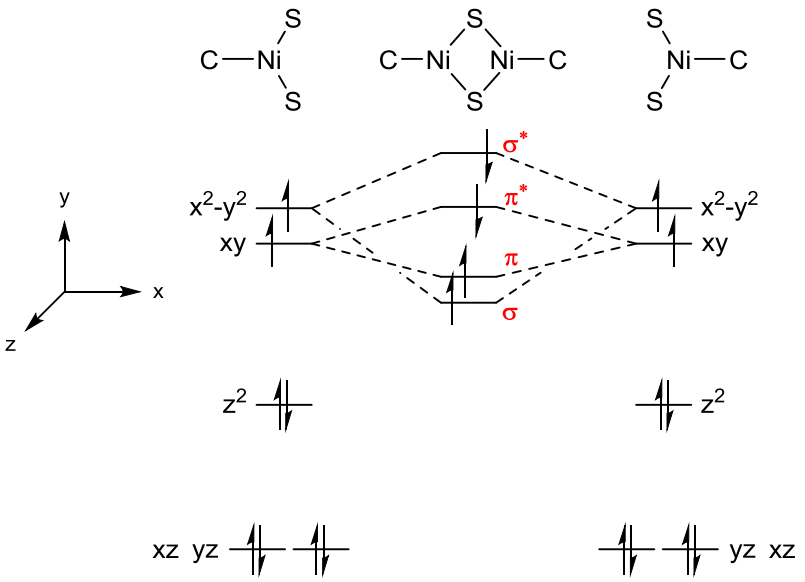

Figure 39. D-orbital splitting diagram predicted from angular overlap model, filled to produce four singly occupied molecular orbitals.

CASSCF analysis of the Trip spin state produced an alternative state that is 61 kcal/mol higher in energy than that found from the CSS and OSS states (Figure 40). The CASSCF Trip spin state contains two σ-bonded Ni centers, each with three filled d orbitals, and the remaining d electrons populating Ni-S π-antibonding orbitals, splitting S lone pairs and resulting in two sulfur-based radicals.

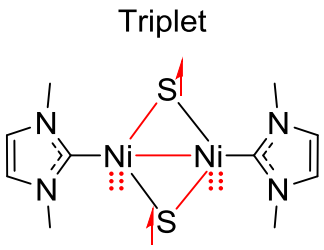

Figure 40. Triplet state electronic structure of **6** determined by CASSCF analysis.

Several structurally similar dinuclear Ni(II) species with two bridging X-type ligands have been reported (Chart 4).[117] These are diamagnetic in solution by ^{1}H and ^{31}P NMR, and feature Ni-Ni distances in range of 2.281(1) to 2.4389(9) Å. The Ni-Ni distance of **6**, 2.3666(5) Å, is in the middle of this range. The $\{ClNi(\mu\text{-}C(TMS)PMe_3)\}_2$ compound was postulated to have a double bond based on two available electrons on each Ni center. However CASSCF calculations on both $\{ClNi(\mu\text{-}C(TMS)PMe_3)\}_2$ and $[\{(IPr)Ni\}_2(\mu\text{-}Cl)(\mu\text{-}NMes)]^+$ complexes predict that both species have a similar electronic structure to **6**, with 4 SOMOs that result in a formal Ni-Ni bond order of 0.

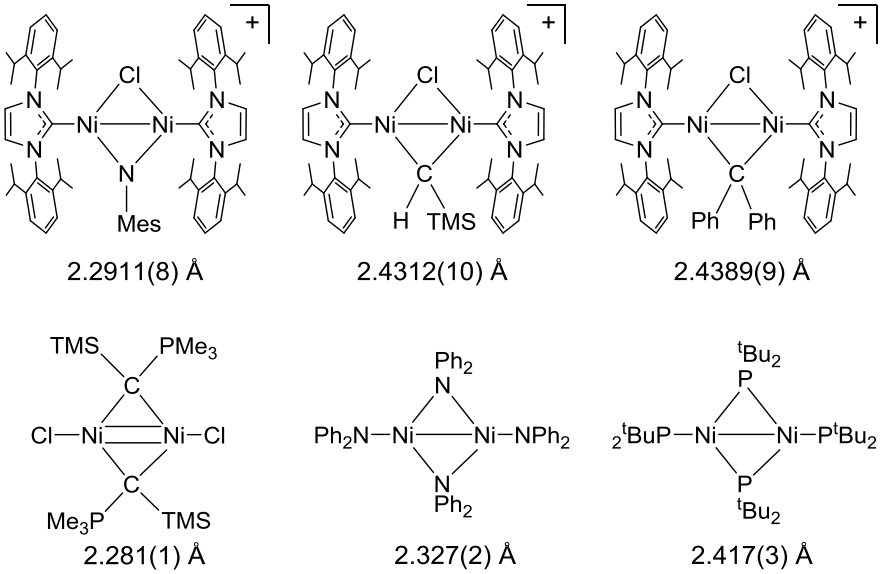

Chart 4. Ni(II)-Ni(II) complexes with two bridging ligands that exhibit short Ni-Ni contacts.

3.4.5. Determination of Reaction Pathway

B3PW91 was chosen to probe the reaction pathway for the reaction of **6** with H_2 to form **7** since it was accurate at geometry reproduction and is reasonably time-efficient. Geometry optimizations with CASSCF were attempted, however this method proved to be poor for reproducing the geometry of **6** and was too time intensive to permit exploration of the full reaction in a reasonable amount of time. The starting point of the reaction pathway is the OSS

structure of **6** and H_2. The OSS state was chosen since it is the closest electronic structure to the CASSCF calculations. The calculated reaction pathway is shown in Figure 41.

The first and rate-limiting step in the hydrogenation of **6** is heterolytic addition of H_2 across the Ni-S bond within the plane of the Ni_2S_2 diamond, which has a barrier of 30.9 kcal/mol. This activation produces a *cis*-hydride-hydrosulfide structure as a local minimum at 6.0 kcal/mol relative to separated reactants. In the *cis* conformation, there is no way for the H atom to transfer to the remaining bridging sulfide (to which it is *trans*), so the complex must undergo an isomerization. This isomerization occurs via a pseudo-tetrahedral transition state at 14.7 kcal/mol, and produces the *trans*-hydride-hydrosulfide structure at a relative free energy of 6.6 kcal/mol. The H atom then migrates to the bridging sulfide to form the product $\{(IPr)Ni(\mu\text{-}SH)\}_2$ (**7**). There are two product isomers with syn- and anti-configurations of the μ-SH ligands at -3.0 and -4.0 kcal/mol, respectively, and transition states were found for both configurations, at 27.4 and 22.2 kcal/mol, respectively. The KIE, calculated by substituting D_2 in place of H_2 for relevant structures, is 1.9, in good agreement with the experimental value of 1.8 (1). Overall, the reaction is thermodynamically favored by 4 kcal/mol. The barrier calculated from the experimental k_{obs} value determined at 80 °C and 1 atm H_2 by the Eyring equation is 29.1 kcal/mol, in close agreement with the computationally predicted barrier of 30.9 for TS1(3).

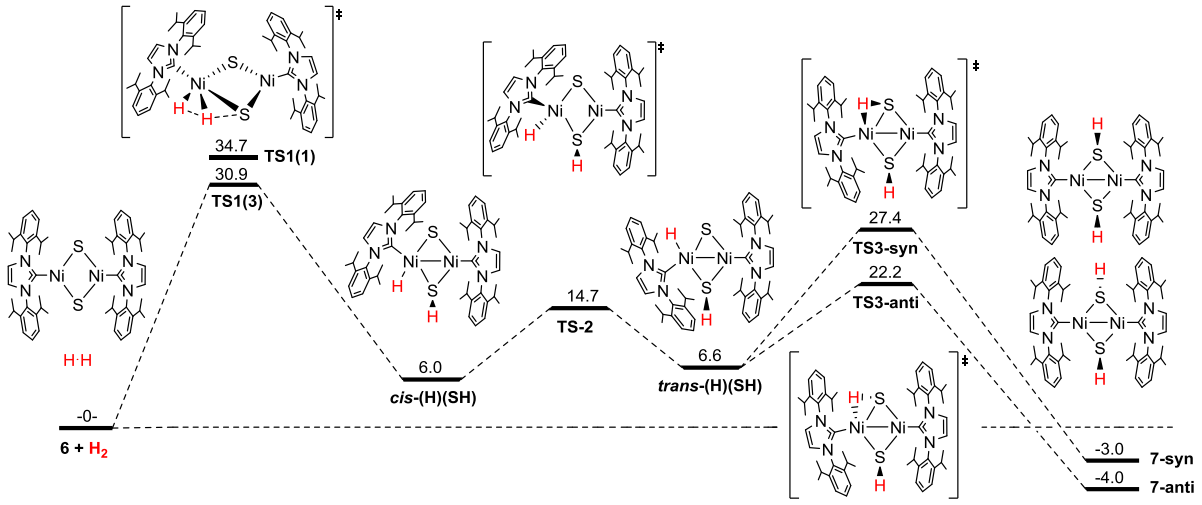

Figure 41. Calculated reaction pathway for the hydrogenation of **6**. All structures were optimized with B3PW91/6-31+G(d) as functional and basis set. Energies are ΔG-corrected and reported in kcal/mol, with the starting materials defined as 0. The spin state of all species is a singlet, except for the first transition state, for which single (TS1(1)) and triplet (TS1(3)) states were found.

3.4.6. Comparison of Rh_2S_2 and Ni_2S_2 Systems

H_2 addition proceeds in a heterolytic manner across the M-S bond for $\{MeC(CH_2PPh_2)_3Rh(\mu\text{-}S)\}_2^{2+}$ (Scheme 8) and **6**, to produce hydride-hydrosulfide intermediates. The barriers calculated by DFT for these reactions are 8.0 and 30.9 kcal/mol, respectively, consistent with the observed hydrogenation of the Rh complex at 23 °C and the requirement for heating to 80 °C to achieve hydrogenation of **6**. Furthermore, DFT predicts an H atom migration from the metal center to the remaining μ-S to produce bis-hydrosulfide species for both complexes. In the Rh system the bis-hydrosulfide is 12.3 kcal/mol higher in energy than the hydride-hydrosulfide, whereas for **6** the bis-hydrosulfide is ca. 10 kcal/mol lower in energy. It is peculiar that these two systems display opposite preferences for the hydride-hydrosulfide ←→ bis-hydrosulfide equilibrium. The Rh-H and Ni-H bond dissociation energies are very similar, 57.4 and 57.6 kcal/mol, respectively,[118] and the S-H BDE should be nearly equal. One possible explanation for this difference is the coordination number of the hydride-hydrosulfide complexes, four and six for **6** and the Rh system respectively.

3.4.7. H Migration in Between Metal and Ligand Positions

The migration of hydrogen between metal and ligand sites has been well documented in multinuclear systems (Scheme 11). Hydride migration between edge positions and μ_3-S ligands was observed in the trinuclear $(L_2Rh)_3(\mu\text{-}S)_2(\mu\text{-}H)$ complex.[119] DFT calculations predict that this process occurs through a (μ-SH) intermediate with a barrier of 19.7 kcal/mol, but the resting states are the hydride complexes, which are 12.0 kcal/mol lower than the hydrosulfide intermediate. The dinuclear complex $\{(Cp^*)Rh(\mu\text{-}NTs)\}_2$ reacts with H_2 at room temperature to produce $\{(Cp^*)Rh(\mu\text{-}NHTs)\}_2$.[120] DFT calculations suggest that this reaction occurs by heterolytic activation across the Rh-N bond with a barrier of 32 kcal/mol, to form an intermediate bridging hydride-amido-imido species, followed by H migration to generate the product. For the mononuclear (P~P)Ni(H)(PHAr), interconversion is observed at 298 K between the hydride and P-H atoms. DFT results imply that this occurs via sequential reductive elimination and oxidative addition, with a calculated barrier of 7.4 - 9.6 kcal/mol depending on the Ar substituent.[121] The transition state for the reductive elimination is similar to that for the H migration observed for **6,** although the barrier is 15.6 kcal/mol lower.

Scheme 11. Examples of H migration between metal and ligand sites.

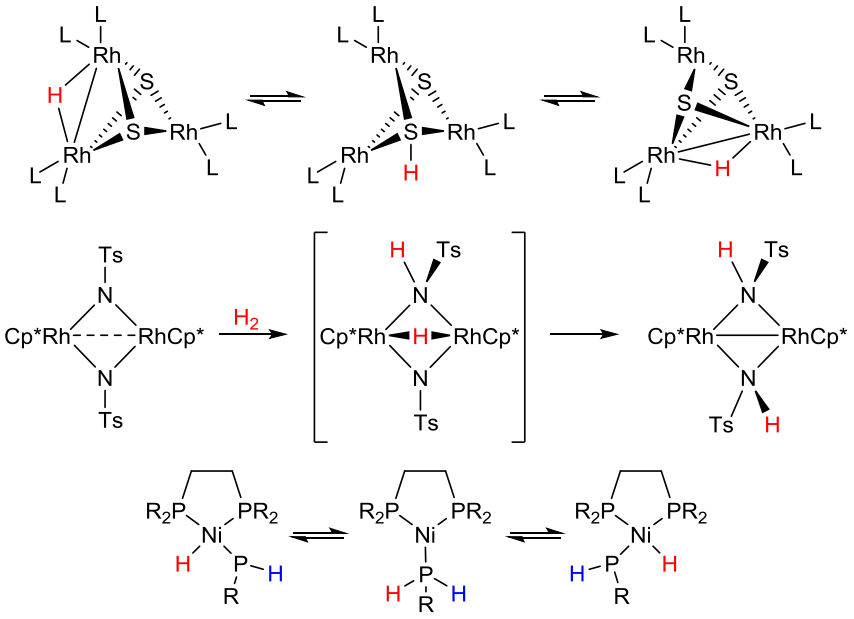

3.4.8. KIE Values for Heterolytic H_2 Activation Reactions

The H_2 activation reactions shown in Schemes 2 - 4 are complicated by isomerization and isotopic scrambling, which precludes determination of the KIE. However, the KIE for heterolytic cleavage of H_2 has been measured in two systems (Figure 42). A KIE of 2.0 ± 0.1 was measured for H_2 addition to a mononuclear Ru-amide complex, and the barrier predicted by DFT is 16.6 kcal/mol.[122] For the addition of H_2 to a dinuclear Zr-N_2 complex, a KIE of 1.8 - 2.4 (R = Me, Ph) was reported, and the DFT-predicted barrier is 18 kcal/mol.[123] The KIE of 1.8(1) for {(IPr)Ni(μ-S)}$_2$ is similar to these values, and the comparatively slightly reduced value is in line with the elevated temperature at which the reaction is performed.

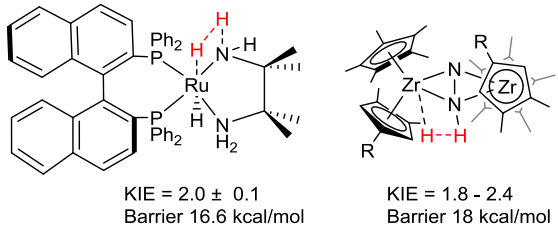

Figure 42. Kinetic Isotope Effects for Heterolytic H_2 Cleavage.

3.4.9. Alternate H_2 Activation Mechanisms

As noted above and shown in Scheme 9, $\{(Ph_3P)_2Ir(\mu\text{-}S)\}_2$ reacts with H_2 by homolytic addition across the Ir-Ir bond followed by heterolytic addition across an Ir-S bond. Although there is formally no Ni-Ni bond in $\{(IPr)Ni(\mu\text{-}S)\}_2$, there is close contact of the Ni centers, and a homolytic activation pathway involving addition of H_2 across the Ni-Ni contact is plausible. Therefore, a thorough exploration of all possible H_2 activation modes for **6** was performed.

Five possible activation modes that cleave the H-H bond were found using B3PW91 functional and 6-31+G(d) basis set and are shown in Figure 43. These additions occur across the following bonds: 1) Ni-S from in the N_2S_2 plane; 2) Ni-S from above the Ni_2S_2 plane; 3) Ni-Ni; 4) Ni-C; 5) the S-S gap in a Ni_2S_2 seesaw geometry (Figure 43). Each activation mode was found to have a transition state for both the singlet and triplet spin states. The energies for these transition states for the truncated model system and the full IPr system are shown in Figure 44.

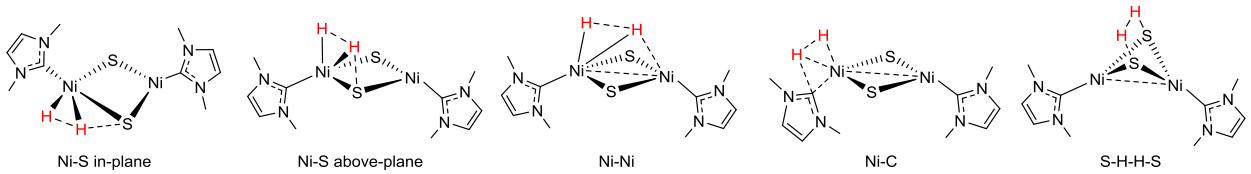

Figure 43. Five possible activation modes of H_2 by **6**, found through optimization at the B3PW91/6-31+G(d) level of theory.

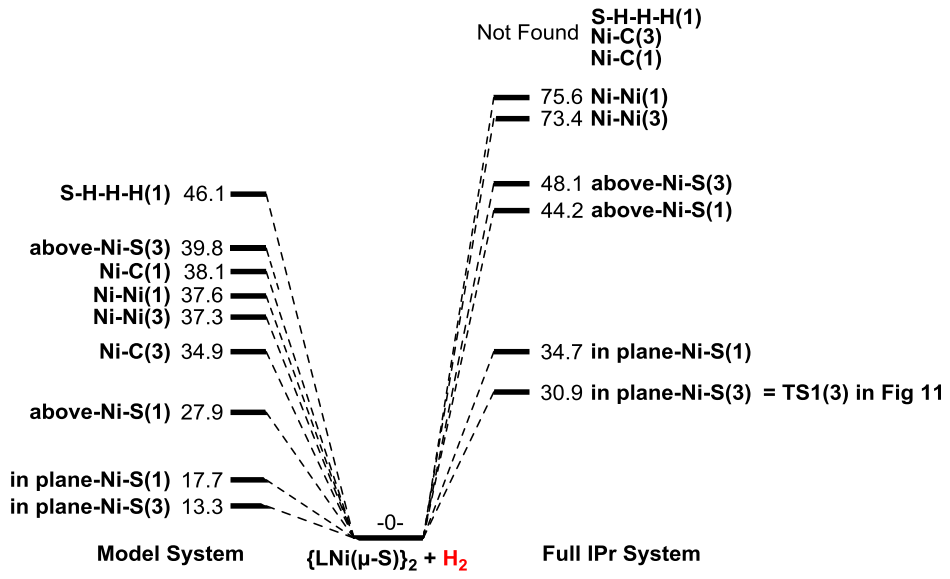

Figure 44. Activation barriers for H_2 bond cleavage in the truncated model and full IPr complex **6**. All structures were optimized with B3PW91/6-31+G(d) level of theory. Energies are ΔG-corrected and reported in kcal/mol, with the both sets of starting materials defined as 0. The spin state of each transition state is denoted by the number in parentheses.

One important conclusion is that the steric properties of the ligand have a significant effect on the activation barriers. At the truncated model level, activation across the Ni-Ni, the Ni-C, and the Ni-S bond from above are predicted to have similar barriers, while for the full IPr level the energy distribution is much greater. The imidazole rings of these transition states undergo significant rotation and bending from the Ni_2S_2 plane. At the truncated model level there are no energetic penalties, while for the full IPr ligand, steric repulsion between the four large di*iso*propylphenyl rings is increased and thus strongly disfavors activation by pathways other than Ni-S from in plane. For the Ni-S in-plane transition state the full IPr ligands orient perpendicular to each other to reduce steric repulsion, however the model barriers are still 18 kcal/mol lower in energy.

These calculations were performed without dispersion effects. Calculations with dispersion forces included were attempted, but are computationally demanding for a system of

this size. Dispersion effects may be expected to lower the barrier further due to attractive forces between the four dipp rings.[124]

3.5. Experimental Section

General Procedures. All experiments were performed under nitrogen using drybox or Schlenk techniques. Nitrogen was purified by passage through activated molecular sieves and Q-5 oxygen scavenger. Anhydrous Et_2O and THF were purified by passage through activated alumina.[125] Anhydrous benzene, pentane, and toluene were purified by passage through activated alumina and BASF R3-11 oxygen scavenger. $\{(IPr)Ni(\mu\text{-}S)\}_2$ was prepared by a literature method.[94] All other chemicals were used as received. NMR spectra were recorded on a Bruker DRX-500 spectrometer at room temperature using Teflon-valved tubes. ^1H chemical shifts are reported relative to $SiMe_4$ and were determined by reference to the residual ^1H and solvent resonances (^1H: residual C_6D_5H in C_6D_6 δ 7.16). Coupling constants are given in hertz (Hz). C_6D_6 was distilled from Na/benzophenone and stored under vacuum.

Kinetic Data. Kinetic runs at 1 atm H_2 and D_2 were performed in J Young NMR tubes. $\{(IPr)Ni(\mu\text{-}S)\}_2$ **6** and the internal standard C_6Me_6 were loaded into a J Young NMR tube inside the glovebox. C_6D_6 was vacuum transferred into the tube from a Na-benzophenone ketyl solution, and the tube was pressurized with H_2 or D_2. The first ^1H NMR was taken prior to heating, and the C_6Me_6 standard integral was set based on 1 full equiv of **6**. The J Young tube was heated to 80 °C, and NMR spectra were taken periodically until the reaction had proceeded for five half-lives.

Reactions at 3 and 6 atm H_2 were performed in a Fischer Porter bottle (Figure 45). **6** and the internal standard C_6Me_6 were both dissolved in C_6D_6, and loaded into the bottle along with a stir bar inside the glovebox. The apparatus was removed from the glovebox and attached to a Schlenk line vacuum and an H_2 cylinder. The headspace was saturated with H_2

by 10 cycles of charging with H_2 and discharging via vacuum. The apparatus was then pressurized to the desired pressure of H_2, and immersed in an oil bath maintained at 80 °C, which was denoted as the start of the reaction. The reaction mixture was sampled at evenly spaced intervals of 1 hour for 12 hours, or until the reaction had proceeded for five half-lives. The sampling was performed by first reducing the pressure by vacuum to ~1.1 atm, at which point a 12" needle was used to withdraw 0.6 mL of the reaction mixture and transfer it into a nitrogen-flushed NMR tube. The apparatus was repressurized with H_2 and then reaction resumed. This entire process was typically completed within 3 min, a negligible amount of time for a reaction that takes more than eight hours to go to completion. The sample was cooled to room temperature and a ^{1}H NMR spectrum was collected.

Figure 45. Fischer Porter bottle setup for high pressure hydrogenation reactions.

Table 5. Kinetic data for the hydrogenation of **6**. Runs at 1 atm were performed in J Young NMR tubes. Runs at 3 and 6 atm were performed in Fischer Porter bottles, and the reaction mixture was sampled and assayed by NMR.

Run	$[6]_0$ (M)	Temp (K)	H_2 Pressure (atm)	k_{obs} (s^{-1})
1	2.6E-03	353	1	7.1E-06
2	3.8E-03	353	1	8.0E-06
3	5.2E-03	353	1	7.1E-06
4	3.2E-03	353	3	5.5E-05
5	3.4E-03	353	3	4.8E-05
6	3.4E-03	353	6	1.1E-04
7	3.5E-03	353	6	1.0E-04
8-D_2	4.0E-03	353	1	4.2E-06
9-D_2	4.3E-03	353	1	4.2E-06

Cyclic Voltammetry. Electrochemical measurements were performed at room temperature in a nitrogen-filled glovebox using a Bioanalytical Systems 100 B/W Electrochemical Workstation. A three-electrode configuration was used, which consisted of a working electrode (Pt /Au disk, area = 0.2 cm^2), auxiliary electrode (Pt/Au disk, area 0.2 cm^2), and quasi-reference electrode (Ag wire). Electrodes were polished prior to each experiment. Samples ranged in concentration from $(0.3 – 2) \times 10^{-3}$ M analyte in THF solution with 0.1 M $[nBu_4N][PF_6]$. Cyclic voltammetry (CV) was conducted over a range of scan rates (0.05 – 0.5 V s^{-1}). Peak currents in CV experiments were determined from scans in which the switching potential was at least 0.3 V beyond the peak potentials. Differential pulse voltammetry (DPV) was conducted using a scan rate of 0.2 V s^{-1}, a pulse amplitude of 0.05 V, a sampling width of 0.017 s, a pulse width of 0.05 s, and a pulse period of 0.2 s. Electrode potentials are referenced to the $FeCp_2^{0/+}$ couple; this was used as an internal electrode potential standard for CV and DPV experiments. Under the conditions of the CV experiment, the $FeCp_2^{0/+}$ signal exhibited i_{pa}/i_{pc} = 1 and ΔE_p = 0.9 – 0.27 V.

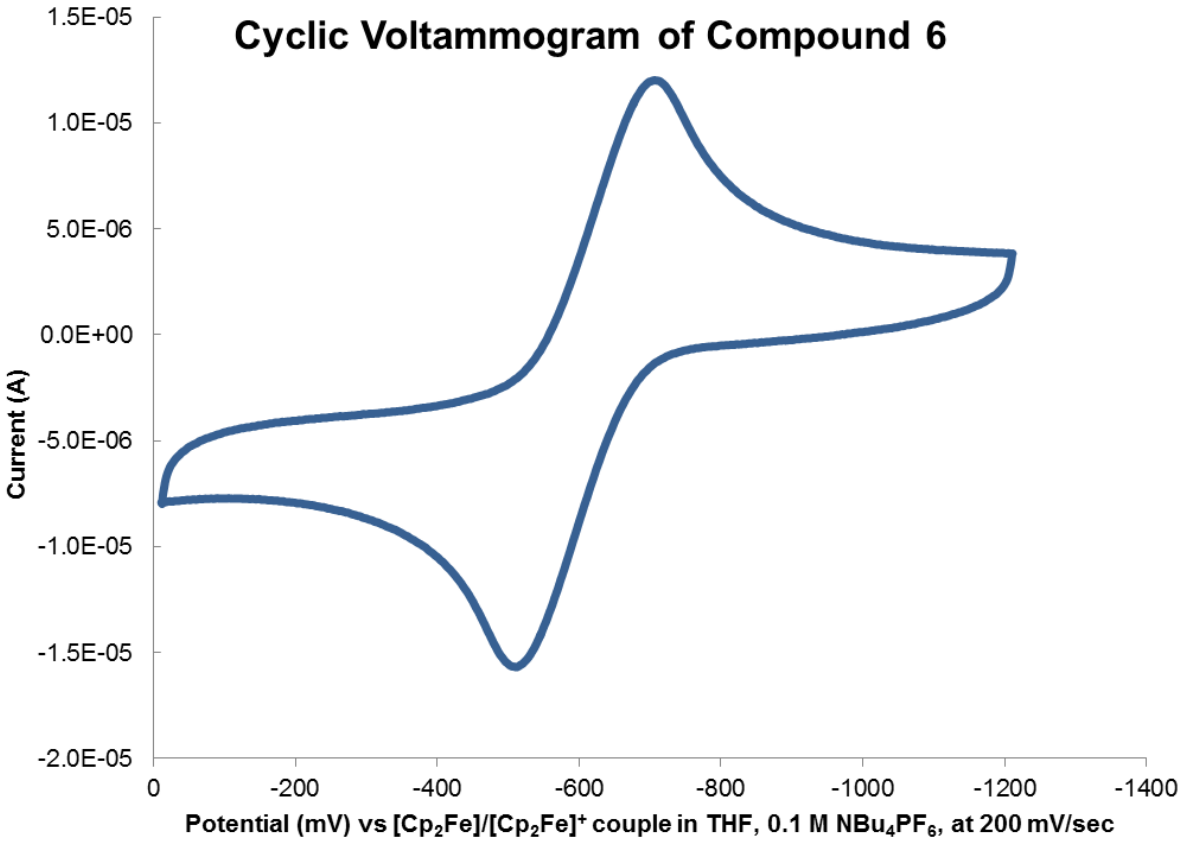

Figure 46. Cyclic voltammogram of Compound **6**. Referenced to $Cp_2Fe/[Cp_2Fe]^+$ couple in THF, 0.1 M $N(Bu)_4PF_6$ as electrolyte, scan speed 250 mV/sec.

Magnetometry. Magnetic measurements were performed on a Quantum Design MPMS 3 equipped with a superconducting quantum interference device (SQUID). Corrections were made for the diamagnetic contributions from the polycarbonate capsules and eicosane used to secure the sample by measuring field vs. moment in triplicate for each to determine a moment per gram correction.

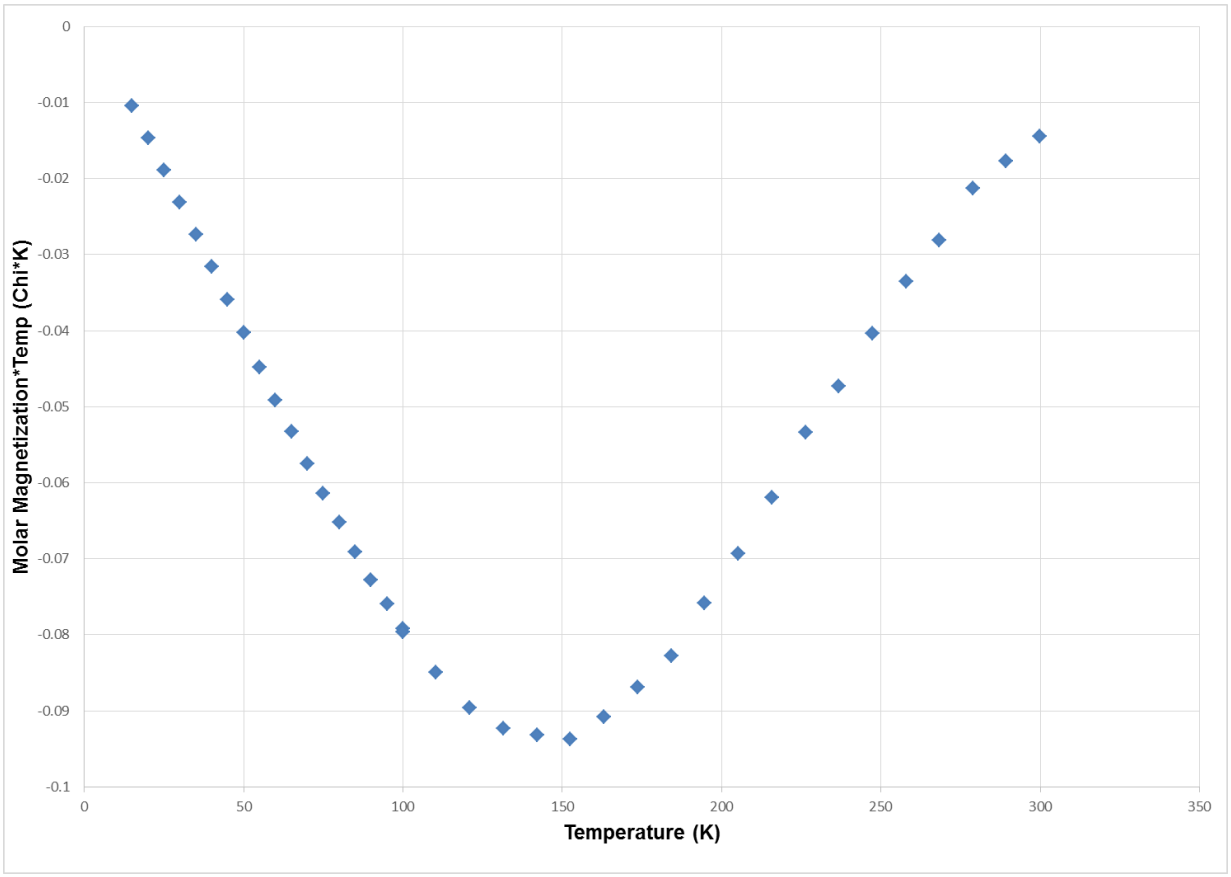

Figure 47. Temperature dependent molar magnetic susceptibilities (X_T) for {(IPr)Ni(μ-S)}$_2$ (6). The negative values indicate a diamagnetic ground state at all examined temperatures.

Continuous-wave EPR spectra were collected on samples of **6**. A crystalline sample was dissolved in toluene and loaded into a quartz tube under a dinitrogen atmosphere. Measurements were performed at the University of Chicago EPR facility using a Bruker Elexsys 500 X-band EPR spectrometer. The temperature of the samples was held at 77 K using an Oxford Systems continuous-flow He Cryostat coupled with a 10 K He stinger from Bruker. Spectra were acquired with the Bruker Win-EPR software suite. The spectrometer was equipped with a dual mode cavity, operating in both parallel and perpendicular modes. Data were collected using the following instrumental parameters: radiation frequency = 9.384 GHz; microwave power = 1.99 mW; modulation amplitude = 5 G; modulation frequency = 100 kHz.

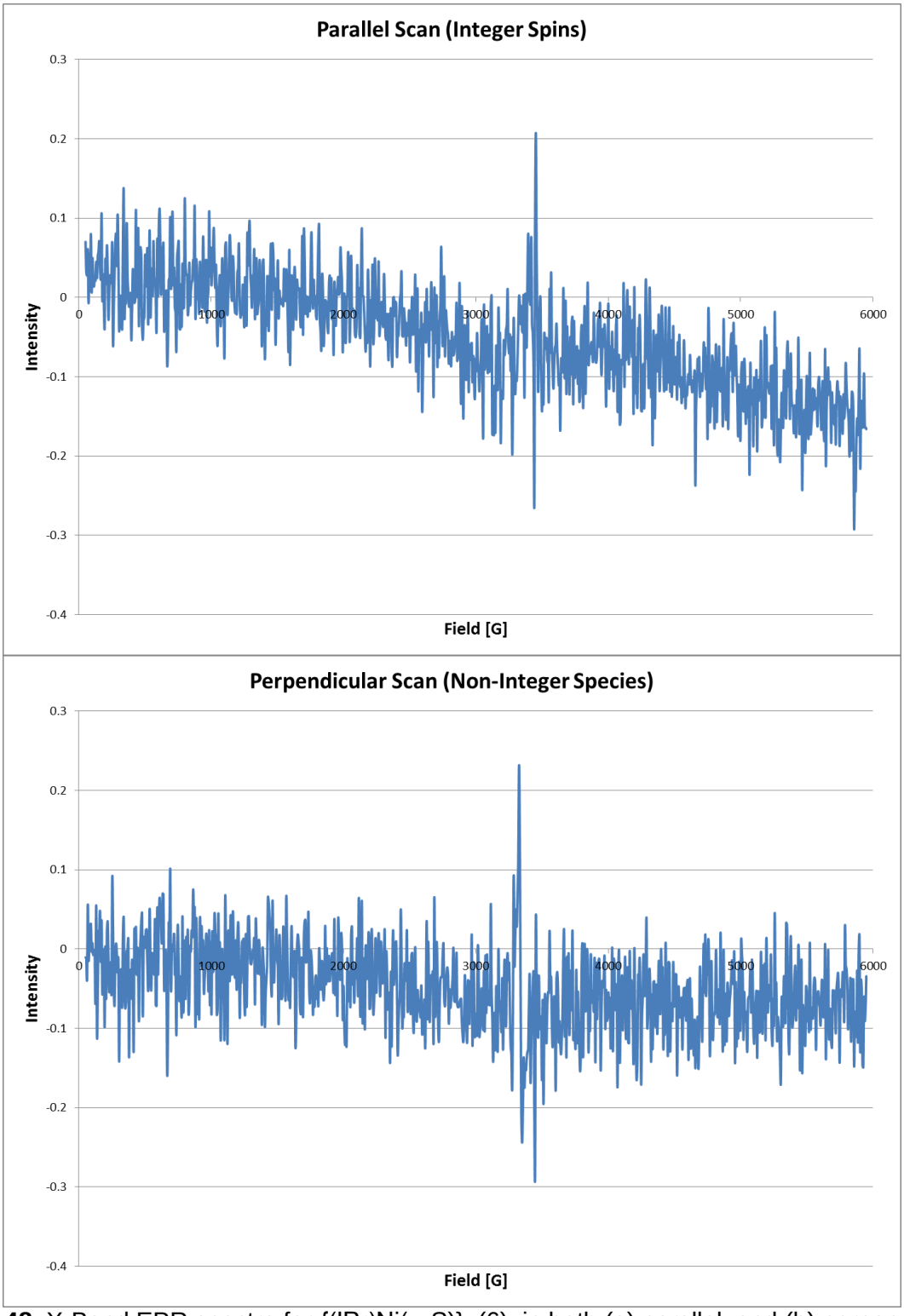

Figure 48. X-Band EPR spectra for $\{(IPr)Ni(\mu\text{-}S)\}_2$ (6), in both (a) parallel, and (b) perpendicular modes. The lack of strong signal indicates the absence of a paramagnetic species under experimental conditions. Data collected in toluene at 77 K under N_2 atmosphere: microwave frequency = 9.384 GHz: microwave power = 1.99 mW.

DFT Calculations. All density functional theory (DFT) calculations were made with the Gaussian 09[126] package. Various functionals were screened by optimization utilizing a truncated dimethyl-imidazolin-2-ylidene ligand, and by comparing calculated metrical parameters with experimental structural data for **6**. The B3PW91 functional was used to explore the reaction coordinate based on the results of the truncated model simulations. The reaction coordinate for the full IPr ligand was explored at the ONIOM[127] (B3PW91/6-31+G(d):UFF)[128] level of theory. The 2,6-$^{i}Pr_2$-Ar substituents were included in the UFF partition, and the remainder of the complex modeled with B3PW91/6-31+G(d).

Unless otherwise noted, calculations were in the gas phase and assumed 298.15 K and 1 atm. Solvent calculations were performed in benzene solvent using the SMD solvation model.[129] All calculated free energies are reported in kcal/mol. Optimized ground states contained no imaginary vibrational frequencies, and optimized transition states contained one imaginary vibrational frequency.

Multi-Configurational Calculations. MCSCF[114] calculations were performed on the model system through the GAMESS[130] program. For these multi-reference calculations, no dispersion or solvent corrections were considered. The input geometries were from previous DFT optimizations. For the bimetallic system an (8,8) active space was chosen was chosen to provide good coverage of the Ni- and S-based orbitals near the HOMO-LUMO gap, while also balancing the computational demand of the system (Figure 37).

3.6. References

(80) (a) Gutiérrez, O.; Singh, S.; Schachtl, E.; Kim, J.; Kondratieva, E.; Hein, J.; Lercher, J. A. *ACS Catal.* **2014**, *4*, 1487. (b) Robbie, A.; Cowley, A. R.; Jones, M. W.; Dilworth, J. R. *Polyhedron* **2011**, *30*, 1849. (c) Torres-Nieto, J.; Brennessel, W. W.; Jones, W. D.; Garcia, J. J. *J. Am. Chem. Soc.* **2009**, *131*, 4120. (d) Vicic, D. A.; Jones, W. D. *J. Am. Chem. Soc.* **1999**, *121*, 4070. (e) Vicic, D. A.; Jones, W. D. *J. Am. Chem. Soc.* **1999**, *121*, 7606.

(81) (a) Kabe, T. *Hydrodesulfurization and Hydrodenitrogenation: Chemistry and Engineering*; Wiley-VCH: New York, **1999**. (b) Topsøe, H.; Clausen, B. S.; Massoth, F. E. *Hydrotreating Catalysis, Science and Technology*; Springer-Verlag: Berlin, **1996**.

(82) (a) Chen, Y.; Wang, L.; Liu, X.; Liu, T.; Huang, B.; Li, P.; Jiang, Z.; Li, C. *Appl. Catal. A* **2015**, *504*, 319. (b) Baston, E. P.; Franca, A. B.; da Silva Neto, A. V.; Urquieta-Gonzalez, E. A. *Catal. Today* **2015**, *246*, 184. (c) Eijsbouts, S. *Appl. Catal. A* **1997**, *158*, 53. (d) Prins, R.; De Beer, V. H. J.; Somorjai, G. A. *Catal. Rev.* **1989**, *31*, 1.

(83) (a) Nagai, M.; Tung, N. T.; Adachi, Y.; Kobayashi, K. *Catal. Today* **2016**, *271*, 91. (b) Lai, W.; Chen, Z.; Zhu, J.; Yang, L.; Zheng, J.; Yi, X.; Fang, W. *Nanoscale* **2016**, *8*, 3823. (c) Scott, C. E.; Perez-Zurita, M. J.; Carbognani, L. A.; Molero, H.; Vitale, G.; Guzman, H. J.; Pereira-Almao, P. *Catal. Today* **2015**, *250*, 21. (d) Dugulan, A. I.; van Veen, J. A. R.; Hensen, E. J. M. *Appl. Catal. B* **2013**, *142*, 178. (e) Louwers, S. P. A.; Prins, R. *J. Catal.* **1992**, *133*, 94. (f) Pratt, K. C.; Sanders, J. V.; Tamp, N. *J. Catal.* **1980**, *66*, 82.

(84) (a) Wen, X. D.; Zeng, T.; Tend, B. T.; Zhang, F.-Q.; Li, Y. W.; Wang, J.; Jiao, H. *J. Mol. Catal. A: Chem.* **2006**, *249*, 191. (b) Cristol, S.; Paul, J. F.; Payen, E.; Bougeard, D.; Clémendot, S.; Hutschka, F. *J. Phys. Chem. B* **2002**, *106*, 5659. (c) Hwang, D. Y.; Mebel, A. M. *J. Phys. Chem. A* **2002**, 106, 520. (d) Alexiev, V.; Prins, R.; Weber, Th. *Phys. Chem. Chem. Phys.* **2001**, *3*, 5326. (e) Cristol, S.; Paul, J. F.; Payen, E.; Bougeard, D.; Clémendot, S.; Hutschka, F. *J. Phys. Chem. B* **20**, *104*, 11220. (f) Neurock, M.; van Santen, R. A. *J. Am. Chem. Soc.* **1994**, *116*, 4427.

(85) (a) Breysse, M.; Furimsky, E. *Catal. Rev.* **2002**, *44*, 651. (b) Lacroix, M.; Yuan, S.; Breysse, M.; Dorémieux-Morin, C.; Fraissard, J. *J. Catal.* **1992**, *138*, 409.

(86) (a) Diaz de León, J. N. *Appl. Catal. B* **2016**, *181*, 524. (b) Rangarajan, S.; Mavrikakis, M. *AIChE J.* **2015**, *61*, 4036. (c) Sigurdson, S.; Dalai, A. K.; Adjaye, J. *Can. J. Chem. Eng.* **2011**, *89*, 562. (d) Hein, J.; Gutiérrez, O. Y.; Schachtl, E.; Xu, P.; Browning, N. D.; Jentys, A.; Lercher, J. A. *ChemCatChem* **2015**, *7*, 3692.

(87) (a) Vicic, D. A.; Jones, W. D. *J. Am. Chem. Soc.* **1999**, *121*, 7606. (b) Vicic, D. A.; Jones, W. D. *J. Am. Chem. Soc.* **1999**, *121*, 4070. (c) Torres-Nieto, J.; Brennessel, W. W.; Jones, W. D.; Garcia, J. J. *J. Am. Chem. Soc.* **2009**, *131*, 4120.

(88) (a) Seyferth, D.; Henderson, R. S.; Song, L.-C. *J. Organomet. Chem.* **1980**, *192*, C1. (b) Kubiak, C. P.; Eisenberg, R. *Inorg. Chem.* **1980**, *19*, 2726. (c) Ruffing, C. J.; Rauchfuss, T. B. *Organometallics* **1985**, *4*, 524. (d) Werner, H.; Luxenburger, G.; Hofmann, W. X.; Nadvornik, M. *J. Organomet. Chem.* **1987,** *323*, 161. (e) Birnbaum, J.; Godziela, G.; Maciejewski, M.; Tonker, T. L.; Haltiwanger, R. C.; Rakowski DuBois, M. *Organometallics* **1990**, *9*, 394. (f) Wang, L. S.; McDonald, R.; Cowie, M. *Inorg. Chem.* **1994**, *33*, 3735. (g) Tang, Z.; Nomura, Y.; Ishii, Y.; Mizobe, Y.; Hidai, M. *Inorg. Chim. Acta* **1998**, *267*, 73. (h) Kuwata, S.; Hidai, M. *Coord. Chem. Rev.* **2001**, *213*, 211. (i) Oster, S. S.; Lachicotte, R. J.; Jones, W. D. *Inorg. Chim. Acta* **2002**, *330*, 118.

(89) (a) Lopez, L. L.; Godziela, G.; Rakowski DuBois, M. *Organometallics* **1991**, *10*, 2660. (b) Bernatis, P.; Laurie, J. C. V.; Rakowski DuBois, M. *Organometallics* **1990**, *9*, 1607. (c) Weberg,

R. T.; Haltiwanger, R. C.; Laurie, J. C. V.; Rakowski DuBois, M. *J. Am. Chem. Soc*. **1986**, *108*, 6242. (d) Laurie, J. C. V.; Duncan, L.; Haltiwanger, R. C.; Weberg, R. T.; Rakowski DuBois, M. *J. Am. Chem. Soc.* **1986**, *108*, 6234. (e) McKenna, M.; Wright, L. L.; Miller, D. J.; Tanner, L.; Haltiwanger, R. C.; Rakowski DuBois, M. *J. Am. Chem. Soc.* **1983**, *105*, 5329.

(90) (a) Appel, A. M.; Lee, S.-J.; Franz, J. A.; DuBois, D. L.; DuBois, M. R. *J. Am. Chem. Soc.* **2009**, *131*, 5224. (b) Appel, A. M.; Lee, S.-J.; Franz, J. A.; DuBois, D. L.; Rakowski DuBois, M.; Twamley, B. *Organometallics* **2009**, *28*, 749. (c) Casewit, C. J.; Coons, D. E.; Wright, L. L.; Miller, W. K.; Rakowski DuBois, M. *Organometallics* **1986**, *5*, 951.

(91) (a) Ref. 90. (b) Appel, A. M.; Lee, S.-J.; Franz, J. A.; DuBois, D. L.; Rakowski DuBois, M.; Birnbaum, J. C.; Twamley, B. *J. Am. Chem. Soc.* **2008**, *130*, 8940. (c) Bursten, B. E.; Cayton, R. H. *Inorg. Chem.* **1989**, *28*, 2846.

(92) (a) Ienco, A.; Calhorda, M. J.; Reinhold, J.; Reineri, F.; Bianchini, C.; Peruzzini, M.; Vizza, F.; Mealli, C. *J. Am. Chem. Soc.* **2004**, *126*, 11954. (b) Bianchini, C.; Mealli, C.; Meli, A.; Sabat, M. *Inorg. Chem.* **1986**, *25*, 4617.

(93) (a) Algarra, A. G. *Inorg. Chem.* **2016**, Article ASAP. **DOI**: 10.1021/acs.inorgchem.6b01888. (b) Rauchfuss, T. B. *Inorg. Chem*. **2004**, *43*, 14. (c) Linck, R. C.; Pafford, R. J.; Rauchfuss, T. B. *J. Am. Chem. Soc.* **2001**, *123*, 8856. (d) Mueting, A. M.; Boyle, P. D.; Wagner, R.; Pignolet, L. H. *Inorg. Chem.* **1988**, *27*, 271.

(94) Olechnowicz, F.; Hillhouse, G. L.; Jordan, R. F. *Inorg. Chem.* **2015**, *54*, 2705.

(95) Reactions at 100-500 psi of H_2 and temperatures 40-80 °C were performed in collaboration with John Linehan at Pacific Northwest National Laboratory. Results were insufficiently reproducible to enable conclusions to be made. A positive correlation of the reaction rate was observed for both temperature and H_2 pressure, however neither variable was able to be fit in any meaningful way.

(96) The concentration of dissolved hydrogen in benzene is linearly proportional to the applied pressure, see: (a) Sartori, E.; Ruzzi, M.; Turro, N. J.; Decatur, J. D.; Doetschman, D. C.; Lawler, R. G.; Buchachenko, A. L.; Murata, Y.; Komatsu, K. *J. Am. Chem. Soc.* **2006**, *128*, 14752. (b) Tsuji, T.; Shinya, Y.; Hiaki, T.; Itoh, N. *Fluid Phase Equilib.* **2005**, *228*, 499. (c) Park, J.; Robinson, R. L.; Gasem, K. A. M. *J. Chem. Eng. Data* **1996**, *41*, 70. (d) Brainard, A. J.; Williams, B. *AlChE J.* **1967**, *13*, 60.

(97) Bai, G. C.; Wei, P. R.; Stephan, D. W. *Organometallics* **2005**, *24*, 5901.

(98) Ni(I)–Ni(I) complexes with bridging ligands that exhibit short Ni–Ni distances include: (a) $[(IPr)Ni]_2(\mu\text{-}I)(\mu\text{-}NO)$, 2.314(1) Å, Varonka, M. S.; Warren, T. H. *Organometallics* **2010**, *29*, 717. (b) $[(Ph_3P)Ni(\mu\text{-}STipp)]_2$, $[(Ph_3P)Ni(\mu\text{-}SAd)]_2$, $[(IMe')Ni(\mu\text{-}STipp)]_2$, and $[(^tBuNC)Ni(\mu\text{-}SDmp)]_2$, 2.3353(4), 2.3510(3), 2.3941(13), and 2.3354 Å respectively, Ito, M.; Matsumoto, T.; Tatsumi, K. *Inorg. Chem.* **2009**, *48*, 2215. (c) $[(Cy_2MeP)Ni(\mu\text{-}PCy_2)]_2$, 2.3910(8) Å, Kriley, C. E.; Woolley, C. J.; Krepps, M. K.; Popa, E. M.; Fanwick, P. E.; Rothwell, I. P. *Inorg. Chim. Acta* **20**, *300*, 200.

(99) High spin 3-coordinate Y-shaped Ni(II) species include (a) Hartmann, N. J.; Wu, G.; Hayton, T. W. *Angew. Chem. Int. Ed.* **2015**, *54*, 14956. (b) Holze, P.; Horn, B.; Limberg, C.;

Matlachowski, C.; Mebs, S. *Angew. Chem.* **2014**, *126*, 2788. *Angew. Chem. Int. Ed.* **2014**, *53*, 2750. (c) Horn, B.; Limberg, C.; Herwig, C.; Braun, B. *Inorg. Chem.* **2014**, *53*, 6867. (d) Laskowski, C. A.; Morello, G. R.; Saouma, C. T.; Cundari, T. R.; Hillhouse, G. L. *Chem. Sci*. **2013**, *4*, 170. (e) Eckert, N. A.; Bones, E. M.; Lachicotte, R. J.; Holland, P. L. *Inorg. Chem.* **2003**, *42*, 1720. (f) Holland, P. L.; Cundari, T. R.; Perez, L. L.; Eckert, N. A.; Lachicotte, R. J. *J. Am. Chem. Soc.* **2002**, *124*, 14416.

(100) Co=Co double bond distances show a 6% contraction over Co-Co single bond distances, based on averages of 2.31 and 2.46 Å respectively (CCSD searches performed on 2016/12/29). Calculated radii for Co and Ni single and double bonds are significantly shorter than all Ni-Ni contacts and all but 2 Co-Co contacts reported, see: (a) Pyykkö, P.; Atsumi, M. *Chem. - Eur. J.* **2009**, *15*, 12770. (b) Pyykkö, P.; Atsumi, M. *Chem. - Eur. J.* **2009**, *15*, 186.

(101) (a) Fondo, M.; Doejo, J.; Garcia-Deibe, A. M.; Sanmartin-Matalobos, J.; Vincente, R.; El-Fallah, M. S.; Amoza, M.; Ruiz, E. *Inorg. Chem.* **2016**, asap DOI: 10.1021/acs.inorgchem.6b01739. (b) Bu, X.-H.; Du, M.; Zhang, L.; Liao, D.-Z.; Tang, J.-K.; Zhang, R.-H.; Shionoya, M. *J. Chem. Soc., Dalton Trans.* **2001**, 593. (c) Blanchet-Boiteux, C.; Mouesca, J. M. *J. Phys. Chem. A* **20**, *104*, 2091. (d) Nanda, K. K.; Thompson, L. K.; Bridson, J. N.; Nag, K. *J. Chem. Soc., Chem. Commun*. **1994**, 1337. (e) Ghilardi, C. A.; Mealli, C.; Midollini, S.; Nefedov, V. I.; Orlandini, A.; Sacconi, L. *Inorg. Chem*. **1980**, *19*, 2454. (f) Martin, R. L. *New Pathways Inorg. Chem.* **1968**, 175.

(102) Two Ni(II)-Ni(II) complexes have been postulated to contain a double bond, see: (a) $\{ClNi(\mu\text{-}C(TMS)PMe_3)\}_2$, 2.281(1) Å: König, H.; Menu, M. J.; Dartiguenave, M.; Dartiguenave, Y.; Klein, H. F. *J. Am. Chem. Soc.* **1990**, *112*, 5351. (b) $\{(C_5{}^{i}Pr_4H)Ni\}_2(\mu\text{-}CH_2)$, 2.3158(10) Å, Weismann, D.; Saurenz, D.; Boese, R.; Blaser, D.; Wolmershauser, G.; Sun, Y.; Sitzmann, H. *Organometallics* **2011**, *30*, 6351.

(103) Antiferromagnetic coupling in a trinuclear Ni(II) complex has been reported, see: (a) Cotton, F. A.; Murillo, C. A.; Wang, Q.; Young, M. D. *Eur. J. Inorg. Chem.* **2008**, *2008*, 5257. (b) Berry, J. F.; Cotton, F. A.; Murillo, C. A. *Dalton Trans.* **2003**, 3015. (c) Clérac, R.; Cotton, F. A.; Dunbar, K. R.; Murillo, C. A.; Pascual, I.; Wang, X. P. *Inorg. Chem.* **1999**, *38*, 2655.

(104) Zhao, Y.; Truhlar, D. G. *Theor. Chem. Acc.* **2008**, *120*, 215.

(105) Grimme, S. *J. Comp. Chem.* **2006**, *27*, 1787.

(106) Becke, A. D. *J. Chem. Phys.* **1993**, *98*, 1372.

(107) (a) Becke, A. D. *Phys. Rev. A* **1988**, *38*, 3098. (b) Perdew, J. P. *Phys. Rev. B* **1986**, *33*, 8822.

(108) (a) Becke, A. D. Phys. Rev. A **1988**, 38, 3098. (b) Lee, C.; Yang, W. Parr, R. G. *Phys. Rev. B* **1988**, *37*, 785.

(109) (a) Becke, A. D. Phys. Rev. A **1988**, 38, 3098. (b) Lee, C.; Yang, W. Parr, R. G. *Phys. Rev. B* **1988**, *37*, 785. (c) Vosko, S. H.; Wilk, L.; Nusair, M. *Can. J. Phys.* **1980**, *58* (8), 1200.

(110) (a) Perdew, J. P.; Burke, K.; Wang, Y. *Phys. Rev. B*, **1996,** *54* 16533. (b) Becke, A. D. *J. Chem. Phys.* **1993**, *98*, 5648. (c) Becke, A. D. *J. Chem. Phys.* **1993**, *98*, 1372.

(111) Koch, W.; Holthausen, M. C. *A Chemist's Guide to Density Functional Theory*, 2nd ed.; Wiley-VCH: Weinheim, Germany, **2001**.

(112) (a) Paier, J.; Marsman, M.; Kresse, G. *J. Chem. Phys.* **2007**, *127*, 024103. (b) Wodrich, M. D.; Corminboeuf, C.; Schleyer, P. v. R. *Org. Lett.* **2006**, *8*, 3631. (c) Grimme, S. *Angew. Chem. Int. Ed*. **2006**, *45*, 4460. (d) Check, C. E.; Gilbert, T. M. *J. Org. Chem.* **2005**, *70*, 9828. (e) Csonka, G. I.; Ruzsinszky, A.; Tao, J.; Perdew, J. P. *Int. J. Quantum Chem.* **2005**, *101*, 506. (f) Redfern, P. C.; Zapol, P.; Curtiss, L. A.; Raghavachari, K. *J. Phys. Chem. A* **20**, *104*, 5850.

(113) (a) Csonka, G. I.; Ruzsinszky, A.; Tao, J.; Perdew, J. P. *Int. J. Quantum Chem.* **2005**, *101*, 506. (b) Staroverov, V. N.; Scuseria, G. E.; Tao, J.; Perdew, J. P. *J. Chem. Phys.* **2004**, *121*, 11507. (c) Staroverov, V. N.; Scuseria, G. E.; Tao, J.; Perdew, J. P. *J. Chem. Phys.* **2003**, *119*, 12129.

(114) Schmidt, M. W.; Gordon, M. S. *Annu. Rev. Phys. Chem.* **1998**, *49*, 233.

(115) Line broadening in the NMR spectra of paramagnetic compounds can be separated into two contributions, the orbital contribution, which is temperature-insensitive, and the paramagnetic contribution, which is temperature-sensitive. The insensitivity in ^{1}H NMR of **6** would suggest that the broadness is due to orbital contribution rather than the paramagnetic contribution, consistent with the overall singlet spin state resulting from Ni-Ni interaction. (a) Novotny, J.; Sojka, M.; Komorovsky, S.; Necas, M.; Marek, R. *J. Am. Chem. Soc.* **2016**, *138*, 8432. (b) Martin, B.; Autschbach, J. *J. Chem. Phys.* **2015**, *142*, 54108. (c) Hiller, M.; Maier, M.; Wadephol, H.; Enders, M. *Organometallics* **2016**, *35*, 1916. (d) Banci, L.; Bertini, I.; Luchinat, C.; Pierattelli, R.; Shokhirev, N. V.; Walker, F. A. *J. Am. Chem. Soc.* **1998**, *120,* 8472.

(116) (a) Bencini, A.; Benelli, C.; Gatteschi, D. *Coord. Chem. Rev.* **1984**, *60*, 131. (b) Schäffer, C. R. *Pure and Applied Chem.* **1970**, *24*, 361. (c) Schäffer, C. R.; Jørgensen, C. K. *Mol. Phys.* **1965**, *9*, 401.

(117) Ni(II)-Ni(II) complexes with bridging ligands that exhibit short Ni-Ni distances include: (a) $\{ClNi(\mu\text{-}C(TMS)PMe_3)\}_2$, 2.281(1) Å, König, H.; Menu, M. J.; Dartiguenave, M.; Dartiguenave, Y.; Klein, H. F. *J. Am. Chem. Soc.* **1990**, *112*, 5351. (b) $[\{(IPr)Ni\}_2(\mu\text{-}Cl)(\mu\text{-}NMes)][B(Ar^F)_4]$, 2.2911(8) Å, Laskowski, C. A.; Hillhouse, G. L. *Organometallics* **2009**, *28*, 6114. (c) $\{Ni(NPh_2)_2\}_2$, 2.327(2) Å, Hope, H.; Olmstead, M. M.; Murray, B. D.; Power, P. P. *J. Am. Chem. Soc.* **1985**, *107*, 712. (d) $\{Ni(P^tBu_2)_2\}_2$, 2.417(3) Å, Kundu, S.; Brennessel, W. W.; Jones, W. D. *Inorg. Chem.* **2011**, *50*, 9443. (e) $[\{(IPr)Ni\}_2(\mu\text{-}Cl)(\mu\text{-}CHSiMe_3)][B(Ar^F)_4]$, 2.4312(10) Å, Laskowski, C. A.; Hillhouse, G. L. *Chem. Sci.* 2011, 2, 321. (f) $[\{(IPr)Ni\}_2(\mu\text{-}Cl)(\mu\text{-}CPh_2)][B(Ar^F)_4]$, 2.4389(9) Å, Ref 117e.

(118) Luo, Y. R. *Comprehensive Handbook of Chemical Bond Energies*, CRC Press: Boca Raton, Fl, **2007**.

(119) (a) Jiménez, M. V.; Lahoz, F. J.; Lukešová, L.; Miranda, J. R.; Modrego, F. J.; Nguyen, D. H.; Oro, L. A.; Pérez-Torrente, J. J. *Chem. Eur. J.* **2011**, 17, 8115. (b) Perez-Torrente, J. J.;

Jimenez, M. V.; Hernandez-Gruel, M. A.; Fabra, M. J.; Lahoz, F. J.; Oro, L. A. *Chem. Eur. J.* **2009**, *15*, 12212.

(120) Ishiwata, K.; Kuwata, S.; Ikariya, T. *J. Am. Chem. Soc*. **2009**, *131*, 5001.

(121) Latypov, S. K.; Polyancev, F. M.; Ganushevich, Y. S.; Miluykov, V. A.; Sinyashin, O. G. *Dalton Trans.* **2016**, *45*, 2053.

(122) Zimmer-De Iuliis, M.; Morris, R. H. *J. Am. Chem. Soc*. **2009**, *131*, 11263.

(123) Bernskoetter, W. H.; Lobkovsky, E.; Chirik, P. J. *J. Am. Chem. Soc*. **2005**, *127*, 14051.

(124) (a) Liptrot, D. J.; Guo, J.-D.; Nagase, S.; Power, P. P. *Angew. Chem. Int. Ed.* **2016**, *55*, 14766. (b) Wagner, J. P.; Schreiner, P. R. *Angew. Chem. Int. Ed*. **2015**, *54*, 12274.

(125) Pangborn, A. B.; Giardello, M. A.; Grubbs, R. H.; Rosen, R. K.; Trimmers, F. *J. Organometallics* **1996**, *15*, 1518.

(126) Frisch, M. J.; Trucks, G. W.; Schlegel, H. B.; Gaussian 09, Revisions, D.01; Gaussian, Inc.: Wallingford, CT, 2009.

(127) Svensson, M.; Humbel, S.; Froese, R. D.; Matsubara, T.; Sieber, S.; Morokuma, K. *J. Phys. Chem*. **1996**, *100*, 19357.

(128) Rassolov, V. A.; Ratner, M. A.; Pople, J. A.; Redfern, P. C.; Curtiss, L. A. *J. Comp. Chem.* **2001**, *22*, 976.

(129) Marenich, A. V.; Cramer, C. J.; Truhlar, D. G. *J. Phys. Chem. B* **2009**, *113*, 6378.

(130) Schmidt, M. W.; Baldridge, K. K.; Boatz, J. A.; Elbert, S. T.; Gordon, M. S.; Jensen, J. H.; Koseki, S.; Matsunaga, N.; Nguyen, K. A. *J. Comput. Chem.* **1993**, *14* (11) 1347.

Chapter 4 - {(IPr)Ni(μ-S)}$_2$ Reactivity with Pinacolborane

4.1. Introduction

Kinetic studies in chapter 3 detail the reaction of {(IPr)Ni(μ-S)}$_2$ (**6**) with H_2 to produce {(IPr)Ni(μ-SH)}$_2$ (**7**).[131] DFT calculations show that H_2 is cleaved in a heterolytic manner across the Ni-S bond in the Ni_2S_2 plane of **6**, to form a hydride-hydrosulfide intermediate, which rearranges by a Ni→S H shift to afford **7**. This mechanism suggests that other substrates with reactive E-H groups might undergo similar reactions. The goal of this chapter is to determine if this heterolytic reactivity can be extended to other functional groups or is limited to H_2.

Mono-nuclear transition metal complexes supported by thiolate and sulfide ligands have shown competency at activating H-H, H-B, and H-Si bonds (Scheme 12).[132] The [(Ar$_3$P)Ru(2,6-(dimesitylphenyl)thiolate)]$^+$ complex is capable of activating H_2, H-B, and H-Si type bonds, and is catalytically active for the hydrosilation of ketones and N-heterocycles. (Cp*)$_2$Ti(Py)=S will reversibly react with both H_2 and tertiary silanes.

Scheme 12. Heterolytic activation of H-E type bonds by mononuclear transition metal complexes.

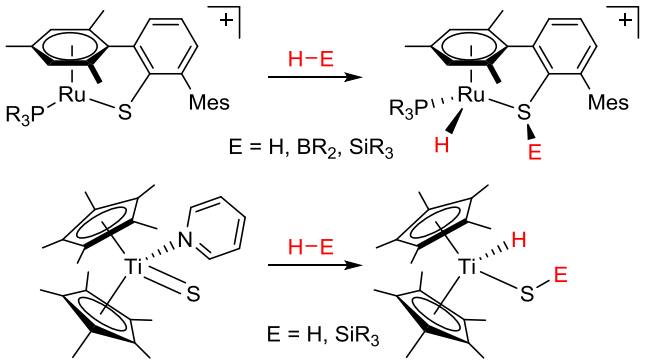

Research into the activation of E-H bonds by heterolytic addition across M-L bonds of dinuclear complexes is limited (Scheme 13).[133] The dinuclear $\{(Cp^*)Ru\}_2(\mu\text{-}NPh)(\mu\text{-}CH_2)$ complex reacts with a wide range of substrates, including alkynes, amines, and alcohols, in a heterolytic fashion to produce $\{(Cp^*)Ru\}_2(\mu\text{-}NHPh)(\mu\text{-}CH_2)(\mu\text{-}E)$ type species.[134] Dinuclear Ta complexes react with boranes and silanes to add the E-H bond across a bridging N_2 unit to form a hydride and $\mu\text{-}\eta^1,\eta^2\text{-}N{=}N\text{-}E$ groups.[135] Rh and Ir dimers activate multiple functional groups including amines, alcohols, and phosphines, however these processes can also be described as acid-base reactions at the ligands.[136] Lastly, the dinuclear complex $\{(PNP)Ni\}_2$ complex (PNP = $N[2\text{-}P(CHMe_2)_2\text{-}4\text{-}MeC_6H_3]_2$) will heterolytically cleave an H-Si bond and disproportionate into (PNP)Ni-H and (PNP)Ni-SiR_3 species.[137]

Scheme 13. Heterolytic activation of E-H bonds by dinuclear complexes.

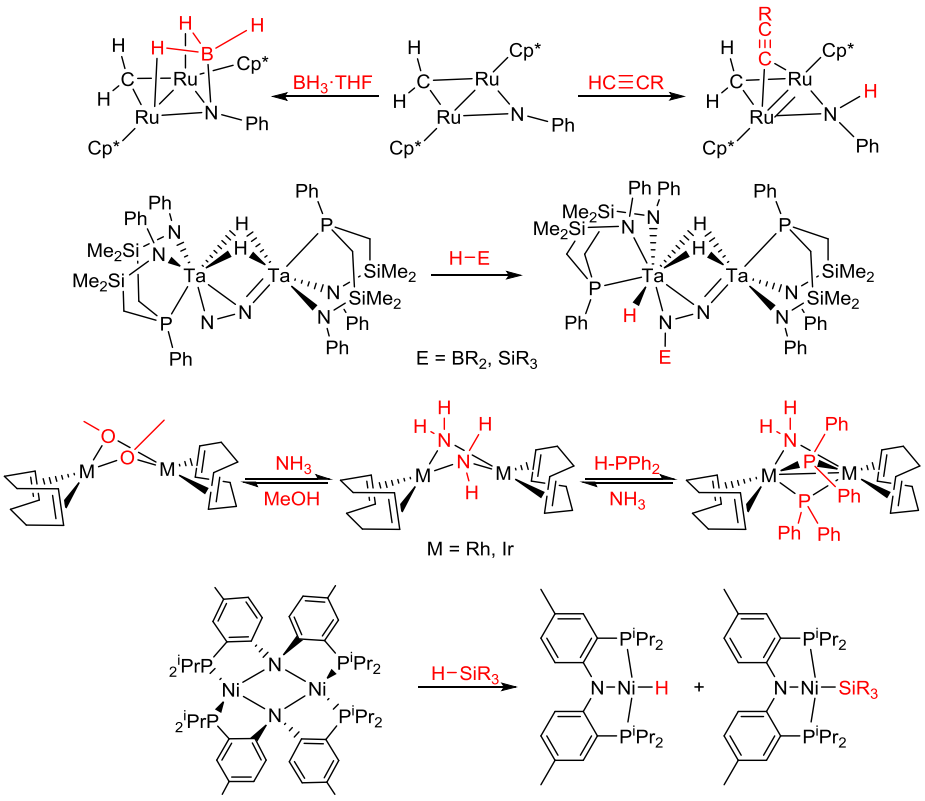

While the borylthiolate functional group, -SBR_2, was first reported in 1975 this unit is rare and only accessible by a few methods with limited functional group tolerance and selectivity (Scheme 14).[138] For example, heterolytic addition of H-BPin across thioketone affords R_2B-$SCHR_2$ products.[139] Borylthiolates are primarily used for Pd-catalyzed coupling reactions, and will react with diazo- compounds to insert a :CR_2 fragment into the R'S-BR"$_2$ bond to afford α,α-borylthiols of the form R'S-CR_2-BR"$_2$.[140]

Scheme 14. Synthetic routes to borylthiolate complexes.

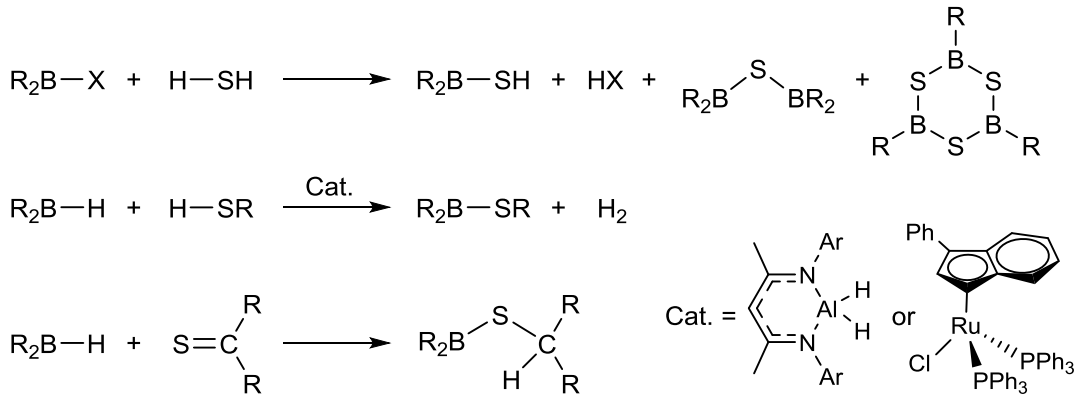

4.2. Results and Discussion

The reaction of the dinuclear μ-sulfide complex {(IPr)Ni(μ-S)}$_2$ (**6**) with HBPin (Pin = 4,4,5,5-tetramethyl-diolate) in solvent produces {(IPr)Ni}$_2$(μ-SH)(μ-SBPin) (**8**) within seconds at room temperature. The reaction is quantitative as measured by ^{1}H NMR, and is accompanied by a color change from turquoise to yellow.

Scheme 15. Reaction of HBPin with **6**.

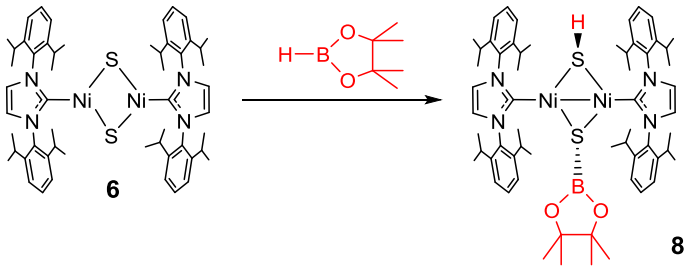

Chilling a concentrated pentane solution of **8** yields X-ray quality yellow plates. In the solid state, **8** assumes a bimetallic structure with planar Ni centers (sum of angles: 359.2(2)°, 359.2(2)°, Figure 49) linked by μ-SH and μ-SBPin ligands. The SH hydrogen was located in the difference map and its position refined isotropically. The Ni_2(SH)(SBPin) core forms a diamond with only the anti-isomer observed. Both imidazolin-2-ylidene rings are almost perpendicular to the Ni plane (72.3° and 85.9°). Two di-*iso*-propylphenyl rings are positioned above the μ-SH group. The Ni-Ni distance is 2.4302(5) Å, longer than that in **7** (2.3601(7) Å) but still within the range for Ni(I)-Ni(I) species with antiferromagnetically coupled Ni centers (2.314(1) - 2.559(2) Å).[141] The B center is trigonal planar (sum of angles: 360.0(7)°), and the S-B distance is 1.804(3) Å, in the range for typical B-S bonds in 3-coordinate B compounds.[142] The BPin fragment is disordered (82:18) over two rotational conformers (Figure 49b).

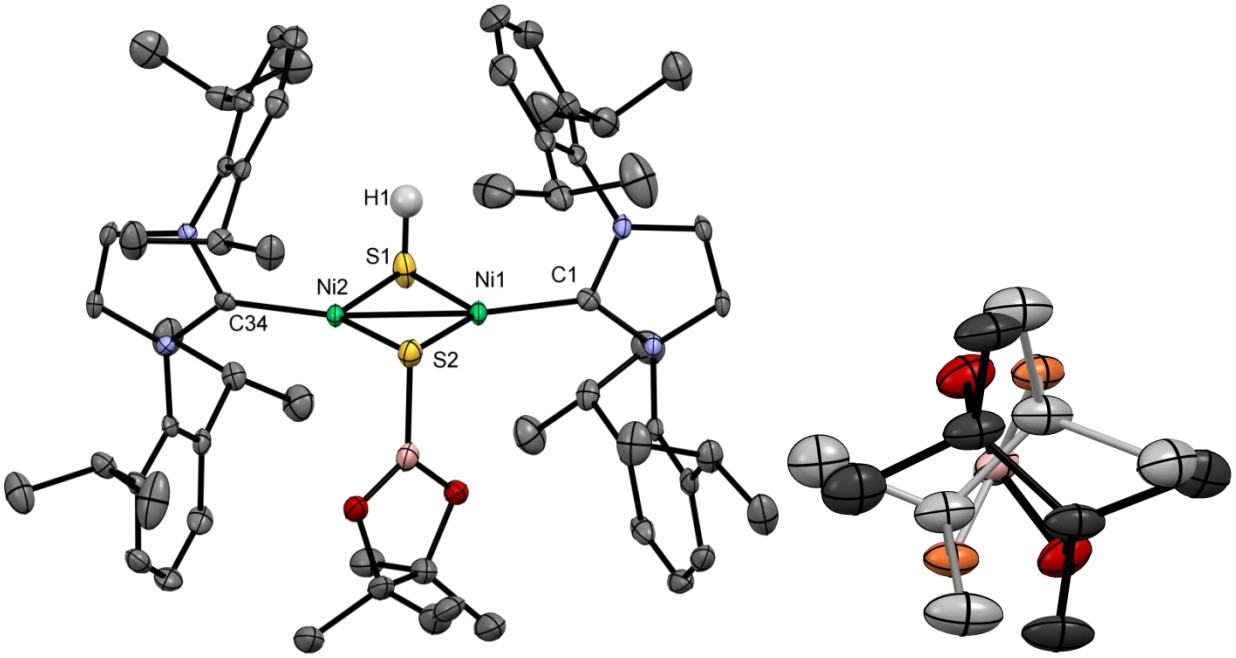

Figure 49. Molecular structure of {(IPr)Ni}$_2$(μ-SH)(μ-SBPin) (**8**). (a) Full structure with hydrogen atoms omitted. (b) Substructure viewed along S-B bond, showing two rotamers. Selected bond distances (Å) and angles (°): Ni(1)-Ni(2) = 2.4302(5), Ni(1)-S(1) = 2.1945(8), Ni(1)-S(2) = 2.2220(8), Ni(2)-S(1) = 2.2089(8), Ni(2)-S(2) = 2.2260(8), Ni(1)-C(1) = 1.889(2), Ni(2)-C(34) = 1.892(2), S(2)-B(1) = 1.804(3); Ni(1)-S(1)-Ni(2) = 66.99(2), Ni(1)-S(2)-Ni(2) = 66.24(2), S(1)-Ni(1)-S(2) = 113.67(3), S(1)-Ni(2)-S(2) = 112.94(3), C(1)-Ni(1)-S(1) = 121.16(8), C(1)-Ni(1)-S(2) = 124.35(8), C(34)-Ni(2)-S(1) = 115.51(8), C(34)-Ni(2)-S(2) = 130.74(8).

The ^{1}H NMR spectrum of **8** in solution contains a high-field resonance integrating for 1H at δ = -6.1 (Figure 50a). This resonance is ca. 1.3 ppm further upfield from that of **7 (**δ = -4.8). The high-field chemical shift is consistent with the anisotropic shielding by the two dipp rings expected for the solid state structure. Two methyl resonances and one methine resonance are observed, indicating that all four isopropyl groups are equivalent on the NMR time scale. The N-dipp bond rotation is assumed to be slow, so this equivalence suggests that inversion of the S centers is fast. VT ^{1}H NMR studies were performed to probe this possibility. At 215 K all of the ^{1}H NMR resonances begin to broaden (Figure 50b), indicating that the inversion at S can be slowed, although the barrier is low. Sulfur inversion barriers are reported to two dimeric systems, {(Cp)(CO)Fe(μ-SPh)}$_2$ and {(dippe)Rh(μ-SR)}$_2$. The Fe complex has an inversion

barrier of 30.7 kcal/mol,[143] while the Rh complexes have barriers 7.7 – 14.7 kcal/mol, for R = Ph and 2-phenylthiophenol respectively.[144] In monomeric Ru-, Pd-, and Pt-thioether complexes the inversion barriers have been measured as low as 11.2 kcal/mol.[145]

Figure 50. ^{1}H NMR spectra of {(IPr)Ni}$_2$(μ-SH)(μ-SBPin) (**8**), taken (a) at 298 K in C_6D_6 and (b) at 215 K in toluene-d8.

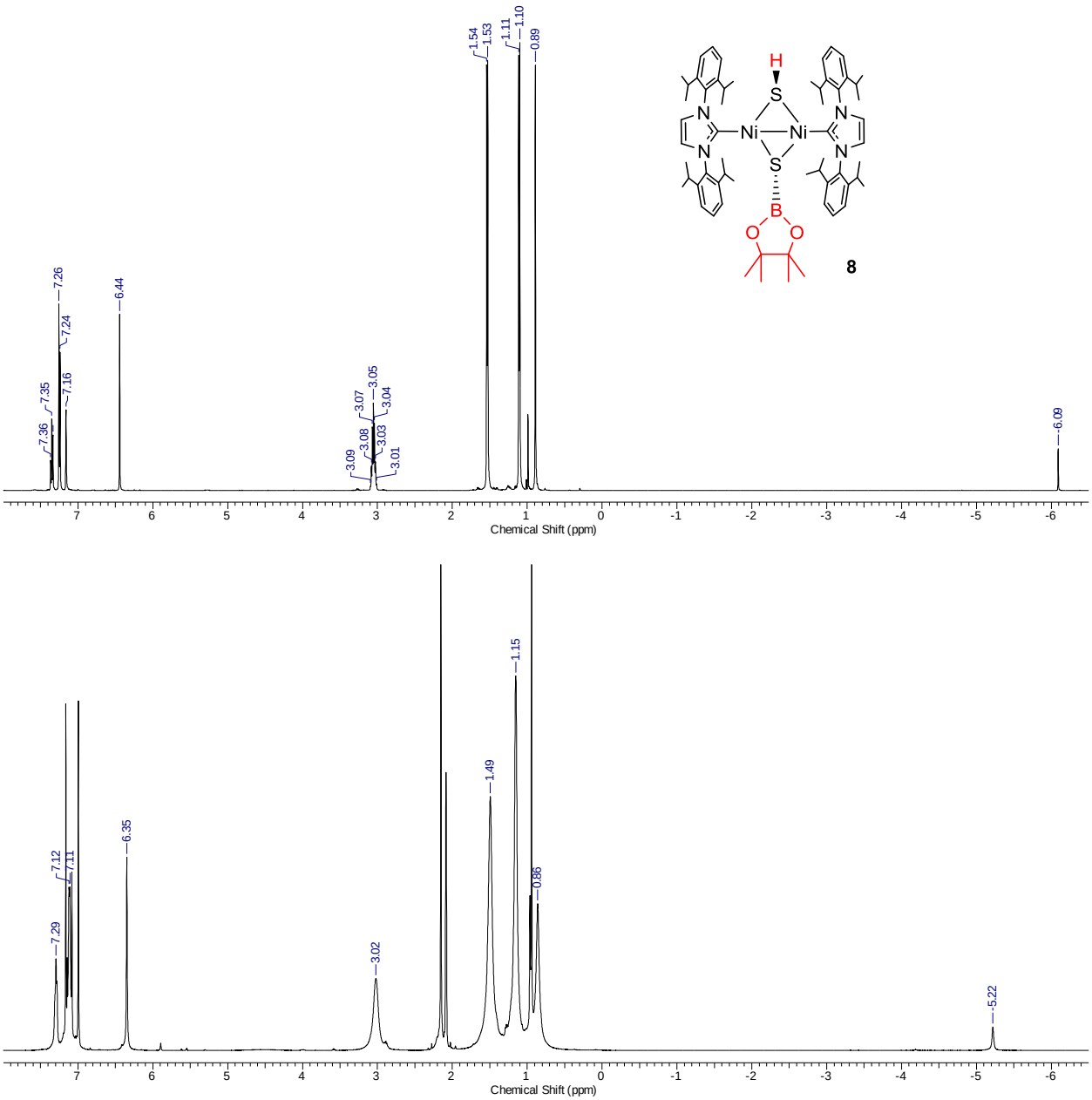

Complex **8** is the first crystallographically characterized example of a borylthiolate unit bridging two metal centers,[146] and one of now three examples of a borylthiolate coordinated to a metal center. The two other complexes, based on Rh and Os, feature terminal borylthiolates (Scheme 16). The dinuclear Rh(III) complex $\{(PinBS)(Et_3P)_2Rh\}_2(\mu\text{-}C)$ was formed by the reaction of CS_2 with the rhodium-boryl complex $(Et_3P)_3Rh\text{-}BPin$, which results in complete C-S bond cleavage and produces the terminal borylthiolate.[147] The mononuclear Os(II) complex $Os(P^iPr_3)_2(H)(H_2)(SBPin)$ was synthesized from $Os(P^iPr_3)_2(H)(SH)$ by heterolytic cleavage of the H-B bond across the Os-S bond and subsequent H migration from S to Os.[148] Both of these complexes contain electrophilic d^6 metal centers, while **8** contains two Ni(I) d^9 centers. The S-B bond in **8**, 1.804(3) Å, is 0.02 Å longer than those in the Rh and Os complexes (1.777(10) and 1.784(3) Å respectively). The ^{11}B NMR resonance of **8** appears at δ = 25.2, slightly upfield from those of the Rh and Os complexes, which are observed at δ = 33.6 and 35 respectively, and organic borylthiolates, which are observed in the range δ = 32.8-33.7.

Scheme 16. Synthesis of crystallographically characterized metal-borylthiolates.

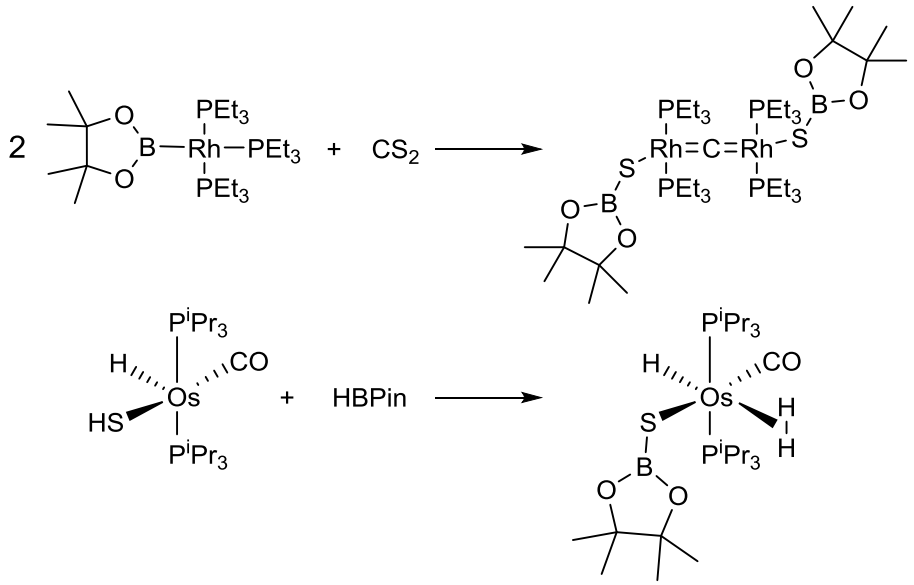

4.3. Experimental Section

General Procedures. All experiments were performed under nitrogen using drybox or Schlenk techniques. Nitrogen was purified by passage through activated molecular sieves and Q-5 oxygen scavenger. Anhydrous Et_2O was purified by passage through activated alumina.[149] Anhydrous pentane was purified by passage through activated alumina and BASF R3-11 oxygen scavenger. C_6D_6 was purchased from Cambridge Isotope Laboratories, degassed by freeze-pump-thaw cycles, and dried over Na-benzophenone ketyl or activated Linde 4 Å molecular sieves. Celite and 4 Å molecular sieves were activated by evacuation overnight at 180 ºC. Pinacolborane was purchased from Sigma Aldrich and used as received. $\{(IPr)Ni(\mu\text{-}S)\}_2$ (**6**) was prepared by the literature preparation. [131] NMR spectra were recorded on a Bruker DRX-500 spectrometer at room temperature using Teflon-valved tubes. ^1H and ^{13}C chemical shifts are reported relative to $SiMe_4$ and were determined by reference to the residual ^1H and solvent resonances (^1H: residual C_6D_5H in C_6D_6 δ 7.16; ^{13}C: C_6D_6 δ 128.1). Coupling constants are given in hertz (Hz). ^{11}B NMR spectra were collected on a Bruker DRX-400 spectrometer,

and reported relative to an externally referenced $BF_3{\cdot}Et_2O$: δ = 0. C_6D_6 was distilled from Na-benzophenone and stored under vacuum.

Synthesis of {(IPr)Ni}$_2$(μ-SH)(μ-SBPin) (8). Neat HBPin (5.5 μL, 0.038 mmol) was added dropwise via microsyringe into a solution of **6** (0.0360 g, 0.038 mmol) in 5 mL Et_2O while the mixture was stirred. The color turned from turquoise to bright green to neon yellow within 10 sec. The solution was stirred for 5 min and transferred to a scintillation vial. The solution was chilled to -35 °C overnight, and the resulting yellow crystals were collected by vacuum filtration. Yield: 0.0187 g (46 %). X-ray quality crystals were grown by liquid diffusion of pentane into an Et_2O solution of **8** at -35 °C. ^{1}H NMR (22 °C, 500 MHz, C_6D_6): δ 7.35 (t, J = 7.5, 4H), 7.25 (d, J = 7.5, 8H), 6.45 (s, 4H), 3.05 (sept, J = 6.5, 8H), 1.53 (d, J = 6.5, 24H), 1.11 (d, J = 6.5, 24H), 0.89 (s, 12H), -6.09 (s, 1H). ^{13}C{^{1}H} NMR (22 °C, 500 MHz, C_6D_6): δ 187.2 (Ni-*C*N_2), 146.9 (*o*-*C*$_6{}^{i}Pr_2H_3$), 138.0 (*i*-*C*$_6{}^{i}Pr_2H_3$), 129.4 (*p*-*C*$_6{}^{i}Pr_2H_3$), 124.4 ($CN_2C_2H_2$), 124.2 (*m*-*C*$_6{}^{i}Pr_2H_3$), 82.1 ($BO_2C_2Me_4$), 28.9 (Ar-*C*HMe_2), 25.1 (ArCH(*C*$H_3)_2$), 25.0 (ArCH(*C*$H_3)_2$), 24.4 (BO_2C_2(*C*$H_3)_4$). ^{11}B{^{1}H} NMR (22 °C, 400 MHz, C_6D_6): δ 25.2.

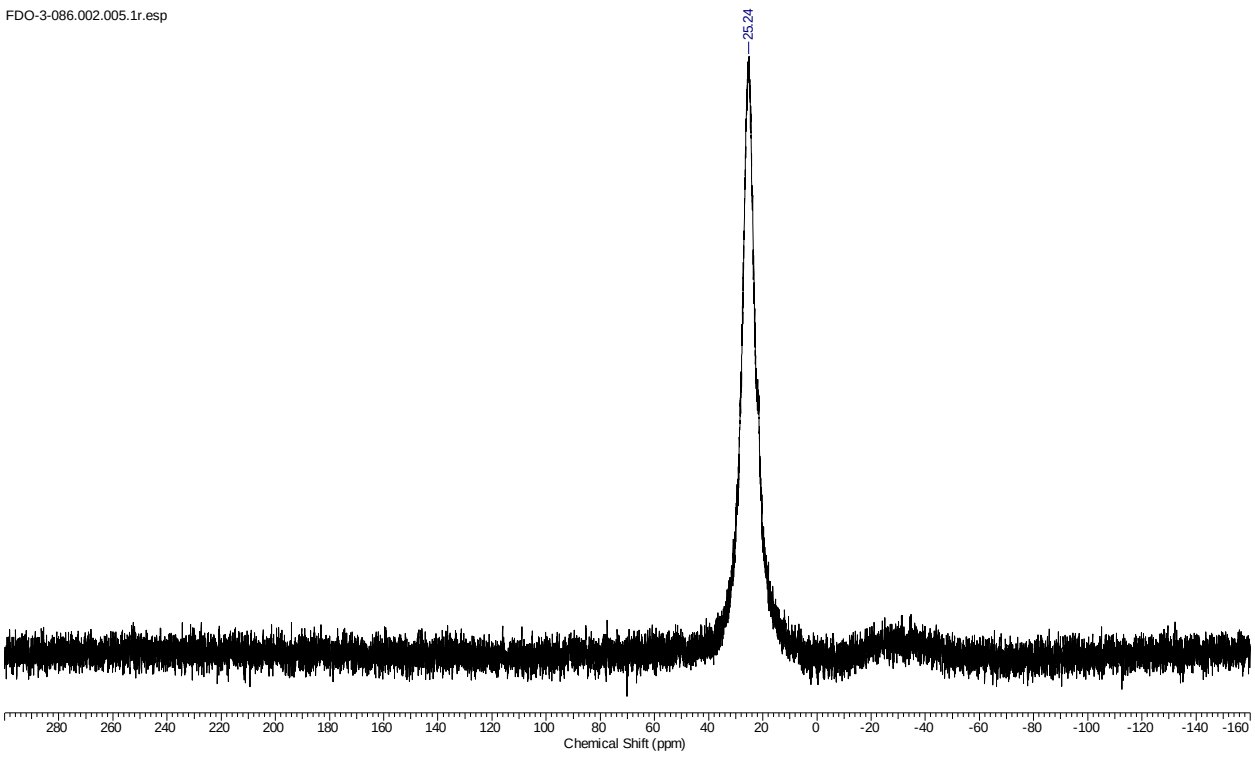

Figure 51. ^{11}B NMR spectrum of {(IPr)Ni}$_2$(μ-SH)(μ-SBPin) (**8**), taken in C_6D_6 at 22 °C, d1 = 3 sec, lb = 3 Hz, 9000 scans.

X-ray Data Collection and Structure Refinement. A yellow plate grown from the mixture of ether/pentane was mounted on a Dual-Thickness MicroMount (MiTeGen) with 30 μm sample aperture with Fluorolube™ oil. The diffraction data were measured at 100 K on a Bruker D8 VENTURE diffractometer equipped with a microfocus Mo-target X-ray tube (λ = 0.71073 Å) and PHOTON 100 CMOS detector. Data reduction and integration were performed with the Bruker APEX3 software package (Bruker AXS, version 2015.5-2, 2015). Data were scaled and corrected for absorption effects using the multi-scan procedure as implemented in SADABS (Bruker AXS, version 2014/5, 2015, part of Bruker APEX3 software package). The structure was solved by SHELXT (Version 2014/5)[150] and refined by a full-matrix least-squares procedure using OLEX2[151] (XL refinement program version 2014/7)[152]. Crystallographic data and details of the data collection and structure refinement are listed in Table 6.

All atoms were refined with anisotropic thermal parameters. Hydrogen atoms were included in idealized positions for structure factor calculations except the H-atom attached to S1, which was found in the difference Fourier map and refined without any geometric restraints. Its thermal parameter was constraint to be 1.2 times of the S1 atom. The boronic ester group was found to be disordered over two rotational orientations (refined to 82:18 occupancies ratio). This disorder was modelled with the application of geometric (SADI) restraints and using enhanced rigid body restraints (RIGU) for thermal parameters. A solvent molecule was located on the edge of two unit cells. It was modeled as purely Et_2O, although it could also be modeled as purely pentane, or as partial occupations of both. All structures are drawn with thermal ellipsoids at 50% probability.

Table 6. Crystal data and structure refinement for $(IPrNi)_2(\mu\text{-}SH)(\mu\text{-}SBPin)$ (**8**).

Identification code	0273_frankolec
Empirical formula	$C_{62}H_{90}BN_4Ni_2O_{2.5}S_2$
Formula weight	1123.72
Temperature/K	100(2)
Crystal system	monoclinic
Space group	$P2_1/c$
a/Å	25.528(3)
b/Å	12.3656(13)
c/Å	20.065(2)
α/°	90
β/°	103.772(3)
γ/°	90
Volume/Å^3	6152.1(11)
Z	4
ρ_{calc}g/cm^3	1.213
μ/mm^{-1}	0.724
F(000)	2412.0
Crystal size/mm^3	0.08 × 0.06 × 0.02
Radiation	MoKα (λ = 0.71073)
2Θ range for data collection/°	4.662 to 51.506
Index ranges	-31 ≤ h ≤ 31, -15 ≤ k ≤ 15, -24 ≤ l ≤ 22
Reflections collected	82382
Independent reflections	11404 [R_{int} = 0.0742, R_{sigma} = 0.0724]
Data/restraints/parameters	11404/481/787

Goodness-of-fit on F^2	1.007
Final R indexes [I>=2σ (I)]	R_1 = 0.0441, wR_2 = 0.0760
Final R indexes [all data]	R_1 = 0.0910, wR_2 = 0.0876
Largest diff. peak/hole / e $Å^{-3}$	0.44/-0.48

4.4. References

(131) Olechnowicz, F.; Hillhouse, G. L.; Jordan, R. F. *Inorg. Chem.* **2015**, *54*, 2705.

(132) (a) Bähr, S.; Simonneau, A.; Irran, E.; Oestreich, M. *Organometallics* **2016**, 35, 925. (b) Milstein, D. *Philos. Trans. R. Soc. A* **2015**, *373*, 20140189. (c) Khusnutdinova, J. R.; Milstein, D. *Angew. Chem. Int. Ed.* **2015**, *54*, 12236. (d) Stevenson, L.; Mellino, S.; Clot, E.; Mountford, P. *J. Am. Chem. Soc.* **2015**, *137*, 10140. (e) Stahl, T.; Hrobarik, P.; Konigs, C. D.; Ohki, Y.; Tatsumi, K.; Kemper, S.; Kaupp, M.; Klare, H. F. T.; Oestreich, M. *Chem. Sci.* **2015**, *6,* 4324. (f) Stahl, T.; Muther, K.; Ohki, Y.; Tatsumi, K.; Oestreich, M. *J. Am. Chem. Soc.* **2013**, 135, 10978. (g) Klare, H. F. T.; Oestreich, M.; Ito, J.-i.; Nishiyama, H.; Ohki, Y.; Tatsumi, K. *J. Am. Chem. Soc.* **2011**,133, 3312. (h) Ikariya, T. *Bull. Chem. Soc. Jpn.* **2011**, *84*, 1. (i) Seino, H.; Misumi, Y.; Hojo, Y.; Mizobe, Y. *Dalton Trans.* **2010**, 39, 3072. (j) Misumi, Y.; Seino, H.; Mizobe, Y. *J. Am. Chem. Soc.* **2009**, 131, 14636. (k) Ohki, Y.; Sakamoto, M.; Tatsumi, K. *J. Am. Chem. Soc.* **2008**,130, 11610. (l) Sellmann, D.; Prakash, R.; Heinemann, F. W.; Moll, M.; Klimowicz, M. *Angew. Chem. Int. Ed.* **2004**, 43, 1877. (m) Sweeney, Z. K.; Polse, J. L.; Bergman, R. G.; Andersen, R. A. *Organometallics* **1999**, 18, 5502. (n) Sellmann, D.; Rackelmann, G. H.; Heinemann, F. W. *Chem. Eur. J.* **1997**, *3*, 2071.

(133) (a) Saha, B.; Rahaman, S. M. W.; Daw, P.; Sengupta, G.; Bera, J. K. *Chem. - Eur. J.* **2014**, *20*, 6542. (b) Kimura, T.; Koiso, N.; Ishiwata, K.; Kuwata, S.; Ikariya, T. *J. Am. Chem. Soc.* **2011**, *133*, 8880. (c) Zhu, M.; Fujita, K.; Yamaguchi, R. *Org. Lett.* **2010**, *12*, 1336. (d) Ishiwata, K.; Kuwata, S.; Ikariya, T. *J. Am. Chem. Soc*. **2009**, *131*, 5001. (e) MacKay, B. A.; Munha, R. F.; Fryzuk, M. D. *J. Am. Chem. Soc*. **2006**, *128*, 9472. (f) Fryzuk, M. D.; Love, J. B.; Rettig, S. J.; Young, V. G. *Science*, **1997**, *275*, 1445.

(134) Takemoto, S.; Ito, T.; Yamazaki, Y.; Tsujita, M.; Matsuzaka, H. *J. Organomet. Chem.* **2016**, 812, 158.

(135) Fryzuk, M. D.; MacKay, B. A.; Johnson, S. A.; Patrick, B. O. *Angew. Chem. Int. Ed.* **2002**, *41*, 3709.

(136) (a) Velez, E.; Betoré, M. P.; Casado, M. A.; Polo, V. *Organometallics* **2015**, *34*, 3959. (b) Mena, I.; Casado, M. A.; Polo, V.; García-Orduña, P.; Lahoz, F. J.; Oro, L. A. *Dalton Trans.* **2014**, *43*, 1609. (c) Mena, I.; Casado, M. A.; Polo, V.; García-Orduña, P.; Lahoz, F. J.; Oro, L. A. *Angew. Chem. Int. Ed.* **2012**, *51*, 8259.

(137) Adhikari, D.; Pink, M.; Mindiola, D. J. *Organometallics* **2009**, *28*, 2072.

(138) (a) Romero, E. A.; Peltier, J. L.; Jazzar, R.; Bertrand, G. *Chem. Commun.* **2016**, *52*, 10563. (b) Yang, Z.; Zhong, M.; Ma, X.; Nijesh, K.; De, S.; Parameswaran, P.; Roesky, H. W. *J.*

Am. Chem. Soc. **2016**, 138, 2548. (c) Fernandez-Salas, J. A.; Manzini, S.; Nolan, S. P. *Chem. Commun.* **2013**, *49*, 5829. (d) Siebert, W.; Gast, E.; Riegel, F.; Schmidt, M. *J. Organomet. Chem.* **1975**, *90*, 13.

(139) Carter, C. A. G.; Vogels, C. M.; Harrison, D. J.; Gagnon, M. K. J.; Norman, D. W.; Langler, R. F.; Baker, R. T.; Westcott, S. A. *Organometallics* **2001**, 20, 2130.

(140) (a) Civit, M. G.; Royes, J.; Vogels, C. M.; Westcott, S. A.; Cuenca, A. B.; Fernández, E. *Org. Lett*. **2016**, *18*, 3830. (b) Ishiyama, T.; Mori, M.; Suzuki, A.; Miyaura, N. *J. Organomet. Chem.* **1996**, *525*, 225. (c) Ishiyama, T.; Nishijima, K.; Miyaura, N.; Suzuki, A. *J. Am. Chem. Soc.* **1993**, *115*, 7219.

(141) Ni(I)-Ni(I) complexes with bridging ligands exhibit short Ni-Ni distances in the range 2.314(1) - 2.559(2) Å, see: (a) Jones, R. A.; Norman, N. C.; Seeberger, M. H.; Atwood, J. L.; Hunter, W. E. *Organometallics* **1983**, *2*, 1629. (b) Jones, R. A.; Whittlesey, B. R. *Inorg. Chem.* **1986**, *25*, 852. (c) Morgenstern, D. A.; Ferrence, G. M.; Washington, J.; Henderson, J. I.; Rosenhein, L.; Heise, J. D.; Fanwick, P. E.; Kubiak, C. P. *J. Am. Chem. Soc.* **1996**, *118*, 2198. (d) Kriley, C. E.; Woolley, C. J.; Krepps, M. K.; Popa, E. M.; Fanwick, P. E.; Rothwell, I. P. *Inorg. Chim. Acta* **2000**, *300*, 200. (e) Dorta, R.; Stevens, E. D.; Hoff, C. D.; Nolan, S. P. *J. Am. Chem. Soc.* **2003**, *125*, 10490. (f) Ito, M.; Matsumoto, T.; Tatsumi, K. *Inorg. Chem.* **2009**, *48*, 2215. (g) Inosako, A.; Kunishita, A.; Kubo, M.; Ogura, T.; Sugimoto, H.; Itoh, S. *Dalton Trans.* **2009**, 9410. (h) Varonka, M. S.; Warren, T. H. *Organometallics* **2010***, 29*, 717.

(142) CSD search performed 2016/12/10 found 202 3-coordinate B-S complexes, with B-S bond lengths spanning of 1.720 - 1.895 Å and an average of 1.82 Å.

(143) Dekker, M.; Knox, G. R.; Robertson, C. G. *J. Organomet. Chem.* **1969**, *18*, 161.

(144) Oster, S. S.; Jones, W. D. *Inorg. Chim. Acta* **2004**, *357*, 1836.

(145) (a) Chauhan, R.; Mashuta, M. S.; Grapperhaus, C. A. *Inorg. Chem.* **2012**, *51*, 7913. (b) Adams, H.; Amado, A. M.; Félix, V.; Mann, B. E.; Antelo-Martinez, J.; Newell, M.; Ribeiro-Claro, P. J. A.; Spey, S. E.; Thomas, J. A. *Chem.—Eur. J.* **2005**, *11*, 2031. (c) Baradello, L.; Lo Schiavo, S.; Nicolò, F.; Lanza, S.; Alibrandi, G.; Tresoldi, G. *Eur. J. Inorg. Chem.* **2004**, *2004*, 3358. (d) Tresoldi, G.; Lo Schiavo, S.; Lanza, S.; Cardiano, P. *Eur. J. Inorg. Chem.* **2002**, *2002*, 181. (e) Abel, E. W.; Ahmed, A. K. S.; Farrow, G. W.; Orrell, J. G.; Sik, V. *J. Chem. Soc. Dalton Trans.* **1977**, 47. (f) Rauk, A.; Allen, L. C.; Mislow, K. *Angew. Chem. Int. Ed.* **1970**, *9*, 400.

(146) CSD search performed 2016/12/09.

(147) Kalläne, S. I.; Braun, T.; Teltewskoi, M.; Braun, B.; Herrmanna, R.; Laubensteina, R. *Chem. Commun.* **2015**, *51*, 14613.

(148) Esteruelas, M. A.; López, A. M.; Mora, M.; Oñate, E. *Chem. Commun*. **2013**, *49*, 7543.

(149) Pangborn, A. B.; Giardello, M. A.; Grubbs, R. H.; Rosen, R. K.; Trimmers, F. *J. Organometallics* **1996**, *15*, 1518.

(150) Sheldrick, G. M. *Acta Cryst*. **2015**, *A71*, 3.

(151) Dolomanov, O. V.; Bourhis, L. J.; Gildea, R. J.; Howard J. A. K.; Puschmann. H. *J. Appl. Cryst.* **2009**, *42*, 339.

(152) (a) *Sheldrick, G. M. Acta Cryst.* **2015**, *C71*, 3. (b) Sheldrick, G. M. *Acta Cryst.* **2008**, *A64*, 112.

Appendix 1 – Calculation Coordinates

5.1. Coordinates for calculations from Chapter 2

5.1.1. Geometry Optimization of 2

B3LYP functional, LANL2DZ for Ni, 6-31+G for other atoms

28	1.5577590	-0.4598160	-0.5875390
28	-1.5576020	-0.4603120	0.5850080
17	-2.1325500	0.1561690	2.6364260
17	2.1356640	0.1598630	-2.6371400
16	-0.3959520	-1.6066170	-0.9657610
16	0.3947060	-1.6103250	0.9588280
7	-4.1972980	-0.8384630	-0.6035580
7	-3.8089190	1.2710750	-0.3470400
7	4.1951700	-0.8432880	0.6047700
7	3.8106420	1.2669990	0.3485580
6	3.2327790	0.0390920	0.2026030
6	5.3572470	-0.1761230	0.9795540
1	6.2321210	-0.7069250	1.3180450
6	5.1128390	1.1459690	0.8268910
1	5.7282900	2.0101410	1.0153220
6	-3.2328390	0.0421820	-0.2025220
6	-5.3588610	-0.1692440	-0.9762360
1	-6.2351070	-0.6984610	-1.3136560
6	-5.1120900	1.1523900	-0.8233220
1	-5.7265100	2.0176230	-1.0102850
6	4.0611430	-2.2823370	0.7069730
6	4.2747000	-3.0727330	-0.4407490
6	4.1832290	-4.4624280	-0.2871480
1	4.3397680	-5.1027930	-1.1493120
6	3.9045530	-5.0369680	0.9492570
1	3.8405170	-6.1179330	1.0429120
6	3.7129910	-4.2310320	2.0676520
1	3.5006370	-4.6917600	3.0274450
6	3.7856570	-2.8359800	1.9760900
6	3.6127200	-1.9842790	3.2328830
1	3.4554970	-0.9463790	2.9226640
6	2.3896370	-2.3939590	4.0749870
1	1.4724490	-2.4021010	3.4789390
1	2.2529830	-1.6849850	4.8994680
1	2.5134040	-3.3888180	4.5181240
6	4.8896560	-2.0231760	4.0997710
1	5.0969870	-3.0433110	4.4443030
1	4.7708220	-1.3862000	4.9841750
1	5.7691530	-1.6737530	3.5480190
6	4.6614460	-2.4748810	-1.7906690
1	4.3729920	-1.4213070	-1.7963440
6	3.9234540	-3.1279860	-2.9720440
1	4.2178380	-4.1742220	-3.1198910
1	4.1579700	-2.5849410	-3.8936960
1	2.8396170	-3.0842590	-2.8309100
6	6.1901540	-2.5529620	-1.9892320
1	6.7296660	-2.0298710	-1.1909470
1	6.4734460	-2.0946310	-2.9440780
1	6.5348310	-3.5943920	-1.9980030
6	3.2027040	2.5612550	0.1059840
6	2.3207050	3.0824920	1.0793590
6	1.8035080	4.3639710	0.8550770
1	1.1110200	4.7905160	1.5715550
6	2.1645040	5.1025900	-0.2686350
1	1.7558340	6.0991730	-0.4162940
6	3.0516270	4.5717310	-1.1978710
1	3.3302100	5.1594720	-2.0668610
6	3.5925790	3.2889800	-1.0379390
6	4.5984420	2.7669240	-2.0617480
1	4.6939820	1.6869960	-1.9210530
6	4.1344500	2.9838470	-3.5140430
1	3.1444610	2.5510650	-3.6731090
1	4.8344800	2.4928310	-4.2001220
1	4.1074170	4.0467970	-3.7826140
6	5.9838650	3.4145240	-1.8488020
1	5.9348160	4.5002890	-1.9960430
1	6.7074790	3.0108800	-2.5669810
1	6.3763060	3.2362530	-0.8415750
6	1.9865560	2.3338600	2.3699060
1	1.9701970	1.2627510	2.1439700
6	0.6066370	2.6856180	2.9484170
1	0.3681860	2.0035820	3.7701370
1	-0.1884010	2.5812010	2.2059470
1	0.5810610	3.7064330	3.3496950
6	3.0780480	2.5796970	3.4357670
1	3.1334790	3.6449130	3.6917150
1	4.0695420	2.2633260	3.0956070
1	2.8437410	2.0252820	4.3523990
6	-4.0655260	-2.2776830	-0.7065780
6	-3.7921010	-2.8311330	-1.9762080
6	-3.7212140	-4.2262500	-2.0684450
1	-3.5105000	-4.6868270	-3.0286660
6	-3.9125060	-5.0324040	-0.9501810
1	-3.8498140	-6.1134070	-1.0443220

6	-4.1892900	-4.4580480	0.2867460	1	-3.3178620	5.1614990	2.0694820
1	-4.3457240	-5.0986030	1.1487830	6	-2.1546690	5.1032460	0.2696860
6	-4.2789950	-3.0683280	0.4410240	1	-1.7438140	6.0989350	0.4173140
6	-4.6640820	-2.4705620	1.7914430	6	-1.7966690	4.3645220	-0.8549420
1	-4.3734110	-1.4176060	1.7977300	1	-1.1042960	4.7901080	-1.5721070
6	-3.9272570	-3.1259790	2.9722660	6	-2.3167030	3.0842030	-1.0791850
1	-4.2242780	-4.1715090	3.1198620	6	-1.9861090	2.3357530	-2.3707370
1	-4.1600250	-2.5826720	3.8941960	1	-1.9715100	1.2644610	-2.1455420
1	-2.8433620	-3.0849650	2.8307330	6	-3.0789660	2.5844980	-3.4345510
6	-6.1929090	-2.5456110	1.9903700	1	-4.0705300	2.2700720	-3.0928010
1	-6.7315870	-2.0208180	1.1926430	1	-2.8474980	2.0300920	-4.3519140
1	-6.4749670	-2.0873810	2.9456330	1	-3.1325710	3.6499730	-3.6898070
1	-6.5397210	-3.5863370	1.9984960	6	-0.6064980	2.6852060	-2.9513700
6	-3.6197650	-1.9790920	-3.2328550	1	-0.5796980	3.7061640	-3.3521840
1	-3.4599070	-0.9416830	-2.9223120	1	-0.3707690	2.0032190	-3.7739290
6	-2.3990840	-2.3907030	-4.0774800	1	0.1896800	2.5788040	-2.2104080
1	-2.5259520	-3.3847510	-4.5215580	6	-4.5908080	2.7715360	2.0648760
1	-1.4809750	-2.4017010	-3.4829230	1	-4.6896350	1.6920390	1.9231970
1	-2.2621570	-1.6811280	-4.9013980	6	-4.1237510	2.9855600	3.5166130
6	-4.8983540	-2.0150090	-4.0974320	1	-3.1350160	2.5491720	3.6736200
1	-5.1083640	-3.0345930	-4.4419790	1	-4.8243430	2.4963570	4.2034180
1	-4.7798270	-1.3779260	-4.9818010	1	-4.0925760	4.0481670	3.7860600
1	-5.7761350	-1.6640070	-3.5439600	6	-5.9747730	3.4231280	1.8547350
6	-3.1983190	2.5641220	-0.1048090	1	-5.9226330	4.5085770	2.0032170
6	-3.5852070	3.2920070	1.0399930	1	-6.6984540	3.0205360	2.5734340
6	-3.0415570	4.5736470	1.1998370	1	-6.3690800	3.2471410	0.8478120

5.2. Coordinates for calculations from Chapter 3

5.2.1. Functional Panel, Geometry Optimization of {(L)Ni(μ-S)}$_2$ (L = 1,3-dimethyl-imidazolin-2-ylidene)

Specified functional and 6-31+G for all atoms
B3PW91 Closed Shell Singlet
E = -4421.939556 HF

28	1.1936310	-0.1272910	-0.4841480	7	3.8999860	0.9410280	-0.2351120
28	-1.1898650	-0.0414760	-0.4958500	7	3.6328000	-0.8131040	0.9773580
16	-0.0211150	-0.9627500	-1.9807970	6	5.1131970	0.6981290	0.3790150
16	0.0096770	0.3734290	1.1630950	1	5.9792860	1.3248130	0.2245280
6	-2.9676720	0.1411750	0.0936460	6	4.9435130	-0.4122260	1.1444670
7	-3.6462000	1.2518640	0.4909210	1	5.6348970	-0.9412410	1.7838590
7	-3.8817180	-0.8634780	0.1902780	6	3.6315040	2.0458840	-1.1378030
6	-4.9523950	0.9482600	0.8219430	1	4.2851540	1.9890470	-2.0140480
1	-5.6550120	1.6968010	1.1576280	1	2.5895450	1.9708620	-1.4578550
6	-5.1008640	-0.3895400	0.6337400	1	3.7847370	3.0009080	-0.6251750
1	-5.9562820	-1.0329720	0.7782880	6	3.0338120	-1.9775020	1.6071240
6	2.9704360	0.0123420	0.1221140	1	1.9578420	-1.9391150	1.4245200
				1	3.4481880	-2.8968510	1.1804660
				1	3.2200000	-1.9539780	2.6850290
				6	-3.0690570	2.5843170	0.5241150
				1	-1.9818540	2.4801470	0.4949980
				1	-3.4065530	3.1706490	-0.3371810
				1	-3.3619430	3.0897760	1.4490780
				6	-3.5945410	-2.2540510	-0.1190100
				1	-4.3054780	-2.6273360	-0.8627140

1	-2.5814860	-2.3073840	-0.5262460	6	-5.2044490	-0.5842280	0.0657550
1	-3.6551690	-2.8644000	0.7877860	1	-6.0631840	-1.1870690	-0.1908830
				6	3.0368710	-0.0599810	0.0814900
B3PW91 Open Shell Singlet				7	3.9419610	0.9243630	-0.1758030
E = -4421.943629 HF				7	3.7841460	-1.0686810	0.6070890
28	1.1888520	-0.0533270	-0.4354990	6	5.2196830	0.5397370	0.1821550
28	-1.1888990	0.0572440	-0.4354420	1	6.0768470	1.1855350	0.0600150
16	0.0003210	0.0084740	-2.1894000	6	5.1203290	-0.7230460	0.6735790
16	-0.0002610	-0.0045040	1.3112640	1	5.8753310	-1.3939390	1.0564080
6	-2.9956320	0.0719290	0.1208530	6	3.5920660	2.2211520	-0.7286470
7	-3.6739430	1.0005630	0.8478290	1	4.2752380	2.4736900	-1.5451550
7	-3.9301640	-0.8758980	-0.1670580	1	2.5718760	2.1606460	-1.1158180
6	-4.9987850	0.6424070	1.0061960	1	3.6422540	2.9946190	0.0449190
1	-5.7036750	1.2535140	1.5505440	6	3.2426590	-2.3541680	1.0119720
6	-5.1605720	-0.5457130	0.3669210	1	2.1553650	-2.2613250	1.0614690
1	-6.0319030	-1.1733240	0.2505170	1	3.5124450	-3.1294070	0.2869410
6	2.9955650	-0.0731070	0.1207820	1	3.6290670	-2.6249870	1.9991040
7	3.9306450	0.8759830	-0.1612410	6	-3.2140430	2.0387320	1.5276240
7	3.6734820	-1.0068700	0.8414840	1	-2.1255350	1.9519440	1.5116240
6	5.1609610	0.5415750	0.3702880	1	-3.5169880	2.9649870	1.0279200
1	6.0326580	1.1693930	0.2577960	1	-3.5616330	2.0498160	2.5649900
6	4.9986080	-0.6506020	1.0018200	6	-3.5915230	-1.9874730	-1.2530730
1	5.7032750	-1.2657630	1.5418690	1	-4.2305780	-1.9907380	-2.1415250
6	3.6527590	2.0904870	-0.9082150	1	-2.5483880	-1.8725450	-1.5574010
1	4.3671150	2.1956460	-1.7305470	1	-3.7096450	-2.9314560	-0.7110280
1	2.6414940	2.0139510	-1.3156280				
1	3.7145010	2.9650030	-0.2523930	B3PW91 Quintet			
6	3.0819970	-2.2364350	1.3404120	E = -4421.937552			
1	1.9963810	-2.1414240	1.2676360	28	1.2517380	-0.3182080	0.1315070
1	3.4185670	-3.0916470	0.7447770	28	-1.2496030	-0.2806240	0.0167790
1	3.3637350	-2.3841750	2.3871590	16	-0.0204760	-2.0858880	-0.0174580
6	-3.0830690	2.2271820	1.3546510	16	0.0331970	1.5304240	-0.0063330
1	-1.9974110	2.1332070	1.2811900	6	-3.1878550	0.1182770	-0.0546550
1	-3.4201440	3.0860340	0.7645750	7	-3.8716960	1.1029460	-0.6945010
1	-3.3647920	2.3679850	2.4023590	7	-4.1595650	-0.6173130	0.5530400
6	-3.6518040	-2.0850350	-0.9225030	6	-5.2329250	0.9851060	-0.4922830
1	-4.3635190	-2.1827790	-1.7480550	1	-5.9446220	1.6724710	-0.9255840
1	-2.6390920	-2.0069420	-1.3259860	6	-5.4158350	-0.1022320	0.3014920
1	-3.7171310	-2.9644540	-0.2736350	1	-6.3168350	-0.5436320	0.7016320
				6	3.1891740	0.0704540	0.0657530
B3PW91 Triplet				7	4.1118260	-0.6174680	-0.6609100
E = -4421.948624 HF				7	3.9121480	1.0421980	0.6827530
28	1.1584770	-0.0001970	-0.2550770	6	5.3766420	-0.0863250	-0.5035330
28	-1.1773270	0.0794330	-0.3056170	1	6.2435310	-0.4892010	-1.0064500
16	0.0427480	0.3410450	-2.0199130	6	5.2501480	0.9627520	0.3508640
16	-0.0605430	-0.2620120	1.4591110	1	5.9870680	1.6480410	0.7434530
6	-3.0261290	0.0367670	0.0688860	6	3.7999990	-1.7492600	-1.5192420
7	-3.7633930	0.8859270	0.8358520	1	4.4611540	-2.5883220	-1.2824700
7	-3.9337560	-0.8651310	-0.3974530	1	2.7630040	-2.0448720	-1.3395940
6	-5.0967840	0.5247840	0.8436760	1	3.9204820	-1.4727330	-2.5716180
1	-5.8447530	1.0781150	1.3923830	6	3.3550250	2.0200010	1.6041490

1	2.2689520	2.0219130	1.4851030
1	3.6167240	1.7625430	2.6359110
1	3.7454630	3.0131790	1.3642890
6	-3.2585130	2.1284800	-1.5241060
1	-2.1805760	2.1117240	-1.3475520
1	-3.4637240	1.9317700	-2.5816070
1	-3.6572420	3.1095650	-1.2497720
6	-3.9026530	-1.7824980	1.3839700
1	-4.5703000	-2.5987490	1.0928700
1	-2.8670140	-2.0984850	1.2321560
1	-4.0576190	-1.5415850	2.4407400

Hartree Fock Closed Shell Singlet
E = -4413.604037 HF

28	1.1341900	0.2357150	-0.0192940
28	-1.1341990	0.2357580	0.0198300
16	0.0329360	-0.2094010	1.6880100
16	-0.0329940	-0.2083330	-1.6877570
6	3.1516340	0.0337630	-0.0332800
7	3.8723090	-1.0029240	-0.4837080
7	4.0621610	0.9068540	0.4264940
6	5.3446980	0.4213450	0.2615200
6	5.2239480	-0.7816940	-0.3083550
1	6.2111630	0.9692020	0.5638140
1	5.9648620	-1.4944830	-0.6003580
6	-3.1516060	0.0338090	0.0333180
7	-4.0619290	0.9071110	-0.4264750
7	-3.8724890	-1.0030140	0.4830770
6	-5.2240550	-0.7816820	0.3072770
6	-5.3445410	0.4215700	-0.2622070
1	-5.9651030	-1.4945550	0.5987330
1	-6.2108730	0.9695660	-0.5646310
6	3.7517210	2.2006640	1.0038480
1	3.9810170	2.9955100	0.3042370
1	4.3274620	2.3433520	1.9094130
1	2.7020760	2.2289990	1.2507570
6	3.3222050	-2.2193180	-1.0570750
1	2.2575820	-2.1005170	-1.1693850
1	3.5276130	-3.0616150	-0.4078260
1	3.7644820	-2.3975960	-2.0292480
6	-3.7512560	2.2010610	-1.0033980
1	-4.3260440	2.3436660	-1.9095840
1	-2.7013550	2.2297390	-1.2491660
1	-3.9815540	2.9957660	-0.3039580
6	-3.3226370	-2.2195500	1.0563770
1	-2.2579530	-2.1010610	1.1684700
1	-3.7647690	-2.3976860	2.0286420
1	-3.5284350	-3.0617860	0.4071750

Hartree Fock Open Shell Singlet
E = -4414.037715 HF

28	-1.2982240	-0.1732460	0.7029010
28	1.3755020	0.1510870	0.2000100
16	-0.0921460	-1.2062920	-1.0155730
16	0.1697380	1.1841670	1.9184020
6	-3.4219960	-0.1186300	0.8475770
7	-4.1609970	0.5773890	1.7219890
7	-4.3076760	-0.7637090	0.0764830
6	-5.5974810	-0.4736210	0.4656970
6	-5.5052460	0.3696990	1.5004240
1	-6.4508910	-0.8875500	-0.0266220
1	-6.2620930	0.8386780	2.0914110
6	3.4995820	0.0932470	0.0570470
7	4.3855220	0.7371880	0.8288170
7	4.2383570	-0.6034240	-0.8170360
6	5.5827080	-0.3973580	-0.5945300
6	5.6752510	0.4455970	0.4404590
1	6.3393830	-0.8670720	-1.1851540
1	6.5288140	0.8584430	0.9334250
6	-3.9866650	-1.6558510	-1.0305320
1	-4.4739010	-1.3034540	-1.9303130
1	-4.3292860	-2.6574430	-0.8038250
1	-2.9202820	-1.6666240	-1.1862720
6	-3.6474900	1.4451450	2.7744860
1	-2.5737140	1.5022180	2.7017380
1	-3.9238420	1.0479070	3.7428890
1	-4.0649150	2.4369700	2.6594800
6	4.0648810	1.6291320	1.9360860
1	4.5493980	1.2745770	2.8364930
1	2.9982460	1.6426810	2.0898430
1	4.4107070	2.6299810	1.7109670
6	3.7245980	-1.4709290	-1.8696110
1	2.6505160	-1.5248260	-1.7990780
1	4.0042270	-1.0755850	-2.8378480
1	4.1388390	-2.4638620	-1.7526140

Hartree Fock Triplet
E = -4413.989641 HF

28	-1.2795890	-0.1468570	0.6707400
28	1.3583680	0.3092960	0.0636780
16	-0.0870310	-1.1088480	-1.0913090
16	0.1748070	1.2650170	1.8303060
6	-3.4031540	-0.1232100	0.8480440
7	-4.1393490	0.5601690	1.7346290
7	-4.2906730	-0.7760870	0.0856620
6	-5.5788900	-0.5033180	0.4923570
6	-5.4837070	0.3369540	1.5292960
1	-6.4334370	-0.9252680	0.0088990
1	-6.2386290	0.7947270	2.1314240
6	3.4805830	0.1420000	0.0179630
7	4.3630470	0.7400950	0.8294820
7	4.2198710	-0.6055570	-0.8125890

6	5.5610850	-0.4769870	-0.5231630
6	5.6510930	0.3691720	0.5093590
1	6.3172080	-0.9977320	-1.0700660
1	6.5014780	0.7344340	1.0436140
6	-3.9726470	-1.6588390	-1.0296220
1	-4.4846760	-1.3145590	-1.9186730
1	-4.2895260	-2.6681070	-0.7993470
1	-2.9096040	-1.6459210	-1.2067130
6	-3.6227960	1.4306320	2.7833510
1	-2.5523250	1.5119080	2.6883180
1	-3.8705870	1.0206480	3.7542190
1	-4.0635800	2.4140160	2.6844690
6	4.0411680	1.6608570	1.9125940
1	4.4985780	1.3106800	2.8286210
1	2.9724280	1.7004950	2.0453330
1	4.4162270	2.6489650	1.6775240
6	3.7100530	-1.4513490	-1.8845870
1	2.6336920	-1.4802300	-1.8391910
1	4.0238100	-1.0575480	-2.8430970
1	4.0961250	-2.4550160	-1.7639080

M06 Closed Shell Singlet
E = -4421.686500 HF

28	-1.2022240	-0.2535870	-0.4861040
28	1.2019040	-0.1320580	-0.5172180
16	0.0086070	-0.7860440	-2.1240770
16	-0.0081540	0.3740120	1.1205740
6	-2.9602160	-0.0369130	0.1613500
7	-3.5963200	-0.6466310	1.1943360
7	-3.8971000	0.7902150	-0.3735160
6	-5.0938430	0.6988730	0.3132300
6	-4.9037430	-0.2086000	1.3021130
1	-5.9630780	1.2824180	0.0374290
1	-5.5753730	-0.5832620	2.0641380
6	2.9574440	0.1417720	0.1157340
7	3.5707530	1.2787820	0.5344470
7	3.9217330	-0.8130380	0.1963080
6	5.1130570	-0.2819870	0.6548250
6	4.8916150	1.0384120	0.8667740
1	6.0012760	-0.8866440	0.7869270
1	5.5485170	1.8238910	1.2183730
6	-3.6543500	1.6682400	-1.5033630
1	-3.7028520	2.7170470	-1.1883950
1	-4.3960370	1.4848790	-2.2891330
1	-2.6518780	1.4546120	-1.8927670
6	-2.9873100	-1.6431670	2.0560780
1	-1.9194460	-1.6902900	1.8168570
1	-3.4482830	-2.6238460	1.8890550
1	-3.1092290	-1.3530770	3.1058910
6	2.9299000	2.5797200	0.5941270
1	3.0802870	3.0235980	1.5849020
1	1.8573710	2.4376580	0.4219120
1	3.3431570	3.2444180	-0.1736500
6	3.7087310	-2.2103350	-0.1329330
1	2.7136240	-2.3073770	-0.5830340
1	4.4658670	-2.5474510	-0.8499060
1	3.7566020	-2.8273810	0.7718510

M06 Open Shell Singlet
E = -4421.686469

28	-1.0876240	0.5236860	1.3014700
28	1.3081700	0.5488100	1.0723420
16	-0.0056300	-0.5478070	-0.1428190
16	0.2330910	1.5531120	2.5798470
6	-2.8730700	0.0478510	0.9301580
7	-3.7041310	-0.6249480	1.7691860
7	-3.6332460	0.3063140	-0.1649100
6	-4.9138990	-0.1929480	-0.0108940
6	-4.9587440	-0.7819470	1.2091370
1	-5.6707860	-0.0810070	-0.7769050
1	-5.7606870	-1.2947780	1.7249140
6	2.9872150	0.1739740	0.3026710
7	3.7927880	1.0681290	-0.3288490
7	3.6829050	-0.9914480	0.2701090
6	4.8995510	-0.8273030	-0.3666560
6	4.9687710	0.4722300	-0.7461920
1	5.6008480	-1.6429710	-0.4885250
1	5.7403090	1.0218520	-1.2703270
6	-3.1676600	1.0381510	-1.3286790
1	-3.6111140	2.0405830	-1.3528980
1	-3.4384250	0.4934140	-2.2401710
1	-2.0769000	1.1185480	-1.2650950
6	-3.3091460	-1.1246430	3.0733510
1	-2.2899100	-0.7761270	3.2772240
1	-3.3250260	-2.2205520	3.0824000
1	-3.9857670	-0.7389730	3.8444430
6	3.4387430	2.4571020	-0.5544650
1	4.2024120	3.1176710	-0.1283560
1	2.4783380	2.6460040	-0.0608290
1	3.3372530	2.6539680	-1.6280440
6	3.2111830	-2.2380450	0.8448240
1	2.1592420	-2.1058300	1.1201720
1	3.2934280	-3.0421220	0.1047610
1	3.7969360	-2.4953120	1.7352260

M06 Triplet
E = -4421.688497

28	-1.0789880	0.1876730	0.7942770
28	1.2706370	0.2933490	0.6703340
16	0.0559320	-0.7565660	-0.7252260
16	0.1261430	1.2414910	2.1820240
6	-3.0071000	-0.0257680	0.8147080

7	-3.7710920	-0.4467620	1.8571970	1	-3.3910710	0.0721650	-2.8930440
7	-3.9012500	0.1927000	-0.1847750	1	-3.2504080	-1.6604890	-2.4747090
6	-5.1927320	-0.0866030	0.2246800	1	-1.9121100	-0.5463640	-2.0909810
6	-5.1099270	-0.4925670	1.5150320	6	-3.5860910	1.0415160	2.3989440
1	-6.0441820	0.0298070	-0.4338420	1	-2.6178960	1.5418440	2.3357560
1	-5.8740060	-0.8073170	2.2145770	1	-3.5615680	0.3136330	3.2133860
6	3.0937360	0.1209760	0.2121990	1	-4.3685380	1.7814770	2.5832390
7	3.9574030	1.1285900	-0.0873230	6	3.7338270	0.7609930	-2.2268170
7	3.8493410	-1.0055830	0.1170150	1	4.6142740	1.3661180	-2.4547730
6	5.1553810	-0.7055170	-0.2260510	1	2.8496130	1.4006480	-2.1983200
6	5.2231360	0.6412010	-0.3596960	1	3.5982270	-0.0036920	-2.9952990
1	5.9104200	-1.4724080	-0.3443250	6	2.8537250	-0.6946990	2.3739990
1	6.0475610	1.2907190	-0.6252710	1	1.7803080	-0.5385260	2.2472910
6	-3.5487430	0.6673280	-1.5099750	1	3.0342010	-1.7111620	2.7294010
1	-3.9685010	1.6656440	-1.6809120	1	3.2601900	0.0257130	3.0883300
1	-3.9290800	-0.0256140	-2.2692720				
1	-2.4565830	0.7117100	-1.5776730	M06-2X Open Shell Singlet			
6	-3.2438440	-0.8253670	3.1552810	E = -4421.679863			
1	-2.1868240	-0.5392020	3.1929660	28	-1.1525530	0.2339720	0.3522670
1	-3.3334210	-1.9080050	3.3030080	28	1.1767560	0.2649590	0.1165170
1	-3.7885350	-0.3002350	3.9480720	16	-0.0856520	-1.0959830	-0.8527930
6	3.5816310	2.5280820	-0.1385120	16	0.1590350	1.0738790	1.7517090
1	4.2809290	3.1262910	0.4569520	6	-3.0907990	0.0056880	0.6854990
1	2.5734860	2.6246330	0.2805000	7	-3.7196990	-0.2644450	1.8548100
1	3.5786020	2.8885880	-1.1739420	7	-4.0948280	0.0555880	-0.2249070
6	3.3571930	-2.3409590	0.3986890	6	-5.3238080	-0.1720120	0.3617290
1	2.2652450	-2.3287720	0.3158260	6	-5.0849200	-0.3774560	1.6815120
1	3.7705010	-3.0466340	-0.3304930	1	-6.2439370	-0.1724630	-0.2025300
1	3.6412380	-2.6505250	1.4117680	1	-5.7549760	-0.5972690	2.4987720
				6	3.1523160	0.1204090	0.0897260
M06-2X Closed Shell Singlet				7	4.0512280	1.1339690	0.1560390
E = -4421.734513				7	3.9187620	-0.9961400	0.0380390
28	-1.2881970	1.3454380	-0.0192950	6	5.2646010	-0.6881800	0.0672360
28	1.3361150	1.2708050	0.0417040	6	5.3490840	0.6639260	0.1398980
16	-0.0289140	-0.4284390	0.1022110	1	6.0315850	-1.4473370	0.0380470
16	0.0775870	3.0621670	-0.1077030	1	6.2044570	1.3208470	0.1831430
6	-2.9803720	0.3908490	0.0833290	6	-3.8945340	0.3420940	-1.6377800
7	-3.8294380	0.3595360	1.1359940	1	-4.1101280	1.3931450	-1.8471670
7	-3.5664700	-0.3920160	-0.8493480	1	-4.5522300	-0.2949540	-2.2332390
6	-4.7637660	-0.9043740	-0.3917750	1	-2.8539450	0.1234020	-1.8858220
6	-4.9305840	-0.4302600	0.8689290	6	-3.0432180	-0.4319660	3.1337380
1	-5.3807840	-1.5546860	-0.9927400	1	-1.9750520	-0.2697860	2.9795020
1	-5.7174910	-0.5885300	1.5904120	1	-3.2135870	-1.4428340	3.5126610
6	2.9847590	0.2367270	0.0795770	1	-3.4224790	0.3006700	3.8504620
7	3.8882730	0.1326440	-0.9224770	6	3.6855810	2.5418240	0.2098170
7	3.4905890	-0.5275150	1.0732430	1	4.3228860	3.0545850	0.9338560
6	4.6901390	-1.1005100	0.7020780	1	2.6437360	2.6104070	0.5292090
6	4.9418790	-0.6854830	-0.5653870	1	3.8011690	3.0022140	-0.7748970
1	5.2508460	-1.7452930	1.3614020	6	3.3947930	-2.3537180	-0.0233610
1	5.7605240	-0.9005340	-1.2350710	1	2.3064270	-2.2978800	-0.0814050
6	-2.9971930	-0.6439310	-2.1675090	1	3.7817670	-2.8572240	-0.9128920

1	3.6898030	-2.9059570	0.8724140

M06-2X Triplet
E = -4421.682094

28	-1.1111570	-0.0316310	0.5804930
28	1.1958930	-0.0022950	0.3422820
16	-0.0874780	-1.0930880	-0.9398320
16	0.1744190	1.0574900	1.8637430
6	-3.0883370	-0.0554570	0.7720280
7	-3.8166870	-0.0987160	1.9155670
7	-4.0225440	-0.0373630	-0.2110890
6	-5.3029710	-0.0698090	0.3045400
6	-5.1721730	-0.1107610	1.6540510
1	-6.1803040	-0.0591540	-0.3243160
1	-5.9121820	-0.1484780	2.4391390
6	3.1690810	0.0295620	0.1387180
7	4.0004330	1.0950760	0.2489340
7	3.9976600	-1.0058460	-0.1444640
6	5.3156540	-0.5986550	-0.2067980
6	5.3167720	0.7356340	0.0383530
1	6.1234360	-1.2839290	-0.4146340
1	6.1253810	1.4494600	0.0819290
6	-3.7227210	0.0246540	-1.6347750
1	-4.0602970	0.9795250	-2.0458290
1	-4.2239940	-0.7975870	-2.1509880
1	-2.6431690	-0.0724800	-1.7602060
6	-3.2468490	-0.1527750	3.2546360
1	-2.1786860	0.0573090	3.1798220
1	-3.3985800	-1.1449780	3.6873980
1	-3.7242300	0.6017990	3.8843160
6	3.5589120	2.4570870	0.5154410
1	4.2146560	2.9099030	1.2625780
1	2.5381350	2.4165560	0.8992040
1	3.5831250	3.0475750	-0.4042050
6	3.5596310	-2.3828270	-0.3243770
1	2.4750090	-2.3824640	-0.4447430
1	4.0264370	-2.7990620	-1.2201410
1	3.8339840	-2.9815970	0.5480390

B97D Closed Shell Singlet
E = -4423.231693

28	-1.1790000	-0.2860690	-0.0463390
28	1.1789930	-0.2860040	0.0468050
16	-0.0695410	0.0355240	1.7234320
16	0.0695290	0.0334150	-1.7233630
6	-3.0560460	-0.0123570	-0.0682940
7	-3.7580780	1.0234990	-0.6365540
7	-4.0300170	-0.7780810	0.5292190
6	-5.2949300	-0.2370900	0.3369270
6	-5.1218240	0.9040980	-0.4002880
1	-6.1911660	-0.7011300	0.7349430
1	-5.8381620	1.6311300	-0.7679000
6	3.0560510	-0.0123080	0.0682840
7	4.0299020	-0.7786010	-0.5286980
7	3.7582090	1.0240140	0.6355320
6	5.1219120	0.9043730	0.3991330
6	5.2948580	-0.2374610	-0.3371170
1	5.8383320	1.6317120	0.7659790
1	6.1910120	-0.7018730	-0.7348870
6	-3.7511170	-2.0153190	1.2582080
1	-4.0636100	-2.8882470	0.6634730
1	-4.2907180	-2.0060570	2.2172860
1	-2.6689170	-2.0598910	1.4429640
6	-3.1383580	2.1250070	-1.3754260
1	-2.0589670	1.9316500	-1.4267940
1	-3.3266670	3.0759700	-0.8530710
1	-3.5556060	2.1706110	-2.3931770
6	3.7508460	-2.0165260	-1.2564640
1	4.2907540	-2.0084160	-2.2153770
1	2.6686880	-2.0609720	-1.4415030
1	4.0628940	-2.8889260	-0.6607210
6	3.1386440	2.1261610	1.3735780
1	2.0592300	1.9329730	1.4251130
1	3.5559120	2.1724960	2.3912880
1	3.3270640	3.0766970	0.8504870

B97D Open Shell Singlet
E = -4423.233631

28	-1.1432250	0.0556110	0.4965960
28	1.2050230	0.0878360	0.2508400
16	-0.0919260	-1.0899870	-0.9493390
16	0.1666570	1.1046800	1.7980250
6	-3.0237270	-0.0374490	0.7275450
7	-3.7247200	-0.3793710	1.8595850
7	-4.0051910	0.2054270	-0.2040740
6	-5.2736450	0.0214140	0.3316350
6	-5.0957590	-0.3509010	1.6377030
1	-6.1763110	0.1694140	-0.2516960
1	-5.8131970	-0.5958270	2.4137330
6	3.0972930	0.0667790	0.1270940
7	3.9531330	1.1367260	0.0124990
7	3.9359820	-1.0222140	0.1486720
6	5.2682600	-0.6410310	0.0517960
6	5.2792670	0.7257940	-0.0365180
1	6.0787220	-1.3622070	0.0557870
1	6.1007670	1.4281870	-0.1299730
6	-3.7317350	0.6379470	-1.5751850
1	-3.9854680	1.7030820	-1.6950670
1	-4.3259170	0.0328050	-2.2765060
1	-2.6606510	0.4874930	-1.7675670
6	-3.0918670	-0.7614750	3.1227780
1	-2.0210070	-0.5304640	3.0446650

1	-3.2289190	-1.8394360	3.3026950
1	-3.5395700	-0.1865630	3.9476470
6	3.5044690	2.5264470	-0.0798790
1	4.0796730	3.1461570	0.6246020
1	2.4386520	2.5531210	0.1850460
1	3.6431000	2.9022910	-1.1059190
6	3.4717400	-2.4023790	0.2965250
1	2.3804570	-2.4045530	0.1727180
1	3.9375230	-3.0320350	-0.4766900
1	3.7344250	-2.7839660	1.2958000

B97D Triplet
E = -4423.239204

28	-1.1303000	-0.0231200	0.5583200
28	1.2064000	0.0123470	0.3170660
16	-0.0881840	-1.1070010	-0.9500710
16	0.1654000	1.0964390	1.8249250
6	-3.0172050	-0.0572830	0.7567410
7	-3.7465970	-0.3509520	1.8846850
7	-3.9761040	0.2017620	-0.1937650
6	-5.2580240	0.0745950	0.3267610
6	-5.1127540	-0.2783720	1.6419350
1	-6.1460630	0.2451270	-0.2726150
1	-5.8494530	-0.4824120	2.4116990
6	3.0942950	0.0375820	0.1390580
7	3.9213430	1.1275180	0.0048300
7	3.9576870	-1.0322200	0.1181110
6	5.2770630	-0.6201360	-0.0230020
6	5.2537910	0.7471380	-0.0977830
1	6.1030260	-1.3227200	-0.0561340
1	6.0549810	1.4691020	-0.2151990
6	-3.6703140	0.6008050	-1.5681880
1	-3.8907870	1.6706010	-1.7104860
1	-4.2724380	0.0009210	-2.2672890
1	-2.6017180	0.4157470	-1.7419430
6	-3.1453940	-0.7328180	3.1629590
1	-2.0743870	-0.4943990	3.1142970
1	-3.2786150	-1.8122460	3.3374220
1	-3.6196220	-0.1630290	3.9763150
6	3.4402300	2.5079590	-0.0593010
1	4.0226680	3.1330480	0.6344320
1	2.3825060	2.5084780	0.2367080
1	3.5404150	2.8971030	-1.0849070
6	3.5288860	-2.4230650	0.2694620
1	2.4377980	-2.4528030	0.1468590
1	4.0097060	-3.0417200	-0.5033150
1	3.8011830	-2.7973380	1.2690320

B97D3 Closed Shell Singlet
E = -4423.290819

28	-1.1781850	-0.2746330	-0.0606640
28	1.1769460	-0.2392040	-0.1607640
16	-0.0796540	0.6492690	-1.6064520
16	0.0776950	-0.5484890	1.6140090
6	3.0493250	0.0067750	-0.0705700
7	4.0006880	-0.9118860	0.3093870
7	3.7755060	1.1490890	-0.3085400
6	5.2757610	-0.3585770	0.3034530
1	6.1567710	-0.9277320	0.5752140
6	5.1327100	0.9452930	-0.0865660
1	5.8650350	1.7329040	-0.2178560
6	-3.0483670	-0.0356370	0.0650420
7	-4.0194380	-0.5179760	-0.7818160
7	-3.7546680	0.7008440	0.9858330
6	-5.2872380	-0.0969580	-0.3976070
1	-6.1813800	-0.3750520	-0.9427540
6	-5.1189560	0.6747340	0.7199580
1	-5.8384110	1.2015370	1.3353860
6	-3.7378250	-1.3790260	-1.9274560
1	-4.2816110	-1.0115800	-2.8079700
1	-2.6592380	-1.3398240	-2.1206290
1	-4.0371640	-2.4145250	-1.7117090
6	-3.1424550	1.4325950	2.0931290
1	-2.0604250	1.2668420	2.0497370
1	-3.3611050	2.5051960	1.9974350
1	-3.5319270	1.0581350	3.0498320
6	3.6938250	-2.2983140	0.6514330
1	2.6157770	-2.3680780	0.8388220
1	3.9688900	-2.9676840	-0.1760720
1	4.2435890	-2.5841550	1.5580150
6	3.1895940	2.4199920	-0.7301190
1	3.5887830	2.7090120	-1.7122020
1	2.1050710	2.2842190	-0.8029630
1	3.4205460	3.1999910	0.0085450

B97D3 Open Shell Singlet
E = -4423.293792

28	-1.1805340	-0.0139010	-0.0744670
28	1.1804730	0.0152850	-0.0745500
16	0.0220640	-1.7583260	0.0100910
16	-0.0221450	1.7600340	0.0026030
6	3.0703110	0.0187530	-0.0033280
7	3.8865370	0.6906060	0.8760620
7	3.9509980	-0.6621100	-0.8112590
6	5.2290840	0.4347430	0.6222700
1	6.0241570	0.8730990	1.2135880
6	5.2700390	-0.4200190	-0.4455900
1	6.1077370	-0.8677700	-0.9669110
6	-3.0702830	-0.0192930	-0.0029150
7	-3.8857080	-0.6863910	0.8807950
7	-3.9517860	0.6553970	-0.8151510
6	-5.2285600	-0.4336080	0.6254960

1	-6.0230980	-0.8691720	1.2195880
6	-5.2705210	0.4142540	-0.4478130
1	-6.1087760	0.8577060	-0.9719130
6	-3.3936780	-1.5312620	1.9668130
1	-3.8622280	-2.5230630	1.9078460
1	-2.3087160	-1.6298870	1.8504260
1	-3.6226430	-1.0699150	2.9377670
6	-3.5426870	1.4972430	-1.9369580
1	-2.4559400	1.6270760	-1.8800900
1	-3.8095100	1.0173690	-2.8891890
1	-4.0348610	2.4764910	-1.8645250
6	3.3956450	1.5426050	1.9570120
1	2.3107450	1.6416180	1.8403860
1	3.6244240	1.0869740	2.9307070
1	3.8651800	2.5335490	1.8918490
6	3.5409400	-1.5099450	-1.9282160
1	4.0353420	-2.4877950	-1.8523090
1	2.4545920	-1.6416740	-1.8682910
1	3.8045810	-1.0340000	-2.8833040

B97D3 Triplet
E = -4423.297156

28	-1.1937960	0.1239710	-0.2488380
28	1.1139060	0.1467790	0.1861820
16	-0.0155120	-1.6373390	-0.0717970
16	-0.0649260	1.9082670	0.0077050
6	2.9724550	0.1642010	0.5368430
7	3.6423330	0.8360410	1.5327140
7	3.9719610	-0.4908260	-0.1440570
6	5.0119500	0.6044390	1.4722650
1	5.7060050	1.0460990	2.1772930
6	5.2206590	-0.2322250	0.4101060
1	6.1324500	-0.6565930	0.0070730
6	-3.0527680	0.1075060	-0.5972640
7	-4.0359520	-0.5834630	0.0714920
7	-3.7397530	0.7851170	-1.5774890
6	-5.2910570	-0.3431880	-0.4757730
1	-6.1920900	-0.7970470	-0.0805550
6	-5.1036710	0.5211040	-1.5199630
1	-5.8091000	0.9619760	-2.2142030
6	-3.7865130	-1.4359720	1.2312020
1	-4.2671690	-2.4123210	1.0831430
1	-2.7027770	-1.5699570	1.3229380
1	-4.1797290	-0.9624590	2.1418830
6	-3.1034830	1.6462270	-2.5715360
1	-2.0626150	1.7999110	-2.2656950
1	-3.1324440	1.1692520	-3.5613940
1	-3.6225910	2.6134550	-2.6104150
6	2.9855620	1.6608880	2.5442240
1	1.9400910	1.7924610	2.2440990
1	3.0300380	1.1661710	3.5247580
1	3.4788610	2.6405840	2.6003550
6	3.7453830	-1.3243580	-1.3223970
1	4.2395780	-2.2962620	-1.1895860
1	2.6648630	-1.4725990	-1.4264100
1	4.1392200	-0.8272600	-2.2201340

BHandHLYP Closed Shell Singlet
E = -4421.596120

28	1.1567240	0.2420950	-0.0203940
28	-1.1567390	0.2423680	0.0204370
16	0.0342400	-0.0959490	1.6854090
16	-0.0343790	-0.0980210	-1.6849460
6	3.0813480	0.0168360	-0.0421520
7	3.7903170	-0.9989350	-0.5733430
7	4.0121430	0.8307080	0.4977730
6	5.2818080	0.3336440	0.3047200
6	5.1407300	-0.8232210	-0.3694650
1	6.1585980	0.8372240	0.6595180
1	5.8709360	-1.5273690	-0.7146880
6	-3.0813370	0.0171060	0.0422450
7	-4.0121410	0.8302750	-0.4987210
7	-3.7902440	-0.9983950	0.5740380
6	-5.1406240	-0.8231900	0.3695200
6	-5.2817500	0.3330660	-0.3057010
1	-5.8707900	-1.5272060	0.7150950
1	-6.1585440	0.8361300	-0.6612230
6	3.7130120	2.0753530	1.1745280
1	3.9473410	2.9231310	0.5369250
1	4.2908890	2.1412550	2.0909410
1	2.6581150	2.0862820	1.4184930
6	3.2113490	-2.1428210	-1.2497930
1	2.1517810	-1.9643620	-1.3773210
1	3.3619730	-3.0423400	-0.6599600
1	3.6741400	-2.2661070	-2.2241570
6	-3.7130370	2.0744780	-1.1762990
1	-4.2911930	2.1399020	-2.0925680
1	-2.6582120	2.0851190	-1.4205950
1	-3.9470570	2.9226730	-0.5391370
6	-3.2112250	-2.1416630	1.2514930
1	-2.1519100	-1.9624620	1.3800920
1	-3.6750130	-2.2649210	2.2253860
1	-3.3605980	-3.0414910	0.6618100

BHandHLYP Open Shell Singlet
E = -4421.678383

28	-1.2693360	-0.1275000	-0.1155610
28	1.2758580	-0.6466860	0.1203440
16	-0.1014480	-1.5308650	-1.3894880
16	0.1082270	0.7623330	1.4003530
6	-3.1697730	0.0401120	0.5029560
7	-3.8009740	1.0663110	1.1015680

7	-4.0992600	-0.9314740	0.4180460	1	-4.3896040	-2.1592420	-1.3669980
6	-5.2953440	-0.5199480	0.9597010	1	-2.7909770	-1.3999840	-1.4150090
6	-5.1069630	0.7427520	1.3884180	6	-3.3331750	0.9333190	3.0483790
1	-6.1584560	-1.1537630	0.9967540	1	-2.2580950	0.9954220	2.9395240
1	-5.7753900	1.4282540	1.8693730	1	-3.5864070	0.2846630	3.8820210
6	3.2325420	-0.2165390	0.2209480	1	-3.7292960	1.9268460	3.2299980
7	3.9916510	0.1367220	1.2740230	6	3.6266390	2.0012220	1.5747940
7	4.0743900	-0.1952780	-0.8308410	1	4.1012970	1.9126270	2.5466500
6	5.3425590	0.1701120	-0.4415810	1	2.5531870	1.9319740	1.6939170
6	5.2900990	0.3769320	0.8881180	1	3.8863880	2.9572740	1.1302540
1	6.1551400	0.2547260	-1.1348610	6	3.7187670	-1.8504660	-1.4735380
1	6.0495710	0.6736320	1.5832600	1	2.6414370	-1.9529070	-1.4428040
6	-3.8757940	-2.2531160	-0.1408330	1	4.0365090	-1.6520270	-2.4926050
1	-4.5746970	-2.4329270	-0.9517280	1	4.1746320	-2.7715580	-1.1247660
1	-4.0107330	-3.0071480	0.6283950				
1	-2.8634540	-2.3104910	-0.5217030	BP86 Closed Shell Singlet			
6	-3.2029160	2.3572160	1.3933740	E = -4422.894934			
1	-2.1263380	2.2625960	1.3321300	28	1.1783400	0.2583080	-0.0328350
1	-3.4758550	2.6590460	2.3990190	28	-1.1783360	0.2584680	0.0339500
1	-3.5534300	3.1015940	0.6841670	16	0.0504290	-0.0684180	1.7178650
6	3.5234710	0.2341440	2.6453150	16	-0.0504740	-0.0670800	-1.7170130
1	3.8753930	-0.6162420	3.2222940	6	3.0491830	0.0165160	-0.0553480
1	2.4414160	0.2593560	2.6415050	7	3.7705250	-1.0238030	-0.6025440
1	3.8979460	1.1513010	3.0875320	7	4.0159450	0.8226530	0.5110800
6	3.7027070	-0.4893810	-2.2035990	6	5.2913790	0.2994850	0.3221430
1	2.6576030	-0.7720160	-2.2352780	6	5.1353200	-0.8679400	-0.3807000
1	3.8537870	0.3890150	-2.8233260	1	6.1872630	0.7924690	0.6953940
1	4.3072190	-1.3081460	-2.5811770	1	5.8695390	-1.5895890	-0.7342950
				6	-3.0491970	0.0167160	0.0551210
BHandHLYP Triplet				7	-4.0156740	0.8229840	-0.5115720
E = -4421.703309				7	-3.7707750	-1.0238900	0.6014770
28	-1.2214130	-0.5587590	0.7122840	6	-5.1354490	-0.8680550	0.3788670
28	1.2389610	-0.0151760	0.0310660	6	-5.2911850	0.2996300	-0.3236140
16	-0.0457870	-1.6330530	-0.8678570	1	-5.8698330	-1.5898750	0.7317700
16	0.0443370	1.0755110	1.6033260	1	-6.1868670	0.7926940	-0.6972410
6	-3.2043400	-0.2094690	0.8449230	6	3.7185150	2.0726550	1.2087390
7	-3.8994820	0.4093650	1.8174830	1	4.0511200	2.9397080	0.6112660
7	-4.1275580	-0.5358530	-0.0805810	1	4.2202190	2.0842790	2.1914040
6	-5.3820180	-0.1254560	0.3067530	1	2.6270990	2.1228030	1.3551020
6	-5.2377570	0.4695670	1.5062400	6	3.1659890	-2.1543900	-1.3077020
1	-6.2512150	-0.2850750	-0.2991330	1	2.0856360	-1.9557450	-1.3955950
1	-5.9571750	0.9288070	2.1539920	1	3.3285760	-3.0883810	-0.7418920
6	3.2735510	0.0685100	0.0476660	1	3.6055200	-2.2492130	-2.3155040
7	4.0761000	0.9180930	0.7164440	6	-3.7179030	2.0733210	-1.2085010
7	4.1167750	-0.7522340	-0.6091120	1	-4.2197000	2.0856710	-2.1911070
6	5.4268340	-0.4212160	-0.3545990	1	-2.6264840	2.1232150	-1.3549270
6	5.4008120	0.6339130	0.4820790	1	-4.0501910	2.9401270	-0.6104910
1	6.2487000	-0.9605410	-0.7809330	6	-3.1665910	-2.1547490	1.3064850
1	6.1958010	1.1964430	0.9288930	1	-2.0863250	-1.9560050	1.3952830
6	-3.8549220	-1.2148910	-1.3356920	1	-3.6068520	-2.2501580	2.3139150
1	-4.1720870	-0.5910110	-2.1654380	1	-3.3286180	-3.0884730	0.7400760

BP86 Open Shell Singlet
E = -4422.897277

28	-1.1398930	0.0257960	0.5185340
28	1.2058440	0.0661700	0.2812590
16	-0.0827870	-1.0954550	-0.9348240
16	0.1580950	1.0951860	1.8073980
6	-3.0126600	-0.0481210	0.7336600
7	-3.7271670	-0.4356770	1.8484020
7	-3.9898280	0.2633360	-0.1893110
6	-5.2647470	0.0753040	0.3355220
6	-5.0985140	-0.3678440	1.6229050
1	-6.1680820	0.2701990	-0.2397280
1	-5.8294010	-0.6370700	2.3833040
6	3.0864430	0.0596290	0.1374990
7	3.9318120	1.1344530	-0.0463520
7	3.9411630	-1.0212420	0.2043890
6	5.2692220	-0.6291280	0.0685220
6	5.2634320	0.7331490	-0.0916880
1	6.0938150	-1.3391410	0.0976480
1	6.0815890	1.4369400	-0.2339000
6	-3.7041640	0.7507620	-1.5383080
1	-3.9849000	1.8145200	-1.6322130
1	-4.2601030	0.1530290	-2.2806940
1	-2.6216090	0.6380760	-1.7114870
6	-3.1061810	-0.8835560	3.0947030
1	-2.0266430	-0.6734480	3.0240100
1	-3.2635790	-1.9672870	3.2360800
1	-3.5348720	-0.3313190	3.9483660
6	3.4677310	2.5130590	-0.1973240
1	4.0160110	3.1731290	0.4963280
1	2.3934470	2.5324550	0.0482590
1	3.6161410	2.8589630	-1.2353760
6	3.4937350	-2.3970020	0.4200460
1	2.3973970	-2.4128980	0.3095090
1	3.9508710	-3.0628570	-0.3316010
1	3.7678020	-2.7374710	1.4340870

BP86 Triplet
E = -4422.901925

28	-1.1314610	-0.0176570	0.5565680
28	1.2069500	0.0219630	0.3166050
16	-0.0858290	-1.0912910	-0.9449440
16	0.1615790	1.0962570	1.8175390
6	-3.0080720	-0.0566810	0.7542290
7	-3.7386170	-0.4241480	1.8654880
7	-3.9719020	0.2699190	-0.1772320
6	-5.2543100	0.1108830	0.3393480
6	-5.1068370	-0.3294930	1.6297690
1	-6.1490400	0.3220960	-0.2435190
1	-5.8485450	-0.5803720	2.3859470
6	3.0850080	0.0415820	0.1388180
7	3.9129430	1.1260810	-0.0645580
7	3.9542970	-1.0285130	0.1900940
6	5.2745720	-0.6205650	0.0261680
6	5.2483470	0.7410000	-0.1370550
1	6.1083360	-1.3202490	0.0399520
1	6.0543530	1.4545620	-0.2985840
6	-3.6680870	0.7461500	-1.5263120
1	-3.9309260	1.8138500	-1.6270190
1	-4.2282690	0.1541070	-2.2700760
1	-2.5863600	0.6151640	-1.6908080
6	-3.1360930	-0.8791920	3.1180460
1	-2.0536880	-0.6804690	3.0594240
1	-3.3059430	-1.9613120	3.2575630
1	-3.5681760	-0.3227470	3.9672270
6	3.4291850	2.4984920	-0.2102860
1	3.9799070	3.1667280	0.4735400
1	2.3588020	2.5044970	0.0519870
1	3.5569770	2.8443260	-1.2511180
6	3.5276820	-2.4084340	0.4196760
1	2.4313190	-2.4412500	0.3128900
1	3.9920740	-3.0741730	-0.3275580
1	3.8092420	-2.7364740	1.4358120

BLYP Closed Shell Singlet
E = -4422.2203

28	1.1931220	0.2536800	-0.0303110
28	-1.1930880	0.2539710	0.0329910
16	0.0473220	-0.0786590	1.7395520
16	-0.0474230	-0.0705110	-1.7384340
6	3.0886870	0.0165060	-0.0518050
7	3.8155560	-1.0338910	-0.5832050
7	4.0564230	0.8413740	0.4966170
6	5.3386970	0.3178160	0.3106910
6	5.1859140	-0.8647060	-0.3684380
1	6.2321680	0.8218150	0.6693210
1	5.9215690	-1.5878400	-0.7101160
6	-3.0886820	0.0167270	0.0515220
7	-4.0558210	0.8429300	-0.4959080
7	-3.8160870	-1.0351760	0.5792230
6	-5.1862040	-0.8655430	0.3632310
6	-5.3382810	0.3187700	-0.3129170
1	-5.9221960	-1.5897100	0.7019770
1	-6.2313410	0.8236310	-0.6713550
6	3.7637550	2.1148130	1.1717160
1	4.0926680	2.9652370	0.5510560
1	4.2772880	2.1480180	2.1462160
1	2.6774640	2.1729170	1.3292630
6	3.2181260	-2.1941170	-1.2643320
1	2.1426130	-2.0029100	-1.3801110
1	3.3717630	-3.1070990	-0.6651050

1	3.6784140	-2.3220730	-2.2575760
6	-3.7624750	2.1184390	-1.1668230
1	-4.2782600	2.1561080	-2.1399560
1	-2.6764550	2.1753370	-1.3266500
1	-4.0885100	2.9671110	-0.5422510
6	-3.2194680	-2.1973030	1.2578030
1	-2.1440620	-2.0065350	1.3753210
1	-3.6808950	-2.3279860	2.2501640
1	-3.3724980	-3.1086180	0.6558870

BLYP Open Shell Singlet
E = -4422.220264

28	-1.1548190	0.0247900	0.5229190
28	1.2211890	0.0630810	0.2762130
16	-0.0889020	-1.1084890	-0.9531060
16	0.1646520	1.1061870	1.8231710
6	-3.0507870	-0.0458780	0.7456650
7	-3.7654570	-0.4295790	1.8671970
7	-4.0328500	0.2660440	-0.1786310
6	-5.3115660	0.0815560	0.3539750
6	-5.1428400	-0.3586230	1.6426660
1	-6.2146380	0.2767480	-0.2180650
1	-5.8712990	-0.6234110	2.4042950
6	3.1248490	0.0561860	0.1253410
7	3.9724560	1.1338010	-0.0650100
7	3.9822690	-1.0281840	0.1930820
6	5.3152120	-0.6334840	0.0515000
6	5.3090910	0.7288380	-0.1134030
1	6.1385840	-1.3420800	0.0801810
1	6.1256550	1.4305940	-0.2604970
6	-3.7584320	0.7573010	-1.5380940
1	-4.0305830	1.8227220	-1.6236210
1	-4.3340450	0.1690590	-2.2709460
1	-2.6836900	0.6349230	-1.7315830
6	-3.1479660	-0.8850560	3.1228110
1	-2.0726150	-0.6656950	3.0703740
1	-3.2981760	-1.9700560	3.2522800
1	-3.5939330	-0.3459690	3.9742100
6	3.5147270	2.5226160	-0.2266290
1	4.0795730	3.1830260	0.4510230
1	2.4469390	2.5590490	0.0305550
1	3.6556410	2.8543820	-1.2690250
6	3.5423840	-2.4136120	0.4219980
1	2.4518850	-2.4487090	0.2922090
1	4.0238100	-3.0821160	-0.3097720
1	3.8031000	-2.7353280	1.4443370

BLYP Triplet
E = -4422.226630

28	-1.1462120	-0.0210860	0.5592950
28	1.2221990	0.0188020	0.3161460
16	-0.0871800	-1.1072020	-0.9616980
16	0.1636890	1.1055690	1.8365200
6	-3.0465720	-0.0578930	0.7590380
7	-3.7806560	-0.4270200	1.8729420
7	-4.0123650	0.2737410	-0.1752450
6	-5.3001890	0.1156550	0.3442290
6	-5.1541640	-0.3281620	1.6342610
1	-6.1928830	0.3299350	-0.2371740
1	-5.8956930	-0.5783840	2.3881510
6	3.1236900	0.0406940	0.1349910
7	3.9522420	1.1296870	-0.0720700
7	3.9974630	-1.0313880	0.1877310
6	5.3221680	-0.6182620	0.0212350
6	5.2934780	0.7434530	-0.1452750
1	6.1557990	-1.3151850	0.0356390
1	6.0969460	1.4565710	-0.3088730
6	-3.7151530	0.7605770	-1.5315310
1	-3.9663790	1.8310050	-1.6186560
1	-4.2946880	0.1838800	-2.2704420
1	-2.6411780	0.6181100	-1.7145430
6	-3.1855380	-0.8959680	3.1341620
1	-2.1077490	-0.6851150	3.0992000
1	-3.3459170	-1.9805860	3.2546210
1	-3.6395810	-0.3587470	3.9824220
6	3.4725810	2.5117430	-0.2281140
1	4.0382560	3.1809050	0.4401920
1	2.4084530	2.5333060	0.0449970
1	3.5931760	2.8441260	-1.2728780
6	3.5808210	-2.4219520	0.4274470
1	2.4907250	-2.4757820	0.3002330
1	4.0715250	-3.0875270	-0.3007590
1	3.8483030	-2.7328650	1.4514270

B3LYP Closed Shell Singlet
E = -4422.349842

28	1.2181070	-0.1743960	0.5252270
28	-1.2165470	-0.0855320	0.5326970
16	-0.0192450	-0.8360620	2.1233370
16	0.0114550	0.3015920	-1.1411310
6	2.9813530	-0.0003390	-0.1439430
7	3.6450440	-0.8153490	-1.0135370
7	3.8981940	0.9536660	0.1918870
6	5.1071140	0.7354990	-0.4512500
6	4.9469270	-0.3818410	-1.2104360
1	5.9606630	1.3830640	-0.3172760
1	5.6357890	-0.8967690	-1.8632290
6	-2.9779000	0.1399000	-0.1249340
7	-3.6173220	1.2708760	-0.5407730
7	-3.9207810	-0.8414170	-0.2344820
6	-5.1216830	-0.3317040	-0.7037760
6	-4.9304920	1.0013950	-0.8949020

1	-5.9920580	-0.9509120	-0.8613320	1	-3.9885530	-0.7025990	3.8943340
1	-5.6040020	1.7684690	-1.2466920	6	3.5394210	2.5049330	-0.4449300
6	3.6268230	2.0650390	1.0974300	1	4.3074650	3.1461370	-0.0014910
1	3.7327440	3.0178680	0.5687120	1	2.5856420	2.6828170	0.0558620
1	4.3163030	2.0372640	1.9472760	1	3.4381770	2.7356250	-1.5105940
1	2.6015000	1.9632430	1.4584480	6	3.3002020	-2.2862670	0.7010950
6	3.0633670	-2.0044840	-1.6295870	1	2.2153630	-2.2277940	0.8031630
1	1.9855930	-1.9776830	-1.4620190	1	3.5562250	-3.0682450	-0.0199340
1	3.4852580	-2.9102470	-1.1813460	1	3.7509720	-2.5202300	1.6715680
1	3.2648040	-1.9978900	-2.7050210				
6	-3.0049120	2.5958020	-0.5664800	B3LYP Triplet			
1	-3.2914530	3.1125060	-1.4872270	E = -4422.356859			
1	-1.9211930	2.4686360	-0.5415990	28	-1.1027260	0.2752220	0.9253930
1	-3.3280400	3.1836530	0.2994110	28	1.2409020	0.3085770	0.6874510
6	-3.6827460	-2.2463620	0.0836130	16	-0.0552390	-0.8308350	-0.5746200
1	-2.6747250	-2.3356640	0.4940340	16	0.1930430	1.4133170	2.1852970
1	-4.4098010	-2.5905140	0.8259230	6	-2.9936780	-0.0162870	0.8466630
1	-3.7634660	-2.8573670	-0.8213020	7	-3.7837820	-0.5025640	1.8491090
				7	-3.8636220	0.2234430	-0.1773590
B3LYP Open Shell Singlet				6	-5.1635110	-0.1020910	0.1803810
E = -4422.355233				6	-5.1129530	-0.5634020	1.4584770
28	-1.1096580	0.4260450	1.1486910	1	-5.9977210	0.0211310	-0.4939970
28	1.2903070	0.4584930	0.9117940	1	-5.8935160	-0.9243850	2.1113860
16	-0.0298360	-0.6684680	-0.3370560	6	3.0831150	0.1187720	0.2011510
16	0.2109650	1.5500520	2.4051780	7	3.9404220	1.1218660	-0.1511820
6	-2.9545140	0.0102990	0.9010200	7	3.8508630	-1.0087220	0.1533040
7	-3.7741080	-0.5997630	1.8065180	6	5.1548150	-0.7139250	-0.2157230
7	-3.7661730	0.2728970	-0.1634770	6	5.2108640	0.6305740	-0.4114430
6	-5.0619470	-0.1594250	0.0755740	1	5.9169090	-1.4735520	-0.3052630
6	-5.0667610	-0.7134690	1.3175750	1	6.0294710	1.2683260	-0.7098320
1	-5.8551300	-0.0371010	-0.6467170	6	-3.4806750	0.7828470	-1.4699110
1	-5.8629890	-1.1722460	1.8844480	1	-3.8166770	1.8223180	-1.5501810
6	3.0552710	0.1578500	0.2532830	1	-3.9270270	0.1906300	-2.2745240
7	3.8969810	1.1019320	-0.2607040	1	-2.3933360	0.7405800	-1.5493630
7	3.7809940	-0.9963490	0.2146160	6	-3.2857110	-0.9252380	3.1540320
6	5.0466150	-0.7756350	-0.3074710	1	-2.2389750	-0.6251580	3.2326200
6	5.1191090	0.5480820	-0.6109110	1	-3.3622820	-2.0127810	3.2575270
1	5.7739960	-1.5662630	-0.4150890	1	-3.8624510	-0.4399840	3.9476150
1	5.9191790	1.1327220	-1.0397400	6	3.5581280	2.5258080	-0.2617600
6	-3.3346450	0.9606230	-1.3769910	1	4.2568070	3.1472740	0.3069490
1	-3.6795830	2.0002190	-1.3695650	1	2.5542190	2.6389310	0.1521460
1	-3.7406410	0.4459570	-2.2528530	1	3.5578930	2.8400280	-1.3108660
1	-2.2443270	0.9344970	-1.4133930	6	3.3708980	-2.3457140	0.4886250
6	-3.3343250	-1.0922020	3.1082350	1	2.2801520	-2.3218250	0.5003810
1	-2.3146070	-0.7415190	3.2794010	1	3.7115550	-3.0590400	-0.2678710
1	-3.3496670	-2.1869700	3.1261820	1	3.7432440	-2.6495050	1.4730009

5.2.2. CASSCF Coordinates

{(L)Ni(μ-S)}$_2$ (L = 1,3-dimethyl-imidazolin-2-ylidene), all spin states C2 symmetric

Closed Shell Singlet
E = -459.7080203708

NICKEL	28.0	-1.176767018	0.069389408	0.250660137
SULFUR	16.0	0.099360869	1.715304594	-0.075476884
CARBON	6.0	-3.042408811	0.210616105	0.008887999
NITROGEN	7.0	-3.808760049	-0.271228604	-1.031574571
NITROGEN	7.0	-3.955995337	0.859232875	0.815090456
CARBON	6.0	-5.243035690	0.782618977	0.291829362
CARBON	6.0	-5.148945714	0.069046970	-0.875725655
HYDROGEN	1.0	-6.102879477	1.232677337	0.784853313
HYDROGEN	1.0	-5.911229864	-0.218887797	-1.597460215
CARBON	6.0	-3.598779181	1.527949276	2.065260010
HYDROGEN	1.0	-3.982035996	0.961442608	2.932189553
HYDROGEN	1.0	-4.013016366	2.550560520	2.077247015
HYDROGEN	1.0	-2.498757632	1.578704592	2.115281003
CARBON	6.0	-3.268123558	-1.026281747	-2.162297566
HYDROGEN	1.0	-2.199617955	-1.208406185	-1.963602975
HYDROGEN	1.0	-3.380494901	-0.448184673	-3.096155099
HYDROGEN	1.0	-3.794128960	-1.991743755	-2.257413616

Open Shell Singlet
E = -459.7175212588

NICKEL	28.0	-1.177152798	0.066380507	0.054508024
SULFUR	16.0	0.098404782	1.756229744	-0.004421308
CARBON	6.0	-3.059181702	0.181446109	0.000657576
NITROGEN	7.0	-3.917312318	-0.341907684	-0.944353338
NITROGEN	7.0	-3.900560790	0.817643371	0.890065452
CARBON	6.0	-5.233045636	0.692594913	0.509138650
CARBON	6.0	-5.243287453	-0.038951300	-0.651106660
HYDROGEN	1.0	-6.048816185	1.125059304	1.085688026
HYDROGEN	1.0	-6.069500093	-0.362238478	-1.281786675
CARBON	6.0	-3.435199046	1.511425615	2.090462063
HYDROGEN	1.0	-3.722084727	0.949803124	2.996825471
HYDROGEN	1.0	-3.866491974	2.526255446	2.130196961
HYDROGEN	1.0	-2.336833411	1.580584288	2.031280227
CARBON	6.0	-3.471506957	-1.095188645	-2.116221768
HYDROGEN	1.0	-2.400028342	-1.315829500	-1.983517214
HYDROGEN	1.0	-3.615281754	-0.499904027	-3.034979002
HYDROGEN	1.0	-4.036532984	-2.039686487	-2.193296431

Triplet
E = -459.5463676505

NICKEL	28.0	-1.174399768	0.051061375	0.012769521
SULFUR	16.0	0.076161385	1.764382102	0.013196787
CARBON	6.0	-3.059444730	0.135263271	-0.001036540
NITROGEN	7.0	-3.927487449	-0.403884857	-0.928036582
NITROGEN	7.0	-3.893666393	0.753978294	0.906916647
CARBON	6.0	-5.231543265	0.602832994	0.554757183
CARBON	6.0	-5.252740782	-0.127247172	-0.606087646
HYDROGEN	1.0	-6.042811084	1.018091624	1.149989146
HYDROGEN	1.0	-6.085851124	-0.465770456	-1.219455275

CARBON	6.0	-3.417246078	1.454613498	2.099004974
HYDROGEN	1.0	-3.678277114	0.887831309	3.009969188
HYDROGEN	1.0	-3.864133056	2.462282968	2.147691165
HYDROGEN	1.0	-2.321531977	1.541385785	2.019469831
CARBON	6.0	-3.491909253	-1.145857051	-2.110700329
HYDROGEN	1.0	-2.417108544	-1.359151545	-1.994014407
HYDROGEN	1.0	-3.652122638	-0.546234587	-3.023897245
HYDROGEN	1.0	-4.050653195	-2.094130613	-2.186239770

{ClNi(μ-C(TMS)PMe_3)}$_2$, all spin states C2 symmetric
Closed Shell Singlet
E = -484.3110933783

NICKEL	28.0	0.000000000	0.000000000	1.109080737
CHLORINE	17.0	0.000000000	0.000000000	3.257570448
NICKEL	28.0	0.000000000	0.000000000	-1.154675211
CHLORINE	17.0	0.000000000	0.000000000	-3.299995388
CARBON	6.0	1.504756569	0.021807526	-0.020578435
PHOSPHORUS	15.0	2.267878332	1.605980323	-0.238242490
SILICON	14.0	2.595256461	-1.507968840	0.269703994
CARBON	6.0	1.246664447	2.901801345	-1.013481952
HYDROGEN	1.0	1.842416020	3.821539464	-1.130607486
HYDROGEN	1.0	0.909567417	2.555981555	-1.989502856
HYDROGEN	1.0	0.380790924	3.103848425	-0.391531235
CARBON	6.0	2.889462508	2.363770040	1.309922051
HYDROGEN	1.0	3.649274016	1.715072290	1.758224720
HYDROGEN	1.0	3.322360378	3.360739363	1.115346691
HYDROGEN	1.0	2.053270631	2.443506928	2.017633034
CARBON	6.0	3.717176523	1.537963597	-1.363207422
HYDROGEN	1.0	4.473554249	0.852322264	-0.974001616
HYDROGEN	1.0	4.160013366	2.538493250	-1.480581386
HYDROGEN	1.0	3.378036281	1.180452524	-2.338674606
CARBON	6.0	4.104012075	-1.088807717	1.349341972
HYDROGEN	1.0	4.701916304	-2.002286102	1.499913748
HYDROGEN	1.0	3.791313558	-0.746921792	2.340268025
HYDROGEN	1.0	4.770704417	-0.334167892	0.916841022
CARBON	6.0	3.222972148	-2.216123831	-1.369921471
HYDROGEN	1.0	2.397413343	-2.387690582	-2.076552947
HYDROGEN	1.0	3.927858003	-1.537881714	-1.871015163
HYDROGEN	1.0	3.742062481	-3.173251477	-1.196811693
CARBON	6.0	1.732867365	-2.889112466	1.224762252
HYDROGEN	1.0	1.014941705	-3.406554381	0.630572939
HYDROGEN	1.0	1.243824558	-2.512791812	2.102913858
HYDROGEN	1.0	2.467210853	-3.628146921	1.557999755

Open Shell Singlet
E = -484.3110934011

NICKEL	28.0	0.000000000	0.000000000	-1.109080696
NICKEL	28.0	0.000000000	0.000000000	1.154675261
CHLORINE	17.0	0.000000000	0.000000000	-3.257570395
CHLORINE	17.0	0.000000000	0.000000000	3.299995459
CARBON	6.0	-0.115513783	-1.500474753	0.020578476

PHOSPHORUS	15.0	-1.744152767	-2.163417691	0.238242534
SILICON	14.0	1.343351004	-2.684163597	-0.269703966
CARBON	6.0	-2.973833334	-1.063456043	1.013482006
HYDROGEN	1.0	-3.928900968	-1.600749212	1.130607541
HYDROGEN	1.0	-2.607683689	-0.748558965	1.989503904
HYDROGEN	1.0	-3.121542686	-0.186676759	0.391531799
CARBON	6.0	-2.539196017	-2.736582913	-1.309922003
HYDROGEN	1.0	-1.939095843	-3.535333237	-1.758224675
HYDROGEN	1.0	-3.561198795	-3.106527126	-1.115346641
HYDROGEN	1.0	-2.566681996	-1.897047720	-2.017632481
CARBON	6.0	-1.766561634	-3.614137974	1.363207453
HYDROGEN	1.0	-1.129375716	-4.411762827	0.974001640
HYDROGEN	1.0	-2.792737038	-3.993780037	1.480581421
HYDROGEN	1.0	-1.388615674	-3.297930247	2.338674129
CARBON	6.0	0.831006401	-4.163873879	-1.349342441
HYDROGEN	1.0	1.705459906	-4.817527690	-1.499913727
HYDROGEN	1.0	0.509266227	-3.830482809	-2.340267979
HYDROGEN	1.0	0.036296628	-4.782255877	-0.916840995
CARBON	6.0	2.011022672	-3.354778994	1.369920975
HYDROGEN	1.0	2.233689698	-2.541512814	2.076552952
HYDROGEN	1.0	1.290182679	-4.016040005	1.871015164
HYDROGEN	1.0	2.933950867	-3.932491432	1.196811688
CARBON	6.0	2.775539717	-1.909497153	-1.224762216
HYDROGEN	1.0	3.336704280	-1.225203580	-0.630572911
HYDROGEN	1.0	2.430418215	-1.397959031	-2.102913800
HYDROGEN	1.0	3.467387801	-2.688457045	-1.557999733

Triplet

E = -484.3173210325

NICKEL	28.0	0.000000000	0.000000000	-1.146309269
NICKEL	28.0	0.000000000	0.000000000	1.185373904
CHLORINE	17.0	0.000000000	0.000000000	-3.207198250
CHLORINE	17.0	0.000000000	0.000000000	3.233396156
CARBON	6.0	0.066448585	1.531593778	0.011226997
PHOSPHORUS	15.0	1.641194541	2.311209486	0.193397458
SILICON	14.0	-1.441140477	2.660754716	-0.218545540
CARBON	6.0	2.958769272	1.277900314	0.894445250
HYDROGEN	1.0	3.892265907	1.852489970	0.979849435
HYDROGEN	1.0	2.660404059	0.940708895	1.877275676
HYDROGEN	1.0	3.109948703	0.417557090	0.260368721
CARBON	6.0	2.330453340	2.928314716	-1.378077543
HYDROGEN	1.0	1.679278536	3.699474168	-1.793766701
HYDROGEN	1.0	3.336891472	3.342513934	-1.212443671
HYDROGEN	1.0	2.369726381	2.101416017	-2.097620806
CARBON	6.0	1.661015571	3.749517784	1.329700992
HYDROGEN	1.0	0.985323568	4.519816387	0.968210652
HYDROGEN	1.0	2.675554712	4.162892223	1.417046251
HYDROGEN	1.0	1.332320029	3.419367127	2.310388370
CARBON	6.0	-1.095473399	4.163556381	-1.311395266
HYDROGEN	1.0	-2.018744314	4.752985507	-1.418114476
HYDROGEN	1.0	-0.803627750	3.858168341	-2.311521940

HYDROGEN	1.0	-0.323948746	4.827012452	-0.912467624
CARBON	6.0	-2.054586663	3.288736738	1.446090593
HYDROGEN	1.0	-2.199307942	2.468239198	2.159221987
HYDROGEN	1.0	-1.351244140	3.985771872	1.912337012
HYDROGEN	1.0	-3.014650503	3.815056260	1.311569851
CARBON	6.0	-2.871412596	1.814826229	-1.083708782
HYDROGEN	1.0	-3.301048628	1.049045263	-0.484650465
HYDROGEN	1.0	-2.557867348	1.380022341	-2.008140782
HYDROGEN	1.0	-3.663050283	2.539578801	-1.319773083

$[\{(L)Ni\}_2(\mu\text{-}Cl)(\mu\text{-}NPh)]^+$ (L = 1,3-dimethyl-imidazolin-2-ylidene), all spin states C1 symmetric
Closed Shell Singlet
E = -499.8087657950

NICKEL	28.0	16.8005040	17.4810270	4.3797260
NICKEL	28.0	18.0850420	19.4063420	4.3662950
CHLORINE	17.0	18.2341590	17.8869400	6.0019750
NITROGEN	7.0	16.6540260	18.9600140	3.3897130
CARBON	6.0	19.2981580	20.9217560	4.3534710
NITROGEN	7.0	20.6443860	20.8396990	4.0521190
NITROGEN	7.0	19.1543030	22.2574320	4.6539680
CARBON	6.0	20.3478540	22.9733880	4.5443240
CARBON	6.0	21.3033980	22.0652910	4.1715050
HYDROGEN	1.0	20.4172460	24.0422380	4.7345250
HYDROGEN	1.0	22.3590010	22.2025830	3.9507240
CARBON	6.0	15.9095550	15.7721970	4.5445590
NITROGEN	7.0	16.5083130	14.5405880	4.6344650
NITROGEN	7.0	14.5706590	15.4482620	4.5593050
CARBON	6.0	15.5894950	13.4914220	4.7203680
CARBON	6.0	14.3501140	14.0733950	4.6936410
HYDROGEN	1.0	15.8858030	12.4477080	4.7982590
HYDROGEN	1.0	13.3582450	13.6325540	4.7602170
CARBON	6.0	15.4815760	19.6554070	3.1337020
CARBON	6.0	14.7719900	20.3723990	4.1606660
CARBON	6.0	13.6289490	21.0942330	3.8140810
CARBON	6.0	13.1272220	21.1232160	2.4918590
CARBON	6.0	13.8240570	20.3993540	1.5059130
CARBON	6.0	14.993152000	19.6728250	1.7795330
HYDROGEN	1.0	15.118733111	20.352040842	5.183287514
HYDROGEN	1.0	13.0916310	21.6364100	4.6032000
HYDROGEN	1.0	12.237076660	21.683361261	2.246342076
HYDROGEN	1.0	13.457159000	20.418280000	0.471612000
HYDROGEN	1.0	15.512249666	19.141314132	0.995674715
CARBON	6.0	21.312250616	19.593923168	3.648510984
HYDROGEN	1.0	22.014994740	19.251038794	4.416423385
HYDROGEN	1.0	20.587686137	18.788890327	3.481071492
HYDROGEN	1.0	21.877931573	19.727372602	2.719368920
CARBON	6.0	17.876319083	22.866796280	5.049356775
HYDROGEN	1.0	17.224214753	23.024097774	4.182682305
HYDROGEN	1.0	17.334249092	22.231836697	5.759352546
HYDROGEN	1.0	18.029797592	23.840676780	5.528010920
CARBON	6.0	13.491100078	16.439551451	4.446177826

HYDROGEN	1.0	13.298464595	16.702052155	3.399710719
HYDROGEN	1.0	12.554218286	16.059199872	4.868898451
HYDROGEN	1.0	13.741504551	17.364636364	4.977801917
CARBON	6.0	17.965285961	14.345393322	4.639834354
HYDROGEN	1.0	18.355825649	14.283581127	5.661972534
HYDROGEN	1.0	18.245896201	13.420706323	4.122804964
HYDROGEN	1.0	18.480587900	15.172941302	4.139097973

Open Shell Singlet
E = -499.8087672001

NICKEL	28.0	16.8005110	17.4814400	4.3793840
NICKEL	28.0	18.0853720	19.4065030	4.3658840
CHLORINE	17.0	18.2342190	17.8871570	6.0015900
NITROGEN	7.0	16.6544410	18.9602860	3.3890320
CARBON	6.0	19.2987110	20.9217280	4.3535220
NITROGEN	7.0	20.6451590	20.8394010	4.0532480
NITROGEN	7.0	19.1548290	22.2574690	4.6536500
CARBON	6.0	20.3485650	22.9732330	4.5448520
CARBON	6.0	21.3042760	22.0649100	4.1729970
HYDROGEN	1.0	20.4179660	24.0420940	4.7349900
HYDROGEN	1.0	22.3600560	22.2020230	3.9529550
CARBON	6.0	15.9091290	15.7729010	4.5447530
NITROGEN	7.0	16.5077090	14.5412030	4.6344880
NITROGEN	7.0	14.5701790	15.4491880	4.5600580
CARBON	6.0	15.5887800	13.4921490	4.7204370
CARBON	6.0	14.3494810	14.0743180	4.6942120
HYDROGEN	1.0	15.8849770	12.4483730	4.7979480
HYDROGEN	1.0	13.3575790	13.6335690	4.7608550
CARBON	6.0	15.4820070	19.6557190	3.1329740
CARBON	6.0	14.7724020	20.3723960	4.1601230
CARBON	6.0	13.6288580	21.0936200	3.8139470
CARBON	6.0	13.1266900	21.1223740	2.4918920
CARBON	6.0	13.8237640	20.3991370	1.5056530
CARBON	6.0	14.9933190	19.6731740	1.7788810
HYDROGEN	1.0	15.119525728	20.352272912	5.182620031
HYDROGEN	1.0	13.0914480	21.6353910	4.6032820
HYDROGEN	1.0	12.236048181	21.681878546	2.246714895
HYDROGEN	1.0	13.4565520	20.4179570	0.4714610
HYDROGEN	1.0	15.512558731	19.142125114	0.994803719
CARBON	6.0	21.313137189	19.593461179	3.650334733
HYDROGEN	1.0	22.015176201	19.250533878	4.418872660
HYDROGEN	1.0	20.588568321	18.788540493	3.482375843
HYDROGEN	1.0	21.879620132	19.726707844	2.721652294
CARBON	6.0	17.876615461	22.867099574	5.047884336
HYDROGEN	1.0	17.225299848	23.024474086	4.180630227
HYDROGEN	1.0	17.333803496	22.232284867	5.757442650
HYDROGEN	1.0	18.029860238	23.840979029	5.526615488
CARBON	6.0	13.490728471	16.440676516	4.447643244
HYDROGEN	1.0	13.297468616	16.703232357	3.401305100
HYDROGEN	1.0	12.554049080	16.060487758	4.870958457
HYDROGEN	1.0	13.741643183	17.365705576	4.979123928

CARBON 6.0 17.9646560 14.345808997 4.639647742
HYDROGEN 1.0 18.355334211 14.283942858 5.661729720
HYDROGEN 1.0 18.245065380 13.421083878 4.122577556
HYDROGEN 1.0 18.479999136 15.173286724 4.138837665

Triplet
E = -499.8216596746
NICKEL 28.0 16.7696210 17.4630250 4.3996600
NICKEL 28.0 18.2290900 19.3306970 4.4213600
CHLORINE 17.0 18.9118110 17.3409550 5.1449960
NITROGEN 7.0 16.5979370 19.1727900 3.7697990
CARBON 6.0 19.3709760 20.8523750 4.3678590
NITROGEN 7.0 20.5966920 20.8626240 3.7223040
NITROGEN 7.0 19.3098880 22.1170710 4.9136570
CARBON 6.0 20.4500870 22.8744760 4.6288870
CARBON 6.0 21.2611980 22.0817950 3.8581200
HYDROGEN 1.0 20.5837840 23.8967190 4.9766230
HYDROGEN 1.0 22.2251600 22.3020190 3.4074120
CARBON 6.0 15.8630560 15.7554280 4.5827660
NITROGEN 7.0 16.4025260 14.4941810 4.5263310
NITROGEN 7.0 14.5183160 15.4891110 4.7440330
CARBON 6.0 15.4510750 13.4855360 4.6739560
CARBON 6.0 14.2478450 14.1218130 4.8345480
HYDROGEN 1.0 15.7015670 12.4268810 4.6633240
HYDROGEN 1.0 13.2519500 13.7193420 5.0052810
CARBON 6.0 15.4587310 19.7796520 3.3024050
CARBON 6.0 14.5946060 20.4448920 4.2490250
CARBON 6.0 13.4568020 21.1002930 3.7798540
CARBON 6.0 13.1123250 21.1103270 2.4059690
CARBON 6.0 13.9668830 20.4552720 1.4962680
CARBON 6.0 15.1362000 19.7943290 1.8992670
HYDROGEN 1.0 14.826002337 20.434934300 5.303897779
HYDROGEN 1.0 12.8047530 21.6122400 4.4994170
HYDROGEN 1.0 12.216821936 21.607707121 2.063788816
HYDROGEN 1.0 13.7134560 20.4649770 0.4283120
HYDROGEN 1.0 15.776894922 19.309864086 1.177322567
CARBON 6.0 17.835955981 14.233816723 4.3304058
HYDROGEN 1.0 18.361716069 14.154376701 5.288718411
HYDROGEN 1.0 18.0550681 13.297557049 3.785025003
HYDROGEN 1.0 18.312881430 15.037495865 3.757904972
CARBON 6.0 13.483602131 16.530989441 4.8130568
HYDROGEN 1.0 13.128555857 16.807515760 3.813708923
HYDROGEN 1.0 12.615222645 16.193363286 5.390090847
HYDROGEN 1.0 13.864433645 17.440519237 5.291364006
CARBON 6.0 18.174725971 22.612853885 5.705178636
HYDROGEN 1.0 17.280333978 22.739045141 5.084495799
HYDROGEN 1.0 17.919591335 21.919469581 6.514642698
HYDROGEN 1.0 18.399860320 23.583777030 6.160954285
CARBON 6.0 21.136996474 19.716459364 2.977134421
HYDROGEN 1.0 22.105914344 19.399764835 3.379640558
HYDROGEN 1.0 20.461710013 18.854649979 3.025922972

HYDROGEN 1.0 21.283349790 19.961611632 1.919027742

5.2.3. Full Reaction Coordinate

H_2
E = -1.175919
1 0.0000000 0.0000000 0.3714840
1 0.0000000 0.0000000 -0.3714840

{(IPr)Ni(μ-S)}$_2$ Open Shell Singlet
E = -4263.707515
28 1.1832150 -0.6711030 0.2052560
28 -1.1750530 -0.6772400 -0.2111210
16 0.0131010 -2.4299380 -0.0275640
16 -0.0052240 1.0509020 0.0218580
6 -2.9083000 -0.0238860 -0.5303060
7 -3.3589830 0.9271840 -1.3898790
7 -4.0608310 -0.4827140 0.0231340
6 -4.7406390 1.0519050 -1.3801990
1 -5.2753620 1.7517830 -2.0042800
6 -5.1916640 0.1532270 -0.4652850
1 -6.1929240 -0.0852360 -0.1399750
6 2.9175190 -0.0228190 0.5312700
7 4.0668500 -0.4926550 -0.0193940
7 3.3746000 0.9290650 1.3860930
6 5.2021530 0.1375010 0.4660950
1 6.2017820 -0.1093330 0.1421010
6 4.7571330 1.0441100 1.3764380
1 5.2961410 1.7442100 1.9966510
6 -4.0523250 -1.4333420 1.0641120
6 -4.2257660 -2.8095960 0.7657330
6 -4.1417730 -3.7469000 1.8114070
6 -3.8908690 -3.3370640 3.1179690
6 -3.7340250 -1.9858380 3.4130420
6 -3.8213430 -1.0133480 2.4008250
1 -4.2686210 -4.8038860 1.6175360
1 -3.8243210 -4.0722790 3.9096210
1 -3.5471870 -1.6993310 4.4396680
6 -3.6784300 0.4636970 2.7609810
1 -3.7985780 1.1025030 1.8625150
6 -4.7724840 0.9040580 3.7410450
1 -5.7742420 0.6711900 3.3205760
1 -4.7133230 2.0009210 3.9080910
1 -4.6659480 0.3940750 4.7215720
6 -2.2849180 0.7667800 3.3199520
1 -2.1233090 0.2578260 4.2931470
1 -2.1650690 1.8610830 3.4697490
1 -1.5084800 0.4304170 2.6020320
6 -4.5086130 -3.2889040 -0.6556010
1 -4.5373010 -2.4331840 -1.3613190
6 -3.4028350 -4.2218930 -1.1626770
1 -2.4221380 -3.7057060 -1.1157080
1 -3.5940750 -4.4976280 -2.2217970
1 -3.3509200 -5.1533900 -0.5608270
6 -5.8819600 -3.9651380 -0.7436620
1 -5.9102070 -4.8994590 -0.1441700
1 -6.1144050 -4.2181650 -1.8002270
1 -6.6690770 -3.2745890 -0.3718620
6 -2.4813650 1.7195980 -2.1631830
6 -2.2118160 3.0649310 -1.7842720
6 -1.3129330 3.8205550 -2.5591510
6 -0.6727810 3.2598930 -3.6597890
6 -0.9380850 1.9464290 -4.0333000
6 -1.8521510 1.1613820 -3.3084250
1 -1.0983020 4.8512800 -2.3105490
1 0.0275020 3.8519700 -4.2348580
1 -0.4318730 1.5448390 -4.9012810
6 -2.1650670 -0.2555570 -3.7841230
1 -2.9273830 -0.7311930 -3.1340530
6 -2.7655080 -0.2465550 -5.1953870
1 -3.6606640 0.4110760 -5.2224780
1 -3.0809010 -1.2731150 -5.4802590
1 -2.0308240 0.1146060 -5.9454920
6 -0.9218210 -1.1496800 -3.7220300
1 -0.1583830 -0.8266530 -4.4598550
1 -1.1994750 -2.2026270 -3.9420630
1 -0.4790310 -1.1142170 -2.7051640
6 -2.8900280 3.7142730 -0.5785330
1 -3.4697320 2.9636380 -0.0047280
6 -1.8774400 4.3039270 0.4149170
1 -1.1540180 3.5298400 0.7370230
1 -2.4062380 4.6684840 1.3214280
1 -1.3208980 5.1567450 -0.0257200
6 -3.8840470 4.7865340 -1.0375410
1 -3.3611200 5.6202930 -1.5526910
1 -4.4331330 5.1976850 -0.1636140
1 -4.6262290 4.3432940 -1.7353380
6 2.5015330 1.7302210 2.1550880
6 1.8669040 1.1802760 3.3012080
6 0.9499140 1.9707570 4.0163690
6 0.6874620 3.2819520 3.6327230
6 1.3327130 3.8344560 2.5308550
6 2.2344870 3.0727700 1.7652750
1 0.4381670 1.5748800 4.8837350
1 -0.0155670 3.8782520 4.2000090
1 1.1186030 4.8629800 2.2727400

6	2.1738210	-0.2353310	3.7847450	E = -4264.834126			
1	2.9455620	-0.7118940	3.1464370	28	6.1665250	5.9569450	11.1115460
6	0.9317520	-1.1297630	3.7066260	28	4.8892520	5.7578740	8.9262700
1	0.1548740	-0.8004200	4.4274970	16	6.4428930	7.2416510	9.4442910
1	1.2049450	-2.1809870	3.9400610	16	5.3502550	4.0175260	10.5482960
1	0.5081070	-1.1026490	2.6811720	1	4.3358260	4.2674720	9.3577970
6	2.7546650	-0.2236820	5.2042480	1	3.8432220	4.7560530	8.4717020
1	3.6472510	0.4368260	5.2434780	6	7.3141890	6.1353060	12.6679990
1	3.0694130	-1.2491210	5.4938670	7	7.1420590	5.6984530	13.9401770
1	2.0085710	0.1350540	5.9441520	7	8.5246830	6.7488030	12.7282990
6	2.9142040	3.7114650	0.5546890	6	9.0519590	6.7631820	14.0134830
1	3.5054480	2.9591590	-0.0048690	6	8.1749010	6.0716190	14.7880720
6	1.9012360	4.2755060	-0.4529250	1	9.9935170	7.2303160	14.2607470
1	1.1952090	3.4855890	-0.7757960	1	8.2059880	5.8141090	15.8360460
1	2.4320260	4.6421360	-1.3574110	6	4.2730950	6.7867520	7.5117440
1	1.3253450	5.1214480	-0.0241100	7	3.5696880	7.9588810	7.4833260
6	3.8949740	4.8001480	1.0035910	7	4.2490930	6.3923280	6.2104780
1	3.3610390	5.6374270	1.5013670	6	3.4855040	7.2301520	5.4102740
1	4.4466060	5.2023050	0.1270790	6	3.0224300	8.2036950	6.2306840
1	4.6361340	4.3746540	1.7135080	1	3.3366770	7.0684300	4.3535540
6	4.0487030	-1.4533940	-1.0508600	1	2.3544790	9.0259770	6.0248510
6	3.8083320	-1.0454850	-2.3894650	6	9.0064040	7.5324470	11.6558140
6	3.6937010	-2.0281540	-3.3889550	6	9.8324250	6.9513660	10.6475030
6	3.8328640	-3.3782050	-3.0796470	6	8.6184300	8.8999270	11.5557550
6	4.0933090	-3.7766340	-1.7713600	6	10.2316060	7.7501170	9.5596780
6	4.2054550	-2.8284740	-0.7381650	6	9.0495170	9.6526800	10.4491600
1	3.4974620	-1.7508640	-4.4163790	6	9.8407460	9.0801200	9.4617830
1	3.7442730	-4.1216210	-3.8614430	1	10.8532320	7.3431720	8.7717030
1	4.2042700	-4.8332410	-1.5660850	1	8.7650320	10.6910120	10.3411000
6	3.6813520	0.4294140	-2.7640590	1	10.1565980	9.6734390	8.6132760
1	3.8284620	1.0763030	-1.8753580	6	6.0164160	4.9342910	14.3171260
6	2.2823510	0.7475030	-3.3003430	6	4.7638120	5.5740200	14.5136440
1	2.0950030	0.2289390	-4.2637320	6	6.1255400	3.5239020	14.4485990
1	2.1767600	1.8416130	-3.4619900	6	3.6327160	4.7865300	14.7934060
1	1.5142590	0.4327120	-2.5637140	6	4.9732320	2.7796560	14.7616710
6	4.7633720	0.8419930	-3.7692930	6	3.7402200	3.4052190	14.9186850
1	5.7691080	0.5966870	-3.3657680	1	2.6603110	5.2424810	14.9255680
1	4.7189110	1.9379930	-3.9462470	1	5.0236580	1.7051150	14.8777780
1	4.6296170	0.3244620	-4.7424880	1	2.8616810	2.8151440	15.1460890
6	4.4971330	-3.2954130	0.6856350	6	4.7972060	5.1636160	5.7725510
1	4.5595190	-2.4310840	1.3784690	6	6.1876200	5.0669150	5.4897660
6	3.3746390	-4.1910390	1.2221740	6	3.9474980	4.0441330	5.5437710
1	2.4096720	-3.6446880	1.1935250	6	6.6979240	3.8606310	4.9767940
1	3.5798770	-4.4664160	2.2787690	6	4.5025000	2.8635540	5.0172530
1	3.2811290	-5.1237160	0.6271880	6	5.8626380	2.7741370	4.7434120
6	5.8533750	-4.0066700	0.7639850	1	7.7491470	3.7612400	4.7402080
1	5.8469010	-4.9523030	0.1819440	1	3.8795460	2.0035800	4.8102890
1	6.0964680	-4.2466980	1.8211750	1	6.2718830	1.8569550	4.3395680
1	6.6523720	-3.3444670	0.3668750	6	3.2307340	8.6947250	8.6468080
				6	3.8024050	9.9867680	8.9032610
TS1-Triplet (Ni-S in plane activation)				6	2.2707680	8.1594380	9.5577530

6	3.4616690	10.6454190	10.1007950	1	10.6908520	5.1015100	12.8049030
6	1.9559710	8.8768630	10.7240810	1	11.8154680	4.2777980	11.6857460
6	2.5579430	10.0950170	10.9974480	1	8.7437230	4.2732880	11.5738990
1	3.8838370	11.6127590	10.3437020	1	9.6012910	3.5048140	10.2135120
1	1.2331870	8.4935300	11.4322460	1	8.4129730	4.8109840	9.8786270
1	2.3070070	10.6280630	11.9056530	6	7.7375190	9.5710450	12.6080280
6	1.5252370	6.8542150	9.2866290	1	7.4813910	8.8636190	13.4194470
1	1.8741210	6.3836020	8.3498090	6	6.4020090	10.0335930	12.0105720
6	0.0262960	7.1079420	9.0858460	6	8.4725930	10.7370840	13.2798070
6	1.7621240	5.8327770	10.4072610	1	9.4395510	10.3847030	13.6987010
1	2.8464290	5.7472740	10.6233080	1	8.6698750	11.5588620	12.5596970
1	1.2398710	6.1280860	11.3414350	1	7.8608310	11.1416170	14.1143400
1	1.3866470	4.8344140	10.0963720	1	6.5525610	10.8041720	11.2256670
1	-0.4452790	7.4998820	10.0116480	1	5.7571420	10.4639400	12.8062370
1	-0.4844120	6.1621580	8.8041510	1	5.8635160	9.1702310	11.5687190
1	-0.1268620	7.8420820	8.2659530	6	7.4573090	2.8005760	14.2655610
6	4.7286070	10.7565630	7.9479860	1	8.2557780	3.5116240	13.9734540
1	5.0323530	11.7044720	8.4478530	6	7.3868620	1.7618630	13.1390500
6	4.0311100	11.2070700	6.6566400	6	7.9109510	2.1547690	15.5797150
6	6.0498980	10.0459390	7.6582180	1	7.9671900	2.9235330	16.3800320
1	6.6045120	9.8875340	8.6050630	1	7.2087210	1.3553730	15.8978620
1	5.8849790	9.0825310	7.1436980	1	8.9210110	1.7088870	15.4563200
1	6.6854910	10.6796490	7.0032950	1	6.6852550	0.9385860	13.3884610
1	4.1861680	10.4829540	5.8331060	1	8.3926590	1.3234390	12.9645390
1	4.4659680	12.1702410	6.3124770	1	7.0562860	2.2444470	12.1965950
1	2.9444640	11.3662170	6.8246900	6	4.6224680	7.0909900	14.4381550
6	7.1332640	6.2466170	5.6881040	1	5.6115530	7.5703170	14.2971950
1	6.5996550	7.0978720	6.1502410	6	4.0630060	7.6698320	15.7441290
6	7.6676620	6.7529870	4.3438460	6	3.7630000	7.5026250	13.2406380
6	8.2849310	5.8906060	6.6381600	1	4.2091380	7.1138720	12.3005570
1	7.8852950	5.4328290	7.5663690	1	2.7269370	7.1152070	13.3370050
1	8.9931450	5.1768170	6.1675870	1	3.7223440	8.6097580	13.1722010
1	8.8458400	6.8089180	6.9145810	1	3.0123070	7.3527650	15.9114030
1	8.2871990	5.9804920	3.8409620	1	4.0900940	8.7801050	15.7083410
1	8.2906170	7.6597250	4.4996470	1	4.6826270	7.3361850	16.6038770
1	6.8207060	7.0242650	3.6777080				
6	2.4485230	4.0977040	5.8284960	TS1-Singlet (Ni-S in plane activation)			
1	2.1852380	5.0396830	6.3488080	E = -4264.813028			
6	1.9993000	2.9615480	6.7601770	28	6.1746430	6.0761140	11.0541740
6	1.6488170	4.0747130	4.5211030	28	4.2557740	6.1249410	9.3959320
1	1.9641830	4.9147170	3.8664460	16	4.1639090	6.7454210	11.4816810
1	1.8028310	3.1194090	3.9756170	16	6.0804030	4.5776540	9.4148080
1	0.5648610	4.1904950	4.7353540	1	4.5287530	4.3860080	9.3607740
1	2.0426600	1.9768400	6.2494560	1	3.4021370	4.7923850	9.2712110
1	0.9520480	3.1352330	7.0881840	6	7.4023600	6.1918130	12.5483870
1	2.6410520	2.9200050	7.6641610	7	7.2010420	5.7710620	13.8223420
6	10.3300400	5.5032400	10.6741530	7	8.6907500	6.6467800	12.5838600
1	10.9539680	5.3316410	9.7679010	6	9.2384580	6.5809550	13.8618300
6	9.1981450	4.4712070	10.5848430	6	8.2980470	5.9924320	14.6423610
6	11.2574990	5.2222780	11.8622670	1	10.2358370	6.9212600	14.0969960
1	11.9954650	6.0442550	11.9801950	1	8.3185750	5.7226220	15.6874960

6	4.0868350	6.8075410	7.5661590	1	-1.0575790	7.3182970	7.0044300
7	3.5294410	8.0191260	7.2876600	1	-0.1912660	8.8842460	6.8131390
7	4.2800380	6.2834840	6.3317260	6	5.1621800	10.2517700	8.4751780
6	3.8051400	7.1018470	5.3162850	1	5.5553680	11.0192190	9.1785420
6	3.2991360	8.2038080	5.9298380	6	5.1290260	10.9395250	7.1059230
1	3.8686860	6.8431990	4.2698820	6	6.1843070	9.1106930	8.5071420
1	2.8285640	9.0850110	5.5200960	1	6.0471950	8.4752900	9.4061940
6	9.2118920	7.4560320	11.5476840	1	6.1086010	8.4831320	7.6042710
6	10.0588590	6.8982520	10.5425990	1	7.2110920	9.5301260	8.5225070
6	8.8635670	8.8376320	11.4923430	1	4.9516110	10.2159930	6.2886420
6	10.4713040	7.7185210	9.4761550	1	6.1041680	11.4355400	6.9118810
6	9.3027860	9.6101700	10.4035870	1	4.3347090	11.7159500	7.0839560
6	10.0869730	9.0515840	9.4031160	6	7.1499610	6.2882840	5.7075810
1	11.0962400	7.3248550	8.6840370	1	6.5006410	7.1801840	5.7868610
1	9.0365540	10.6559890	10.3237740	6	7.7996260	6.3725480	4.3202840
1	10.4112860	9.6611640	8.5694590	6	8.2040910	6.4099740	6.8149780
6	5.9628640	5.2588560	14.2790280	1	7.7128930	6.4132650	7.8095690
6	5.0799490	6.0870560	15.0297620	1	8.9322180	5.5728780	6.7727570
6	5.6415600	3.8901040	14.0677480	1	8.7593750	7.3664750	6.7095940
6	3.8846460	5.5350240	15.5254230	1	8.5698910	5.5844910	4.1850370
6	4.4386670	3.3822060	14.5911800	1	8.2866980	7.3624890	4.1888760
6	3.5672160	4.2003600	15.3007710	1	7.0257680	6.2604490	3.5308170
1	3.1989760	6.1336780	16.1100920	6	2.6658840	3.8444530	6.3353030
1	4.1761540	2.3402900	14.4641900	1	2.3360980	4.8206930	6.7439190
1	2.6475760	3.7908550	15.6987370	6	2.1874490	2.7815160	7.3380940
6	4.9298400	5.0453480	6.1224000	6	1.9662880	3.6669080	4.9845150
6	6.3266540	5.0115080	5.8558040	1	2.2750590	4.4752770	4.2875820
6	4.1808140	3.8371950	6.1492170	1	2.2243820	2.6856220	4.5315860
6	6.9577600	3.7652210	5.6925330	1	0.8643000	3.7231710	5.1143930
6	4.8472370	2.6187180	5.9242530	1	2.2194240	1.7634130	6.8962450
6	6.2233540	2.5845850	5.7241600	1	1.1382600	2.9922310	7.6371310
1	8.0232150	3.7041850	5.5138960	1	2.8176720	2.7885290	8.2506490
1	4.3031840	1.6843310	5.9024770	6	10.5698390	5.4553280	10.5504610
1	6.7220430	1.6360770	5.5712480	1	11.3160470	5.3419250	9.7316280
6	2.9838690	8.8169000	8.3193290	6	9.4665950	4.4457880	10.2329530
6	3.7670570	9.8339840	8.9435270	6	11.3235290	5.0830340	11.8337680
6	1.6696750	8.5436120	8.7947790	1	11.9284590	5.9409840	12.1974000
6	3.2249490	10.5255640	10.0426030	1	10.6301540	4.7479590	12.6299000
6	1.1713510	9.2748940	9.8872760	1	12.0139890	4.2367930	11.6292700
6	1.9457480	10.2465000	10.5076630	1	8.6976860	4.4225020	11.0265910
1	3.7924510	11.2987240	10.5459800	1	9.8994640	3.4267930	10.1410170
1	0.1768900	9.0882470	10.2706870	1	8.9910230	4.7037340	9.2647720
1	1.5481850	10.7941050	11.3525810	6	8.0517650	9.5141430	12.5954510
6	0.7859000	7.4745850	8.1564470	1	7.8368680	8.8047960	13.4126610
1	1.3133040	6.9695350	7.3246230	6	6.6932630	9.9990080	12.0787790
6	-0.4744830	8.0957240	7.5429610	6	8.8366300	10.6629720	13.2418090
6	0.4239340	6.3759130	9.1638350	1	9.8261460	10.2976300	13.5910160
1	1.3438090	5.9747290	9.6374320	1	8.9916480	11.4996420	12.5287270
1	-0.2468040	6.7626240	9.9596390	1	8.2819790	11.0531690	14.1220340
1	-0.0919360	5.5400240	8.6445500	1	6.8159460	10.7614960	11.2821360
1	-1.1243390	8.5447270	8.3233910	1	6.1070240	10.4480520	12.9086360

1	6.1135490	9.1417480	11.6802390	1	13.8054980	1.0955070	-4.7682230
6	6.5977200	2.9433610	13.3496230	1	12.1107550	0.9833100	-6.5228560
1	7.4305000	3.5082390	12.8867990	6	13.0587890	-5.6336540	-1.1620010
6	5.9005040	2.1874520	12.2094450	6	11.8278070	-6.3394630	-1.0779110
6	7.2355120	1.9659870	14.3426150	6	13.9859490	-5.6869450	-0.0872210
1	7.7683130	2.5292030	15.1386790	6	11.5400840	-7.0688760	0.0900220
1	6.4669080	1.3178660	14.8151470	6	13.6598270	-6.4388680	1.0561590
1	7.9738060	1.3200430	13.8209350	6	12.4455280	-7.1118550	1.1451180
1	5.2293470	1.3937570	12.5999280	1	10.6165780	-7.6251580	0.1817810
1	6.6586250	1.7091920	11.5529150	1	14.3520130	-6.5150250	1.8840780
1	5.2958680	2.8874100	11.5975320	1	12.2113880	-7.6854700	2.0327580
6	5.4213440	7.5369670	15.3642920	6	7.9536260	0.0534550	-2.7200050
1	6.3491740	7.8445130	14.8495060	6	7.2721230	-0.8750210	-3.5528280
6	5.6809700	7.6984750	16.8665360	6	8.8676170	0.9823490	-3.2880260
6	4.3357670	8.5136400	14.8919270	6	7.5132720	-0.8502210	-4.9386110
1	4.1622740	8.3992960	13.8038470	6	9.1029150	0.9452470	-4.6741890
1	3.3785850	8.3518150	15.4296850	6	8.4276530	0.0422250	-5.4881050
1	4.6636100	9.5593960	15.0743180	1	7.0031160	-1.5366870	-5.6012140
1	4.7618320	7.4940220	17.4556290	1	9.8062260	1.6267770	-5.1340440
1	6.0191690	8.7337490	17.0859550	1	8.6138360	0.0344270	-6.5543470
1	6.4791380	6.9976480	17.1922200	6	8.6523970	-0.4983740	1.9817450
				6	8.5905320	-1.7983900	2.5480450
Cis-(H)(SH)				6	9.4220930	0.5181880	2.6083550
E = -4264.873795				6	9.2923570	-2.0560210	3.7396280
28	10.2637960	-1.2576590	-0.628512	6	10.1143380	0.2129000	3.7943520
28	12.2142570	-2.5290710	-1.288830	6	10.0453310	-1.0596260	4.3530120
16	10.3732420	-2.2410040	-2.457356	1	9.2666850	-3.0371600	4.1952280
16	11.8934670	-1.6395280	0.753336	1	10.7189290	0.9610640	4.2898280
1	12.7590660	-0.6010730	0.6867700	1	10.5851580	-1.2772460	5.2656640
1	13.5844030	-2.6470610	-0.7817320	6	14.8138350	-0.9162430	-3.2188750
6	8.6232870	-0.4617310	-0.4353700	1	15.0094060	-1.9056830	-2.7588340
7	8.0038720	-0.2354060	0.7570710	6	14.4326570	0.0319970	-2.0764800
7	7.7281970	0.0491380	-1.3252720	6	16.1353960	-0.4885290	-3.8692990
6	6.6054800	0.5862040	-0.7117750	1	16.3904260	-1.1805420	-4.7003400
6	6.7803120	0.4021940	0.6233740	1	16.0741840	0.5458320	-4.2683650
1	5.7904970	1.0331570	-1.2610530	1	16.9564200	-0.5273790	-3.1217280
1	6.1527760	0.6633530	1.4620030	1	14.3432890	1.0798420	-2.4328460
6	12.9724350	-3.6429620	-2.5495000	1	15.2029230	-0.0053510	-1.2768880
7	13.3815750	-4.9222160	-2.3377180	1	13.4631560	-0.2789990	-1.6382290
7	13.3886700	-3.4061850	-3.8234750	6	11.3355110	-3.5897670	-5.9394080
6	14.0522400	-4.4964760	-4.3771730	1	11.5571420	-4.3815740	-5.1969050
6	14.0344050	-5.4693580	-3.4321330	6	11.8238070	-4.0957450	-7.3014900
1	14.4722700	-4.4883590	-5.3711370	6	9.8060380	-3.4427180	-5.9409040
1	14.4302430	-6.4735700	-3.4425750	1	9.4549770	-3.0215300	-4.9802270
6	13.0376360	-2.2360780	-4.5390000	1	9.4574380	-2.7881510	-6.7665040
6	12.0487920	-2.2901680	-5.5658640	1	9.3312460	-4.4390790	-6.0679870
6	13.6951800	-1.0084700	-4.2527950	1	11.5526580	-3.3838680	-8.1101350
6	11.7458090	-1.1162740	-6.2793490	1	11.3665310	-5.0825130	-7.5283830
6	13.3303030	0.1446570	-4.9705460	1	12.9270670	-4.2195030	-7.2924080
6	12.3681970	0.0878780	-5.9718400	6	10.8400180	-6.3703900	-2.2417600
1	11.0211300	-1.1270580	-7.0820890	1	11.1760630	-5.7034640	-3.0609730

6	9.4536620	-5.8651560	-1.8246070	6	11.1028560	1.7624270	-2.4265450
6	10.7504930	-7.7785300	-2.8402680	1	11.3049890	0.7255590	-2.0866290
1	11.7599880	-8.1221060	-3.1525800	1	11.5385200	1.9026560	-3.4376120
1	10.3361060	-8.5009170	-2.1053770	1	11.6061640	2.4614510	-1.7251140
1	10.0946920	-7.7703460	-3.7371120	1	9.6901240	3.6440720	-3.9118420
1	8.9745980	-6.5469700	-1.0914650	1	9.7216260	4.1814820	-2.1936010
1	8.7942660	-5.7939770	-2.7156690	1	8.1789760	3.6060540	-2.9200940
1	9.5378610	-4.8558410	-1.3742820				
6	15.3403970	-4.9887220	-0.1639380	TS-2 (T_d isomerization)			
1	15.4004500	-4.3532790	-1.0719420	E = -4264.859990			
6	16.4706600	-6.0176520	-0.2750430	28	9.8096630	-1.7938270	-0.2641360
6	15.5691140	-4.0533410	1.0330340	28	12.1062280	-2.8442100	-1.898939
1	14.6986180	-3.3791460	1.1729060	16	10.2223800	-3.6234510	-1.558728
1	15.7268570	-4.6263650	1.9707180	16	11.9695900	-1.3636780	0.017098
1	16.4688940	-3.4264220	0.8551360	1	11.9241290	-0.0709950	-0.3929390
1	16.5199440	-6.6569290	0.6320730	1	12.7837670	-4.0360890	-1.4453380
1	17.4462470	-5.5006530	-0.3985090	6	7.9642520	-2.1613400	-0.5044180
1	16.3069130	-6.6660900	-1.1624280	7	7.2849290	-2.9437200	0.3857150
6	7.7970850	-2.9207430	1.8861450	7	6.9738980	-1.7761050	-1.3653820
1	7.2969950	-2.5583980	0.9639530	6	5.7241150	-2.2936070	-1.0056000
6	6.6801530	-3.4271130	2.8065430	6	5.9251390	-3.0309720	0.1173260
6	8.7199520	-4.0676990	1.4560890	1	4.8233250	-2.1116490	-1.5700200
1	9.5238910	-3.6792450	0.7958320	1	5.2369100	-3.5914390	0.7317000
1	9.1860580	-4.5628480	2.3338240	6	13.6811310	-2.3124890	-2.8810980
1	8.1416390	-4.8284550	0.8897850	7	14.4731220	-3.1294410	-3.6368180
1	7.0942420	-3.9102440	3.7164770	7	14.1614070	-1.0700680	-3.2093620
1	6.0533160	-4.1705150	2.2691250	6	15.2439150	-1.1281800	-4.0920660
1	6.0283830	-2.5809360	3.1126870	6	15.4274680	-2.4418230	-4.3776870
6	9.5372550	1.9189780	2.0123330	1	15.7628970	-0.2524730	-4.4499480
1	8.9046840	2.0164970	1.1080800	1	16.1395040	-2.9360750	-5.0214060
6	10.9726250	2.2103590	1.5604140	6	13.7971210	0.1094610	-2.5156590
6	9.0384960	2.9863180	2.9942760	6	12.6855990	0.8933510	-2.9506490
1	9.0213240	3.9800870	2.4977190	6	14.6000310	0.5553280	-1.4261310
1	8.0048280	2.7458340	3.3232200	6	12.4061340	2.0970490	-2.2767130
1	9.6949280	3.0536760	3.8870790	6	14.2809790	1.7712920	-0.7963130
1	11.6765920	2.1960370	2.4190030	6	13.1933680	2.5272700	-1.2151430
1	11.0244410	3.2087670	1.0757730	1	11.5725940	2.7196050	-2.5765910
1	11.2942390	1.4523660	0.8156970	1	14.8801060	2.1444250	0.0236720
6	6.2953280	-1.8996140	-2.9818920	1	12.9611860	3.4591840	-0.7154790
1	6.2613950	-1.8371560	-1.8751710	6	14.2740690	-4.5242520	-3.7394520
6	6.7292370	-3.3349170	-3.3065740	6	13.5230620	-5.0566810	-4.8195420
6	4.8710830	-1.6314020	-3.4806370	6	14.9410850	-5.3968980	-2.8374720
1	4.5699630	-0.5923230	-3.2274060	6	13.4504610	-6.4524660	-4.9778910
1	4.7985320	-1.7688180	-4.5803060	6	14.8405220	-6.7863330	-3.0339360
1	4.1582670	-2.3280190	-2.9898540	6	14.0988130	-7.3051440	-4.0902900
1	6.6942060	-3.5348650	-4.3979250	1	12.8961760	-6.8875640	-5.7992340
1	6.0588930	-4.0592190	-2.7964910	1	15.3541430	-7.4766200	-2.3783970
1	7.7614960	-3.5095410	-2.9421490	1	14.0363470	-8.3767760	-4.2298190
6	9.5926440	2.0195660	-2.4347760	6	7.2069040	-1.0182090	-2.5426880
1	9.2571340	1.9664630	-1.3801860	6	7.1119290	-1.6398690	-3.8177390
6	9.2784070	3.4470120	-2.8997860	6	7.4816740	0.3743340	-2.4522240

6	7.2631010	-0.8534260	-4.9746240	1	15.9588910	-4.9193910	0.4691690
6	7.6701850	1.1109230	-3.6365620	1	17.5066350	-6.2118520	-2.0379850
6	7.5463810	0.5045350	-4.8815170	1	17.9255110	-4.6673860	-1.2027960
1	7.1837720	-1.2961410	-5.9587070	1	17.5762750	-4.6637800	-2.9681790
1	7.8974400	2.1681740	-3.6009910	6	7.8207240	-5.8282790	0.4331480
1	7.6801760	1.0899600	-5.7820900	1	7.5354980	-5.2435350	-0.4663720
6	7.9149070	-3.4976110	1.5215610	6	6.6092370	-6.6845100	0.8171300
6	8.1940370	-4.8903690	1.5773690	6	8.9988860	-6.7184320	0.0067930
6	8.2398900	-2.6618070	2.6261240	1	9.9195480	-6.1129940	-0.1203850
6	8.8019830	-5.4162900	2.7322230	1	9.2002810	-7.5123280	0.7564420
6	8.8967210	-3.2239310	3.7352560	1	8.7677590	-7.2106730	-0.9619090
6	9.1685640	-4.5867330	3.7870740	1	6.8439890	-7.3395610	1.6832470
1	9.0026490	-6.4757130	2.8193600	1	6.3053150	-7.3216930	-0.0406070
1	9.1780760	-2.6098390	4.5804970	1	5.7508860	-6.0333950	1.0860840
1	9.6537190	-5.0061710	4.6591250	6	7.8548570	-1.1838170	2.6584460
6	15.8139030	-0.2365750	-0.9398160	1	7.2729090	-0.9098240	1.7570310
1	15.8976850	-1.2016430	-1.4771540	6	9.0967430	-0.2859340	2.6694450
6	15.7038210	-0.6000000	0.5472880	6	6.9389060	-0.8697330	3.8486520
6	17.1105370	0.5322370	-1.2179150	1	6.5732800	0.1772530	3.7791040
1	17.1842570	0.7735870	-2.2998710	1	6.0568030	-1.5451690	3.8380710
1	17.1485950	1.4770990	-0.6354300	1	7.4730000	-0.9884270	4.8145860
1	17.9891880	-0.0891090	-0.9414480	1	9.7018350	-0.4469090	3.5864360
1	15.7138760	0.3045200	1.1904260	1	8.7948420	0.7823970	2.6265450
1	16.5575360	-1.2465080	0.8435770	1	9.7251570	-0.4989680	1.7810620
1	14.7694130	-1.1664700	0.7348940	6	6.8850250	-3.1412560	-3.9648190
6	11.7761780	0.5227640	-4.1266530	1	6.8687250	-3.6377890	-2.9736890
1	11.0566040	1.3573010	-4.2885070	6	8.0348300	-3.7963590	-4.7348220
6	10.9030460	-0.7050720	-3.8433600	6	5.5374940	-3.4350470	-4.6332190
6	12.5336320	0.3839360	-5.4531470	1	4.7156750	-2.9573700	-4.0585840
1	13.2776390	1.2015270	-5.5630390	1	5.5151510	-3.0530960	-5.6758050
1	13.0466240	-0.5936890	-5.5326190	1	5.3547490	-4.5308160	-4.6546730
1	11.8179900	0.4503640	-6.3007070	1	8.0297010	-3.5019290	-5.8052720
1	11.4711540	-1.6474030	-3.9185630	1	7.9569540	-4.9030270	-4.6730260
1	10.0923680	-0.7650590	-4.5973760	1	8.9981730	-3.4851290	-4.2838640
1	10.4397740	-0.6307260	-2.8372840	6	7.5501010	1.0970690	-1.1104230
6	12.8123940	-4.1510510	-5.8179970	1	7.3202860	0.4046280	-0.2781020
1	12.8695920	-3.0930110	-5.4928240	6	6.5029700	2.2150260	-1.0244490
6	11.3205100	-4.4877980	-5.9075190	6	8.9589750	1.6421540	-0.8518820
6	13.4789350	-4.2251490	-7.1953820	1	9.6986880	0.8173310	-0.9085360
1	14.5514280	-3.9471240	-7.1122550	1	9.2303640	2.4206260	-1.5953970
1	13.4057120	-5.2484760	-7.6210390	1	9.0161090	2.0884380	0.1637980
1	12.9890350	-3.5131320	-7.8934600	1	6.7202490	3.0306550	-1.7457720
1	11.1505220	-5.4376000	-6.4570100	1	6.4930390	2.6481870	-0.0013080
1	10.7777620	-3.6744420	-6.4351420	1	5.4921810	1.8056120	-1.2373190
1	10.9024600	-4.5913000	-4.8854540				
6	15.8130370	-4.8602270	-1.7048870	*Trans*-(H)(SH)			
1	15.6979570	-3.7609210	-1.6119990	E = -4264.872882			
6	17.2944930	-5.1223170	-1.9960500	28	10.0982260	-1.4774870	-0.773160
6	15.4120210	-5.4452590	-0.3425520	28	12.2712100	-2.6258320	-1.234155
1	14.3245430	-5.3118460	-0.1669970	16	10.3281670	-3.3028600	-1.751845
1	15.6544510	-6.5265680	-0.2773010	16	11.9629130	-0.7234570	0.054525

1	12.4130600	0.1685350	-0.8596550	1	8.7738480	-3.9106070	4.6973880
1	12.4169070	-3.9581750	-1.8007280	6	13.4000550	-0.5306170	-4.0357840
6	8.2823570	-1.4824480	-0.9215410	1	13.9445980	-0.4211890	-3.0760940
7	7.3734250	-1.9972930	-0.0469390	6	11.9702120	-0.0332910	-3.7858610
7	7.4908160	-1.0462080	-1.9416200	6	14.1246540	0.3704010	-5.0425010
6	6.1398970	-1.2556940	-1.6991760	1	15.1581910	-0.0020060	-5.2088180
6	6.0648290	-1.8633080	-0.4872310	1	13.5912230	0.3977280	-6.0161450
1	5.3641240	-0.9695860	-2.3931650	1	14.1888030	1.4067920	-4.6472770
1	5.2124360	-2.2088350	0.0777550	1	11.3992500	0.0269570	-4.7340990
6	14.1279160	-2.5157010	-1.4044890	1	11.9913810	0.9780680	-3.3267520
7	15.1583380	-2.3810090	-0.5248970	1	11.4387700	-0.7196580	-3.0936920
7	14.7778290	-2.6791400	-2.5906720	6	14.6977090	-5.4854720	-3.4593600
6	16.1591000	-2.6698590	-2.4588000	1	15.0909830	-5.1219010	-2.4888740
6	16.4037240	-2.4863980	-1.1360330	6	15.8905660	-6.0537330	-4.2358720
1	16.8364300	-2.7930210	-3.2904360	6	13.6934910	-6.5939070	-3.1107290
1	17.3369380	-2.4203400	-0.5977720	1	12.8107600	-6.1670250	-2.5907960
6	14.0791850	-3.0022650	-3.7767300	1	13.3487760	-7.1306470	-4.0191730
6	14.0394510	-4.3480850	-4.2370420	1	14.1682150	-7.3331150	-2.4305240
6	13.4032170	-1.9835440	-4.5020220	1	15.5623470	-6.5170340	-5.1904940
6	13.3673660	-4.6369870	-5.4387710	1	16.4088780	-6.8252740	-3.6273140
6	12.7290470	-2.3245350	-5.6890600	1	16.6173080	-5.2442470	-4.4612660
6	12.7173050	-3.6355740	-6.1517380	6	14.0711420	-4.5620990	1.1315500
1	13.3374090	-5.6463800	-5.8270850	1	14.3165980	-4.6353760	0.0542900
1	12.2097880	-1.5713020	-6.2669370	6	12.5674120	-4.8366990	1.2624160
1	12.1963380	-3.8782350	-7.0690520	6	14.8922080	-5.6633530	1.8142820
6	14.9605430	-2.1520820	0.8581160	1	15.9767190	-5.4396700	1.7231150
6	14.4250910	-3.1825100	1.6826580	1	14.6327480	-5.7558540	2.8897860
6	15.3115740	-0.8958050	1.4315810	1	14.6976070	-6.6407120	1.3228170
6	14.2354160	-2.9290880	3.0533500	1	12.2658310	-4.9303400	2.3270420
6	15.1433860	-0.7081920	2.8156700	1	12.3066530	-5.7804430	0.7374160
6	14.5992080	-1.7093920	3.6115240	1	11.9864040	-4.0104520	0.8017880
1	13.8180810	-3.6868610	3.7033700	6	15.8687530	0.2513060	0.5905220
1	15.4258460	0.2238560	3.2865500	1	15.8065360	0.0089000	-0.4896440
1	14.4624750	-1.5400590	4.6719200	6	17.3474800	0.4905600	0.9171560
6	7.9962740	-0.3861170	-3.0853790	6	15.0608560	1.5455000	0.7714670
6	8.1120510	-1.0857560	-4.3173850	1	13.9808550	1.3545640	0.6126100
6	8.3138870	0.9985460	-3.0241240	1	15.2008900	1.9757900	1.7850430
6	8.5016590	-0.3790100	-5.4698440	1	15.3895830	2.3024990	0.0276030
6	8.7377630	1.6540520	-4.1945400	1	17.4740020	0.8259040	1.9686110
6	8.8149420	0.9741120	-5.4048850	1	17.7657570	1.2688090	0.2436430
1	8.5711330	-0.8769920	-6.4277280	1	17.9290080	-0.4436910	0.7700140
1	8.9946780	2.7049820	-4.1777730	6	7.6086340	-4.8993370	0.2749860
1	9.1270320	1.4985800	-6.2988440	1	7.5330910	-4.3644180	-0.6949140
6	7.7448280	-2.5092840	1.2162300	6	6.2686650	-5.6072490	0.4993570
6	7.8825350	-3.9110850	1.4043720	6	8.7435270	-5.9235830	0.1143450
6	7.9514620	-1.6213550	2.3068200	1	9.7295490	-5.4160060	0.1193630
6	8.2367750	-4.3955420	2.6770430	1	8.7313650	-6.6756590	0.9309420
6	8.3490490	-2.1485900	3.5487060	1	8.6322060	-6.4617190	-0.8511960
6	8.4873140	-3.5207310	3.7290600	1	6.2871950	-6.2051850	1.4356170
1	8.3232390	-5.4578800	2.8613180	1	6.0474830	-6.2848990	-0.3527890
1	8.5314200	-1.4970080	4.3931640	1	5.4504930	-4.8589510	0.5690550

6	7.7126990	-0.1197320	2.1750160	1	-0.1936520	-10.5128420	1.5093140
1	7.3515180	0.1308010	1.1590530	1	-2.6197170	-11.2168760	0.4080510
6	9.0080530	0.6710820	2.3847820	6	0.0219970	-7.7039750	1.7787780
6	6.6161540	0.3553030	3.1367120	6	1.0447850	-7.2217680	0.9020980
1	6.3779540	1.4231190	2.9429260	6	0.0186880	-7.2459940	3.1342000
1	5.6906860	-0.2394830	2.9806360	6	1.9336810	-6.2423730	1.3901240
1	6.9349500	0.2549350	4.1955090	6	0.9629720	-6.2696870	3.5109150
1	9.4002470	0.5374200	3.4149180	6	1.8648420	-5.7923900	2.6472200
1	8.8255900	1.7534090	2.2127840	1	2.7138330	-5.8439170	0.7524670
1	9.7758740	0.3337240	1.6598280	1	0.9744100	-5.8791710	4.5215410
6	7.8086160	-2.5762190	-4.4237320	1	2.5704620	-5.0408580	2.9801910
1	7.6681190	-3.0143660	-3.4134180	6	-4.2870210	-8.9808020	0.1055940
6	8.9702170	-3.3479230	-5.0711330	6	-4.6733810	-8.5284210	-1.1880900
6	6.5054490	-2.8079260	-5.1954830	6	-5.2867980	-9.3644070	1.0468920
1	5.6686570	-2.2728070	-4.6981460	6	-6.0412930	-8.4452010	-1.5042730
1	6.5914560	-2.4438270	-6.2414940	6	-6.6411480	-9.2855680	0.6734110
1	6.2616890	-3.8916430	-5.2147490	6	-7.0109390	-8.8188650	-0.5822420
1	9.0342360	-3.1474870	-6.1612660	1	-6.3639740	-8.1045470	-2.4793750
1	8.8249320	-4.4399600	-4.9282070	1	-7.4227080	-9.5867920	1.3581290
1	9.9356970	-3.0601180	-4.6057590	1	-8.0586080	-8.7583780	-0.8478610
6	8.1856110	1.7968720	-1.7308170	6	-3.8659980	-1.9598710	-1.9237670
1	7.8051840	1.1580490	-0.9120250	6	-2.6996170	-1.7030360	-2.6985000
6	7.1725400	2.9389280	-1.8771230	6	-4.9211410	-2.7468080	-2.4664670
6	9.5496380	2.3237470	-1.2717760	6	-2.6073110	-2.2522000	-3.9905440
1	10.2652630	1.4814500	-1.1756210	6	-4.7638670	-3.3054980	-3.7475130
1	9.9601300	3.0621430	-1.9923390	6	-3.6191770	-3.0603440	-4.4974380
1	9.4547620	2.8128430	-0.2788260	1	-1.7462140	-2.0569070	-4.6153150
1	7.5255670	3.7034740	-2.6006590	1	-5.5424340	-3.9179880	-4.1829220
1	7.0143740	3.4334180	-0.8947860	1	-3.5239450	-3.4848730	-5.4886450
1	6.1962380	2.5375940	-2.2240170	6	-4.3276960	-1.6932940	2.8286980
				6	-5.6464940	-1.7871150	3.3551050
TS3-anti				6	-3.2117740	-2.0212040	3.6457010
E = -4264.848082				6	-5.8172490	-2.1603060	4.7006460
28	-3.7363990	-4.0412320	0.7156350	6	-3.4339170	-2.4039510	4.9811740
28	-2.6083620	-6.1765040	0.6545750	6	-4.7220320	-2.4659160	5.5011440
16	-4.4474220	-5.8445390	1.6505690	1	-6.8057240	-2.2223020	5.1363110
16	-1.8489330	-4.4519890	-0.4717350	1	-2.6048880	-2.6527390	5.6305420
1	-0.9425760	-3.8379670	0.3255730	1	-4.8731330	-2.7572260	6.5326910
1	-5.0430960	-4.1150590	1.4222910	6	-4.9361310	-9.8770760	2.4419640
6	-3.9300580	-2.1967800	0.4951400	1	-3.8510550	-9.7827450	2.6323390
7	-3.9843410	-1.4211770	-0.6217250	6	-5.2772380	-11.3656280	2.5730930
7	-4.1271280	-1.2879300	1.4897710	6	-5.6257720	-9.0615820	3.5454590
6	-4.3202310	0.0028350	1.0136880	1	-5.4257110	-7.9795490	3.4088430
6	-4.2360110	-0.0838380	-0.3387180	1	-6.7236500	-9.2247870	3.5474160
1	-4.4959300	0.8523860	1.6562670	1	-5.2291180	-9.3608710	4.5392540
1	-4.3235860	0.6775210	-1.0988190	1	-6.3708920	-11.5351170	2.4785590
6	-2.1969330	-7.9622130	0.8289330	1	-4.9434010	-11.7474610	3.5615940
7	-2.9147080	-9.0596390	0.4514310	1	-4.7553240	-11.9466690	1.7831670
7	-1.0314220	-8.5116310	1.2884690	6	-3.6482840	-8.1778390	-2.2595760
6	-1.0138450	-9.8959930	1.1754740	1	-2.6268720	-8.2664910	-1.8544070
6	-2.2153850	-10.2450690	0.6477180	6	-3.8019150	-6.7288720	-2.7374010

6	-3.7269270	-9.1550370	-3.4381300	1	-7.2085190	-1.2628030	-2.7030720
1	-3.6025730	-10.1977650	-3.0749610	1	-7.5765090	-2.8597170	-3.4659410
1	-4.7005020	-9.0716720	-3.9658590	1	-8.3434420	-2.4052050	-1.8998430
1	-2.9130600	-8.9414820	-4.1637290	1	-7.3993180	-4.5497270	-0.7970650
1	-4.7462740	-6.5856030	-3.3029480	1	-6.6571800	-5.0100210	-2.3737830
1	-2.9524590	-6.4531880	-3.3982310	1	-5.6356850	-4.8714890	-0.8937920
1	-3.7991500	-6.0432770	-1.8675400	6	-1.5663580	-0.8191320	-2.1804280
6	1.3267890	-7.7568560	-0.5052300	1	-1.7111310	-0.5923340	-1.1044060
1	2.0324870	-7.0578090	-1.0088270	6	-1.5501510	0.5206380	-2.9252550
6	0.1103330	-7.8147770	-1.4311910	6	-0.1963020	-1.5067080	-2.2809270
6	2.0562300	-9.1031880	-0.4512170	1	-0.2264130	-2.5059510	-1.8041230
1	2.9618020	-9.0217980	0.1873880	1	0.5696670	-0.8985130	-1.7538410
1	1.4068660	-9.9011170	-0.0466910	1	0.1255850	-1.6240160	-3.3366270
1	2.3786200	-9.4013370	-1.4718720	1	-0.7760590	1.1893310	-2.4917640
1	-0.4684610	-8.7435880	-1.2678630	1	-2.5353480	1.0240020	-2.8294840
1	0.4446220	-7.8247200	-2.4907850	1	-1.3290870	0.3732880	-4.0039710
1	-0.5355670	-6.9260800	-1.2857790				
6	-0.9107130	-7.7645620	4.2364030	TS3-syn			
1	-0.5375840	-7.3783290	5.2120740	E = -4264.839745			
6	-0.8909910	-9.2909310	4.3882680	28	-3.5558610	-3.9679450	0.7871370
6	-2.3351850	-7.2219120	4.1177400	28	-2.6124640	-6.1348520	0.7030510
1	-2.3182910	-6.1237380	3.9586900	16	-4.2640600	-5.6805540	1.9262770
1	-2.8805470	-7.7051310	3.2912620	16	-1.9628510	-4.5396340	-0.6503060
1	-2.8961130	-7.4268960	5.0545570	1	-0.8703180	-3.9476410	-0.1112050
1	-1.5980830	-9.7795370	3.6921950	1	-4.7387540	-4.0649720	1.7151470
1	-1.2079660	-9.5685230	5.4164830	6	-3.8107700	-2.1494430	0.5786290
1	0.1329210	-9.6890710	4.2231520	7	-4.2062120	-1.4322160	-0.5066210
6	-1.7816940	-1.9600960	3.1173170	7	-3.7767900	-1.2060610	1.5601840
1	-1.7681560	-1.6607510	2.0493270	6	-4.1490260	0.0546210	1.1081370
6	-0.9616230	-0.9039260	3.8673720	6	-4.4219610	-0.0894290	-0.2140550
6	-1.1053900	-3.3355850	3.1929890	1	-4.1790120	0.9283900	1.7411820
1	-0.9602980	-3.6601380	4.2447550	1	-4.7381510	0.6328990	-0.9514280
1	-1.7257480	-4.0927580	2.6689740	6	-2.1814800	-7.9034040	0.8840900
1	-0.1106730	-3.2982830	2.6998810	7	-2.8045520	-8.9742760	0.3045600
1	0.0458610	-0.8092230	3.4086520	7	-1.1349160	-8.4891350	1.5507520
1	-0.8364020	-1.1748720	4.9369480	6	-1.1010350	-9.8671560	1.3752660
1	-1.4662420	0.0838620	3.8028700	6	-2.1675670	-10.1771530	0.5969480
6	-6.8792100	-1.5016980	2.5001720	1	-0.3691750	-10.5103410	1.8402080
1	-6.5922240	-1.3003100	1.4496820	1	-2.5216160	-11.1354520	0.2481170
6	-7.6125400	-0.2526250	3.0015570	6	-0.1761170	-7.7221400	2.2589430
6	-7.8254410	-2.7094120	2.4470960	6	0.9598370	-7.1665220	1.5890500
1	-7.2770320	-3.6140090	2.1115120	6	-0.3818230	-7.3819900	3.6333840
1	-8.2803460	-2.9128810	3.4390180	6	1.7205870	-6.1905530	2.2646470
1	-8.6443280	-2.5164550	1.7213300	6	0.4504960	-6.4007370	4.2093990
1	-8.0164130	-0.4081780	4.0243680	6	1.4446690	-5.8295140	3.5220030
1	-8.4563880	-0.0077140	2.3216630	1	2.5725830	-5.7273610	1.7815310
1	-6.9178150	0.6142560	3.0176970	1	0.3010300	-6.0891180	5.2363570
6	-6.2408660	-2.9527880	-1.7247110	1	2.0600580	-5.0799680	4.0048560
1	-6.2278890	-2.4387480	-0.7441590	6	-4.0657500	-8.8796640	-0.3423970
6	-6.4978790	-4.4367430	-1.4365320	6	-4.1553580	-8.4246450	-1.6906430
6	-7.4112470	-2.3363600	-2.5006380	6	-5.2410140	-9.3350870	0.3233690

6	-5.3946480	-8.4897890	-2.3546290	1	-0.1355560	-8.5500890	-0.8806250
6	-6.4611870	-9.3554970	-0.3768340	1	1.0367960	-7.6503350	-1.8768220
6	-6.5327690	-8.9423770	-1.7007630	1	-0.1210320	-6.7294470	-0.8626240
1	-5.4859090	-8.1958580	-3.3914700	6	-1.4021410	-8.0482770	4.5615870
1	-7.3667140	-9.7085030	0.0983020	1	-1.1764720	-7.7345980	5.6062250
1	-7.4779050	-8.9796470	-2.2275880	6	-1.3070310	-9.5795480	4.5836450
6	-4.2734580	-1.9945810	-1.8025900	6	-2.8293720	-7.5729230	4.3083390
6	-3.2873810	-1.6584920	-2.7727880	1	-2.8693670	-6.4639350	4.3497570
6	-5.3372550	-2.8747460	-2.1485940	1	-3.1943300	-7.9245480	3.3289540
6	-3.4112710	-2.1714650	-4.0766290	1	-3.5084640	-7.9727430	5.0915470
6	-5.4043040	-3.3799900	-3.4601280	1	-1.9468810	-10.0382410	3.8051040
6	-4.4547940	-3.0264450	-4.4114650	1	-1.6702710	-9.9624730	5.5614970
1	-2.6932630	-1.9132160	-4.8435710	1	-0.2549720	-9.9122000	4.4541710
1	-6.2031170	-4.0474620	-3.7556170	6	-1.0314480	-1.6098370	2.5056400
1	-4.5286630	-3.4183900	-5.4176580	1	-1.3368350	-1.4517710	1.4510520
6	-3.5720850	-1.5537600	2.9158980	6	-0.1856060	-0.3934970	2.8978930
6	-4.6854320	-1.7070750	3.7886730	6	-0.1900200	-2.8935600	2.5256740
6	-2.2525310	-1.7359670	3.4104120	1	0.3134950	-3.0305390	3.5053880
6	-4.4520390	-1.9880630	5.1473870	1	-0.8336510	-3.7781930	2.3311290
6	-2.0692360	-2.0253110	4.7751800	1	0.5920570	-2.8481080	1.7378670
6	-3.1580360	-2.1465290	5.6314410	1	0.6570640	-0.2701440	2.1844800
1	-5.2756430	-2.0861730	5.8419280	1	0.2311850	-0.5067670	3.9211820
1	-1.0761940	-2.1533190	5.1853400	1	-0.8073410	0.5267570	2.8631610
1	-2.9974910	-2.3661630	6.6793660	6	-6.1222400	-1.5639630	3.2930850
6	-5.2167720	-9.8186460	1.7705180	1	-6.1465020	-1.4641180	2.1889150
1	-4.2121070	-9.6803730	2.2118820	6	-6.7675340	-0.2988160	3.8684790
6	-5.5275310	-11.3177700	1.8528460	6	-6.9684950	-2.8036680	3.6206680
6	-6.1817800	-9.0135380	2.6520050	1	-6.4628370	-3.7250790	3.2668220
1	-5.9938690	-7.9271590	2.5350090	1	-7.1505560	-2.8952430	4.7118850
1	-7.2403840	-9.2213430	2.3900970	1	-7.9528200	-2.7340800	3.1101520
1	-6.0281000	-9.2776070	3.7198040	1	-6.8494730	-0.3601880	4.9746390
1	-6.5620350	-11.5324690	1.5105500	1	-7.7853050	-0.1635600	3.4444020
1	-5.4219830	-11.6701350	2.9009880	1	-6.1594610	0.5921350	3.6029870
1	-4.8153630	-11.8899660	1.2211240	6	-6.4188770	-3.2734430	-1.1485720
6	-2.9360570	-7.9311950	-2.4572000	1	-6.2244270	-2.8250200	-0.1545850
1	-2.1226610	-7.7043580	-1.7503510	6	-6.4489520	-4.7951890	-0.9456600
6	-3.2084650	-6.6204050	-3.2140160	6	-7.7926860	-2.7508110	-1.5848510
6	-2.4220470	-9.0159910	-3.4078180	1	-7.7533990	-1.6485270	-1.7191550
1	-2.1758840	-9.9361630	-2.8356520	1	-8.1184760	-3.2174580	-2.5384180
1	-3.1858560	-9.2639290	-4.1758150	1	-8.5508490	-2.9780180	-0.8048370
1	-1.4986570	-8.6689820	-3.9196520	1	-5.4285940	-5.1712080	-0.7243200
1	-3.8236240	-6.7919690	-4.1221730	1	-7.1097750	-5.0522890	-0.0903560
1	-2.2478690	-6.1625930	-3.5343830	1	-6.8268770	-5.3177650	-1.8496860
1	-3.7379310	-5.8977370	-2.5587040	6	-2.1017810	-0.7550050	-2.4388630
6	1.5101490	-7.6473550	0.2430100	1	-2.0707770	-0.5336300	-1.3529550
1	2.3088080	-6.9423550	-0.0816090	6	-2.2219360	0.5884200	-3.1674670
6	0.5006220	-7.6447130	-0.9036150	6	-0.7601750	-1.4292090	-2.7593560
6	2.2012250	-9.0077380	0.3799860	1	-0.7028720	-2.4230580	-2.2709150
1	2.9574070	-8.9714880	1.1932830	1	0.0761320	-0.8076850	-2.3740300
1	1.4761950	-9.8112970	0.6040890	1	-0.6197410	-1.5581400	-3.8527430
1	2.7232800	-9.2651010	-0.5662940	1	-1.4005820	1.2671880	-2.8530790

1	-3.1881830	1.0746290	-2.9156170	1	0.8574080	-3.9834510	1.5481480
1	-2.1675230	0.4515410	-4.2683150	1	0.8114030	-2.2060700	1.2376360
				1	1.4014620	-2.8268420	2.8190590
{(IPr)Ni(μ-SH)}$_2$-anti Open Shell Singlet				6	3.4893440	2.1288110	1.0271300
E = -4264.889748				6	3.5613690	2.2077200	2.4450620
28	1.1968610	0.0508360	-0.0397050	6	3.0676340	3.3580410	3.0873790
28	-1.1007890	0.0469820	0.0101970	1	3.1187190	3.4552770	4.1637760
16	0.0905570	0.7956290	1.6943780	6	2.4892970	4.3912390	2.3570110
16	0.0170020	-0.6729310	-1.7343330	1	2.1027500	5.2626910	2.8697150
1	-0.0002600	0.4027380	-2.5634540	6	2.4062440	4.3104490	0.9710260
1	0.1084970	-0.2642570	2.5427370	1	1.9484220	5.1304580	0.4334650
6	3.0500990	0.0244570	-0.0769500	6	2.9106770	3.1924780	0.2826000
7	3.9336220	0.9664910	0.3604220	6	2.8284930	3.1535270	-1.2413880
7	3.8834680	-0.9452650	-0.5507340	1	3.2939210	2.2279360	-1.6379520
6	5.2607120	0.6032940	0.1671940	6	3.6056820	4.3168170	-1.8696140
6	5.2284100	-0.6270080	-0.4111070	1	4.6556600	4.3115630	-1.5062200
1	6.0949360	1.2257770	0.4542270	1	3.1430760	5.2947170	-1.6195380
1	6.0291810	-1.2753380	-0.7339650	1	3.6210630	4.2094390	-2.9753530
6	-2.9552110	0.0019400	0.0623360	6	1.3701470	3.1470760	-1.7151420
7	-3.8635390	0.7400790	-0.6414710	1	0.8622520	4.1039690	-1.4712480
7	-3.7705570	-0.7907610	0.8184450	1	0.8196020	2.3156480	-1.2287450
6	-5.1826250	0.4217790	-0.3394620	1	1.3265870	2.9949250	-2.8147300
6	-5.1228700	-0.5596460	0.5965180	6	4.1509940	1.0777940	3.2867520
1	-6.0304480	0.9044920	-0.8019160	1	4.4386730	0.2181140	2.6496960
1	-5.9085340	-1.0944610	1.1087420	6	3.1298440	0.5252300	4.2894400
6	3.3762700	-2.1147300	-1.1574290	1	3.5586300	-0.3490100	4.8245160
6	2.8131850	-3.1420410	-0.3516550	1	2.2197160	0.1845670	3.7553040
6	2.2509680	-4.2684120	-0.9787970	1	2.8433420	1.2888860	5.0422960
1	1.8043140	-5.0615470	-0.3936060	6	5.4265380	1.5390730	4.0008760
6	2.2615850	-4.3926250	-2.3639710	1	6.1579340	1.9250920	3.2588820
1	1.8302100	-5.2696780	-2.8291490	1	5.8939960	0.6847510	4.5356510
6	2.8274530	-3.3971390	-3.1541120	1	5.2063890	2.3393240	4.7387750
1	2.8251460	-3.5296960	-4.2279190	6	-3.2560540	-1.6917260	1.7752680
6	3.3791330	-2.2403330	-2.5734700	6	-2.7987140	-2.9743040	1.3674260
6	3.9610640	-1.1553590	-3.4770050	6	-2.3123110	-3.8645700	2.3418560
1	4.2940400	-0.2818940	-2.8814710	1	-1.9689640	-4.8528410	2.0661830
6	5.1960070	-1.6736190	-4.2226690	6	-2.2796650	-3.5040620	3.6848090
1	5.9476010	-2.0497370	-3.4959380	1	-1.9083940	-4.2049080	4.4214800
1	5.6610740	-0.8513890	-4.8074680	6	-2.7410500	-2.2552430	4.0882790
1	4.9279230	-2.4951690	-4.9202560	1	-2.7255820	-2.0182670	5.1436700
6	2.9149720	-0.6129650	-4.4595850	6	-3.2266920	-1.3272680	3.1491330
1	3.3421390	0.2333420	-5.0389880	6	-3.7500430	0.0239440	3.6314950
1	2.0323470	-0.2349130	-3.9048780	1	-3.9804050	0.6838110	2.7700200
1	2.5847820	-1.3939660	-5.1758750	6	-5.0549880	-0.1543680	4.4151010
6	2.8134890	-3.0587370	1.1730790	1	-5.8074390	-0.6767140	3.7864530
1	3.3093690	-2.1284750	1.5177070	1	-5.4686060	0.8370470	4.6985420
6	3.6114240	-4.2131160	1.7912790	1	-4.8872020	-0.7468090	5.3396900
1	4.6415210	-4.2275590	1.3750750	6	-2.7110120	0.7795540	4.4715290
1	3.1281860	-5.1923520	1.5901380	1	-3.0704680	1.8102110	4.6788870
1	3.6840840	-4.0775610	2.8916500	1	-1.7530610	0.8554660	3.9206080
6	1.3834680	-3.0218320	1.7255030	1	-2.5270190	0.2755490	5.4431710

6	-2.8778030	-3.4293490	-0.0878050	6	5.2703140	0.1516980	0.3962710
1	-3.2013010	-2.5949820	-0.7430810	6	5.0667720	1.0790620	-0.5759350
6	-3.9233480	-4.5377880	-0.2512980	1	6.1833050	-0.2282060	0.8298210
1	-4.9116680	-4.1825110	0.1116590	1	5.7690440	1.6672840	-1.1474910
1	-3.6364950	-5.4463450	0.3197210	6	-2.9985000	-0.3451070	0.1060310
1	-4.0252560	-4.8104100	-1.3235390	7	-4.0063270	0.2779550	0.7838960
6	-1.5113820	-3.8867220	-0.6162710	7	-3.6967790	-1.1802360	-0.7185690
1	-1.1870080	-4.8359770	-0.1408350	6	-5.2727350	-0.1428470	0.3974250
1	-0.7467990	-3.1111510	-0.4157790	6	-5.0732370	-1.0693240	-0.5765920
1	-1.5628100	-4.0466920	-1.7144600	1	-6.1840310	0.2398980	0.8320320
6	-3.4672200	1.6511130	-1.6440580	1	-5.7780070	-1.6540700	-1.1486510
6	-3.5161510	1.2675790	-3.0122330	6	3.0371210	1.9600110	-1.6989880
6	-3.1507020	2.2057650	-3.9947700	6	2.5692590	1.3421280	-2.8911170
1	-3.1978610	1.9533990	-5.0456980	6	1.8523470	2.1154420	-3.8210920
6	-2.7267870	3.4823080	-3.6400660	1	1.4746860	1.6722760	-4.7331940
1	-2.4468380	4.1901800	-4.4096640	6	1.6289230	3.4706710	-3.5990760
6	-2.6760420	3.8589020	-2.3020850	1	1.0825950	4.0527380	-4.3301090
1	-2.3599470	4.8655840	-2.0625520	6	2.1273770	4.0871900	-2.4550330
6	-3.0451610	2.9599660	-1.2850780	1	1.9636470	5.1493060	-2.3303500
6	-3.0291100	3.4283390	0.1677970	6	2.8323760	3.3492830	-1.4863900
1	-3.2818090	2.5935510	0.8530850	6	3.3951620	4.0629020	-0.2591640
6	-4.0872900	4.5123630	0.4007700	1	3.8552700	3.3355180	0.4407900
1	-5.0901130	4.1309910	0.1117320	6	4.5039650	5.0396200	-0.6669190
1	-3.8649870	5.4243810	-0.1928990	1	5.2963970	4.5005650	-1.2291740
1	-4.1183140	4.7892370	1.4763360	1	4.9668150	5.4907630	0.2367220
6	-1.6383440	3.9240200	0.5859380	1	4.1032160	5.8560730	-1.3045580
1	-1.3720820	4.8713640	0.0720350	6	2.3019820	4.7834590	0.5410360
1	-0.8738770	3.1609230	0.3403520	1	2.7361460	5.2211440	1.4653320
1	-1.6118030	4.1016890	1.6823170	1	1.5142540	4.0659880	0.8443350
6	-3.9876580	-0.1203200	-3.4403520	1	1.8385190	5.6031020	-0.0464570
1	-4.1257630	-0.7764240	-2.5568260	6	2.8687570	-0.1224380	-3.2069170
6	-2.9570380	-0.8289560	-4.3300620	1	3.4428040	-0.5930270	-2.3847600
1	-3.2648880	-1.8830600	-4.4989040	6	3.7479290	-0.2462950	-4.4569010
1	-1.9648800	-0.8362470	-3.8368870	1	4.6784420	0.3466270	-4.3259140
1	-2.8621750	-0.3332530	-5.3186620	1	3.2154440	0.1153750	-5.3618030
6	-5.3459250	-0.0338320	-4.1449070	1	4.0332220	-1.3081290	-4.6171800
1	-6.0882250	0.4571120	-3.4798950	6	1.5829540	-0.9422550	-3.3595480
1	-5.7168140	-1.0531220	-4.3851850	1	1.0264010	-0.6483680	-4.2730970
1	-5.2699850	0.5479410	-5.0881620	1	0.9312240	-0.7962740	-2.4744690
				1	1.8275020	-2.0234310	-3.4337610
{(IPr)Ni(μ-SH)}$_2$-syn Open Shell Singlet				6	3.7449300	-1.3420270	1.6677150
E = -4264.888256				6	3.8837600	-2.6868390	1.2262370
28	1.1475240	0.1201860	0.2182280	6	3.5532500	-3.7291480	2.1115920
28	-1.1500680	-0.1257970	0.2183050	1	3.6553840	-4.7634990	1.8108090
16	0.2008310	-1.8592760	0.1797020	6	3.0803790	-3.4560670	3.3913190
16	-0.2030960	1.8535140	0.1990830	1	2.8210060	-4.2708930	4.0550190
1	-0.2051330	2.1585870	1.5230620	6	2.9452580	-2.1410130	3.8243260
1	0.2050480	-2.1750660	1.5012220	1	2.5766780	-1.9630810	4.8259710
6	2.9951070	0.3451630	0.1059120	6	3.2854130	-1.0669470	2.9825430
7	4.0057170	-0.2747570	0.7827100	6	3.1556460	0.3630620	3.4996180
7	3.6898240	1.1849860	-0.7171510	1	3.5084570	1.0904770	2.7394320

6	4.0308940	0.5908710	4.7384930	1	-3.4475320	0.5973640	-2.3858680
1	5.0841590	0.3172090	4.5144210	6	-3.7425700	0.2558230	-4.4603010
1	3.6776210	-0.0123540	5.6010400	1	-4.6746950	-0.3359810	-4.3358100
1	4.0057460	1.6630740	5.0285750	1	-3.2059680	-0.1041260	-5.3634470
6	1.6917550	0.7094420	3.7872540	1	-4.0254220	1.3185330	-4.6191760
1	1.2894430	0.0926560	4.6181890	6	-1.5816730	0.9443570	-3.3501180
1	1.0814590	0.5320350	2.8778750	1	-1.0199160	0.6492500	-4.2600480
1	1.5988770	1.7813320	4.0638240	1	-0.9361140	0.7967150	-2.4607350
6	4.3882350	-3.0288110	-0.1743500	1	-1.8233410	2.0260800	-3.4257210
1	4.5630750	-2.1099630	-0.7665690	6	-3.7399700	1.3411890	1.6720480
6	3.3595140	-3.8451120	-0.9670720	6	-3.8707810	2.6880940	1.2342370
1	3.7247270	-4.0117500	-2.0031060	6	-3.5311180	3.7258480	2.1214950
1	2.4018710	-3.2904790	-1.0311560	1	-3.6269150	4.7615970	1.8235660
1	3.1750810	-4.8339380	-0.4977790	6	-3.0568330	3.4463250	3.3992870
6	5.7330150	-3.7614590	-0.1049740	1	-2.7903290	4.2577190	4.0643500
1	6.4677410	-3.1522230	0.4639250	6	-2.9297750	2.1292790	3.8287230
1	6.1338970	-3.9197510	-1.1290060	1	-2.5597930	1.9463430	4.8289710
1	5.6265640	-4.7504680	0.3888140	6	-3.2796050	1.0597460	2.9851380
6	-3.0467450	-1.9563370	-1.7012160	6	-3.1590040	-0.3724890	3.4980550
6	-2.5751700	-1.3384890	-2.8917500	1	-3.5212700	-1.0951290	2.7377660
6	-1.8575030	-2.1124410	-3.8206450	6	-4.0304120	-0.5964170	4.7402720
1	-1.4763200	-1.6691660	-4.7312400	1	-5.0822470	-0.3127700	4.5219240
6	-1.6372160	-3.4683200	-3.5990970	1	-3.6677550	0.0009890	5.6029650
1	-1.0898370	-4.0508470	-4.3289840	1	-4.0132960	-1.6697260	5.0268520
6	-2.1393330	-4.0846870	-2.4565550	6	-1.6967130	-0.7314400	3.7779610
1	-1.9771930	-5.1470360	-2.3317000	1	-1.2851030	-0.1185860	4.6072360
6	-2.8453090	-3.3461670	-1.4891320	1	-1.0895250	-0.5587490	2.8655540
6	-3.4107110	-4.0593630	-0.2627760	1	-1.6116240	-1.8043060	4.0533180
1	-3.8751310	-3.3322480	0.4345620	6	-4.3762070	3.0373050	-0.1643180
6	-4.5158480	-5.0395750	-0.6723080	1	-4.5594520	2.1211210	-0.7582320
1	-5.3074100	-4.5037100	-1.2388200	6	-3.3435560	3.8479930	-0.9578760
1	-4.9810910	-5.4894740	0.2307310	1	-3.7110990	4.0216070	-1.9919210
1	-4.1110430	-5.8568890	-1.3062320	1	-2.3909090	3.2856140	-1.0278530
6	-2.3181530	-4.7756540	0.5419430	1	-3.1489530	4.8335220	-0.4857510
1	-2.7545090	-5.2159290	1.4639630	6	-5.7152770	3.7799180	-0.0896370
1	-1.5352310	-4.0546230	0.8493370	1	-6.4529290	3.1750080	0.4800460
1	-1.8482730	-5.5926510	-0.0441430	1	-6.1178350	3.9434540	-1.1121640
6	-2.8701150	0.1272780	-3.2060580	1	-5.6000950	4.7670850	0.4058900

5.2.4. Kinetic Isotope Effect Coordinates

D_2
E = -1.180517

1	0.0000000	0.0000000	0.3714710	16	6.4428930	7.2416510	9.4442910
1	0.0000000	0.0000000	-0.3714710	16	5.3502550	4.0175260	10.5482960
				1	4.3358260	4.2674720	9.3577970
				1	3.8432220	4.7560530	8.4717020
				6	7.3141890	6.1353060	12.6679990

TS1(D_2)-Triplet (Ni-S in plane activation)
E = -4264.838029

28	6.1665250	5.9569450	11.1115460	7	7.1420590	5.6984530	13.9401770
28	4.8892520	5.7578740	8.9262700	7	8.5246830	6.7488030	12.7282990
				6	9.0519590	6.7631820	14.0134830
				6	8.1749010	6.0716190	14.7880720

1	9.9935170	7.2303160	14.2607470	1	1.3866470	4.8344140	10.0963720
1	8.2059880	5.8141090	15.8360460	1	-0.4452790	7.4998820	10.0116480
6	4.2730950	6.7867520	7.5117440	1	-0.4844120	6.1621580	8.8041510
7	3.5696880	7.9588810	7.4833260	1	-0.1268620	7.8420820	8.2659530
7	4.2490930	6.3923280	6.2104780	6	4.7286070	10.7565630	7.9479860
6	3.4855040	7.2301520	5.4102740	1	5.0323530	11.7044720	8.4478530
6	3.0224300	8.2036950	6.2306840	6	4.0311100	11.2070700	6.6566400
1	3.3366770	7.0684300	4.3535540	6	6.0498980	10.0459390	7.6582180
1	2.3544790	9.0259770	6.0248510	1	6.6045120	9.8875340	8.6050630
6	9.0064040	7.5324470	11.6558140	1	5.8849790	9.0825310	7.1436980
6	9.8324250	6.9513660	10.6475030	1	6.6854910	10.6796490	7.0032950
6	8.6184300	8.8999270	11.5557550	1	4.1861680	10.4829540	5.8331060
6	10.2316060	7.7501170	9.5596780	1	4.4659680	12.1702410	6.3124770
6	9.0495170	9.6526800	10.4491600	1	2.9444640	11.3662170	6.8246900
6	9.8407460	9.0801200	9.4617830	6	7.1332640	6.2466170	5.6881040
1	10.8532320	7.3431720	8.7717030	1	6.5996550	7.0978720	6.1502410
1	8.7650320	10.6910120	10.3411000	6	7.6676620	6.7529870	4.3438460
1	10.1565980	9.6734390	8.6132760	6	8.2849310	5.8906060	6.6381600
6	6.0164160	4.9342910	14.3171260	1	7.8852950	5.4328290	7.5663690
6	4.7638120	5.5740200	14.5136440	1	8.9931450	5.1768170	6.1675870
6	6.1255400	3.5239020	14.4485990	1	8.8458400	6.8089180	6.9145810
6	3.6327160	4.7865300	14.7934060	1	8.2871990	5.9804920	3.8409620
6	4.9732320	2.7796560	14.7616710	1	8.2906170	7.6597250	4.4996470
6	3.7402200	3.4052190	14.9186850	1	6.8207060	7.0242650	3.6777080
1	2.6603110	5.2424810	14.9255680	6	2.4485230	4.0977040	5.8284960
1	5.0236580	1.7051150	14.8777780	1	2.1852380	5.0396830	6.3488080
1	2.8616810	2.8151440	15.1460890	6	1.9993000	2.9615480	6.7601770
6	4.7972060	5.1636160	5.7725510	6	1.6488170	4.0747130	4.5211030
6	6.1876200	5.0669150	5.4897660	1	1.9641830	4.9147170	3.8664460
6	3.9474980	4.0441330	5.5437710	1	1.8028310	3.1194090	3.9756170
6	6.6979240	3.8606310	4.9767940	1	0.5648610	4.1904950	4.7353540
6	4.5025000	2.8635540	5.0172530	1	2.0426600	1.9768400	6.2494560
6	5.8626380	2.7741370	4.7434120	1	0.9520480	3.1352330	7.0881840
1	7.7491470	3.7612400	4.7402080	1	2.6410520	2.9200050	7.6641610
1	3.8795460	2.0035800	4.8102890	6	10.3300400	5.5032400	10.6741530
1	6.2718830	1.8569550	4.3395680	1	10.9539680	5.3316410	9.7679010
6	3.2307340	8.6947250	8.6468080	6	9.1981450	4.4712070	10.5848430
6	3.8024050	9.9867680	8.9032610	6	11.2574990	5.2222780	11.8622670
6	2.2707680	8.1594380	9.5577530	1	11.9954650	6.0442550	11.9801950
6	3.4616690	10.6454190	10.1007950	1	10.6908520	5.1015100	12.8049030
6	1.9559710	8.8768630	10.7240810	1	11.8154680	4.2777980	11.6857460
6	2.5579430	10.0950170	10.9974480	1	8.7437230	4.2732880	11.5738990
1	3.8838370	11.6127590	10.3437020	1	9.6012910	3.5048140	10.2135120
1	1.2331870	8.4935300	11.4322460	1	8.4129730	4.8109840	9.8786270
1	2.3070070	10.6280630	11.9056530	6	7.7375190	9.5710450	12.6080280
6	1.5252370	6.8542150	9.2866290	1	7.4813910	8.8636190	13.4194470
1	1.8741210	6.3836020	8.3498090	6	6.4020090	10.0335930	12.0105720
6	0.0262960	7.1079420	9.0858460	6	8.4725930	10.7370840	13.2798070
6	1.7621240	5.8327770	10.4072610	1	9.4395510	10.3847030	13.6987010
1	2.8464290	5.7472740	10.6233080	1	8.6698750	11.5588620	12.5596970
1	1.2398710	6.1280860	11.3414350	1	7.8608310	11.1416170	14.1143400

1	6.5525610	10.8041720	11.2256670	1	7.0562860	2.2444470	12.1965950
1	5.7571420	10.4639400	12.8062370	6	4.6224680	7.0909900	14.4381550
1	5.8635160	9.1702310	11.5687190	1	5.6115530	7.5703170	14.2971950
6	7.4573090	2.8005760	14.2655610	6	4.0630060	7.6698320	15.7441290
1	8.2557780	3.5116240	13.9734540	6	3.7630000	7.5026250	13.2406380
6	7.3868620	1.7618630	13.1390500	1	4.2091380	7.1138720	12.3005570
6	7.9109510	2.1547690	15.5797150	1	2.7269370	7.1152070	13.3370050
1	7.9671900	2.9235330	16.3800320	1	3.7223440	8.6097580	13.1722010
1	7.2087210	1.3553730	15.8978620	1	3.0123070	7.3527650	15.9114030
1	8.9210110	1.7088870	15.4563200	1	4.0900940	8.7801050	15.7083410
1	6.6852550	0.9385860	13.3884610	1	4.6826270	7.3361850	16.6038770
1	8.3926590	1.3234390	12.9645390				

5.2.5. Alternative Activation Pathways

Model L Level (L = 1,3-dimethyl-imidazolin-2-ylidene)
Ni-S in plane activation Triplet
E = -4423.098319

28	6.2174420	6.0802400	11.0170230	1	5.3092210	6.4407040	14.8109400
28	4.7430630	5.7076620	8.9914580	6	9.5119620	6.8406280	11.3846470
16	6.4203880	7.1881590	9.2023780	1	10.2764620	6.0757790	11.2140950
16	5.2560010	4.1353810	10.7016700	1	8.8299530	6.8729400	10.5315030
1	4.0970980	4.3520080	9.6116120	1	9.9904320	7.8171820	11.5076580
1	3.5737510	4.7758670	8.7009240				
6	7.4153870	6.1959980	12.5612550	Ni-S in plane activation Singlet			
7	7.1252790	5.9465670	13.8677450	E = -4423.091327			
7	8.7367350	6.5163120	12.5716040	28	6.4939220	5.2327890	10.9383790
6	9.2573820	6.4674700	13.8502160	28	4.8724860	5.4631140	9.0449230
6	8.2361120	6.1111500	14.6722930	16	6.2656020	6.9646140	9.7720000
1	10.2945840	6.6816070	14.0625010	16	5.6417510	3.4529340	10.1028830
1	8.2074940	5.9603690	15.7415080	1	4.2820450	3.9330260	9.3520340
6	4.1346860	6.7097070	7.5553270	1	3.7040520	4.5335590	8.6475550
7	3.2397020	7.7280590	7.5690500	6	7.4569200	6.0256880	12.2930880
7	4.4864490	6.5722480	6.2531920	7	6.9978710	6.3874010	13.5231260
6	3.8201340	7.4910830	5.4617670	7	8.7830410	6.3316210	12.3229290
6	3.0324840	8.2210910	6.2925890	6	9.1450380	6.8554480	13.5497430
1	3.9735180	7.5542050	4.3947510	6	8.0179120	6.8929650	14.3069460
1	2.3648000	9.0457630	6.0922220	1	10.1578530	7.1552300	13.7752290
6	5.4445710	5.5894800	5.7794950	1	7.8568600	7.2347490	15.3187920
1	6.1039810	5.3315120	6.6112870	6	4.1929170	6.6511730	7.7980490
1	4.9323800	4.6895930	5.4225860	7	3.1897310	7.5517540	7.9453790
1	6.0383430	6.0210650	4.9691460	7	4.5871120	6.7770260	6.5060070
6	2.6080350	8.2233550	8.7781420	6	3.8328580	7.7341450	5.8507290
1	1.6482300	7.7236830	8.9478600	6	2.9499300	8.2228860	6.7592740
1	3.2798740	8.0232020	9.6159560	1	3.9965230	7.9897240	4.8143510
1	2.4503510	9.3017030	8.6904370	1	2.1924930	8.9873440	6.6698750
6	5.8049570	5.5791090	14.3509870	6	5.6557440	5.9947550	5.9095370
1	5.2139600	5.2248330	13.5024510	1	6.2335180	5.5427690	6.7189410
1	5.8929240	4.7738330	15.0860260	1	5.2453800	5.2072680	5.2688350
				1	6.3071840	6.6478350	5.3217990
				6	2.4685460	7.7523700	9.1891230
				1	1.5426860	7.1672620	9.1982470
				1	3.1162850	7.4297010	10.0074060

1	2.2343450	8.8138290	9.3083160
6	5.6141590	6.2548640	13.9398380
1	5.0486190	5.8593110	13.0930700
1	5.5346500	5.5640940	14.7856090
1	5.2088910	7.2318260	14.2218580
6	9.6952770	6.0962380	11.2173540
1	10.3364570	5.2330680	11.4260450
1	9.0964250	5.9018430	10.3250400
1	10.3133530	6.9836870	11.0524520

Ni-S above plane activation Triplet
E = -4423.056068

28	-1.0536950	-0.7159600	0.6356060
28	1.2697300	-1.0700150	-0.2250700
16	-0.5172550	-1.3444910	-1.3555380
16	0.3440820	-1.6499590	1.9467370
1	1.3885530	-2.3609740	0.7899210
1	1.9111960	-2.4655730	-0.1686260
6	-2.8406140	-0.0838380	0.9253090
7	-4.0226980	-0.6734830	0.5700310
7	-3.2247820	1.0362640	1.6150600
6	-4.6046670	1.1364540	1.6907000
6	-5.1082940	0.0551580	1.0261220
1	-5.1044030	1.9524230	2.2005180
1	-6.1324820	-0.2471790	0.8387130
6	2.8933370	-0.0341180	-0.0647800
7	3.3250380	0.8548820	-1.0173150
7	3.8687740	0.0223810	0.8942290
6	4.8754840	0.9111240	0.5468450
6	4.5293570	1.4411180	-0.6612540
1	5.7342240	1.0925010	1.1832220
1	5.0251380	2.1781810	-1.2827030
6	-2.2879760	1.9735700	2.2201920
1	-2.2892780	1.8695250	3.3144490
1	-2.5560250	3.0031270	1.9462610
1	-1.2852290	1.7407530	1.8408010
6	-4.1173820	-1.9144940	-0.1920130
1	-3.0977590	-2.2610600	-0.4001490
1	-4.6392360	-1.7351120	-1.1421310
1	-4.6586620	-2.6724440	0.3909670
6	2.6085590	1.1343430	-2.2559640
1	2.3794520	2.2069180	-2.3274560
1	1.6725740	0.5592430	-2.2436610
1	3.2128010	0.8279220	-3.1216400
6	3.8712200	-0.7871020	2.1067910
1	4.3710900	-1.7501140	1.9271410
1	4.4002140	-0.2445030	2.9008960
1	2.8309430	-0.9663400	2.4078460

Ni-S above plane activation Singlet
E = -4423.050130

28	-1.0958470	-1.0461220	1.1077020
28	1.2136950	-1.0219010	-0.2174240
16	-0.6876100	-1.4004650	-0.9418350
16	0.5347940	-1.9529220	2.0354710
1	1.4865400	-2.4475560	0.4725070
1	1.8490870	-2.4160270	-0.4310700
6	-2.8005520	-0.2091170	0.9991100
7	-3.9986840	-0.7569060	0.6549440
7	-3.1069080	1.0816770	1.3130960
6	-4.4591860	1.3293790	1.1720980
6	-5.0220150	0.1656410	0.7534670
1	-4.8991820	2.2944110	1.3769710
1	-6.0481380	-0.0787710	0.5206590
6	2.8429230	-0.0072260	0.0146120
7	3.1642080	1.0551140	-0.7814550
7	3.8955320	-0.1014210	0.8704280
6	4.8461100	0.8680910	0.6135490
6	4.3820310	1.6038790	-0.4291380
1	5.7554780	0.9523960	1.1902530
1	4.8042850	2.4581880	-0.9375790
6	-2.1257840	2.0576310	1.7491530
1	-2.2981570	2.3376960	2.7937030
1	-2.1746340	2.9506210	1.1178110
1	-1.1371780	1.6009200	1.6560800
6	-4.1721550	-2.1403270	0.2453100
1	-3.1876100	-2.6114090	0.2302240
1	-4.6069160	-2.1846790	-0.7579880
1	-4.8224880	-2.6648620	0.9528830
6	2.3258980	1.5480420	-1.8594590
1	1.9645590	2.5568680	-1.6335380
1	1.4701950	0.8738650	-1.9623380
1	2.8883130	1.5628980	-2.7985210
6	4.0266130	-1.1216310	1.8979390
1	4.5733820	-1.9878990	1.5098320
1	4.5674950	-0.7037120	2.7514030
1	3.0232370	-1.4252350	2.2111990

Ni-Ni activation Triplet
E = -4423.060032

28	-1.1115900	-0.3037950	0.7087110
28	1.1276140	-0.4248950	0.3317440
16	-0.4790600	-2.1447040	-0.1051540
16	0.2375090	0.6131320	2.1041900
1	0.0715320	0.2097780	-0.5374290
1	1.3672120	-0.1829290	-1.1140150
6	-2.9046680	-0.5552580	1.2830240
7	-3.3758930	-0.9263710	2.5004830
7	-4.0169080	-0.4363230	0.5090300
6	-5.1599460	-0.7185480	1.2312360
6	-4.7531000	-1.0339010	2.4884340
1	-6.1475860	-0.6728350	0.7966710

1	-5.3169950	-1.3256810	3.3620690	6	-2.3391720	-1.8873390	3.1986680
6	2.9926700	-0.6669190	0.6054530	1	-1.3296360	-1.5347280	2.9820380
7	3.9258970	0.3141280	0.7242710	1	-2.3833100	-2.9695540	3.0451410
7	3.7028500	-1.8227800	0.6872290	1	-2.6037110	-1.6420110	4.2312820
6	5.0519280	-1.5675980	0.8531190	6	3.5840630	1.7179250	0.1907730
6	5.1929990	-0.2173530	0.8719880	1	4.1573600	2.4209550	0.8016680
1	5.7817570	-2.3577010	0.9503710	1	2.5160110	1.8948020	0.3389640
1	6.0711990	0.4014720	0.9824240	1	3.8336550	1.8600240	-0.8661510
6	-3.9916880	-0.0417290	-0.8886840	6	3.0887800	-3.0541810	1.2429360
1	-4.1301830	1.0397780	-0.9898910	1	2.0274290	-3.0099020	0.9871950
1	-4.7861310	-0.5643460	-1.4282780	1	3.5881920	-3.7810650	0.5946240
1	-3.0242460	-0.3284520	-1.3086760	1	3.2015320	-3.3563000	2.2891590
6	-2.5422290	-1.2286910	3.6535160				
1	-1.5230990	-0.9019760	3.4336370	Ni-C activation Triplet			
1	-2.5505140	-2.3054970	3.8504160	E = -4423.063927			
1	-2.9171010	-0.6899030	4.5287920	28	-1.1646160	0.1649000	0.8903250
6	3.6243070	1.7334000	0.6570370	28	1.3146740	0.2625730	0.4737690
1	4.2518990	2.2734940	1.3715720	16	-0.2828070	0.1381920	-1.0705480
1	2.5718930	1.8703730	0.9184990	16	0.2840040	0.3109530	2.4876140
1	3.8035940	2.1165020	-0.3532260	1	2.1483000	0.2448180	-0.8178830
6	3.1235210	-3.1535940	0.6271500	1	2.7664930	0.3132450	0.0799730
1	2.0498410	-3.0488830	0.4549310	6	-3.1018840	0.0950960	1.1055610
1	3.5713530	-3.7198590	-0.1955820	7	-3.8102440	-0.6199880	2.0244690
1	3.2926480	-3.6815310	1.5712210	7	-4.0616410	0.7341540	0.3805840
				6	-5.3297460	0.4274330	0.8354550
Ni-Ni activation Singlet				6	-5.1710570	-0.4350560	1.8729450
E = -4423.059522				1	-6.2225030	0.8430050	0.3913980
28	-1.1414680	-0.4386940	0.4380870	1	-5.8986040	-0.9249720	2.5034650
28	1.1223070	-0.4924140	0.1739990	6	2.9274450	0.3857570	1.4701630
16	-0.3981680	-2.3692680	-0.0102970	7	3.4977300	1.5205250	1.9507040
16	0.1021150	0.7048080	1.7333650	7	3.6094290	-0.6364290	2.0479000
1	0.0981730	-0.1726980	-0.8851470	6	4.5431680	-0.1468830	2.9357520
1	1.4670800	-0.6239300	-1.2660070	6	4.4727770	1.2112610	2.8744160
6	-2.8894600	-0.5922660	1.1483780	1	5.1775700	-0.7951420	3.5215220
7	-3.2599360	-1.2155390	2.2941010	1	5.0342740	1.9712880	3.3968780
7	-4.0536340	-0.1459110	0.6071590	6	-3.7827990	1.6439500	-0.7173330
6	-5.1339480	-0.4919910	1.3973030	1	-3.9902790	2.6773840	-0.4193300
6	-4.6300130	-1.1694000	2.4615130	1	-4.4004900	1.3816880	-1.5817740
1	-6.1490370	-0.2253990	1.1425510	1	-2.7266630	1.5424690	-0.9801620
1	-5.1224380	-1.6120430	3.3147270	6	-3.2036090	-1.4888160	3.0174660
6	2.9600410	-0.6401370	0.6444520	1	-2.1368850	-1.2534360	3.0661720
7	3.8809410	0.3587620	0.6069180	1	-3.3336700	-2.5403000	2.7392160
7	3.6606100	-1.7338530	1.0410960	1	-3.6621620	-1.3103550	3.9950050
6	4.9935480	-1.4241840	1.2440750	6	2.9691200	2.8458700	1.6737360
6	5.1336370	-0.1029500	0.9657670	1	3.7395930	3.5907200	1.8870310
1	5.7133910	-2.1590920	1.5728250	1	2.0804040	3.0165590	2.2890910
1	6.0008280	0.5399530	0.9975750	1	2.6790440	2.9039890	0.6218250
6	-4.1446440	0.5852110	-0.6430960	6	3.2218220	-2.0282060	1.8911790
1	-4.6530570	1.5415940	-0.4864630	1	2.9508570	-2.2105570	0.8483020
1	-4.6863480	-0.0024190	-1.3910510	1	4.0615300	-2.6681990	2.1726390
1	-3.1304290	0.7732390	-1.0018460	1	2.3484180	-2.2330910	2.5179930

Ni-C activation Singlet
E = -4423.058769

28	-0.8596000	0.7768050	0.5238510
28	1.3505160	1.3366960	-0.0534010
16	-0.0707750	0.4731920	-1.4076890
16	0.0002340	2.4697290	1.4156470
1	2.8130940	1.7704130	-0.4518530
1	2.1520630	2.1370580	-1.1573590
6	-2.5715940	0.1753220	1.0165530
7	-2.9659350	-0.2444640	2.2719500
7	-3.7206260	0.0775770	0.2604550
6	-4.7889530	-0.3902790	1.0203970
6	-4.3130030	-0.5938700	2.2895100
1	-5.7833760	-0.5316450	0.6009780
1	-4.8113080	-0.9487780	3.1898280
6	2.4753230	0.5201630	1.5244880
7	3.2046980	1.1331290	2.5107030
7	2.5522520	-0.8151970	1.8365060
6	3.3049130	-1.0268980	2.9916070
6	3.7166840	0.2088300	3.4188660
1	3.4740100	-2.0193600	3.4055190
1	4.3138840	0.5054160	4.2793650
6	-3.8124740	0.4417160	-1.1537090
1	-4.5495050	1.2522820	-1.2875900
1	-4.1119180	-0.4356550	-1.7528550
1	-2.8188300	0.7868060	-1.4799880
6	-2.0786170	-0.3019100	3.4324740
1	-1.1360090	0.2014410	3.1604180
1	-1.8774800	-1.3505760	3.7152470
1	-2.5395900	0.2280080	4.2835180
6	3.3969770	2.5819740	2.5864520
1	3.7266580	2.8467500	3.6037460
1	2.4327360	3.0674430	2.3618650
1	4.1577600	2.9095520	1.8569160
6	1.9404730	-1.8809480	1.0413580
1	1.2269780	-1.4160700	0.3401430
1	2.7130220	-2.4310020	0.4753420
1	1.4043090	-2.5792540	1.7062560

S-H-H-S activation Singlet
E = -4423.045987

28	-1.1884760	0.6630560	-0.0005270
28	1.1463980	0.7230060	-0.1923860
16	-0.1680850	0.6372210	-2.0473840
16	-0.0357420	2.5729890	0.4465980
1	-0.1479140	2.6922490	-0.9795680
1	-0.1946280	2.0518750	-1.8049440
6	-2.8636290	0.0081490	0.6312910
7	-3.1808480	-0.4272700	1.8871180
7	-4.0372120	-0.1151400	-0.0559920
6	-5.0486870	-0.6056180	0.7466700
6	-4.5060490	-0.8077420	1.9760750
1	-6.0533260	-0.7669130	0.3836850
1	-4.9450020	-1.1845490	2.8884550
6	2.9295850	0.1367070	0.1385990
7	4.0502550	0.8967130	0.3165620
7	3.3932820	-1.1449600	0.2371480
6	4.7547010	-1.1791070	0.4699160
6	5.1707360	0.1137930	0.5153720
1	5.3043450	-2.1023010	0.5824690
1	6.1543240	0.5334300	0.6687350
6	-4.1966090	0.2589990	-1.4497080
1	-4.7245490	-0.5331300	-1.9899470
1	-3.2001100	0.3931090	-1.8787740
1	-4.7576330	1.1958140	-1.5352710
6	-2.2305860	-0.4773120	2.9810750
1	-1.3222130	0.0372650	2.6566610
1	-1.9878310	-1.5143010	3.2379090
1	-2.6397830	0.0303430	3.8604790
6	4.0538380	2.3475570	0.2657100
1	4.6151980	2.7492640	1.1151640
1	3.0165460	2.6884860	0.3188570
1	4.5042500	2.6990060	-0.6688080
6	2.5455070	-2.3145160	0.1126890
1	1.5684350	-1.9805200	-0.2463920
1	2.9756640	-3.0174420	-0.6079840
1	2.4248410	-2.8126610	1.0809860

Full IPr Level (IPr = 1,3-di(2,6-di-*iso*-propylphenyl)imidazolin-2-ylidene)
Ni-S in plane activation Triplet
E = -4264.834126

28	6.1665250	5.9569450	11.1115460
28	4.8892520	5.7578740	8.9262700
16	6.4428930	7.2416510	9.4442910
16	5.3502550	4.0175260	10.5482960
1	4.3358260	4.2674720	9.3577970
1	3.8432220	4.7560530	8.4717020
6	7.3141890	6.1353060	12.6679990
7	7.1420590	5.6984530	13.9401770
7	8.5246830	6.7488030	12.7282990
6	9.0519590	6.7631820	14.0134830
6	8.1749010	6.0716190	14.7880720
1	9.9935170	7.2303160	14.2607470
1	8.2059880	5.8141090	15.8360460
6	4.2730950	6.7867520	7.5117440
7	3.5696880	7.9588810	7.4833260
7	4.2490930	6.3923280	6.2104780
6	3.4855040	7.2301520	5.4102740
6	3.0224300	8.2036950	6.2306840
1	3.3366770	7.0684300	4.3535540

1	2.3544790	9.0259770	6.0248510	1	6.6045120	9.8875340	8.6050630
6	9.0064040	7.5324470	11.6558140	1	5.8849790	9.0825310	7.1436980
6	9.8324250	6.9513660	10.6475030	1	6.6854910	10.6796490	7.0032950
6	8.6184300	8.8999270	11.5557550	1	4.1861680	10.4829540	5.8331060
6	10.2316060	7.7501170	9.5596780	1	4.4659680	12.1702410	6.3124770
6	9.0495170	9.6526800	10.4491600	1	2.9444640	11.3662170	6.8246900
6	9.8407460	9.0801200	9.4617830	6	7.1332640	6.2466170	5.6881040
1	10.8532320	7.3431720	8.7717030	1	6.5996550	7.0978720	6.1502410
1	8.7650320	10.6910120	10.3411000	6	7.6676620	6.7529870	4.3438460
1	10.1565980	9.6734390	8.6132760	6	8.2849310	5.8906060	6.6381600
6	6.0164160	4.9342910	14.3171260	1	7.8852950	5.4328290	7.5663690
6	4.7638120	5.5740200	14.5136440	1	8.9931450	5.1768170	6.1675870
6	6.1255400	3.5239020	14.4485990	1	8.8458400	6.8089180	6.9145810
6	3.6327160	4.7865300	14.7934060	1	8.2871990	5.9804920	3.8409620
6	4.9732320	2.7796560	14.7616710	1	8.2906170	7.6597250	4.4996470
6	3.7402200	3.4052190	14.9186850	1	6.8207060	7.0242650	3.6777080
1	2.6603110	5.2424810	14.9255680	6	2.4485230	4.0977040	5.8284960
1	5.0236580	1.7051150	14.8777780	1	2.1852380	5.0396830	6.3488080
1	2.8616810	2.8151440	15.1460890	6	1.9993000	2.9615480	6.7601770
6	4.7972060	5.1636160	5.7725510	6	1.6488170	4.0747130	4.5211030
6	6.1876200	5.0669150	5.4897660	1	1.9641830	4.9147170	3.8664460
6	3.9474980	4.0441330	5.5437710	1	1.8028310	3.1194090	3.9756170
6	6.6979240	3.8606310	4.9767940	1	0.5648610	4.1904950	4.7353540
6	4.5025000	2.8635540	5.0172530	1	2.0426600	1.9768400	6.2494560
6	5.8626380	2.7741370	4.7434120	1	0.9520480	3.1352330	7.0881840
1	7.7491470	3.7612400	4.7402080	1	2.6410520	2.9200050	7.6641610
1	3.8795460	2.0035800	4.8102890	6	10.3300400	5.5032400	10.6741530
1	6.2718830	1.8569550	4.3395680	1	10.9539680	5.3316410	9.7679010
6	3.2307340	8.6947250	8.6468080	6	9.1981450	4.4712070	10.5848430
6	3.8024050	9.9867680	8.9032610	6	11.2574990	5.2222780	11.8622670
6	2.2707680	8.1594380	9.5577530	1	11.9954650	6.0442550	11.9801950
6	3.4616690	10.6454190	10.1007950	1	10.6908520	5.1015100	12.8049030
6	1.9559710	8.8768630	10.7240810	1	11.8154680	4.2777980	11.6857460
6	2.5579430	10.0950170	10.9974480	1	8.7437230	4.2732880	11.5738990
1	3.8838370	11.6127590	10.3437020	1	9.6012910	3.5048140	10.2135120
1	1.2331870	8.4935300	11.4322460	1	8.4129730	4.8109840	9.8786270
1	2.3070070	10.6280630	11.9056530	6	7.7375190	9.5710450	12.6080280
6	1.5252370	6.8542150	9.2866290	1	7.4813910	8.8636190	13.4194470
1	1.8741210	6.3836020	8.3498090	6	6.4020090	10.0335930	12.0105720
6	0.0262960	7.1079420	9.0858460	6	8.4725930	10.7370840	13.2798070
6	1.7621240	5.8327770	10.4072610	1	9.4395510	10.3847030	13.6987010
1	2.8464290	5.7472740	10.6233080	1	8.6698750	11.5588620	12.5596970
1	1.2398710	6.1280860	11.3414350	1	7.8608310	11.1416170	14.1143400
1	1.3866470	4.8344140	10.0963720	1	6.5525610	10.8041720	11.2256670
1	-0.4452790	7.4998820	10.0116480	1	5.7571420	10.4639400	12.8062370
1	-0.4844120	6.1621580	8.8041510	1	5.8635160	9.1702310	11.5687190
1	-0.1268620	7.8420820	8.2659530	6	7.4573090	2.8005760	14.2655610
6	4.7286070	10.7565630	7.9479860	1	8.2557780	3.5116240	13.9734540
1	5.0323530	11.7044720	8.4478530	6	7.3868620	1.7618630	13.1390500
6	4.0311100	11.2070700	6.6566400	6	7.9109510	2.1547690	15.5797150
6	6.0498980	10.0459390	7.6582180	1	7.9671900	2.9235330	16.3800320

1	7.2087210	1.3553730	15.8978620	6	4.9956760	2.7723600	14.6663460
1	8.9210110	1.7088870	15.4563200	6	3.7563680	3.3875470	14.8180000
1	6.6852550	0.9385860	13.3884610	1	2.6629960	5.2177640	14.8321360
1	8.3926590	1.3234390	12.9645390	1	5.0551130	1.6980280	14.7806460
1	7.0562860	2.2444470	12.1965950	1	2.8815620	2.7895510	15.0389560
6	4.6224680	7.0909900	14.4381550	6	4.7913080	5.1376620	5.8728100
1	5.6115530	7.5703170	14.2971950	6	6.1839400	5.0064940	5.6210650
6	4.0630060	7.6698320	15.7441290	6	3.9247740	4.0265480	5.6678510
6	3.7630000	7.5026250	13.2406380	6	6.6881240	3.7622070	5.2019770
1	4.2091380	7.1138720	12.3005570	6	4.4710960	2.8120460	5.2141240
1	2.7269370	7.1152070	13.3370050	6	5.8385210	2.6805840	4.9981080
1	3.7223440	8.6097580	13.1722010	1	7.7452370	3.6296340	5.0124120
1	3.0123070	7.3527650	15.9114030	1	3.8369790	1.9560590	5.0254980
1	4.0900940	8.7801050	15.7083410	1	6.2420060	1.7350420	4.6590810
1	4.6826270	7.3361850	16.6038770	6	3.3009350	8.7525260	8.6757170
				6	3.9175550	10.0196000	8.9441370
Ni-S in plane activation Singlet				6	2.2916780	8.2607640	9.5568950
E = -4264.828073				6	3.5547580	10.7074450	10.1181360
28	6.2902410	5.5507590	11.1118060	6	1.9656130	8.9995680	10.7066740
28	4.8755160	5.7550070	9.0041910	6	2.5992150	10.2005750	10.9870700
16	6.2141250	7.2275400	9.8346470	1	4.0070220	11.6594740	10.3672100
16	5.4032200	3.7714890	10.2764120	1	1.2091150	8.6470860	11.3954180
1	4.2186670	4.2367730	9.3266080	1	2.3369050	10.7519420	11.8809580
1	3.7450130	4.8320960	8.5339250	6	1.5121910	6.9783790	9.2717230
6	7.3335490	6.1056910	12.5647930	1	1.8607560	6.5003070	8.3385020
7	7.1392750	5.7090490	13.8515930	6	0.0240190	7.2743470	9.0486860
7	8.5171170	6.7774200	12.6423580	6	1.7038920	5.9478110	10.3926010
6	9.0053890	6.8441890	13.9430410	1	2.7840220	5.8089360	10.6056700
6	8.1317380	6.1476450	14.7142500	1	1.1974260	6.2685130	11.3269940
1	9.9200950	7.3561850	14.2021620	1	1.2809770	4.9681100	10.0831400
1	8.1396830	5.9262830	15.7707630	1	-0.4529950	7.6696130	9.9701720
6	4.3076560	6.8061070	7.5798170	1	-0.5069210	6.3452380	8.7493770
7	3.6461640	8.0008190	7.5252690	1	-0.0958140	8.0197390	8.2334170
7	4.2654080	6.3839640	6.2863400	6	4.9309640	10.7227190	8.0279690
6	3.5373830	7.2325920	5.4670790	1	5.2450290	11.6714640	8.5197240
6	3.1093640	8.2396620	6.2662260	6	4.3348890	11.1607330	6.6833530
1	3.3858190	7.0547530	4.4133310	6	6.2324640	9.9432070	7.8406930
1	2.4838680	9.0896640	6.0396870	1	6.7165500	9.7853670	8.8242890
6	8.9941630	7.5766850	11.5794250	1	6.0550240	8.9710580	7.3476130
6	9.8143200	7.0089410	10.5593540	1	6.9380910	10.5261300	7.2108770
6	8.6336370	8.9555160	11.5174590	1	4.4834190	10.3919180	5.9002410
6	10.2118540	7.8230300	9.4829100	1	4.8517500	12.0773960	6.3259750
6	9.0815890	9.7282490	10.4318370	1	3.2542860	11.3976510	6.7855300
6	9.8452550	9.1618290	9.4196040	6	7.1391130	6.1868330	5.7620910
1	10.8281570	7.4258120	8.6858740	1	6.5901280	7.0970260	6.0692760
1	8.8331050	10.7788090	10.3597490	6	7.8041050	6.5286270	4.4231590
1	10.1693530	9.7702200	8.5850200	6	8.1888080	5.9222140	6.8463610
6	6.0212960	4.9360410	14.2296910	1	7.6855030	5.6407240	7.7930590
6	4.7648550	5.5660350	14.4270780	1	8.8783210	5.1034980	6.5512250
6	6.1437580	3.5277190	14.3649050	1	8.7863230	6.8405470	7.0280250
6	3.6387660	4.7691090	14.6998610	1	8.4683950	5.7077510	4.0800550

1	8.4130980	7.4521380	4.5270770	1	4.6886700	7.3132250	16.5308000
1	7.0275230	6.7108090	3.6496580				
6	2.4185340	4.1246370	5.8978560	Ni-S above plane activation Triplet			
1	2.1612440	5.0888130	6.3790280	E = -4264.806751			
6	1.9060980	3.0296450	6.8464240	28	5.8174530	6.1779680	11.4094300
6	1.6660540	4.0799940	4.5633500	28	4.3355320	6.1843120	9.3842860
1	2.0236150	4.8933240	3.8967240	16	3.9127050	7.1147440	11.3205510
1	1.8186790	3.1057900	4.0518330	16	6.3298670	4.9885380	9.6382560
1	0.5778810	4.2251470	4.7340770	1	4.8805460	4.4908280	9.4253270
1	1.9339730	2.0297760	6.3649380	1	3.6796510	4.7204230	9.2569370
1	0.8550570	3.2441530	7.1359440	6	7.3019210	6.1205610	12.5827500
1	2.5176110	2.9941170	7.7711120	7	7.1896880	5.6899790	13.8683570
6	10.3433110	5.5718750	10.5851110	7	8.6015610	6.5433840	12.5231120
1	10.9428370	5.4029870	9.6620610	6	9.2287310	6.4738680	13.7639110
6	9.2389200	4.5072640	10.5489620	6	8.3424660	5.8946100	14.6110920
6	11.3133030	5.3360240	11.7485520	1	10.2395320	6.8121100	13.9361150
1	12.0707410	6.1477530	11.7885560	1	8.4328900	5.6251270	15.6525910
1	10.7831970	5.2870820	12.7188930	6	4.0869380	6.8449630	7.5601300
1	11.8454070	4.3714340	11.6039160	7	3.4910880	8.0281640	7.2482440
1	8.8628740	4.2726480	11.5631820	7	4.2941260	6.2882000	6.3424730
1	9.6434510	3.5617790	10.1284910	6	3.7964030	7.0615470	5.3033630
1	8.3964270	4.8356550	9.9079650	6	3.2599660	8.1664720	5.8856990
6	7.7927430	9.6266910	12.6041530	1	3.8680300	6.7748970	4.2649240
1	7.4671550	8.8914320	13.3635010	1	2.7580430	9.0176540	5.4507150
6	6.5019060	10.2382510	12.0414260	6	9.0898240	7.3232050	11.4470220
6	8.6158240	10.6827620	13.3506370	6	9.9691440	6.7587810	10.4700300
1	9.5406170	10.2228850	13.7603790	6	8.7143810	8.6958070	11.3478630
1	8.8978890	11.5204770	12.6783250	6	10.3492880	7.5504180	9.3698930
1	8.0287040	11.0938790	14.1995210	6	9.1353780	9.4416360	10.2339690
1	6.7146560	11.0439280	11.3084610	6	9.9239830	8.8668010	9.2474780
1	5.8946010	10.6688400	12.8660780	1	10.9928570	7.1518350	8.5953660
1	5.8900580	9.4558890	11.5509110	1	8.8587100	10.4823820	10.1278210
6	7.4872570	2.8206820	14.2056630	1	10.2322120	9.4556740	8.3930440
1	8.2838230	3.5438490	13.9381210	6	5.9660420	5.2223430	14.4018090
6	7.4519550	1.7902830	13.0704870	6	5.1526460	6.0837150	15.1912340
6	7.9210340	2.1696630	15.5241760	6	5.5600560	3.8801060	14.1696830
1	7.9486240	2.9319570	16.3321560	6	3.9444430	5.5882960	15.7149010
1	7.2241820	1.3571000	15.8198520	6	4.3472370	3.4283690	14.7208160
1	8.9400070	1.7394770	15.4193290	6	3.5476260	4.2770120	15.4779580
1	6.7472320	0.9624980	13.2951110	1	3.3052230	6.2168260	16.3208540
1	8.4640770	1.3578140	12.9192380	1	4.0173680	2.4088530	14.5704570
1	7.1446340	2.2793270	12.1237850	1	2.6171760	3.9121080	15.8937460
6	4.6169980	7.0830180	14.3640250	6	4.9559560	5.0496630	6.1786570
1	5.6035210	7.5674440	14.2215240	6	6.3529780	5.0199690	5.9133980
6	4.0610490	7.6481270	15.6773350	6	4.2205480	3.8349960	6.2596960
6	3.7521120	7.5026800	13.1740280	6	6.9997980	3.7750680	5.8139980
1	4.1893220	7.1121060	12.2310900	6	4.9026820	2.6153690	6.0956030
1	2.7141350	7.1225690	13.2777390	6	6.2800870	2.5884910	5.9036650
1	3.7203190	8.6102860	13.1073650	1	8.0656030	3.7183170	5.6358730
1	3.0141380	7.3207600	15.8487320	1	4.3707980	1.6741300	6.1132870
1	4.0789200	8.7587960	15.6494810	1	6.7906870	1.6399190	5.7974660

6	2.9180300	8.8370450	8.2561920	6	9.5472240	4.2421910	10.3776030
6	3.6636910	9.9022530	8.8446920	6	11.4310740	5.1382320	11.8128060
6	1.6228640	8.5186510	8.7550080	1	11.9512370	6.0755220	12.1047620
6	3.1077110	10.5929390	9.9373490	1	10.8206050	4.7649180	12.6578990
6	1.1123330	9.2445650	9.8454880	1	12.2043790	4.3657960	11.6121620
6	1.8515570	10.2636590	10.4322260	1	8.7877670	4.2620910	11.1817210
1	3.6462070	11.4038770	10.4122430	1	10.0491430	3.2512880	10.4009000
1	0.1365500	9.0167820	10.2538400	1	9.0566260	4.3466440	9.3879930
1	1.4441880	10.8087770	11.2740670	6	7.9239130	9.4028290	12.4472370
6	0.7771760	7.4011600	8.1485050	1	7.6763460	8.7021960	13.2633160
1	1.2918890	6.9406930	7.2836990	6	6.5891920	9.9474180	11.9273190
6	-0.5513180	7.9411920	7.6046860	6	8.7552190	10.5182520	13.0928850
6	0.5415530	6.2731810	9.1599890	1	9.7197360	10.1076750	13.4613710
1	1.5134750	5.8968060	9.5418590	1	8.9640330	11.3357420	12.3709740
1	-0.0700780	6.6226840	10.0182570	1	8.2080540	10.9467480	13.9598940
1	0.0128540	5.4276170	8.6701880	1	6.7438140	10.7351450	11.1613140
1	-1.1992110	8.3215960	8.4220850	1	6.0029270	10.3831370	12.7641700
1	-1.0986470	7.1347700	7.0712130	1	5.9943270	9.1243710	11.4862490
1	-0.3592110	8.7646930	6.8839140	6	6.4215490	2.9074360	13.3708690
6	5.0256100	10.3794700	8.3370140	1	7.3069150	3.4232060	12.9494880
1	5.4207510	11.1394510	9.0478480	6	5.6498540	2.3239590	12.1795320
6	4.9068250	11.1024910	6.9914300	6	6.9636860	1.7922980	14.2719060
6	6.0904840	9.2780280	8.2892090	1	7.5373120	2.2327410	15.1155150
1	6.0102090	8.6045220	9.1672710	1	6.1396210	1.1717700	14.6835000
1	6.0077920	8.6839280	7.3629220	1	7.6471320	1.1343990	13.6935790
1	7.1006680	9.7369500	8.2862290	1	4.8687900	1.6093710	12.5143710
1	4.6662120	10.4002500	6.1715190	1	6.3476930	1.7871290	11.5018960
1	5.8693640	11.5998800	6.7451690	1	5.1601630	3.1372860	11.6054010
1	4.1170180	11.8821120	7.0433420	6	5.5624890	7.5198010	15.5065080
6	7.1567940	6.2969460	5.6817020	1	6.5162860	7.7724080	15.0096870
1	6.4968310	7.1835250	5.7208200	6	5.7996300	7.7048660	17.0099780
6	7.7839280	6.3090090	4.2814800	6	4.5344200	8.5311480	14.9847570
6	8.2265580	6.4976930	6.7618800	1	4.3866190	8.3939540	13.8946450
1	7.7485490	6.5933650	7.7571650	1	3.5570070	8.4196230	15.4989140
1	8.9455470	5.6519900	6.7841050	1	4.9020750	9.5662060	15.1519070
1	8.7904340	7.4354630	6.5700030	1	4.8592170	7.5712160	17.5852360
1	8.5633020	5.5247260	4.1803880	1	6.1931450	8.7243700	17.2104670
1	8.2544680	7.2960700	4.0844830	1	6.5493170	6.9677160	17.3693320
1	6.9999150	6.1404900	3.5123060				
6	2.7026260	3.8359360	6.4242910	Ni-S above plane activation Singlet			
1	2.3654630	4.8137310	6.8222780	E = -4264.813028			
6	2.2075620	2.7792450	7.4262370	28	6.1746430	6.0761140	11.0541740
6	2.0251430	3.6472670	5.0638090	28	4.2557740	6.1249410	9.3959320
1	2.3403110	4.4525800	4.3663900	16	4.1639090	6.7454210	11.4816810
1	2.2960520	2.6645970	4.6213660	16	6.0804030	4.5776540	9.4148080
1	0.9209550	3.6985110	5.1758600	1	4.5287530	4.3860080	9.3607740
1	2.2458730	1.7583260	6.9914130	1	3.4021370	4.7923850	9.2712110
1	1.1532230	2.9915650	7.7053000	6	7.4023600	6.1918130	12.5483870
1	2.8205310	2.7921230	8.3502300	7	7.2010420	5.7710620	13.8223420
6	10.5793990	5.3547340	10.5551590	7	8.6907500	6.6467800	12.5838600
1	11.2873430	5.2275870	9.7048240	6	9.2384580	6.5809550	13.8618300

6	8.2980470	5.9924320	14.6423610	1	-0.2468040	6.7626240	9.9596390
1	10.2358370	6.9212600	14.0969960	1	-0.0919360	5.5400240	8.6445500
1	8.3185750	5.7226220	15.6874960	1	-1.1243390	8.5447270	8.3233910
6	4.0868350	6.8075410	7.5661590	1	-1.0575790	7.3182970	7.0044300
7	3.5294410	8.0191260	7.2876600	1	-0.1912660	8.8842460	6.8131390
7	4.2800380	6.2834840	6.3317260	6	5.1621800	10.2517700	8.4751780
6	3.8051400	7.1018470	5.3162850	1	5.5553680	11.0192190	9.1785420
6	3.2991360	8.2038080	5.9298380	6	5.1290260	10.9395250	7.1059230
1	3.8686860	6.8431990	4.2698820	6	6.1843070	9.1106930	8.5071420
1	2.8285640	9.0850110	5.5200960	1	6.0471950	8.4752900	9.4061940
6	9.2118920	7.4560320	11.5476840	1	6.1086010	8.4831320	7.6042710
6	10.0588590	6.8982520	10.5425990	1	7.2110920	9.5301260	8.5225070
6	8.8635670	8.8376320	11.4923430	1	4.9516110	10.2159930	6.2886420
6	10.4713040	7.7185210	9.4761550	1	6.1041680	11.4355400	6.9118810
6	9.3027860	9.6101700	10.4035870	1	4.3347090	11.7159500	7.0839560
6	10.0869730	9.0515840	9.4031160	6	7.1499610	6.2882840	5.7075810
1	11.0962400	7.3248550	8.6840370	1	6.5006410	7.1801840	5.7868610
1	9.0365540	10.6559890	10.3237740	6	7.7996260	6.3725480	4.3202840
1	10.4112860	9.6611640	8.5694590	6	8.2040910	6.4099740	6.8149780
6	5.9628640	5.2588560	14.2790280	1	7.7128930	6.4132650	7.8095690
6	5.0799490	6.0870560	15.0297620	1	8.9322180	5.5728780	6.7727570
6	5.6415600	3.8901040	14.0677480	1	8.7593750	7.3664750	6.7095940
6	3.8846460	5.5350240	15.5254230	1	8.5698910	5.5844910	4.1850370
6	4.4386670	3.3822060	14.5911800	1	8.2866980	7.3624890	4.1888760
6	3.5672160	4.2003600	15.3007710	1	7.0257680	6.2604490	3.5308170
1	3.1989760	6.1336780	16.1100920	6	2.6658840	3.8444530	6.3353030
1	4.1761540	2.3402900	14.4641900	1	2.3360980	4.8206930	6.7439190
1	2.6475760	3.7908550	15.6987370	6	2.1874490	2.7815160	7.3380940
6	4.9298400	5.0453480	6.1224000	6	1.9662880	3.6669080	4.9845150
6	6.3266540	5.0115080	5.8558040	1	2.2750590	4.4752770	4.2875820
6	4.1808140	3.8371950	6.1492170	1	2.2243820	2.6856220	4.5315860
6	6.9577600	3.7652210	5.6925330	1	0.8643000	3.7231710	5.1143930
6	4.8472370	2.6187180	5.9242530	1	2.2194240	1.7634130	6.8962450
6	6.2233540	2.5845850	5.7241600	1	1.1382600	2.9922310	7.6371310
1	8.0232150	3.7041850	5.5138960	1	2.8176720	2.7885290	8.2506490
1	4.3031840	1.6843310	5.9024770	6	10.5698390	5.4553280	10.5504610
1	6.7220430	1.6360770	5.5712480	1	11.3160470	5.3419250	9.7316280
6	2.9838690	8.8169000	8.3193290	6	9.4665950	4.4457880	10.2329530
6	3.7670570	9.8339840	8.9435270	6	11.3235290	5.0830340	11.8337680
6	1.6696750	8.5436120	8.7947790	1	11.9284590	5.9409840	12.1974000
6	3.2249490	10.5255640	10.0426030	1	10.6301540	4.7479590	12.6299000
6	1.1713510	9.2748940	9.8872760	1	12.0139890	4.2367930	11.6292700
6	1.9457480	10.2465000	10.5076630	1	8.6976860	4.4225020	11.0265910
1	3.7924510	11.2987240	10.5459800	1	9.8994640	3.4267930	10.1410170
1	0.1768900	9.0882470	10.2706870	1	8.9910230	4.7037340	9.2647720
1	1.5481850	10.7941050	11.3525810	6	8.0517650	9.5141430	12.5954510
6	0.7859000	7.4745850	8.1564470	1	7.8368680	8.8047960	13.4126610
1	1.3133040	6.9695350	7.3246230	6	6.6932630	9.9990080	12.0787790
6	-0.4744830	8.0957240	7.5429610	6	8.8366300	10.6629720	13.2418090
6	0.4239340	6.3759130	9.1638350	1	9.8261460	10.2976300	13.5910160
1	1.3438090	5.9747290	9.6374320	1	8.9916480	11.4996420	12.5287270

1	8.2819790	11.0531690	14.1220340	6	-3.4472300	0.5075940	-3.0875000
1	6.8159460	10.7614960	11.2821360	6	-3.5181700	-0.7084340	-3.7526420
1	6.1070240	10.4480520	12.9086360	1	-3.8531790	-2.8000500	-3.6059500
1	6.1135490	9.1417480	11.6802390	1	-3.2693530	1.3998460	-3.6755280
6	6.5977200	2.9433610	13.3496230	1	-3.3993300	-0.7421770	-4.8281400
1	7.4305000	3.5082390	12.8867990	6	-2.8049710	-0.9370880	3.7206850
6	5.9005040	2.1874520	12.2094450	6	-2.3029660	-2.2483950	3.9761770
6	7.2355120	1.9659870	14.3426150	6	-2.6039890	0.0968800	4.6891100
1	7.7683130	2.5292030	15.1386790	6	-1.5589130	-2.4819700	5.1453370
1	6.4669080	1.3178660	14.8151470	6	-1.8266860	-0.1883700	5.8275770
1	7.9738060	1.3200430	13.8209350	6	-1.3040820	-1.4567610	6.0448280
1	5.2293470	1.3937570	12.5999280	1	-1.1777320	-3.4686300	5.3722060
1	6.6586250	1.7091920	11.5529150	1	-1.6303170	0.5750350	6.5702650
1	5.2958680	2.8874100	11.5975320	1	-0.7195850	-1.6539990	6.9343830
6	5.4213440	7.5369670	15.3642920	6	3.9480010	1.7393730	1.0345150
1	6.3491740	7.8445130	14.8495060	6	3.8369280	2.6565830	-0.0641270
6	5.6809700	7.6984750	16.8665360	6	3.8974970	2.2507660	2.3771040
6	4.3357670	8.5136400	14.8919270	6	3.5056420	3.9977140	0.2047620
1	4.1622740	8.3992960	13.8038470	6	3.5661110	3.6042050	2.5723770
1	3.3785850	8.3518150	15.4296850	6	3.3487690	4.4556200	1.5021830
1	4.6636100	9.5593960	15.0743180	1	3.3806540	4.7130090	-0.5989540
1	4.7618320	7.4940220	17.4556290	1	3.4783110	4.0163370	3.5703690
1	6.0191690	8.7337490	17.0859550	1	3.0952650	5.4928770	1.6810730
1	6.4791380	6.9976480	17.1922200	6	3.0047970	-2.9503940	0.4544660
				6	2.6378750	-3.6578500	1.6318550
Ni-Ni activation Triplet				6	2.7110280	-3.5003960	-0.8236730
E = -4264.766453				6	1.9018930	-4.8500480	1.5093420
28	-1.1054190	-0.2991660	0.8931280	6	1.9770110	-4.6987620	-0.8968020
28	1.1620890	-0.3091610	0.6384080	6	1.5621560	-5.3531720	0.2583040
16	-0.3971770	-2.0034100	-0.1129080	1	1.5973770	-5.4042020	2.3874560
16	0.1403500	0.4407530	2.4501010	1	1.7314220	-5.1395600	-1.8538720
1	0.1366690	0.3675990	-0.2324240	1	0.9966080	-6.2730490	0.1832550
1	1.2737040	-0.1750240	-0.8168850	6	4.2230500	1.4542830	3.6495520
6	-2.9440830	-0.5300780	1.3229280	1	4.3689100	2.1798050	4.4824070
7	-3.5437770	-0.6911640	2.5367160	6	5.5439920	0.6771490	3.5986010
7	-3.9904450	-0.5828940	0.4540080	6	3.0623880	0.5742380	4.1021310
6	-5.1962570	-0.8473170	1.0953940	1	2.1798410	1.2077430	4.3305000
6	-4.9041110	-0.9479980	2.4152060	1	2.7969460	-0.1561030	3.3211650
1	-6.1385580	-0.9300230	0.5755570	1	3.3343710	0.0216390	5.0268680
1	-5.5470130	-1.1408270	3.2610050	1	5.3947440	-0.3488100	3.2094770
6	3.0599230	-0.5284770	0.7272070	1	5.9527510	0.5658360	4.6261320
7	4.1073810	0.3502900	0.7963300	1	6.2986200	1.2198210	2.9908260
7	3.6961300	-1.7209270	0.5558480	6	4.1271600	2.3165550	-1.5326820
6	5.0751410	-1.6022490	0.5092830	1	4.0309320	3.2505000	-2.1318980
6	5.3373380	-0.2801000	0.6528200	6	3.1093810	1.3616770	-2.1502490
1	5.7387300	-2.4439620	0.3812670	6	5.5691860	1.8482890	-1.7742200
1	6.2795420	0.2463710	0.6823640	1	6.2710820	2.3515030	-1.0753100
6	-3.8180840	-0.6183890	-0.9526220	1	5.6669160	0.7502350	-1.6766690
6	-3.9123040	-1.8633310	-1.6496370	1	5.8764530	2.1030780	-2.8113800
6	-3.6170660	0.5889040	-1.6932480	1	3.2633540	0.3327330	-1.7850000
6	-3.7664930	-1.8773230	-3.0481380	1	3.2300310	1.3446830	-3.2546860

1	2.0781790	1.7049220	-1.9223600	6	-4.2284480	-3.1786020	-0.9382770
6	3.0736810	-3.1908030	3.0169940	1	-4.1868670	-3.0470810	0.1562850
1	3.6596000	-2.2547930	2.9435190	6	-3.2118040	-4.2836480	-1.2634580
6	4.0058850	-4.2151570	3.6750940	6	-5.6504200	-3.6432710	-1.2745390
6	1.8681670	-2.8927260	3.9165880	1	-6.3837380	-2.8497220	-1.0185000
1	1.1849480	-2.1777760	3.4142170	1	-5.7468780	-3.8813050	-2.3552960
1	1.3074310	-3.8193240	4.1579860	1	-5.9038920	-4.5515090	-0.6869330
1	2.2081600	-2.4342150	4.8694000	1	-3.3069560	-4.6306670	-2.3133940
1	3.4766120	-5.1696760	3.8798080	1	-3.3781760	-5.1562800	-0.5959600
1	4.3921760	-3.8142430	4.6366400	1	-2.1781950	-3.9232460	-1.1012230
1	4.8734880	-4.4195910	3.0116680				
6	3.2148090	-2.8556350	-2.1113840	Ni-Ni activation Singlet			
1	3.7527390	-1.9142280	-1.8905340	E = -4264.763033			
6	2.0627450	-2.4876390	-3.0556600	28	-1.1172610	-0.3448540	0.8129690
6	4.2265110	-3.7676400	-2.8154560	28	1.1630880	-0.2765210	0.5732670
1	5.0585380	-4.0172820	-2.1224900	16	-0.3486450	-2.0515350	-0.1487860
1	3.7484910	-4.7099850	-3.1573860	16	0.0961760	0.4319980	2.3599460
1	4.6561380	-3.2492220	-3.6992450	1	0.0608080	0.2627830	-0.3247630
1	1.5340310	-3.3921580	-3.4224530	1	1.3503980	-0.1696710	-0.8736100
1	2.4562840	-1.9323980	-3.9338050	6	-2.9458750	-0.5302300	1.3291250
1	1.3341690	-1.8327220	-2.5376150	7	-3.5282440	-0.7270310	2.5473690
6	-2.6184630	-3.4277140	3.0591500	7	-4.0119400	-0.5327320	0.4796580
1	-3.0780080	-3.0741850	2.1212040	6	-5.2080200	-0.8085880	1.1320660
6	-3.6363260	-4.3646380	3.7173040	6	-4.8931680	-0.9635960	2.4405200
6	-1.3588270	-4.1984330	2.6439380	1	-6.1605700	-0.8590240	0.6269470
1	-0.5777240	-3.4929640	2.3009120	1	-5.5232200	-1.1839400	3.2891850
1	-0.9534720	-4.8002620	3.4837680	6	3.0596740	-0.5151030	0.7145090
1	-1.5952570	-4.8892550	1.8063440	7	4.1115560	0.3615570	0.7950160
1	-3.2222230	-4.8142100	4.6449390	7	3.6987390	-1.7110850	0.5749810
1	-3.9109000	-5.1820440	3.0165620	6	5.0783630	-1.5963600	0.5583290
1	-4.5598340	-3.8019710	3.9724690	6	5.3415660	-0.2743980	0.6899960
6	-3.2068140	1.5034420	4.5981900	1	5.7414660	-2.4418350	0.4552560
1	-2.9838880	2.0445480	5.5456630	1	6.2843340	0.2497850	0.7362840
6	-4.7373680	1.5052100	4.4940880	6	-3.8766970	-0.5097280	-0.9309480
6	-2.5674100	2.3496210	3.4973510	6	-4.0010390	-1.7233630	-1.6757670
1	-1.4823700	2.4713920	3.6951090	6	-3.6922880	0.7264770	-1.6264850
1	-2.7100210	1.8855960	2.5075590	6	-3.9066580	-1.6791020	-3.0781190
1	-3.0246650	3.3620250	3.4784330	6	-3.5736900	0.7037370	-3.0283290
1	-5.0730270	1.4223300	3.4421060	6	-3.6775610	-0.4824800	-3.7413530
1	-5.1373930	2.4661700	4.8831760	1	-4.0182870	-2.5774220	-3.6703410
1	-5.1747850	0.6821340	5.0985410	1	-3.4107750	1.6190570	-3.5843360
6	-3.6018420	1.9938820	-1.0849830	1	-3.5969240	-0.4714350	-4.8207590
1	-3.7763110	2.7262680	-1.9059440	6	-2.7828240	-1.0133380	3.7183170
6	-2.2277380	2.3500200	-0.5130880	6	-2.2940110	-2.3365110	3.9331180
6	-4.7352560	2.2635330	-0.0852070	6	-2.5750620	-0.0127270	4.7206860
1	-5.6884010	1.8261490	-0.4514980	6	-1.5581780	-2.6151000	5.0976220
1	-4.5040340	1.8611880	0.9189640	6	-1.7994550	-0.3405540	5.8487710
1	-4.8802380	3.3591580	0.0295480	6	-1.2918570	-1.6207380	6.0277150
1	-1.9595290	1.6953930	0.3314620	1	-1.1914780	-3.6130410	5.2967510
1	-2.2230400	3.4021630	-0.1565120	1	-1.5968000	0.3966990	6.6157420
1	-1.4503550	2.2466410	-1.3000940	1	-0.7109430	-1.8517500	6.9115210

6	3.9619230	1.7556100	1.0059510	6	4.3065850	-3.8020950	-2.7592520
6	3.8945250	2.6567840	-0.1091680	1	5.1290600	-4.0378220	-2.0501020
6	3.8735530	2.2878220	2.3382350	1	3.8414070	-4.7515560	-3.0986970
6	3.5642210	4.0041890	0.1288700	1	4.7469380	-3.2903700	-3.6417320
6	3.5452330	3.6461400	2.5027660	1	1.6185380	-3.4557430	-3.4089450
6	3.3679650	4.4825300	1.4135690	1	2.5400860	-1.9981320	-3.9290100
1	3.4717300	4.7083020	-0.6890530	1	1.3973620	-1.8839020	-2.5508200
1	3.4294740	4.0738390	3.4914070	6	-2.6200400	-3.4827060	2.9786840
1	3.1146190	5.5234450	1.5686250	1	-3.0600340	-3.0936180	2.0448770
6	3.0182750	-2.9464300	0.4808140	6	-3.6640260	-4.4174410	3.5976260
6	2.6411940	-3.6418740	1.6619000	6	-1.3698220	-4.2655590	2.5575380
6	2.7577810	-3.5211230	-0.7938390	1	-0.5702960	-3.5648440	2.2488460
6	1.9287130	-4.8490140	1.5442020	1	-0.9881200	-4.9014010	3.3834850
6	2.0432300	-4.7315590	-0.8620530	1	-1.6072940	-4.9246940	1.6950770
6	1.6194420	-5.3761230	0.2951760	1	-3.2712920	-4.8982880	4.5188210
1	1.6179340	-5.3953010	2.4251270	1	-3.9435960	-5.2110420	2.8719810
1	1.8214340	-5.1898290	-1.8168500	1	-4.5807270	-3.8447780	3.8549770
1	1.0699630	-6.3057720	0.2241210	6	-3.1744840	1.3980940	4.6819380
6	4.1597570	1.5101080	3.6316610	1	-2.9401110	1.9073350	5.6442370
1	4.2876380	2.2480960	4.4564230	6	-4.7062330	1.4079970	4.5958880
6	5.4772750	0.7255830	3.6283340	6	-2.5443600	2.2795310	3.6039900
6	2.9825040	0.6435440	4.0669910	1	-1.4575510	2.3941410	3.7970620
1	2.0955840	1.2845090	4.2542060	1	-2.6957220	1.8477830	2.6009790
1	2.7386770	-0.1032280	3.2944140	1	-3.0013520	3.2920840	3.6220150
1	3.2244430	0.1101490	5.0112090	1	-5.0545100	1.3661340	3.5457680
1	5.3336260	-0.3043750	3.2481130	1	-5.0990060	2.3546990	5.0253620
1	5.8565170	0.6254250	4.6682210	1	-5.1395330	0.5643160	5.1742800
1	6.2517450	1.2561830	3.0349530	6	-3.6425910	2.1032610	-0.9591700
6	4.2338780	2.2934940	-1.5614670	1	-3.8217920	2.8739870	-1.7431030
1	4.1596570	3.2179330	-2.1781980	6	-2.2518930	2.4136080	-0.4007110
6	3.2363960	1.3299160	-2.1981980	6	-4.7521580	2.3436720	0.0740630
6	5.6829140	1.8204500	-1.7458850	1	-5.7191570	1.9386470	-0.2932670
1	6.3603890	2.3278810	-1.0263000	1	-4.5092580	1.8907830	1.0533410
1	5.7748250	0.7231260	-1.6359630	1	-4.8769060	3.4347290	0.2427650
1	6.0290020	2.0654070	-2.7732980	1	-1.9738310	1.7151180	0.4045660
1	3.3716050	0.3082750	-1.8062550	1	-2.2251720	3.4471240	0.0059210
1	3.3994470	1.2903660	-3.2967260	1	-1.4930300	2.3383080	-1.2087350
1	2.1986810	1.6810080	-2.0163370	6	-4.2935400	-3.0660460	-1.0079090
6	3.0408530	-3.1455440	3.0475110	1	-4.2054330	-2.9805030	0.0889210
1	3.6136610	-2.2019780	2.9705120	6	-3.2942620	-4.1567020	-1.4224800
6	3.9742660	-4.1440150	3.7424160	6	-5.7303080	-3.5126650	-1.3044570
6	1.8117600	-2.8516680	3.9155740	1	-6.4495430	-2.7303470	-0.9830380
1	1.1294950	-2.1551060	3.3866050	1	-5.8731950	-3.7014460	-2.3895880
1	1.2590450	-3.7827870	4.1584980	1	-5.9625460	-4.4457480	-0.7478200
1	2.1238700	-2.3729380	4.8681430	1	-3.4476700	-4.4714970	-2.4760370
1	3.4555920	-5.1028570	3.9529320	1	-3.4222540	-5.0503280	-0.7743340
1	4.3342310	-3.7206500	4.7047510	1	-2.2541480	-3.7954230	-1.3077800
1	4.8587380	-4.3462480	3.1009520				
6	3.2769210	-2.8896010	-2.0822150	Ni-C activation Triplet			
1	3.8043800	-1.9418650	-1.8652660	No convergence to local minimum			
6	2.1368400	-2.5426590	-3.0485580				

Ni-C activation Singlet				1	2.5323890	3.6553580	-4.1230430
No convergence to local minimum				1	1.6098910	4.0340330	-8.2353540
				1	2.7719740	4.8056890	-6.2471110
S-H-H-S activation Singlet				6	-3.2632800	-1.2789170	-5.3807550
No convergence to local minimum, but will				6	-4.2876530	-1.1872110	-6.3611910
converge if H-H distance is frozen				6	-3.5558880	-1.8103640	-4.0959480
E = -4264.836257				6	-5.5869390	-1.6152130	-6.0325280
28	-2.7715730	1.9175790	-5.0317510	6	-4.8669390	-2.2366560	-3.8158810
28	-2.6730090	4.0665620	-3.3396980	6	-5.8697470	-2.1349440	-4.7739520
16	-1.8213760	4.1075860	-5.4861100	1	-6.3900520	-1.5498290	-6.7547620
16	-4.6858510	3.0634210	-4.4511560	1	-5.1203180	-2.6455640	-2.8465810
1	-3.8799610	3.8540070	-5.2824130	1	-6.8745220	-2.4622310	-4.5392920
1	-3.1510970	4.3324870	-5.8597520	6	-0.0804490	1.9881340	-8.5787770
6	-1.6226770	0.5017550	-5.5772780	1	0.3589790	2.5998010	-9.3993220
7	-1.9614400	-0.8180380	-5.6722590	6	-1.5587720	2.3846010	-8.5446750
7	-0.3101630	0.4825930	-5.9514350	6	0.1147560	0.5400000	-9.0418090
6	0.1523130	-0.7991240	-6.2304030	1	1.1392860	0.1850510	-8.8015560
6	-0.9053820	-1.6320020	-6.0531960	1	-0.6413480	-0.1336750	-8.5959720
1	1.1693380	-1.0128800	-6.5209690	1	-0.0175910	0.4785170	-10.1435090
1	-0.9942420	-2.6976140	-6.1966500	1	-2.0961300	1.8797290	-7.7240710
6	-2.9892040	4.8286280	-1.6112770	1	-2.0500010	2.1187540	-9.5050540
7	-4.1370720	5.4767710	-1.2388600	1	-1.6513780	3.4824120	-8.4063160
7	-2.1383070	5.1754780	-0.5952420	6	-2.4901270	-1.9163740	-3.0108170
6	-2.7367010	5.9627300	0.3802480	1	-1.5212400	-1.5231790	-3.3737680
6	-4.0222330	6.1255200	-0.0156520	6	-2.2427600	-3.3773690	-2.6183230
1	-2.2169590	6.3230190	1.2545340	6	-2.8595500	-1.0704110	-1.7881000
1	-4.8321010	6.6715430	0.4433440	1	-3.0545510	-0.0244760	-2.1036820
6	-5.3792340	5.2272720	-1.8613970	1	-3.7625010	-1.4657250	-1.2772370
6	-5.8854500	6.1184970	-2.8553090	1	-2.0180940	-1.0655890	-1.0628990
6	-6.1519950	4.0994270	-1.4589610	1	-1.9742830	-3.9709650	-3.5184070
6	-7.1403620	5.8444010	-3.4301150	1	-3.1421830	-3.8258830	-2.1462400
6	-7.3967690	3.8705670	-2.0709380	1	-1.3991420	-3.4394450	-1.8980160
6	-7.8819750	4.7340640	-3.0444230	6	-4.0142860	-0.6394520	-7.7572590
1	-7.5523810	6.4913800	-4.1946980	1	-2.9439280	-0.3814480	-7.8710620
1	-8.0019690	3.0178670	-1.7925980	6	-4.8076640	0.6489090	-8.0074720
1	-8.8428160	4.5416420	-3.5043770	6	-4.3099120	-1.6883090	-8.8362660
6	-0.8215090	4.6785720	-0.4924220	1	-3.7377920	-2.6178630	-8.6285760
6	0.2324940	5.3076890	-1.2074900	1	-5.3921420	-1.9327620	-8.8778190
6	-0.5455490	3.5641700	0.3470660	1	-3.9989820	-1.3055480	-9.8319170
6	1.5375540	4.7957400	-1.0892190	1	-5.9008680	0.4544630	-8.0111030
6	0.7717800	3.0749540	0.4177800	1	-4.5246250	1.0854320	-8.9889740
6	1.7986410	3.6847300	-0.2947460	1	-4.5789030	1.3954330	-7.2171680
1	2.3630830	5.2585920	-1.6134540	6	-0.0090430	6.5458290	-2.0645940
1	1.0100490	2.2142930	1.0286350	1	-1.0938160	6.7643520	-2.1400000
1	2.8069060	3.2973300	-0.2248600	6	0.4935110	6.3436740	-3.4999960
6	0.4890680	1.6476630	-6.0267380	6	0.6388820	7.7797030	-1.4277200
6	1.1875240	2.1193620	-4.8659480	1	0.2406470	7.9287010	-0.4011120
6	0.6430460	2.3439610	-7.2726860	1	1.7426920	7.6684090	-1.3717800
6	2.0008370	3.2615270	-4.9809330	1	0.4031980	8.6854730	-2.0263830
6	1.4790100	3.4750820	-7.3169090	1	1.6028010	6.3503920	-3.5475260
6	2.1436060	3.9260870	-6.1878000	1	0.1104780	7.1551930	-4.1548450

1	0.1318890	5.3739800	-3.8942290
6	-1.6378810	2.8845390	1.1690690
1	-2.5996230	3.4191760	1.0642560
6	-1.3077540	2.9042610	2.6668790
6	-1.8935730	1.4579000	0.6773850
1	-2.2044600	1.4868570	-0.3871530
1	-0.9855790	0.8264830	0.7767090
1	-2.7160400	0.9923260	1.2612920
1	-0.4241420	2.2723840	2.8956580
1	-2.1715640	2.5200220	3.2505760
1	-1.1031940	3.9453680	2.9966920
6	-5.6716130	3.1325600	-0.3785230
1	-4.6927730	3.4488480	0.0248940
6	-5.4625390	1.7221240	-0.9427630
6	-6.6325720	3.1118660	0.8162400
1	-6.7787430	4.1431500	1.2030980
1	-7.6196360	2.6891470	0.5339310
1	-6.2071010	2.4923510	1.6346320
1	-6.4154080	1.2865400	-1.3097810
1	-5.0495680	1.0539810	-0.1570950
1	-4.7349980	1.7557030	-1.7795710
6	-5.1405620	7.3573780	-3.3616150
1	-5.8269670	7.9332720	-4.0229210
6	-3.9444620	6.9889880	-4.2430240
6	-4.7420660	8.3372640	-2.2505940
1	-5.5346720	8.3937100	-1.4743620
1	-3.7766440	8.0543320	-1.7857090
1	-4.6077640	9.3534920	-2.6794840
1	-3.1589110	6.4643090	-3.6686730
1	-3.4972250	7.9078430	-4.6788100
1	-4.2808900	6.3424780	-5.0795950
6	1.1173540	1.4767520	-3.4753720
1	1.8628320	1.9838130	-2.8216640
6	1.5287200	0.0003990	-3.4492150
6	-0.2269200	1.7100450	-2.7808590
1	-0.5127350	2.7811780	-2.8411500
1	-1.0333780	1.0932930	-3.2088920
1	-0.1376340	1.4298560	-1.7121250
1	0.6781880	-0.6632850	-3.6896020
1	1.8716920	-0.2742150	-2.4284440
1	2.3647430	-0.1864690	-4.1563450